A N N U A L R E P O R T

1966

U. S. WATER CONSERVATION LABORATORY
Southwest Branch
Soil and Water Conservation Research Division
Agricultural Research Service
United States Department of Agriculture
Phoenix, Arizona

FOR OFFICIAL USE ONLY

This report contains unpublished and confidential information concerning work in progress. The contents of this report may not be published or reproduced in any form without the prior consent of the research workers involved.

LABORATORY STAFF

Professional:

Dr. H. Bouwer, Research Hydraulic Engineer
Mr. K. J. Brust, Agricultural Engineer
Mr. K. R. Cooley, Hydrologist
Dr. W. L. Ehrler, Research Plant Physiologist
Mr. L. J. Erie, Research Agricultural Engineer
Dr. D. H. Fink, Research Soil Scientist
Mr. G. W. Frasier, Agricultural Engineer
Dr. L. J. Fritschen, Research Meteorologist
Dr. R. D. Jackson, Research Physicist
Mr. L. E. Myers, Research Hydraulic Engineer and Director
Dr. F. S. Nakayama, Research Chemist
Mr. R. J. Reginato, Research Soil Scientist
Dr. J. A. Replogle, Research Agricultural Engineer
Mr. R. C. Rice, Agricultural Engineer
Dr. C. H. M. van Bavel, Research Physicist
Dr. K. K. Watson, Research Civil Engineer
Dr. F. D. Whisler, Research Soil Scientist

Technicians:

F. L. Combs, Physical Science Aid
O. F. French, Hydraulic Engineering Technician
J. L. Gale, Physical Science Aid
L. P. Girdley, Engineering Draftsman
J. R. Griggs, Physical Science Technician
J. J. Gruden, Physical Science Aid
J. B. Miller, Physical Science Technician
S. T. Mitchell, Physical Science Technician
K. G. Mullins, Physical Science Technician
G. D. Overman, Physical Science Aid
J. M. Pritchard, Physical Science Technician
B. A. Rasnick, Physical Science Technician
C. D. Wakefield, Physical Science Aid

Administrative, Clerical and Maintenance:

O. J. Abeyta, Laborer
I. G. Barnett, Janitor
E. D. Bell, General Machinist
E. E. De La Rosa, Janitor
B. E. Fisher, Library Assistant
D. S. Fry, Clerk-Stenographer

Administrative, Clerical and Maintenance (Continued)

C. G. Hiesel, General Machinist
R. C. Klapper, Refrigeration and Air Conditioning Mechanic
J. M. R. Martinez, Laborer
R. S. Miller, Administrative Assistant
A. H. Morse, Clerk-Dictating Machine Transcriber
M. E. Olson, Clerk-Stenographer
L. J. Orneside, Clerk-Stenographer
J. J. Rodriguez, Laborer
M. A. Seiler, Clerk-Stenographer
C. H. Tanner, Secretary
M. F. Witcher, Clerk-Stenographer
M. M. Zamora, Laborer

CHANGES IN PERSONNEL

The Laboratory staff has been strengthened during 1966 by the addition of seven new members. They are as follows:

I. G. Barnett, Janitor
K. R. Cooley, Hydrologist
D. H. Fink, Research Soil Scientist
J. J. Gruden, Physical Science Aid
L. J. Orneside, Clerk-Stenographer
G. D. Overman, Physical Science Aid
J. J. Rodriguez, Laborer

Dr. K. K. Watson, Research Civil Engineer, joined our staff as a visiting scientist during 1966. He has returned to his native Australia, where he is a Senior Lecturer in the School of Civil Engineering, University of New South Wales, Kensington.

Dr. F. D. Whisler, Research Soil Scientist, of the Soil and Water Conservation Research Division, Agricultural Research Service, U. S. Department of Agriculture, Urbana, Illinois, joined our staff on a temporary duty assignment until August, 1967.

During 1966, there were three resignations and one transfer. They are as follows:

F. L. Combs, Physical Science Aid
L. J. Fritschen, Research Meteorologist
M. E. Olson, Clerk-Stenographer
M. M. Zamora, Laborer

The Laboratory staff is now essentially at full strength, with one or two exceptions.

TABLE OF CONTENTS

Title	Line Project	Research Outline Number	Page
Dynamic Similarity in Elbow Flow Meters	SWC X-gG1	Ariz. WCL-2	2-1
Soil Treatment to Reduce Infiltration and Increase Precipitation Runoff	SWC VII-gG3	Ariz. WCL-7	7-1
Application of Hexadecanol-Octadecanol Monofilms to Small Ponds	SWC VII-gG2	Ariz. WCL-9	9-1
Measurement and Calculation of Unsaturated Conductivity and Soil-Water Diffusivity	SWC VII-gG5	Ariz. WCL-13	13-1
Field Application of Falling-Head Technique for Seepage Meters and of Double-Tube Method for Hydraulic Conductivity Measurement	SWC VII-gG1	Ariz. WCL-14	14-1
Evaporation from the Soil Surface and Soil Moisture Movement	SWC VII-gG5	Ariz. WCL-19	19-1
Consumptive Use of Water by Crops Grown in Arizona	SWC IX-gG3	Ariz. WCL-23	23-1
Measuring Horizontal and Vertical Hydraulic Conductivity of Soil with the Double-tube Method	SWC VII-gG1	Ariz. WCL-25	25-1
Water Absorption, Transpiration, and Internal Water Balance of Cotton Plants as Affected by Changes in Evaporative Demand	SWC IX-gG1	Ariz. WCL-29	29-1
Quantitative Measurement of Water Flow with Chemical Tracers	SWC X-gG1	Ariz. WCL-30	30-1
Direct Measurement of Evapotranspiration and the Energy Balance of Irrigated Crops	SWC IX-gG1	Ariz. WCL-33	33-1
Water Management for the Efficient Irrigation of Sugar Beets	SWC IX-gG3	Ariz. WCL-36	36-1

Title	Line Project	Research Outline Number	Page
Clay Dispersants for the Reduction of Seepage Losses from Reservoirs	SWC VII-gG1	Ariz. WCL-37	37-1
Water-borne Sealants to Reduce Seepage Losses from Unlined Channels and Reservoirs	SWC VII-gG1	Ariz. WCL-38	38-1
Crack Sealants for Concrete-lined Canals	SWC VII-gG1	Ariz. WCL-39	39-1
Dispersion and Flocculation of Soil and Clay Materials as Related to the Na and Ca Status of the Ambient Solution	SWC VII-gG4	Ariz. WCL-40	40-1
Materials and Methods for Water Harvesting and Water Storage in the State of Hawaii	SWC VII-gG2	Ariz. WCL-42	42-1
Integrating Velocity Profile Meters	SWC X-gG1	Ariz. WCL-43	43-1
Experimental and Analytical Studies of the Flow and Oxygen Regimes in Soil Intermittently Inundated with Low Quality Water	SWC IV-gG2	Ariz. WCL-44	44-1
Irrigation Outlet Structures to Distribute Water onto Erosive Soils	SWC X-gG1	Ariz. WCL-45	45-1
Flow Measurement in Open Channels with Critical Depth Flumes	SWC X-gG1	Ariz. WCL-48	48-1
Physical and Chemical Characteristics of Hydrophobic Soils	SWC VII-gG4	Ariz. WCL-49	49-1
Use of Floating Solid and Granular Materials to Reduce Evaporation from Water Surfaces	SWC VII-gG5	Ariz. WCL-50	50-1
Manuscripts Approved and/or Published in 1966			AI

TITLE: DYNAMIC SIMILARITY IN ELBOW FLOW METERS

LINE PROJECT: SWC X-gG1 CODE NO.: Ariz.-WCL-2

INTRODUCTION:

See Annual Report for 1965.

PROCEDURE:

Hydraulic facilities at the laboratory were modified to allow the diversion of 10 cfs pumping capacity through a 12-inch diameter pipeline. Elbow No. 41 was installed in series with a venturi meter and recalibrated to include the higher flow rate.

Work with the elbow meters has for the most part been completed. The present phase is concerned with developing a suitable low-cost integrating device that will operate with the elbow meter and certain other differential-head meters.

RESULTS AND DISCUSSION:

Results and techniques developed were published in the Journal of the Irrigation and Drainage Division, ASCE, Vol. 92, No. IR3, Sept. 1966, pp. 17-34, by Replogle, Myers, and Brust, under the title "Evaluation of Pipe Elbows as Flow Meters." This essentially summarized the results reported in Annual Reports 1965 and previous.

As a result of the published paper, a discussion was submitted to the Journal by others which advocated retention of the square root form of the theoretical equation and attributing deviation of experimental data to Reynolds-number effects. Though not specifically reported in the original publication, the advocated procedure had been investigated and disgarded because the deviations did not significantly diminish with increasing Reynolds number.

The elbow data was rearranged to show the Reynolds-number effects in the manner suggested by the author of the discussion. As expected, the rearranged plots clearly show that the discharge coefficient continues to change with increasing Reynolds number. This indicates that the viscous effects are not a satisfactory explanation for the deviation from the theoretical equation. If it were a true Reynolds number effect, the deviations should significantly decrease, if not completely disappear, at higher Reynolds-number values.

To verify that high Reynolds numbers produced little improvement, elbow No. 41 was tested to Reynolds numbers in excess of 1,000,000. As with all the elbows, a Reynolds-number effect can be noted at values below 300,000, but this does not account for the major deviations noted even at higher values. Elbow No. 41 continued to deviate regularly from the theoretical equation even at the values exceeding 1 million. Below 300,000 the deviation was greater, indicating that at least in this range Reynolds-number effects are real. It is apparent that another explanation is necessary.

These deviations may be associated with the strengths of the secondary currents in the bend. Assuming that two spirals are formed in the elbow, the effective head-differential would decrease with increasing secondary flow. This would cause the filament of flow representing the average velocity to be carried outward from the inside pressure tap and would cause a slight decrease in the observed pressure differentials.

The mechanism for causing secondary flow in the elbow originates from a nonuniform velocity profile and depends on the slow-moving fluid near the boundaries. This being the case, as the Reynolds number increases the velocity profile approaches a uniform distribution, and thus the relative influence (not the absolute strength) of the secondary currents should decrease. Note, though, that if the velocity profile remains relatively unchanged, the relative influence of the secondary currents remains unchanged and a constant deviation from the theoretical equation would be produced, at least for a limited interval of flow ranges.

The above discussion does not explain the observation that an increasing value for the exponent in the theoretical equation is required for increasing elbow size. No explanation for why this should be associated with size of elbow is forthcoming.

A reply containing replotted data and supporting the above points in detail is being prepared as a published reply to the discussion submitted in response to the original paper.

Integrating Devices. The most satisfactory integrating device located and tested to date appears to be a low-cost, turbine-type

water meter. It measures flow rates down to 1/8 gallon per minute, looks somewhat like a household water meter, is not easily clogged by sand, and sells for under $25.00. It is attached across the elbow taps and replaces the pressure differential sensing manometer previously used which is capable of indicating flow rate only.

The flow through the water meter is proportional to the square root of the pressure differential across the water meter. However, the pressure differential, itself, is proportional to the square of the velocity through the elbow (approximately). The combined result is that the recorded reading on the water meter is linearly related to the total flow that passed through the large elbow.

Three water meters were tested on a three-inch diameter elbow. Since the three-inch elbows adhere well to a square root equation, the expected linearity was achieved, Figure 1. The exact relation depends on the size of manometer taps, the pipe sizes used on the water meter shunt lines, and the valves and fittings in the shunt line.

To determine the correct calibration, the water meter is mounted in parallel to the manometer with valves provided to shut either out of the system. While preventing flow through the water meter by closing the appropriate valve, the manometer is read and the discharge rate calculated. Without changing the discharge rate, flow is permitted through the water meter and the dial accumulation noted for a measured time interval. This relation can be plotted as in Figure 1. Additional points for various flow rates can be similarly obtained and the linear relation determined for any set of plumbing fittings and manometer tap sizes. However, the tap sizes and pipe sizes must be properly selected to insure that the velocities in the shunt lines remain above a critical Reynolds number, or the square-root relation may not be valid. Manometer taps 1/4-inch in diameter used with a 1/2 - inch shunt line have been satisfactory for the tests to date.

The testing equipment of the water meters on a 10-inch diameter elbow has been assembled, but tests have not been conducted. Since this elbow size does not agree well with the theoretical square root equation, a strictly linear relation with the water meter is doubtful.

However, it should be within practical limits of $\pm$ 5 percent.

A major problem with the system is partial clogging of the shunt circuit by fiberous materials which changes the linear relation.

SUMMARY AND CONCLUSIONS:

Elbow flow meters, constructed from commercial, flanged pipe elbows have the unique advantages of replacing existing elbows, ability to measure flow in either direction and contributing no additional head loss to the piping system. The meter is readily constructed by drilling two holes at specified locations for attaching a manometer which is used to read out pressure differential caused by a fluid flowing around a bend.

Two conflicting theoretical analyses of flow through an elbow flow meter can be reconciled. One mathematical approach produces an equation closely approximating experimental results but is based on assumptions contrary to observation. The other mathematical approach, while analytically more sound, deviates considerably from experiment. Modifications to the latter produced an equation identical with the former without assumptions contrary to observation. This established the equational form used for an empirical relation, which is

$$Q = k \frac{\pi D^2}{4} \sqrt{\frac{g\bar{r}}{D}} H^E$$

and permits more confident generalizations and application of experimental results. In the above equation, k is a constant derived from previous calibrations on several elbows of the nominal size and type under consideration, D is the elbow diameter, g is the gravitational constant, $\bar{r}$ is the centerline radius of bend for the elbow meter, and E is obtained from the empirical equation

$$E = 0.0377D + 0.489$$

The empirical relation between discharge rate and pressure differential for uncalibrated elbow flow meters should be within $\pm$ 3 percent when dimensional data for the elbow is available.

Rearrangement of the original elbow-meter data and a new test of one elbow to Reynolds numbers exceeding 1 million, show that Reynolds-

numbers effects are not responsible for deviations from the theoretically derived square-root expression, as was suggested by a discusser of the published report originating from this project. Although thought to be related to secondary flows in the elbow, no sound explanation for variation of E with elbow size has as yet been tendered.

Low cost integrating devices to be used with the elbow flow meter to convert it from a rate device to a total quantity meter are being investigated. A simple shunt flow system using a new type of household water meter selling for less than $25.00 seems most promising. A strict linear relation is maintained between the water meter and the flow through a 3-inch elbow when the shunt system replaced the differential-pressure sensing manometers. This relation is not expected to hold as well for larger sized elbows which do not adhere closely to a square root equation. Partial clogging of the shunt circuit can cause changes in calibration, and hence an error in total flow, if not recalibrated frequently. Recalibration is not difficult and requires reading the differential pressure across the elbow with no flow going through the shunt, and comparing this to a timed accumulation on the water meter after flow in the shunt is resumed.

PERSONNEL: J. A. Replogle

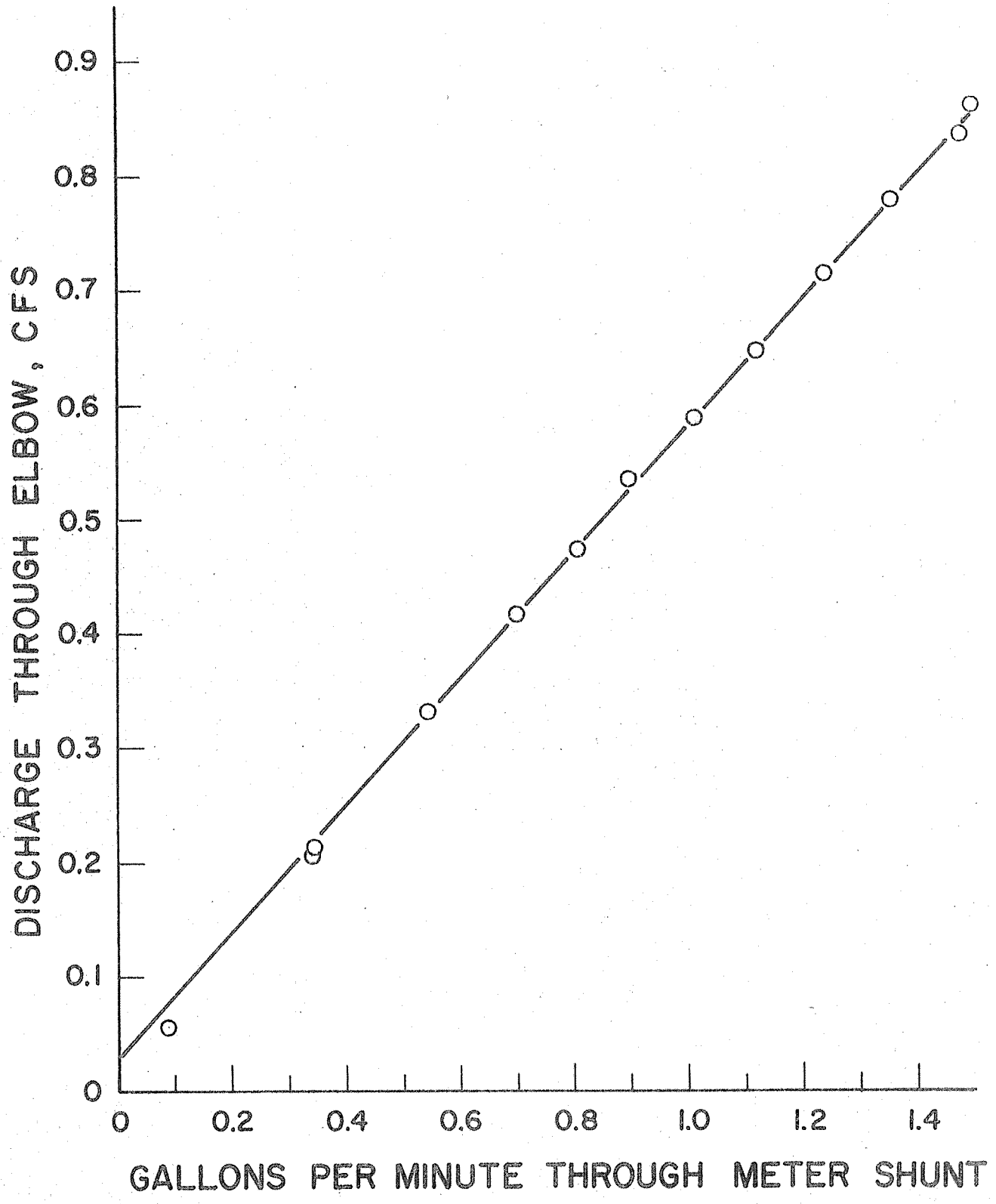
DISCHARGE THROUGH ELBOW, CFS
0.9
0.8
0.7
0.6
0.5
0.4
0.3
0.2
0.1
0
0
0.2
0.4
0.6
0.8
1.0
1.2
1.4
GALLONS PER MINUTE THROUGH METER SHUNT

Figure 1.

TITLE: SOIL TREATMENT TO REDUCE INFILTRATION AND INCREASE PRECIPITATION RUNOFF

LINE PROJECT: SWC VII-gG3 CODE NO.: Ariz.-WCL-7

INTRODUCTION:

The evaluation of different surface treatments for increasing precipitation runoff continued. Observations were made on existing experimental water harvesting installations and periodic maintenance was performed as required. This included a complete new sealcoat on the Flagstaff cinders catchment. Discoloration of runoff water collected from asphalt-treated plots was measured to evaluate materials applied to asphalt surfaces to reduce water discoloration and increase the life expectancy of the treatments. Preliminary work was started in evaluation of low-cost soil stabilizers for use with water repellent soil treatments. Observations and measurements were continued at the Granite Reef study site.

PART I. ANALYSIS OF RUNOFF WATER:

Reducing the degree of discoloration of runoff water from asphalt-treated surfaces serves a two-fold purpose. The quality of the runoff water is improved and since the amount of discoloration is an indication of the rate of asphalt deterioration, any reduction in discoloration represents an increase in treatment life.

Procedure. The analysis of the runoff water was performed as described in the Annual Report 1965, WCL-7. Primary interest was given to water samples collected from plots L-5 and L-6 at the Granite Reef testing site. Plot L-5 was originally a two-phase asphalt treatment with a sealcoat of roofing asphalt-clay emulsion at a rate of 0.5 kg asphalt m^{-2}. It was given a new sealcoat on 16 March 1966 of RSK asphalt emulsion at a rate of 0.6 kg asphalt m^{-2}. Plot L-6, which was also a two-phase asphalt with a top spray of aluminized asphalt, received a new top spray of a specially prepared flaked aluminum-rubber latex coating at a rate of 0.16 kg material m^{-2} on 17 February 1966. These coatings were not applied because the runoff from the plots were decreasing, but to permit evaluation of two other protective coatings.

Results. The correlation of the water color index was found to be directly proportional to the days between rains and inversely proportional to the quantity of runoff. The correlation is shown in Figure 1, where the days between rains divided by the runoff in mm is plotted against the water color index. The figure includes the data obtained for four different sealcoat materials: a standard RSK asphalt emulsion, a roofing asphalt-clay emulsion, an aluminized asphalt paint, and a flaked aluminum-rubber latex coating. The data analysis consisted of computing the best-fit line by the least squares method for each treatment. The effectiveness of the sealcoats for reducing water discoloration is compared to the standard RSK asphalt emulsion. The reduction in water discoloration was 60 percent with the clay emulsion, 80 percent with the aluminized-asphalt paint, and 93 percent with the flaked aluminum-rubber latex coating.

These results show the discoloration of runoff water from asphalt treated surfaces can be significantly reduced with the present treatment, which costs approximately 5 cents m^{-2}. The studies will be continued to determine the long-term effectiveness of the materials and the possibility of using them for protective coatings with types of treatments other than asphalt.

PART II. OPERATIONAL FIELD CATCHMENTS:

Nelson Road catchment. The two-phase asphalt treatment installed on this catchment during the summer of 1964 was considered in excellent condition when inspected 27 September 1966. There were a few minor cracks on the pavement surface. The most serious cracking had occurred at the lower edge of the plot. The asphalt-fiberglass reservoir lining has a tendency to slide downslope and the buried edge pulled away from the soil. Repair was performed by pouring MC-250 cutback asphalt on each crack from a can. Inspection of the reservoir lining showed no signs of deterioration. There were a few holes above the water line which had been caused by animals walking on the lining. These were repaired with an asphaltic crack sealer. A large hole next to the drain outlet was repaired with an asphalt-sand mix covered with a butyl rubber tape. When inspected in September 1966, the lining was holding water.

Blue Mountain catchment. This catchment, treated during the summer of 1964, was considered in good condition on about 70 percent of the area when inspected on 28 September 1966. The upper half, which has a top spray of flaked aluminum on top of a two-phase asphalt treatment looked good and the pavement was undamaged. The lower half, without the top spray, had deteriorated considerably during the summer. Bureau of Indian Affairs personnel had mopped a coating of diluted asphalt-clay emulsion on this portion of the catchment. The coating looked good but it is not known how long it will last because of a partially deteriorated basecoat. At the plot outlet the pavement was starting to break up. During the year a few small yucca plants grew on the plot, but these were being controlled by cutting and spot application of soil sterilent as they appeared.

Metate catchment. The treatment of the Metate catchment, installed during the summer of 1965, consisted of 2-mil black polyethylene bonded to asphalt stabilized soil. The catchment was considered in excellent condition with no holes or vegetation growth when inspected 20 May 1966 and again on 19 July 1966. There were indications the asphalt-fiberglass reservoir lining was leaking when inspected on 20 May 1966. The lining was repaired by brushing an asphaltic crack sealer on all damaged areas and loose seams which might be leaking. The entire lining was then sprayed with asphalt-clay emulsion. Inspection on 19 July 1966 indicated the lining was holding water. The collected water was very dark brown in color, similar to water collected from asphalt pavements. It is believed that asphalt is migrating through the polyethylene to the sheeting surface and undergoing deterioration. The oxidized by-products are then washed into the reservoir when it rains.

Flagstaff cinders catchment. The Flagstaff cinders catchment, installed during the summer of 1964 by stabilizing the cinders with RSK asphalt emulsion and sealing the surface with asphalt-clay emulsion, had weathered very well until the winter of 1965-66. Inspection on 6 May 1966 showed the pavement had cracked with the cracks averaging about 1 cm wide on an irregular grid of about 1 m. The loose, uncompacted

cinders apparently had permitted the pavement to shrink as the volatile fractions evaporated from the asphalt. Repair was accomplished on 1 June 1966 by spraying the cracks with RSK asphalt emulsion, filling them with cinders, and spraying them again with emulsion. This repair put the pavement in good condition, but additional cracking is anticipated. It is expected that periodic maintenance of the cracks will be an essential item in the performance and life of the pavement.

Mescal catchment. This catchment was covered with an experimental 20-mil-thick film of modified polyethylene in September 1966. Inspection of the sheeting on 19 July 1966 showed the catchment to be in good shape. There were a few holes caused by twigs underneath, forcing their way through the sheeting. The BIA had been using the water collected from the catchment and considered it a successful installation.

San Vicente catchment. This catchment, installed during the summer of 1965, is covered with the 20-mil modified polyethylene sheeting. Inspection of the catchment on 28 April 1966 showed no signs of deterioration except a few holes made by animals and ants. These were repaired and measures taken to control the ants and small animals. The water storage for the catchment had originally been a 180,000 liter bag made from 20-mil modified polyethylene sheeting. This failed from rodent damage and the sheeting in the bag sticking together. The bag was removed and the retaining walls reshaped with dimensions 6.1 × 7.3 m bottom, 12.2 × 14.6 m top and 2.5 m deep for installation of a membrane lining. On 28 April 1966 the area was sprayed with 2,270 liters of MC-250 cutback asphalt. On 19 May 1966 a lining of 20-mil modified polyethylene was installed. The sheeting was bonded to the stabilized soil with RSK asphalt emulsion. There were some problems with poor lap joints. These were corrected and a report in December stated the lining appears to be holding water.

PART III. GRANITE REEF TESTING SITE:

During the summer of 1966 an underground water supply to all plots was installed. This system will supply 750 liters min^{-1} (200-gal min^{-1}) at a pressure of 3 kg cm^{-2} (40 lbs in^{-2}) at strategically located outlets within the test area. The water is pumped from

a 36.6 × 12.2 m × 1 m deep storage pond lined with 22-mil blue vinyl sheeting. The pond is kept filled with water collected from six of the 230 m^2 plots.

Results of studies of the rainfall patterns within the test area using a series of twenty-three, 7.62 cm diameter raingages were inconclusive. Trouble was encountered in obtaining watertight fittings between the collection rim and the storage bottles. Also, the plastic bottles would deteriorate and crack in the sunlight. Subsequently, in December the network of 7.62 cm diameter raingages were replaced with a network of fifteen, 20.32 cm (8 in) diameter raingages, 150 mm capacity, on a 45.7 × 39.6 m rectangular grid. These raingages are identical to the standard Weather Bureau raingages except in total capacity. The data from these gages, plus two, 20.32 cm diameter weighing gages, one 20.32 standard storage gage, two 20.32 cm diameter ground level gages and a Vector pluviometer will be used to evaluate the rainfall patterns in the future. Because of the poor data obtained with the 7.62 cm gages, the runoff from the plots is being compared to the standard 20.32 storage raingage, even though it is known some of the rainfall patterns are variable. For the year, a total rainfall of 228.2 mm was measured in 29 separate storms. Following are the results of the runoff measured from the different plots.

Esso plots. The four-plot test unit constructed in cooperation with Esso Research Corporation of Linden, New Jersey in December 1964 with a one-phase treatment of Eastern asphalt is still performing satisfactorily. Plot E-1, treated with 1.95 kg asphalt m^{-2}, averaged 80 percent runoff, plot E-2 treated with 1.85 kg asphalt m^{-2}, averaged 77 percent runoff, plot E-3, smoothed-untreated soil, averaged 44 percent runoff, and plot E-4 treated with 2.2 kg asphalt m^{-2} averaged 86 percent runoff. Runoff from the asphalt plots is approximately 10 percent lower than the preceeding year. Even so, the runoff is quite good considering these treatments do not include a sealcoat. A few cracks are developing in the pavements.

Watersheds. The runoff from the three, 450 m^2 watersheds is presented in Table 1. The majority of the runoff from these watersheds

occurred in two storms on 17-18 August when the rainfall intensity exceeded 75 mm hr^{-1}. Watersheds 1 and 2 are completely untreated with respect to smoothing and brush removal. Watershed 3 has had the brush hand-removed with a minimum of soil disturbance. For the year, watersheds 1 and 2 yielded 30 and 23 percent, respectively, with runoff from watershed 3 yielding 40 percent.

Large 230 m^2 plots. The treatments applied to the 230 m^2 plots are listed in Table 2, and the runoff results presented in Table 3. The bonded 1.5-mil black polyethylene on plot L-1 is considered in good condition after 22 months exposure. It was necessary to repair the lower 3 ft of the plot in May 1966. The film in this area had not bonded to the basecoat and wind movement of the sheeting over underlying pebbles wore holes in the sheeting. The remainder of the sheeting was not damaged because of the excellent bond between the film and the base coat. Repair consisted of bonding a sheet of 4-mil polyethylene on top of the existing sheeting with asphalt emulsion. Runoff for the plot averaged 88 percent for the year. The water collected from the plot is discolored. The bonding asphalt is migrating through the film, undergoing deterioration on the surface and discoloring the collected water. Further studies of asphalt migration through thin films will be conducted.

Runoff from the smoothed-untreated plot L-2 averaged 34 percent, while runoff from plot L-3 treated with a water repellent designated R-9, averaged 76 percent. Runoff from plot L-2 has not changed significantly from the preceeding year but runoff from L-3 has decreased. A detailed study of the degree of water repellency on the plot was checked in November 1966. A rectangular grid on a 1.53 m spacing was laid out and water was applied to the soil surface at all grid intersections, including the plot boundaries, for a total of 121 points. Points were considered to represent the following areas: interior intersections - 2.33 m^2, boundary intersections - 1.16 m^2, and corners - 0.58 m^2. The following criteria were used for defining the degree of repellency.

Zero - water soaked rapidly into soil.

Slight - soil surface was wetted but infiltration was slow.

Fair - sand and gravel on the soil surface was wetted but water did not soak into underlying soil.

Good - soil surface highly water repellent.

On this basis, the plot area in the various categories was: zero - 8, slight - 19, fair - 44, and good - 29 percent. Almost all of the zero and slightly repellent areas were in the upper one-third of the plot. The lower two-thirds of the plot was almost all fair to good. This pattern indicates that erosion may have removed a considerable part of the water repellent soil from the upper part of the plot with much less erosion and some deposition on the lower part of the plot.

Sand and gravel on the plot surface was rarely water repellent. Subsequent tests showed the gravel to be siliceous with a very thin surface coating of calcareous material. The water repellent reached with the surface material to form a hydrophobic coating that was not chemically bonded to the gravel and could be washed off by raindrop impact. Although the underlying soil was still hydrophobic, the deposits of wettable gravel appreciably increased retention of water on the plot surface.

Evidence of non-uniform application of the chemical to the plot surface was also found. When the surface soil was scraped off to a depth of about 2 mm, spots of wettable soil were located in areas of hydrophobic soil. The original solution application was made by spraying at a rate exceeding the infiltration rate. In retrospect, it is obvious that solution distribution was affected by small variations in surface elevation. Solution ran off the slightly higher spots and collected in minor depressions. Accordingly, the high spots received a relatively light application creating a shallow depth of hydrophobic soil that could be removed by relatively minor erosion.

The quantity of soil eroded from the plots and deposited in the tanks was dried and weighed for all storms 30 January 1966 through

13 September 1966. For these storms, plot L-2 eroded 7.4 g soil per liter of runoff and plot L-3 eroded 4.2 g soil per liter of runoff. This is an increase in erosion over the preceeding year where L-2 eroded 2.0 g per liter of runoff and L-3 eroded 3.2 g per liter of runoff. Over 80 percent of the erosion occurred in the two storms on the 17-18 August 1966. Particle size analysis of the eroded soil collected from the plots shows the particle size distribution has not significantly changed since August 1965. For plot L-2 the distribution is roughly 40 percent sand, 50 percent silt and 10 percent clay. For plot L-3 the distribution is 50 percent sand, 45 percent silt and 5 percent clay. The results of the erosion studies and particle size analysis is presented in Table 4.

Reduction in the rainfall runoff from plot L-3 can be attributed to three factors:

1. Inadequate application of water repellent to some parts of the plot;
2. Erosion of water repellent soil from upper parts of the plot;
3. Erosion developed deposits of siliceous gravel that were not made permanently hydrophobic by the chemical.

The above problems can be essentially solved by using a soil stabilizer to stop erosion and by application of the chemical at a rate less than the infiltration rate of the soil. Preliminary laboratory tests have shown that several promising low-cost soil stabilizers are compatible with R-9 so that both materials can be applied in a single solution. The most encouraging observation was the fact that about 30 percent of the plot surface was still highly water repellent after exposure to high solar radiation, rainfall, and related destructive forces for 16 months.

The runoff from plot L-4, the butyl sheeting standard, averaged 99 percent for the year. The cover has no holes at present, but is showing signs of "chalking", which is an indication that the one-year-old butyl sheeting is deteriorating. The magnitude of the deterioration is not presently known.

The runoff from both the two-phase asphalt treatment plots, L-5 and L-6, averaged 98 percent for the year. Both of these plots were given new surface treatments this year in conjunction with studies in reducing the discoloration of the runoff water. The condition of the previous coatings was considered to be excellent at time of retreatment.

The cover on plot L-7 of 10-mil black, modified polyethylene installed in June 1965, underwent serious deterioration this year, partially as a result of installing the sheeting under tension. At areas of high stress, small holes formed which then increased in size until the tension in the immediate material was relieved. Even with many holes in the sheeting, there was no damage by wind as the bonded area between holes prevented any movement of the sheeting. The runoff from the plot for the year averaged 80 percent, showing the pavement below the sheeting was in good condition.

Ridge and furrow plots. The description of these plots is presented in the Annual Report of 1965, WCL-7. Plots R-4, R-5, and R-6 were treated in May 1966. The runoff from the five remaining plots averaged approximately 40 percent runoff from both 10 and 20 percent slopes. Measured erosion from these plots for storms through 13 September 1966 was 12.9 g sediment per liter of runoff for the 20 percent slopes and 10.1 g sediment per liter of runoff for the 10 percent slopes, which compared to 7.4 g sediment per liter of runoff for plot L-2 which has a 5 percent slope. The increase in erosion this year compared to last year can partially be attributed to the high intensity storms of 17-18 August 1966. Particle size analysis of the eroded soil from these plots for a period of sampling from 17 August 1965 to 13 September 1966 show the clay and silt content has decreased with a corresponding increase in the sand content. The size distribution in September 1966 was approximately 45 percent sand, 45 percent silt and 10 percent clay.

Plot R-4 was treated 13 May 1966 with sodium carbonate at a rate of 44.9 g m^{-2} (400 lb $acre^{-1}$) in a 10 percent water solution. Plots

R-5 and R-6 were treated 10 May 1966 with the water repellent R-9, at a rate of 56.1 g m^{-2} (500 lb $acre^{-1}$) as a 10 percent solution combined with a low-cost rubber latex soil stabilizer, at a rate of 37.5 g solids per m^2 (390 lbs $acre^{-1}$). The runoff results from the three treated ridge and furrow plots and an untreated check of R-2 are presented in Table 5. From 1 January 1966 through 16 April 1966, when all plots were untreated, runoff was 26, 21, 17 and 18 percent for plots R-2, R-3, R-5, and R-6, respectively. From 17 April 1966 through 31 December 1966, after treatment, the runoff was 48, 70, 78 and 70 percent for the plots respectively. Erosion measurements from 17 August 1965 through 26 March 1966, and 27 March 1966 through 13 September 1966, show the collected sediment in the tanks increased from 5.0 to 11 g per liter of runoff on plot R-2 and on plot R-4 increased from 4.0 to 12.0 g per liter of runoff. There was no consistent change in particle size distribution. This indicates the salt treatment will increase runoff but does not significantly increase erosion. For the same periods, the erosion on plot R-5 decreased from 7.6 to 4.1 g per liter of runoff and on plot R-6 decreased from 16.9 to 4.7 g per liter of runoff. Again, there was no consistent change in particle size. These results show the combination of the low-cost water repellent in combination with a low-cost soil stabilizer can increase runoff and at the same time reduce the erosion hazard. The degree of soil stabilization was not considered satisfactory.

SUMMARY AND CONCLUSIONS:

Analysis of discolored water collected from asphalt pavements sprayed with four different surface coatings have shown that the discoloration can be significantly reduced by application of low-cost protective coatings to the asphalt surface. Studies at Granite Reef have shown that a specially prepared aluminum coating can reduce the discoloration by over 90 percent. These coatings serve a two-fold purpose. One, better quality water is obtained, and two, by reducing the rate of deterioration, the life of the base material is increased.

With the exception of the Flagstaff cinders catchment, all the experimental operational catchments have performed satisfactorily. At the Flagstaff catchment it was necessary to perform considerable maintenance. During the winter of 1965-1966 the pavement had developed numerous shrinkage cracks. These were repaired by spraying the cracks with RSK asphalt emulsion, filling with cinders and then respraying with RSK at a total cost of about 10 cents per square yard. The resulting pavement is in excellent condition. It is expected other cracks will develop with time, but it has been shown the cracks can be easily repaired.

Observations of the Blue Mountain catchment have shown that a protective coating of flaked aluminum will increase the life of the asphalt pavements. The portion without the top spray had deteriorated after two years exposure and was retreated with asphalt-clay emulsion. It is not known how long this will last as the basecoat is not in good condition. The pavement of the Nelson Road catchment is in excellent condition after two years and expected to last many years if periodic maintenance in control of weeds and repair of cracks is performed.

The 14-month-old 1.5-mil black polyethylene on the Metate catchment is in excellent condition and expected to last several years unless the rate of deterioration rapidly increases. The asphalt-fiberglass lining of the reservoir was resprayed to stop the loss of water by seepage from the lap joints.

The 20-mil experimental-modified polyethylene on the Mescal and San Vicente catchments is performing with excellent results after one year. There have been no signs of deterioration on either of these catchments. The storage reservoir at San Vicente was lined with the sheeting bonded to the soil with asphalt. At present, this is performing satisfactorily.

At the Granite Reef testing site, an underground water supply system was installed to furnish water to all the plots. The water is pumped from a vinyl lined pond which stores water collected on six of the plots during rainstorms.

Runoff from three plots treated in 1964 with a one-phase application of Eastern asphalt is gradually declining. The runoff is still good when considering that the plots do not have a sealcoat. Runoff from two, 230 m^2 plots treated with a two-phase asphalt treatment in 1963 yielded essentially 100 percent runoff for the year. These plots were given new top spray coats in our studies in evaluating and reducing the discoloration of runoff water from asphalt treated surfaces. This was not necessary for maintenance of high runoff performance.

A plot of bonded 1.5-mil black polyethylene is still yielding good runoff ater 22 months of exposure. The runoff water is discolored because of the bonding asphalt migrating through the film. Runoff from the butyl sheeting installed in 1961 standard averaged 99 percent for the year. Observations of the sheeting indicate the butyl is starting to deteriorate. The bonded 10-mil modified, black polyethylene installed in June 1965 underwent serious deterioration this year. The rapid rate of deterioration is a result of installing the sheeting under tension.

The runoff from the smoothed-untreated plot continued to average approximately 34 percent while the runoff from a similar plot treated with a low-cost water repellent in August 1965 averaged 76 percent. A detailed study on the plot indicates the degree of water repellency is decreasing because of uneven initial treatment, minor erosion, and failure of the chemical to render siliceous fine gravel permanently hydrophobic. Analysis of sediment collected in the tank shows the particle size distribution and quantity of eroded soil is not significantly different than from the smoothed-untreated plot.

Runoff from the ridge and furrow plots shows that increasing the slope from 10 to 20 percent does not increase runoff but does increase erosion. Analysis of eroded sediment shows the particle size distribution has gradually changed with an increase in sand content. A ridge and furrow plot treated with salt has had a significant increase in runoff but no significant increase in erosion. Two similar plots treated with a combination low-cost water repellent and low-cost soil stabilizer increased runoff and at the same time reduced erosion.

PERSONNEL: L. E. Myers, G. W. Frasier

TABLE 1. Runoff from 450 m^2 Watersheds at Granite Reef Testing Site

Date	Total Rainfall	W-1 runoff		W-2 runoff		W-3 runoff	
1966	(mm)	(mm)	(%)	(mm)	(%)	(mm)	(%)
17 Jan	3.8	0	0	0.2	5.3	0.5	13.2
18 Jan	3.1	0	0	0	0	0.3	9.7
30 Jan	2.3	0	0	0.1	4.3	0.4	17.4
7 Feb	20.5	2.8	13.7	2.2	10.7	5.0	24.4
8 Feb	1.2	0.3	25.7	0.2	16.7	0.3	25.0
10 Feb	9.9	0.1	1.0	0	0	0.3	3.0
2 Mar	2.5	0	0	0	0	0	0
26 Mar	5.7	0	0	0	0	0	0
16 Apr	0.4	0	0	0	0	0	0
19 Jun	0.8	0	0	0	0	0	0
20 Jul	1.2	0	0	0	0	0	0
22 Jul	2.3	0	0	0	0	0	0
29 Jul	1.4	0	0	0	0	0	0
11 Aug	1.1	0	0	0	0	0	0
17 Aug	38.2	21.1	55.2	15.3	40.1	25.6	67.0
18 Aug	39.4	23.8	60.4	18.6	47.2	29.1	73.9
29 Aug	0.7	0	0	0	0	0	0
12 Sep	9.4	3.2	34.0	2.9	30.9	5.1	54.3
12 Sep	3.5	0.5	14.3	0.3	8.6	0.8	22.9
12-13 Sep	37.0	14.6	39.5	10.2	27.6	18.0	48.6
13 Sep	1.1	0	0	0	0	0	0
4 Oct	6.4	0.3	4.7	0.2	3.1	1.1	17.2
4 Oct	3.0	0	0	0	0	0	0
7 Oct	1.0	0	0	0	0	0	0
7-8 Oct	14.3	2.1	14.7	1.6	11.2	2.8	19.6
9 Nov	0.8	0	0	0	0	0	0
5 Dec	1.0	0	0	0	0	0	0
7 Dec	3.0	0.3	10.0	0.2	6.7	0.5	16.7
26 Dec	13.2	0.1	1.0	0.3	2.0	0.8	5.8
TOTAL	228.2	69.2	30.3	52.3	22.9	90.9	39.7

TABLE 2. Treatments on 230 m^2 Plots at Granite Reef Testing Site

Plot	Treatment date	Treatment
L-1	10 Oct 1963	Basecoat. RC-Special at 2.0 kg asphalt m^{-2}
	1 Feb 1965	Top sheeting. Black polyethylene, 1.5 mil bonded with a mixture of MC-70 and MC-250 at 1.2 kg asphalt m^{-2}
L-2	30 Nov 1961	Smoothed - untreated
L-3	4 Aug 1965	R-9 at 0.057 kg m^{-2}
L-4	30 Nov 1961	Butyl Rubber Sheeting, 15 mil
L-5	18 Sep 1962	Basecoat. S-1 at 1.04 kg asphalt m^{-2}
	25 Jan 1965	Topcoat. Asphalt-clay emulsion at 0.5 kg asphalt m^{-2}
	16 Mar 1966	Topcoat. RSK asphalt emulsion at 0.6 kg asphalt m^{-2}
L-6	19 Apr 1963	Basecoat. RC-Special at 1.5 kg asphalt m^{-2}
	8 May 1963	Topcoat-South Half, SS-2 special asphalt emulsion at 0.65 kg asphalt m^{-2} with 3 percent butyl latex
	9 Jul 1963	Topcoat-North Half, S-1 at 0.5 kg asphalt m^2 with 3 percent butyl latex
	22 Jan 1965	Top Spray. Flaked aluminum at 0.08 kg solution m^{-2}
	17 Feb 1966	Top Spray. Aluminum coating TS-A-1 at 0.16 kg material m^{-2}
L-7	12 Feb 1965	Basecoat. RC-Special at 2.0 kg asphalt m^{-2}
	8 Jun 1965	Top sheeting. Modified polyethylene film, 10 mil bonded with S-1 at 0.7 kg asphalt m^{-2}

TABLE 3. Runoff Results from Rainfall on 230-m^2 Plots at Granite Reef Testing Site

Date	Total Rainfall	L-1 runoff		L-2 runoff		L-3 runoff		L-4 runoff		L-5 runoff		L-6 runoff		L-7 runoff	
1966	(mm)	(mm)	(%)	(mm)	(%)	(mm)	(%)	(mm)	(%)	(mm)	(%)	(mm)	(%)	(mm)	(%)
17 Jan	3.8	3.8	100.0	0.2	5.3	3.1	81.6	4.0	105.3	3.9	102.6	3.8	100.0	3.6	94.7
18 Jan	3.1	3.3	106.5	0	0	3.1	100.0	3.6	116.1	3.5	112.9	3.3	106.5	3.1	100.0
30 Jan	2.3	2.2	95.7	0.1	4.3	1.7	73.9	2.4	104.3	2.4	104.3.	2.3	100.0	2.4	104.3
7 Feb	20.5	17.4	84.9	2.6	12.7	16.0	78.0	19.3	94.1	18.0	87.8	18.0	87.5	20.5	100.0 2/
8 Feb	1.2	1.1	91.7	0	0	0.9	75.0	1.3	108.3	1.1	91.7	0.9	75.0	1.1	91.7
10 Feb	9.9	10.3	104.0	0.4	4.0	9.7	98.0	10.1	102.0	10.5	106.1	10.5	106.1	10.0	101.0
2 Mar	2.5	2.6	104.0	0	0	2.2	88.0	2.7	108.0	2.6	103.9	2.5	100.0	2.6	104.0
26 Mar	5.7	5.2	91.2	0.3	5.3	4.1	71.9	5.3	93.0	5.5	96.5	5.0	87.7	5.8	101.8
16 Apr	0.4	0.6	150.0	0	0	0	0	1.2	300.0	0.9	225.0	0.8	200.0	0.8	200.0
19 Jun	0.8	0.4	50.0	0	0	0	0	0.9	112.5	0.6	75.0	0.5	62.5	0.4	50.0
20 Jul	1.2	1.6	133.3	0	0	0.5	41.7	1.4	116.7	1.1	91.7	0.9	75.3	1.3	108.3
22 Jul	2.3	2.0	87.0	0	0	1.3	56.5	1.9	82.6	2.1	91.3	1.9	82.6	1.3	56.6
29 Jul	1.4	1.3	92.9	0	0	0.7	50.0	1.4	100.0	1.3	92.9	1.3	92.9	0.8	57.1
11 Aug	1.1	0.9	81.8	0	0	0.5	45.5	1.2	109.1	1.1	100.1	1.1	100.0	0.8	72.7
17 Aug	38.2	29.1	76.2	21.0	55.0	28.8	75.4	38.8	101.6	35.3	92.4	35.4	92.7	28.1	73.6
18 Aug	39.4	37.3	94.7	23.5	59.6	34.3	87.1	38.1	96.7	38.8	98.5	39.4	100.0 1/	33.9	86.0
29 Aug	0.7	0.6	85.7	0	0	0	0	1.0	142.9	0.8	114.3	0.6	85.7	0.8	114.3

TABLE 3. Runoff Results from Rainfall on 230-m^2 Plots at Granite Reef Testing Site (continued)

Date	Total Rainfall	L-1 runoff		L-2 runoff		L-3 runoff		L-4 runoff		L-5 runoff		L-6 runoff		L-7 runoff	
1966	(mm)	(mm)	(%)	(mm)	(%)	(mm)	(%)	(mm)	(%)	(mm)	(%)	(mm)	(%)	(mm)	(%)
12 Sep	9.4	8.5	90.4	4.4	46.8	7.2	76.6	9.3	98.9	8.6	91.5	9.1	96.8	7.5	79.8
12 Sep	3.5	3.0	85.7	1.1	31.4	1.7	48.6	3.1	88.6	3.2	91.4	3.2	91.4	2.3	65.0
12-13 Sep	37.0	32.8	88.6	18.5	50.0	33.0	89.2	36.5	98.6	39.3	106.2	39.3	106.2	27.1	73.2
13 Sep	1.1	0.9	81.8	0	0	0	0	1.0	90.9	1.0	90.6	1.0	90.9	0.5	45.5
4 Oct	6.4	5.4	84.4	1.2	18.8	3.2	50.0	5.7	89.1	5.8	90.6	5.6	87.5	3.0	47.1
4 Oct	3.0	2.6	86.7	0.2	6.7	0.9	30.0	2.7	90.0	2.7	90.0	2.6	86.7	1.4	46.7
7 Oct	1.0	1.3	130.0	0	0	0	0	1.3	130.0	1.3	130.0	1.4	140.0	0.7	70.0
7-8 Nov	14.3	12.4	87.1	3.4	23.8	9.7	67.9	13.6	95.1	13.8	96.5	14.1	98.6	10.0	69.9
9 Nov	0.8	0.9	113.1	0	0	0	0	1.1	137.5	1.1	137.5	0.9	112.5	0	0
5 Dec	1.0	0.4	40.0	0	0	0	0	0.8	80.0	0.6	60.0	0.6	60.0	0.3	30.0
7 Dec	3.0	2.9	96.7	0.2	6.7	1.3	43.2	3.1	103.3	3.1	103.3	2.9	96.7	2.2	73.3
26 Dec	13.2	11.0	83.5	0.9	7.1	9.9	74.7	12.8	97.0	13.4	101.4	13.6	102.9	10.6	80.4
TOTAL	228.2	201.8	88.4	78.0	34.2	173.8	76.2	225.6	98.9	223.4	97.9	222.5	97.5	182.9	80.1

1/ Water ran into tank from outside, runoff estimated at 100 percent.

2/ Meter stopped, runoff estimated at 100 percent.

TABLE 4. Results of Particle Size Analysis of Eroded Soil from Plots L-2 and L-3 at the Granite Reef Testing Site

Storm Date	Plot L-2							Plot L-3					
	Total Rainfall	Runoff	Erosion		Particle Size Analysis			Runoff	Erosion		Particle Size Analysis		
					Sand	Silt	Clay				Sand	Silt	Clay
	(mm)	(mm)	(gr/m^2)	(gr/liter) (runoff)	(%)	(%)	(%)	(mm)	(gr/m^2)	(gr/liter) (runoff)	(%)	(%)	(%)
17 Aug 1965	18.5	7.6	58.5	7.7	42.4	51.3	6.3	17.1	162.9	9.5	58.5	36.5	5.0
19 Sep 1965	7.2	1.7	10.0	5.9	18.4	67.6	14.0	7.9	48.9	6.2	57.0	39.1	3.9
16 Oct 1965	6.2	0.6	2.8	4.7	44.4	56.2	10.4	5.3	49.1	9.3	39.0	56.0	5.0
8 to 29 Dec 1965	166.4	83.5	114.1	1.4	50.0	45.8	4.2	136.8	265.0	1.9	48.0	47.6	4.4
30 Jan to 10 Feb 1966	33.9	3.1	1.9	0.6	64.5	29.2	6.3	28.3	8.3	0.3	57.8	35.9	6.3
26 Mar 1966	5.7	0.3	2.9	9.7	75.3	19.7	5.0	4.1	1.9	0.5	38.7	51.3	10.0
17-18 Aug 1966	77.6	44.5	469.4	10.5	44.2	50.0	5.8	63.1	466.1	7.4	37.3	56.7	6.0
12-13 Sep 1966	51.0	24.0	55.4	2.3	46.4	45.0	8.6	41.9	96.4	2.3	53.2	39.3	7.5

TABLE 5. Runoff results from ridge and furrow plots at Granite Reef

Date	Total Rainfall	R-2 Runoff		R-4 Runoff		R-5 Runoff		R-6 Runoff	
1965	(mm)	(mm)	(%)	(mm)	(%)	(mm)	(%)	(mm)	(%)
17 Jan	3.8	1.1	28.9	0.6	15.8	0.7	18.4	0.6	15.8
18 Jan	3.1	1.3	41.9	1.3	41.9	0.6	19.4	0.6	19.4
30 Jan	2.3	0.3	13.0	0	0	0.2	8.7	0.3	13.0
7 Feb	20.5	6.6	32.2	6.1	29.8	5.2	25.4	5.2	25.4
8 Feb	1.2	0	0	0	0	0	0	0	0
10 Feb	9.9	2.3	23.2	1.6	16.2	1.1	11.1	1.2	12.1
2 Mar	2.5	0	0	0	0	0	0	0	0
26 Mar	5.7	1.4	24.6	0.9	15.8	0.8	14.0	0.8	14.0
16 Apr	0.4	0	0	0	0	0	0	0	0
19 Jun	0.8	0	0	0	0	0	0	0.4	50.0
20 Jul	1.2	0	0	0	0	0.4	33.3	0.6	50.0
22 Jul	2.3	0	0	0	0	0.7	30.4	1.1	47.8
29 Jul	1.4	0	0	0	0	0.5	35.7	0.8	57.1
11 Aug	1.1	0	0	0	0	0.5	45.5	0.8	72.7
17 Aug	38.2	23.5	61.5	31.2	81.7	34.2	89.5	36.0	94.2
18 Aug	39.4	26.2	66.5	37.8	95.9	37.0	93.9	28.0	71.1
29 Aug	0.7	0	0	0	0	0.3	42.9	0.4	57.1
12 Sep	9.4	5.1	54.3	7.1	75.5	7.3	77.7	7.1	75.5
12 Sep	3.5	1.6	45.7	2.5	71.4	2.4	68.6	2.3	65.7
12-13 Sep	37.0	20.1	54.3	31.9	86.2	33.0	89.2	33.1	89.5
13 Sep	1.0	0	0	0	0	0.4	36.4	0.4	36.4
4 Oct	6.4	2.0	31.3	2.6	40.7	3.3	51.6	3.5	54.7
4 Oct	3.0	0	0	0	0	1.1	36.7	1.0	33.3
7 Oct	1.0	0	0	0	0	0.4	40.0	0.5	50.0
7-8 Nov	14.3	4.3	30.1	7.3	51.0	9.1	63.6	8.6	60.1
9 Nov	0.8	0	0	0	0	0	0	0	0
5 Dec	1.0	0	0	0	0	0	0	0	0
7 Dec	3.0	0	0	0	0	1.1	36.7	1.2	40.0
26 Dec	13.2	2.0	15.3	4.5	34.2	7.8	59.4	8.0	60.5
TOTAL	228.2	97.8	42.9	135.4	59.3	148.1	164.9	142.5	62.4

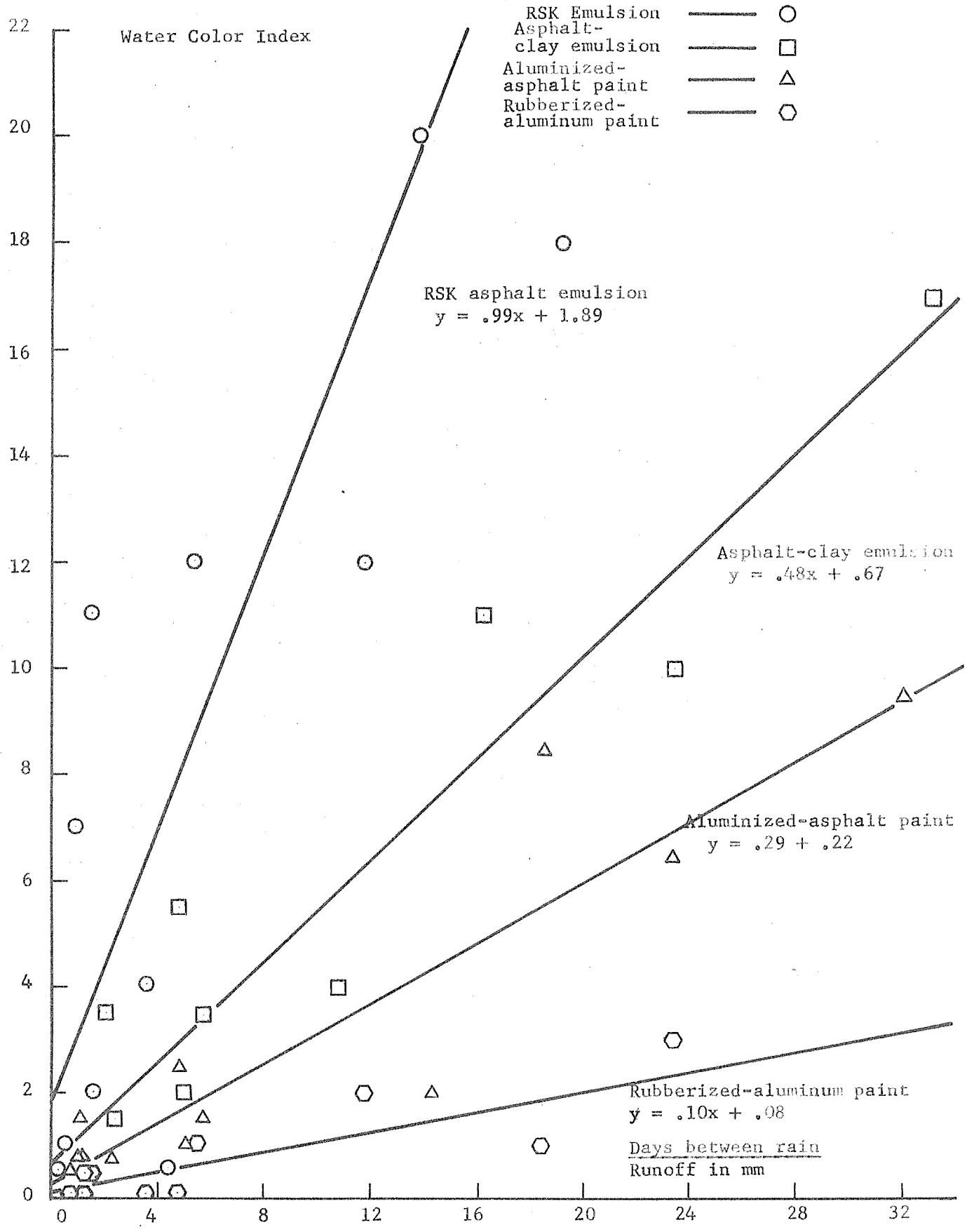

Figure 1. Discoloration of water from asphalt catchments in relation to quantity of runoff and days between rainfall.

TITLE: APPLICATION OF HEXADECANOL-OCTADECANOL MONOFILMS TO SMALL PONDS

LINE PROJECT: SWC VII-gG2 CODE NO.: Ariz.-WCL-9

INTRODUCTION:

Previous studies had shown that it was possible to prepare a stable, long-chain alkanol dispersion that would spread into an effective evaporation reducing monolayer on a water surface. This dispersion was extremely stable, but it was necessary to use distilled water for preparation. Concentrated mixes were quite viscous and became unstable when diluted with either distilled or tap water. Recent studies were concerned with formulation of a concentrated, long-chain alkanol dispersion in tap water which could easily be diluted with tap water to make a stable, lower viscosity dispersion for use with simple application equipment.

PROCEDURES:

All of the alkanol dispersions were prepared by the same basic procedure. The alkanol was melted by heating to 53-55°C. One part surfactant to 10 parts alkanol by weight was added. The surfactant-alkanol was stirred into water, preheated to 55-57°C, with a wire-basket type beater on an eccentric-type mixer set at a slow speed. Mixing was continued until the dispersion had cooled to about 35°C.

The relative viscosities of different dispersions and dilutions were measured with a falling head, tube-type viscometer. This consisted of a 3.8 cm diameter vertical plexiglass tube with a 12.3 cm long discharge tube set in a rubber stopper at the lower end. Two separate discharge tubes of 0.325 and 0.480 cm I.D. were used. The viscometer was filled with the alkanol dispersion and then allowed to drain through the discharge tube into a beaker setting on a weighing balance. Simultaneous measurements of the weight of collected material and the time required for the total head to change from 25.0 to 21.0 cm

were recorded. The viscosity in poises was calculated by the formula,

$$\mu = \frac{\pi d^4 h_L \gamma^2 t g}{128 \ell w}$$

where
μ = viscosity in poises
d = I.D. of discharge tube in cm
h_L = average total head in cm
γ = unit weight of material in grams cm^{-3}
t = elapsed time in seconds
g = force of gravity in cm sec^{-2}
ℓ = length of discharge tube in cm
w = weight of collected fluid in grams.

The size and shape of the alkanol particles was measured with a microscope and calibrated optical grid.

The rate of film release was measured in a 17.5 × 60 cm plexiglass tray containing a 1 cm depth of tap water at 28°C. Talcum powder was sprinkled on the water surface to indicate film movement. A 0.1 g sample of dispersion was placed on the water surface at one end of the tray and the film spreading rate was measured after an initial coverage of 175 cm^2 area.

The effectiveness of the dispersions for reducing evaporation was determined on the 2.74 m diameter tanks as described in previous annual reports.

RESULTS AND DISCUSSION:

The surfactant used in preparing dispersions discussed here is listed as a basic emulsifier for use in water with up to 1,100 ppm soluble salts. We were able to make pourable dispersions with alkanol contents up to 10 percent using tap water containing 1,700 ppm soluble salts. The concentrated dispersions could be diluted with tap water to make a stable, low viscosity dispersion with 1 percent alkanol.

Microscopic examination shows that the dispersion consists of randomly oriented alkanol "strings", approximately 0.5μ in width and 5-10μ long, intermixed with the water in a gel or sol-type structure.

Viscosity measurements were made at temperatures of 12, 23 and 33°C for three diluted dispersions: 10 percent diluted to 1 percent, 10 percent diluted to 3 percent, and 30 percent diluted to 3 percent. Viscosity varied with temperature, but not as much as expected. Viscosity for the 1 percent dispersions at temperatures of 12, 23 and 33°C was 75, 30 and 40 poises, respectively. Concentration of the original dispersion influenced viscosity of the diluted dispersion. Viscosity of the 30 percent diluted to 3 percent was approximately one-half the viscosity of 10 percent diluted to 3 percent. Changing discharge tube diameters did not significantly affect the viscosity measurement, indicating that the values obtained can be used in designing drip-type dispersion applicators.

The film release rate was 8,200 and 8,500 cm^2 min^{-1} for 1 and 3 percent dispersion applications containing 0.001 and 0.003 g of alkanol, respectively. These values compare to 3,900 cm^2 min^{-1} for 0.1 g of dry, powdered alkanol, 150-200μ particle size, scattered on the water surface. The dispersed alkanol spread from two to three times as fast as the powdered alkanol, even though from 100 to 300 times as much powdered alkanol was applied.

Ten percent dispersion diluted to 3 percent was applied to evaporation tanks at a rate of 0.7 g of alkanol m^{-2} $month^{-1}$ for a 30-day period during September 1966. Evaporation from untreated tanks for the period was 120 mm. This dispersion reduced evaporation by 25 percent.

SUMMARY AND CONCLUSIONS:

A stable, long-chain alkanol dispersion was prepared which can be made in pourable concentrations up to 10 percent, and then diluted with tap water to stable, 1 percent dispersions for application with simple automatic equipment. These dispersions reduced evaporation by 25 percent for a period of 30 days when applied at a rate of 0.7 g alkanol m^{-2} $month^{-1}$. The viscosity of the diluted dispersion does change with temperature and concentration of base dispersion. The effect of diurnal temperature fluctuation can be controlled by using insulated containers and applicators. Relatively low viscosity, stable dispersions can be prepared by proper formulation. The film generation

rate of the dispersions is significantly faster than that of powdered alkanol. These dispersions are not discrete alkanol particles as reported by others, instead, microscopic examination indicates a sol-type structure, which is extremely stable, yet permits rapid release of the alkanol particle as needed.

PERSONNEL: L. E. Myers, G. W. Frasier

TITLE: MEASUREMENT AND CALCULATION OF UNSATURATED CONDUCTIVITY AND SOIL WATER DIFFUSIVITY

LINE PROJECT: SWC VII-gG5 CODE NO.: Ariz.-WCL-13

INTRODUCTION:

The objectives and need for study for this project were given in the 1961 Annual Report of the U. S. Water Conservation Laboratory. Annual Reports for 1962, 1963 and 1965 covered work done on conductivity and soil-water diffusivity measurements at several porosities and temperatures. This work was based on the assumption that Darcy's law would describe water flow through saturated and unsaturated soils. Recent literature has questioned the applicability of Darcy's law. Deviations have been reported for porous materials ranging from sands to clays. The greatest deviations reported were for fine materials such as clays. The implications of these reports warrant an investigation into the occurrence and causes of non-Darcy behavior for the flow of water in porous materials.

Darcy's law can be written

$$q = k \, \Delta P/\ell \qquad [1]$$

where q is the flow velocity ($cm^3 \; cm^{-2} \; min^{-1}$), k is the hydraulic conductivity ($cm \; min^{-1}$) and $\Delta P/\ell$ is the hydraulic gradient ($cm \; cm^{-1}$). Equation [1] states that the flow velocity q is directly proportional to the hydraulic gradient $\Delta P/\ell$. Deviations from Darcy's law are evident when the relation between q and $\Delta P/\ell$ is not linear.

This report covers work concerning the applicability of Darcy's law for water flow through a 50-500μ sand, Boise sandstone, and a ceramic plate of 0.1μ nominal pore diameter. An introduction to theoretical aspects of possible causes of non-Darcy behavior is presented.

PART I. EXPERIMENTAL.

SAND AND SANDSTONE:

Flow measurements were made on a column of 50-500μ sand, 20.4 cm long and 38.4 cm^2 cross-sectional area. Gradients ranging from 0.09

to 1.21 cm cm^{-1} were imposed on the column. Plots of flow velocity versus gradient are shown in Figure 1 for three temperatures. The relation between q and $\Delta P/\ell$ is linear, indicating no deviations from Darcy's law for this material.

A block of Boise sandstone, 8.8 cm long and 25.5 cm^2 in area was sealed on all sides. Gradients ranging from 0.3 to 3.15 cm cm^{-1} were imposed. Plots of flow velocity versus gradient at three temperatures are shown in Figure 2. No deviations from Darcy's law are evident.

For both materials the temperature dependence of the conductivity could be attributed to the temperature dependence of the viscosity of water.

CERAMIC PLATES:

Deryagin and Krylov (2) reported that water flow through ceramic filters with pores of 0.1μ diameter was not viscous but more nearly plastic, the flow rate being nonproportional to the pressure gradient. Their results have been cited as evidence of threshold gradients and non-Darcy behavior for flow of water through the fine pores (3, 4, 6, 7). Some proposed explanations of these anomalies are the interaction of water with the pore wall which causes an increase in viscosity of the fluid near the wall; slippage along the wall; and streaming potentials. Low (5) proposed that water near a charged surface has a "quasi-crystalline" structure that extends some distance from the wall. Miller and Low (6) attributed the threshold gradients they observed for water flow through clay plugs to quasi-crystalline water structure. Henniker (4) calculated that the thickness of the structured water would need to be 190 Å to account for the anomalies reported by Deryagin and Krylov and showed that slippage was not likely, but streaming potential was possible. In this report, data are presented which show that dissolution of the ceramic creates an osmotic force that can cause anomalous flow in porous ceramics. This effect may explain the results of Deryagin and Krylov.

The experimental apparatus diagramed in Figure 3 is a simple falling head permeameter so constructed that flow measurements can be made from left to right or right to left. The apparatus consists of

a 25-cm diameter, 0.61-cm thick ceramic plate (a) with nominal pore size of 0.1μ, cemented with epoxy (e) between two glass funnels (L, R). In the neck of each funnel an inlet tube (b), an outlet tube (d) and a bracing rod (c) are cemented. The standpipe (f) is a calibrated capillary tube of 0.0157-cm^2 cross-sectional area. The reservoir (g) is of very large cross-sectional area compared to the tube (f). The rod (c) is necessary to reduce plate deflection caused by imposed pressure differences. Initially, the plate was saturated with de-aired, distilled water, and all air removed from the system. The entire system was encased in insulation and located in a controlled temperature room.

To make a measurement, water is drawn up in the tube (f) to a height h_i. The stopcocks are turned for the desired direction of flow at time 0. Immediately upon initiation of flow, the height of water in tube (f) drops due to plate deflection. Readings of h versus time are taken. The first few readings are used to find h at time 0 by extrapolation. The value h_o is the height of water applied to the plate after deflection has occurred. The volume change due to plate deflection is $(h_i - h_o)$ a, where a is the cross-sectional area of the measuring tube (f). Plots of $(h_i - h_o)$ a versus h_o are linear with a slope b. The flow volume Q passing through the plate is the amount measured by the tube plus the amount displaced by the plate as it returns to its original position. Mathematically, $Q = a(h_o - h) - bh$. The hydraulic gradient is h/ℓ (ℓ the plate thickness). If osmotic or other forces cause water to flow independently of hydraulic pressure, the gradient is modified by a factor β. The equation that describes flow in this system when β is constant is

$$(a + b)\frac{dh}{dt} = \frac{kA}{\ell}(h + \beta) \qquad [2]$$

where k is the conductivity of the plate, A its cross-sectional area, and t the time.

Integrating [2] gives

$$\ln\left(\frac{h + \beta}{h_o + \beta}\right) = -\frac{kA}{(a + b)\ell}t. \qquad [3]$$

A plot of $\ln(h/h_o)$ versus t will be linear only if $\beta = 0$. For $\beta \neq 0$, $\ln(h/h_o)$ versus t is plotted and the deviation from linearity noted. Successive values of β are chosen until a plot of $\ln[(h + \beta)/(h_o + \beta)]$ versus t is linear. The slope of the linear plot is $kA/(a + b)\ell$, from which the conductivity can be calculated. If β is not constant, a linear relation will not obtain.

Factors that could cause β to be nonzero are: slippage along the pore wall, streaming potential, threshold gradient, and osmotic effects. The first two would be velocity dependent, would always oppose flow, and would result in a nonlinear relation because β would not be constant. Furthermore, the greatest deviation would occur at the start of the flow process when the velocity was greatest. Velocity dependent effects should be evident if the selected value of β does not result in a linear relation as given by equation [3], and the selected value of β varies with different initial heads h_o. Threshold and osmotic gradients should give a constant value of β and be independent of the initial head. Only osmotic effects can cause β to be positive because they can both assist or resist hydraulic flow depending on the relative directions, whereas the other effects discussed here can only resist flow.

Figure 4 shows typical pairs of runs ($L \rightarrow R$ and $R \rightarrow L$ at the same h_o) for three temperatures. Both positive and negative values of β were obtained, indicating the presence of osmotic effects and possibly a threshold gradient. The linearity of the $\log[(h + \beta)/(h_o + \beta)]$ plots (open symbols) indicates that velocity dependent effects are negligible.

Assuming that β is composed only of osmotic effects and a threshold gradient, then $\beta = -\psi \pm \pi$ where ψ is a threshold head and π is an osmotic head (gradients are obtained by dividing by the plate thickness ℓ). Since β and π have the same sign, ψ and π can be estimated by solving simultaneous equations obtained from pairs of runs ($L \rightarrow R$ and $R \rightarrow L$) at the same initial head. A comparison of $|\beta|$ for several pairs of runs indicated that ψ would be small, if present. Therefore, only data for small values of β were used to calculate ψ and π. Results of the calculations for twelve pairs of runs are given in Table 1. In two

cases the values of ψ and π are nearly equal. In most cases π is greater than ψ by a factor of 2 or more. In three cases the calculated ψ is negative - a physical impossibility - indicating that ψ, if present, is too small to be accurately measured with this technique. There is no obvious relation between the initial head h_o and ψ and π (hence β), which is additional evidence that velocity dependent effects were negligible.

Additional and more conclusive evidence of the presence of osmotic effects is given in Table 2. After completion of the initial runs (A, Table 2), 3 liters of distilled water was flushed through side R, followed by flushing of both L and R as given in C, Table 2. Electrical conductivity of water samples taken from L and R before and after flushing indicated a concentration difference of 1.25×10^{-4}, 1.6×10^{-5}, and 1.3×10^{-5} mole liter^{-1} for A, B, C, respectively. The calculated values of π along with the direction of osmotic flow are given in Table 2.

Although the values of π calculated from van't Hoff's equation are qualitative, they are in the range of measured β values and the direction of osmotic flow is the same as obtained from the hydraulic flow measurements. Chemical analysis of water samples indicated that the solute was Na and K silicate. Apparently the dilute solution of silicate resulted from dissolution of the ceramic plate, with the concentration in the two sides of the plate being slightly different.

After evaluating β for each run, the hydraulic conductivity k of the ceramic plate was calculated from the slope of the log $[(h + \beta)/(h_o + \beta)]$ versus t plots (accounting for the change from common to naperian logarithms). Permeabilities P were calculated using the relation $P = K\eta/\rho g$, where η is the viscosity of bulk water, ρ is the density of bulk water, and g is the gravitational constant. Conductivity and permeability data are given in Table 3. The permeabilities are constant with temperature. For this system the viscosity of water flowing through 0.1μ pores has the same temperature dependence as bulk water. This suggests no anomalous viscosity effect in 0.1μ pores.

It is concluded that anomalous flow of water through porous ceramic filters is essentially due to osmotic effects and not due to anomalous viscosity or plastic flow as has been previously reported. When osmotic effects are accounted for, the flow rate is proportional to the pressure gradient and in accord with Darcy's law.

REFERENCES:

(1) Chinard, F. P., and Enns, T.
1956. Osmotic pressure. Science 124: 472-474.

(2) Deryagin, B. V., and Krylov, N. A.
1944. Anomalous phenomena in the flow of liquids through fine pores of rigid filters. Conference on Viscosity of Liquids and Colloid Solutions, Proc. (Akad. Nauk, S.S.S.R., Moscow) 2: 52-53.

(3) Henniker, J.C.
1949. The depth of the surface zone of a liquid. Rev. Mod. Phys. 21: 322-341.

(4) Henniker, J. C.
1952. Retardation of flow in narrow capillaries. Jour. Colloid Sci. 7: 443-446.

(5) Low, P. F.
1960. Viscosity of water in clay systems. Eighth National Conference on Clays and Clay Minerals. pp. 170-181. New York.

(6) Miller, R. J., and Low, P. F.
1963. Threshold gradient for water flow in clay systems. Soil Sci. Soc. Amer. Proc. 27: 605-609.

(7) Swartzendruber, D.
1962. Modification of Darcy's law for the flow of water in soils. Soil Sci. 93: 22-29.

PERSONNEL: Ray D. Jackson

Table 1. Osmotic and threshold heads calculated from pairs of runs at the given initial head. Heads may be changed to gradients by dividing by ℓ (0.61 cm).

Temperature (^{o}C)	Initial head (h_o) (cm H_2O)	Osmotic head (π) (cm H_2O)	Threshold head (ψ) (cm H_2O)
9.7	5.4	0.10	0.11
	9.2	0.27	0.15
	10.0	0.29	0.11
	14.5	0.12	0.13
19.7	8.5	0.24	0.09
	9.4	0.52	0.12
	14.0	0.17	-0.01
	24.5	0.53	0.11
29.5	9.1	0.17	-0.07
	9.5	0.20	0
	14.0	0.16	0.06
	15.1	0.10	-0.10

Table 2. Values of β for three concentration differences across ceramic plates all at 19.7 C. Positive values of β indicate direction of osmotic flow. The values of π were calculated using van't Hoff's equation for osmotic pressure (1) using concentrations obtained by electrical conductivity measurements. Osmotic flow direction shown is from lower to higher concentration.

	β (cm) water flow direction		π (cm)
	L → R	R → L	
A. Initial runs.			
	4.75	-4.20	4.5 L → R
	3.16	-5.20	
	3.48	-3.03	
B. Side R diluted by flushing with 3 liters distilled water.			
	-0.64	0.40	0.6 R → L
	-0.63	0.42	
C. 1 1/2 liters flushed through side L and 1/2 liter through side R.			
	-0.16	0.18	0.4 R → L
	-0.33	0.15	

Table 3. Conductivity and permeability data at three temperatures. The 95% confidence limits are given for the conductivity data.

Temperature (^{o} C)	Number of runs	Conductivity (cm $min^{-1} \times 10^{7}$)	Permeability ($cm^{2} \times 10^{14}$)
9.7	8	2.23 $\pm$ 0.02	5.07
19.7	16	2.88 $\pm$ 0.05	5.06
29.5	8	3.68 $\pm$ 0.04	5.09

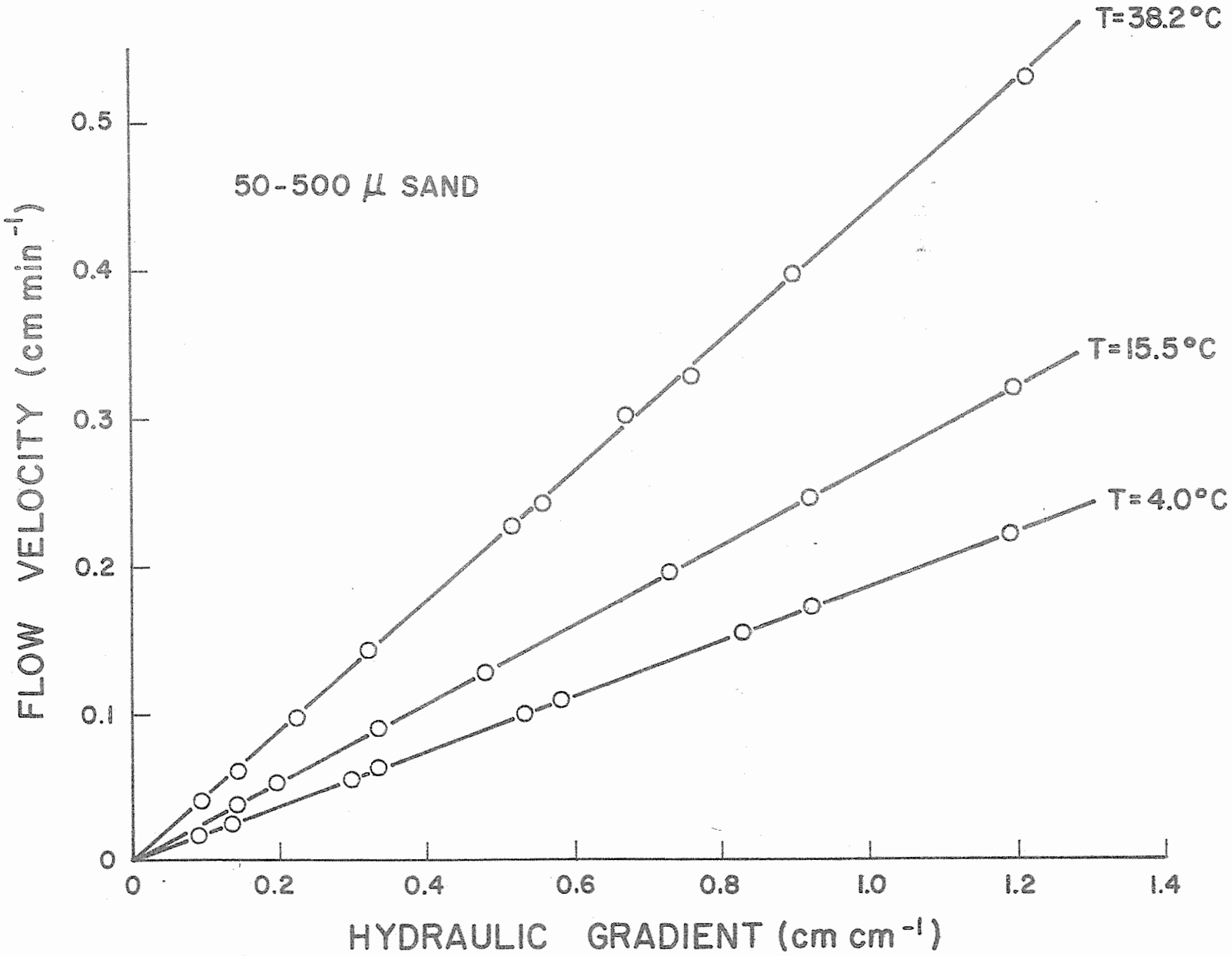

Figure 1. Flow velocity versus hydraulic gradient for 50-500μ sand.

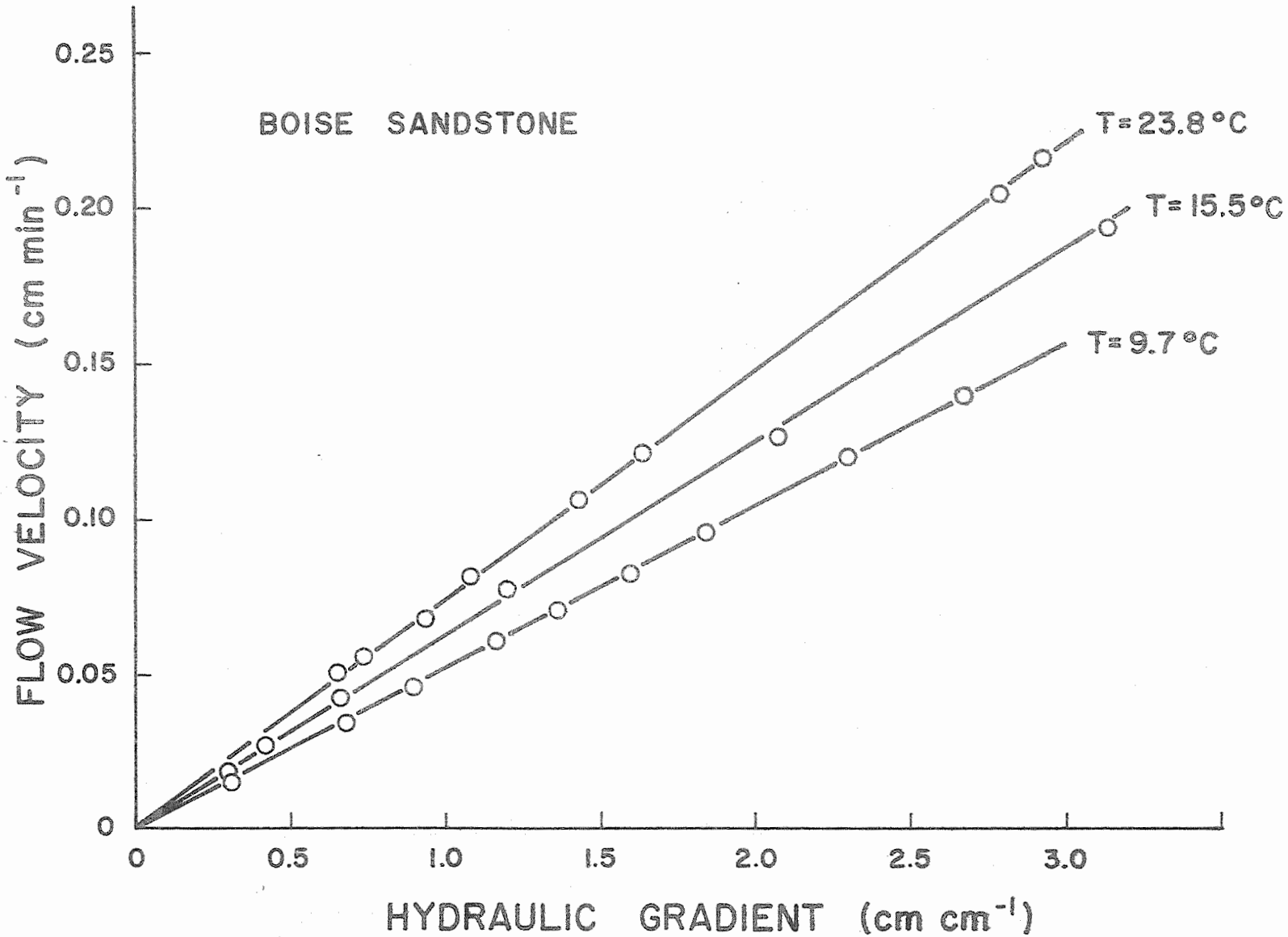

Figure 2. Flow velocity versus hydraulic gradient for Boise sandstone.

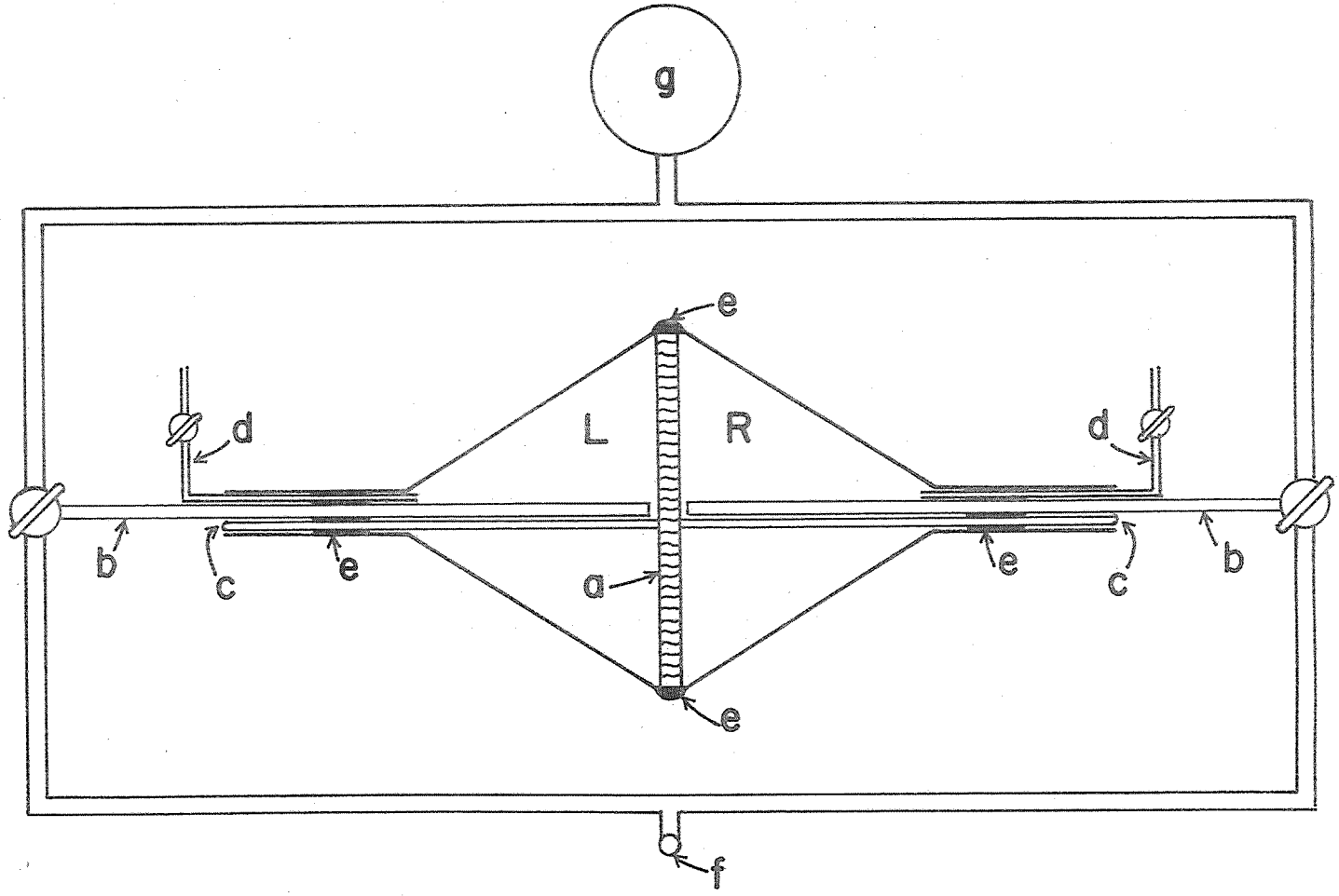

Figure 3. Diagram of measurement apparatus.

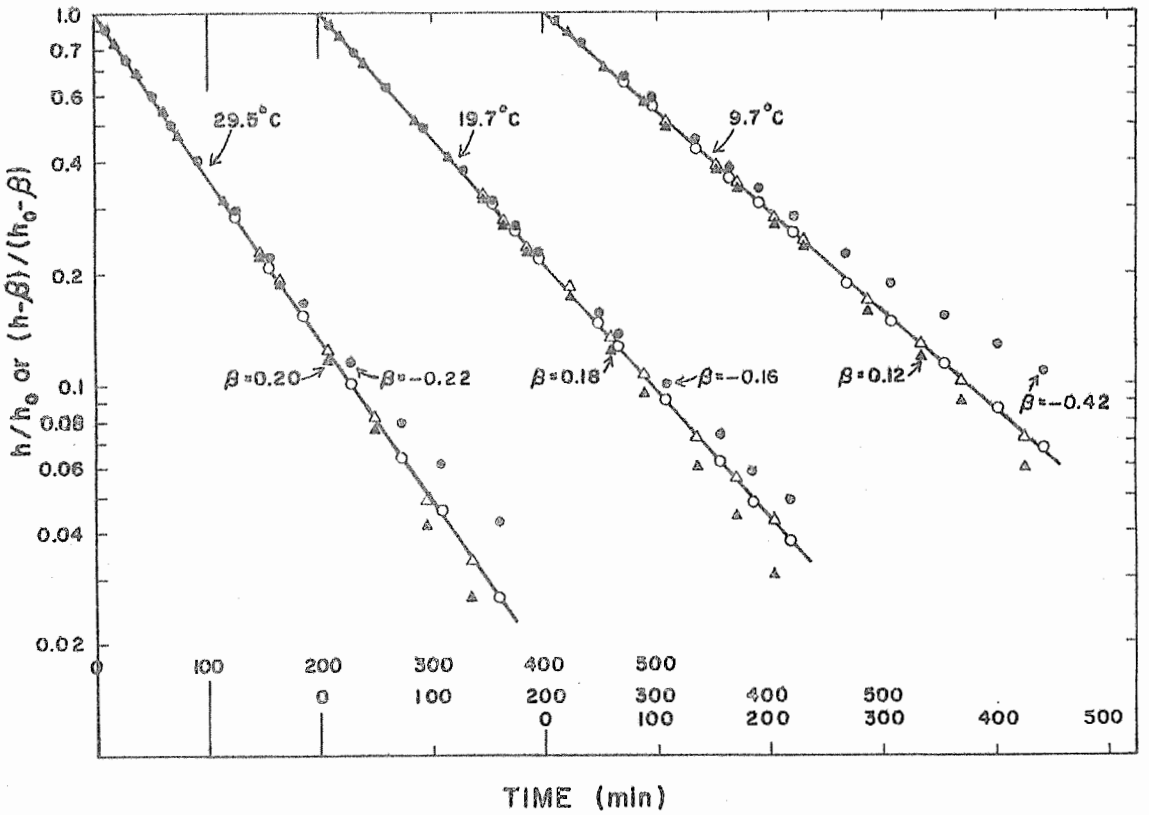

Figure 4. Typical data for paired runs at 3 temperatures.

PART II. THEORETICAL ASPECTS.

Although the experimental results reported above indicate no deviation from Darcy's law it is of interest to examine theoretically some possible causes of deviations reported elsewhere.

The causes of non-proportionality between flow volume and gradient are not clear. Clay-water interaction is frequently mentioned as a probable cause. It has been shown that water near a clay surface has a higher viscosity than water some distance from the clay surface. The higher viscosity occurs because of the orientation of, and the attraction for, the dipolar water molecules by the electrical charges on the clay surfaces. It has been postulated that this "quasi-crystalline" water structure does not flow as bulk water but requires an initial or threshold gradient to initiate flow. Furthermore, the water influenced by the clay surface may be non-Newtonian (shear-rate dependent) which, as will be discussed later, can cause non-proportionality between flow velocity and hydraulic gradient. However, the non-Newtonian concept may not hold for this case because this effect will persist longest in the central axial portion of a pore, contrary to the concept of the greatest effect being near the wall. Another concept is that the water layers near the surface are immobile and the remaining fluid Newtonian. As the gradient increases, the thickness of the immobile layers is reduced causing an increase in the effective cross section and hence an increase in flow volume with an increase in hydraulic gradient.

We begin the theoretical development with the general equations of motion and make the usual assumptions to obtain the Navier-Stokes equations, with the exception that the shear stress components are not yet resolved in terms of viscosity and velocity gradients. For steady laminar flow of an imcompressible fluid through a cylindrical tube, the Navier-Stokes equations reduce to

$$F_z - \frac{\partial p}{\partial z} + \frac{1}{r}\frac{\partial(\tau r)}{\partial r} = 0 \qquad [4]$$

where F_z is the component of all body forces acting in the z or axial

direction, p is the fluid pressure, r is the radial direction from the center of the cylinder, and τ is the shear stress.

In general, the equations of motion are obtained by considering all body and surface forces acting on a fluid element. Body forces are regarded as given external forces that permeate completely through the medium. An example is the gravitational or magnetic fields, but the force fields caused by charges on particle surfaces cannot be considered body forces because they are a decreasing function of distance from the particle surface, and may affect only a small portion of the fluid. The forces caused by particle surface charges must therefore appear in the shear stress τ, a surface force.

Surface forces depend on the state of strain (the velocity field) of the fluid. These forces can be expressed in terms of normal and shear stresses. The negative of the arithmetic mean of the normal stress is the fluid pressure. It is, therefore, the shear stress components that can be influenced by factors such as the charges on the pore wall and the effect of ions in solution on the flow properties of the fluid.

Newton, in 1687, proposed that the shear stress is directly proportional to the velocity gradient. That is

$$\tau = \eta \frac{\partial v}{\partial r} \qquad [5]$$

where η is the fluid viscosity and v the fluid velocity. For η a constant, equation [5] is Newton's law of viscosity and forms the basis for the definition of Newtonian and non-Newtonian fluids. In general η may be a function of v, r, or both. A fluid that exhibits a functional relationship between η and v is called non-Newtonian. A fluid with η a constant is Newtonian. In certain cases η may be a function of r with the fluid exhibiting Newtonian properties.

In the following discussion, several forms of η are considered. These relationships can be demonstrated by simplifying equation [4] by integrating and solving for τ, and then using several forms of variable viscosity to determine their flow rate, gradient relationships.

When gravity is the only body force and the tube is horizontal $F_z = 0$. For this discussion the pressure gradient is constant, consequently, let $\Delta p/\ell = \partial p/\partial z$, where ℓ is the length of the tube. Under these conditions equation [4] is integrated to obtain

$$\frac{r\Delta p}{2\ell} = \tau \qquad [6]$$

The constant of integration is 0 since $\tau = 0$ when $r = 0$.

Viscosity Constant. For η a constant, substitute equation [5] into equation [6] and integrate to obtain

$$v_{(r)} = -\frac{\Delta p\ (R^2 - r^2)}{4\eta\ell} \qquad [7]$$

where R is the radius of the capillary tube.

Now the average velocity $\bar{v}$ is

$$\bar{v} = \frac{-1}{\pi R^2} \int_0^R v_{(r)}\ 2\pi r dr \qquad [8]$$

and the volume of flow per unit time Q is

$$Q = \bar{v}\pi R^2 = \frac{\pi\Delta p}{2\eta\ell} \int_0^R (R^2 - r^2)\ rdr$$

$$= \frac{\pi\Delta p R^2}{8\eta\ell} \qquad [9]$$

Equation [9] is known as Poiseuille's equation. The flow velocity v and the volume Q is directly proportional to the hydraulic gradient $\Delta p/\ell$.

Viscosity a Function Radial Distance. For capillary tubes having surface charges on the walls there is considerable evidence that these charges interact with molecules of a polar liquid. This interaction can cause the shear stress in the liquid within the distance influenced by the charges to be greater than in bulk fluid. The influence of the charges decreases with distance from the wall. For a pure polar liquid flowing through the tube, a molecule always at a

fixed distance from the wall would have the same force exerted on it regardless of its velocity. For this condition the viscosity can be considered a function of radial distance with equation [5] becoming

$$\tau = \eta_{(r)} \frac{\partial v}{\partial r} \qquad [10]$$

Substituting [10] in [6] gives

$$\frac{r\Delta p}{2\ell} = \eta_{(r)} \frac{\partial v}{\partial r} \qquad [11]$$

Integrating [11] yields

$$v_{(r)} = \frac{\Delta p}{2\ell} \int_o^r \frac{r}{\eta_{(r)}} \, \partial r \qquad [12]$$

and

$$Q = \frac{\pi\Delta p}{\ell} \int_o^R r \int_o^r \frac{r}{\eta_{(r)}} \, \partial r \, \partial r \qquad [13]$$

to complete the integration the functional relationship between η and r must be known. For present purposes it is sufficient to note that the flow volume Q is directly proportional to the hydraulic gradient $\Delta p/\ell$ regardless of the functional dependence of the viscosity in the radial direction.

Bingham Bodies. There is a certain class of materials that will not flow until subjected to a yield stress ψ. The yield stress is sometimes referred to as a "threshold gradient." When the applied stress exceeds the yield stress, the material flows and the velocity gradient-shear stress relation becomes linear. Materials possessing these properties are called Bingham bodies. The rheological equation is

$$\tau = \psi + \eta_{pl} \, \partial v/\partial r \qquad [14]$$

where η_{pl} is the plastic viscosity.

Using [14] in [6] and integrating, we have

$$v = -\frac{1}{\eta_{p1}}\left[\frac{(R^2 - r^2)\,\Delta p}{4\ell} - \psi(R - r)\right] \qquad [15]$$

In a viscous liquid the shearing stress τ is zero at the axis and increases with distance from it. Around the axis there will be a cylinder of material with $\tau < \psi$. The stresses in this cylinder will be purely elastic, and the cylinder will move as a solid plug. If r_o is the radius of the cylinder for which $\psi = \tau$, then from equation [3] we obtain

$$\psi = r_o\,\Delta p/2\ell \qquad [16]$$

The velocity of the plug is

$$v_o = \frac{\Delta p}{4\ell\eta_{p1}}(R - r_o)^2 \qquad [17]$$

and the volume of flow is

$$Q = \frac{\pi R^4 \Delta p}{8\ell\eta_{p1}}\left[1 - \frac{8}{3}\frac{\psi\ell}{R\Delta p} + \frac{16}{3}\left(\frac{\psi\ell}{R\Delta p}\right)^4\right] \qquad [18]$$

which is known as the Buckingham-Reiner equation. It is obvious that the flow volume Q is not proportional to the gradient $\Delta p/\ell$.

<u>Yield Stress a Function of Radial Distance</u>. If charges on pore walls structure the water near the wall to the degree that a yield stress is required to initiate flow, then the yield stress will be a function of radial distance. This concept circumvents the difficulty encountered when plug flow (Bingham flow-yield stress across entire pore area) is considered. With plug flow the flow begins near the wall. This is difficult to imagine when the evidence for water structure near the wall is considered.

Assuming that $\psi = 0$ for $0 \leq r < a$, where $a < R$, and $\psi = \psi_{(r)}$ for $a < r \leq R$, then

$$\frac{r\Delta p}{2\ell} = \eta\frac{\partial v}{\partial r} \qquad 0 \leq r < a$$

and

$$\frac{r\Delta p}{2\ell} = \psi_{(r)} + \eta \frac{\partial v}{\partial r} \qquad a < r \leq R \qquad [19]$$

Solving for the average velocity in the two regions and then adding the total flow volumes yields

$$Q = \frac{2}{\eta}\left[-\frac{\Delta p R^4}{16\ell} + \frac{R^2}{2}\int_a^R \psi_{(r)}\,\partial r - \int_a^R r \int_a^r \psi_{(r)}\,\partial r\,\partial r\right] \qquad [20]$$

Equation [20] allows the calculation of Q for any $\psi_{(r)}$ that increases as $r \rightarrow R$, providing $\psi = 0$ at $r = 0$. If $\psi \neq 0$ at the axis, plug flow results and the analysis leading to equation [20] is not correct.

Calculations of assumed values of $\psi_{(r)}$ and $\eta_{(r)}$ using the above equations, plus further development of theory should yield some answers concerning causes of non-Darcy behavior and may form a basis for predicting its occurence.

PERSONNEL: R. D. Jackson

TITLE: FIELD APPLICATION OF FALLING-HEAD TECHNIQUES FOR SEEPAGE METER AND DOUBLE-TUBE METHOD FOR HYDRAULIC CONDUCTIVITY MEASUREMENTS

LINE PROJECT: SWC VII gG1 CODE NO.: Ariz.-WCL-14

PART I. SEEPAGE STUDIES

INTRODUCTION:

Canal conditions are not always favorable for using the seepage meter technique. To obtain local measurements of the seepage under such adverse conditions, a technique was developed whereby seepage is determined from the rate of penetration of a salt wave into the bottom material after applying salt crystals to the channel bottom. When the salt crystals dissolve, part of the salt enters the bottom material with the seepage flow. The depth of penetration of the salt after some time is measured with an electrical conductivity probe. Laboratory studies were performed to relate seepage rate to rate of advance of the salt wave. The amount of salt that should be applied per unit area of channel bottom to obtain an easily detectable salt wave in the bottom material was evaluated from flume studies.

PROCEDURE:

a. Column studies.

When the salt that has been placed on the bottom of the channel or reservoir is completely dissolved, regular channel or pond water will again enter the bottom material. Thus, the salt-concentration profile in the bottom material some time after the complete dissolution of the salt will have the form of a wave. If the amount of salt applied is such that the crystals disappear in a relatively short period (approximately 5 minutes), the wave will have a well-defined peak. The electrical conductivity is measured with a specially designed conductivity probe (Figure 1) using a portable resistance meter. The electrodes, consisting of the brass point and the brass ring, are separated by a 0.1" ring of phenolic resin. The meter (Irrigage, Rayturn Corp., Portland, Oregon) was modified to obtain greater resolution in the range of conductivity values encountered with the technique. The results of the conductivity measurements

are expressed in meter readings, which range from 0 to 200 (full scale). The reading of 200 was essentially obtained with the probe in a saturated NaCl solution.

The rate of advance of the peak of the salt wave (V_s) will be greater than the gross seepage rate (I_s) because of the solid matrix in the bottom material. If true piston flow occurs, $I_s = n V_s$ where n is the porosity of the soil expressed as a volume fraction. To determine the ratio between I_s and V_s, column studies were set up whereby I_s and V_s were determined for different soils (sand, Laveen loam, Adelanto loam, and pine silty clay) and different seepage rates. The columns were packed in 7-cm ID plexiglas cylinders and "saturated" from the bottom. Using tap water, a certain seepage rate was established and maintained. To create a salt wave, the water above the column was temporarily replaced by a saturated solution of NaCl or $CaCl_2$. After 10 ml of the salt solution had entered the column, the solution above the column was replaced by tap water. The outflow at the bottom of the column was then measured in relation to time. After 50 to 70 ml had been collected, the conductivity probe was inserted into the column and readings were taken as rapidly as possible at 0.5-cm increments. Thus, the entire form of the salt wave was measured. After completion of the tests, the density of the soil in the column was determined. The resulting value of n was then compared with I_s/V_s.

The column studies were performed using both NaCl and $CaCl_2$, except for the Pine silty clay where only $CaCl_2$ was used. Comparisons between the flow rate in the columns before and after application of the salt showed excellent agreement for all soils. The use of NaCl (in large-crystal form if it is to be used in flowing channels) will be satisfactory for sandy and gravelly bottom materials. For soils containing clay, however, the Na-ion may cause reduction in the hydraulic conductivity, particularly at the receding end of the wave where the salt concentrations become relatively low. In that case, $CaCl_2$ should be preferred.

b. Flume studies.

In applying the salt penetration technique to the field measurement of seepage in flowing channels, the question arises of how much salt should be applied per unit wetted area to obtain a well-defined, readily-detectable salt wave in the bottom material. It can be expected that this amount depends on the velocity in the channel and on the seepage rate. To determine desired rates of salt application, studies were made in a rectangular flume, 9 m long, 0.6 m wide, and 0.5 m deep. For a 2.4-m section of the flume, the plywood bottom was 0.6 m lower than for the rest of the flume. This section was filled with sand so that the surface of the sand would be flush with the bottom of the flume. A drain was placed in the bottom of the box. By controlling the water level at the drain outlet, different seepage rates could be maintained.

The salt used in the flume studies was rock salt (NaCl) with crystals of about 5 mm diameter. The salt was applied in a band across the upstream portion of the sand bottom at different amounts per unit area. When the depth of salt penetration was expected to have reached a value of approximately 10 cm, the electrical-conductivity probe was inserted to measure the depth of the peak of the salt wave. This was done at a number of points in the area where the salt was applied and at various distances downstream from that area. Measurements were obtained for different seepage rates and different velocities of water in the flume. The water depth in the flume during these studies was held constant at approximately

0.3 m. The results were analyzed to evaluate the amounts of salt necessary to obtain a maximum difference in meter reading between the electrical conductivity of the bottom material prior to application of the salt (referred to as "background") and the electrical conductivity at the peak of the salt wave in the bottom. The length of time that salt should be present on the bottom to obtain a well-defined peak was also determined.

c. Field studies.

A field test of the salt-penetration technique was performed on a small reservoir of approximately 40 x 40 m near Peoria, Arizona. The water depth was approximately 0.3 m and the bottom material consisted of a loam. At ten locations, randomly selected but fairly evenly distributed over the pond bottom, approximately 1 m^2 of bottom area was covered with about 3 kg $CaCl_2$. Approximately 3 to 5 hrs after the application of the salt, the conductivity probe was inserted at 10 to 15 points in each area of salt application to measure the depth of penetration of the peak of the salt wave. At 4 locations, bottom-soil samples were collected to determine the density for calculation of n. During the 5-hour period of salt penetration, periodic measurements of the water level in the pond were made so that the average rate of seepage obtained with the salt penetration technique could be compared with the rate of fall of the water level in the pond.

RESULTS AND DISCUSSION:

a. Column studies.

A typical example of a conductivity wave due to the penetration of salt is shown in Figure 2 (solid line), which applies to a column

of Adelanto loam after application of $CaCl_2$. The curve in Figure 2 has a well-defined peak. If the salt had been applied for a longer period of time, a flatter peak would have been obtained (Curve A). Under continuous salt application, a conductivity profile such as Curve B in Figure 2 will result. Where the conductivity profile exhibits a plateau, such as Curves A and B in Figure 2, the lower point of the plateau should be taken as the location of the peak. Dividing the depth of the peak conductivity by the time between salt application and insertion of the probe yields the average rate of advance of the peak. Plotting the seepage rate against the velocity of the salt wave for different seepage rates yielded graphs such as Figure 3. Similar plots were obtained for the other soils and salts used in the column studies. The slope I_s/V_s of the straight line in each plot appeared to agree very well with n, as shown in Table 1. This indicates that the advance of the salt peak can be considered as a process of piston flow, and that knowledge of the porosity of the soil suffices to calculate I_s from V_s.

b. Flume studies.

An example of the relationship between the peak-minus-background conductivity readings and the rate of salt application is shown in Figure 4, which applies to three different seepage rates (on the curves) and a constant velocity in the channel of 0.2 m/sec. This graph shows, that for a velocity of 0.2 m/sec, the minimum amount of rock salt to obtain maximum conductivity readings at the peak of the salt wave ranges from about 1 kg/m^2 for a seepage rate of 1.5 m/day

to about 1.5 kg/m^2 for a seepage rate of 0.15 m/day. From similarly obtained data for other channel velocities, Figure 5 was constructed. As expected, the minimum rate of salt application for maximum peak conductivity readings increases with increasing velocity in the channel and with decreasing seepage rates. As a general rule, it was found that enough salt should be applied to form a continuous layer on the bottom for at least 5 minutes before it is completely dissolved. Because $CaCl_2$ has a higher solubility than NaCl, the application rate for $CaCl_2$ should be 1.5 to 2 times as high as for NaCl. It was also found that the area of well-defined and easily-detectable salt waves was limited to the area covered by the salt, despite the fact that considerable amounts of dissolved salt pass over the channel bottom downstream from the area of application.

c. Field studies.

The results of the field study to compare the seepage obtained with the salt technique with the rate of fall of the water level in a small reservoir are presented in Table 2. Each column in this table applies to one of the areas of salt application in the reservoir bottom. The values in Table 2 were calculated using an n-value of 0.47 as obtained from the bulk density measurements on the bottom material. The average seepage rate obtained from the salt penetration technique is 0.30 m/day. This figure agrees very well with the rate of fall of the water surface in the same period, which was 0.29 m/day.

SUMMARY AND CONCLUSIONS:

A technique for evaluating channel or reservoir seepage from the rate of advance of a salt wave in the bottom material was developed. The salt wave is created by covering the bottom with a layer of salt crystals. For sandy or gravelly material, NaCl can be used. For soils containing clay, $CaCl_2$ or similar salt should be applied to avoid reductions in the hydraulic conductivity. As the salt dissolves, part of it enters the bottom material due to seepage. After the salt has disappeared the original water of the channel or pond again enters the bottom, so that the salt concentration profile in the bottom after some time tends to assume the form of a wave. The depth of the peak conductivity is measured with a specially constructed conductivity probe, using a portable electric conductivity meter. Dividing this depth by the time elapsed since the application of the salt yields the average velocity of the conductivity peak. Laboratory studies on columns of different soil materials indicated that the seepage rate can be calculated by multiplying the average velocity of the conductivity peak by the porosity of the soil. Thus, the advance of the salt concentration peak is essentially a process of piston flow for the depths of salt penetration considered in these studies (about 10-15 cm).

Sufficient salt should be applied to create a well-defined, easily detected electrical conductivity wave in the bottom. Studies in a hydraulic flume showed that this was achieved if the salt crystals were present on the bottom for at least 5 minutes before they had completely dissolved. For NaCl as rock salt with crystals of about 5 mm diameter, this required from 1 kg/m^2 for low velocities to 2 kg/m^2 for high velocities in the channel. Very low seepage rates may require higher rates of application.

A field study was made to compare the seepage calculated with the salt penetration technique with the rate of fall of the water level in a shallow pond of about 40 x 40 m in size in loam soil. Salt ($CaCl_2$) was applied at ten locations of about $1m^2$ each of the

bottom. At each location, 10 to 15 probe measurements were made for a total of 138 measurements. Soil samples were obtained for density determination. Based on these measurements, an average seepage rate of 0.30 m/day was calculated. The rate of fall of the water surface in the pond during the same period was 0.29 m/day. The salt penetration technique thus appears to be an accurate as well as a convenient tool for seepage measurement. Its field application is not as dependent on favorable water and bottom conditions as is the seepage meter technique.

PERSONNEL: Herman Bouwer and Robert C. Rice.

Table 1. Results of salt penetration studies in soil columns.

Soil	Salt	Number of columns	n*	I_s/V_s
Sand	NaCl	8	0.40	0.38
	$CaCl_2$	4	0.44	0.45
Laveen loam	NaCl	10	0.46	0.51
	$CaCl_2$	8	0.44	0.53
Adelanto loam	NaCl	4	0.47	0.45
	NaCl	5	0.56	0.62
	$CaCl_2$	5	0.44	0.43
Pine silty clay	$CaCl_2$	5	0.46	0.53

* average value for columns

Table 2. Seepage rates in m/day obtained with salt penetration technique in Peoria reservoir. The average values per area of salt application are listed at the bottom of the columns.

Area of salt application									
A	B	C	D	E	F	G	H	I	J
0.23	0.19	0.20	0.38	0.23	0.33	0.10	0.27	0.53	0.28
0.16	0.24	0.14	0.38	0.11	0.23	0.22	0.33	0.23	0.38
0.29	0.20	0.21	0.30	0.32	0.30	0.17	0.36	0.36	0.40
0.24	0.19	0.18	0.38	0.11	0.25	0.22	0.27	0.36	0.41
0.24	0.16	0.15	0.44	0.17	0.40	0.18	0.36	0.31	0.28
0.23	0.28	0.24	0.38	0.26	0.27	0.16	0.31	0.36	0.30
0.26	0.36	0.22	0.26	0.12	0.30	0.16	0.48	0.34	0.33
0.23	0.31	0.18	0.36	0.26	0.32	0.20	0.39	0.39	0.33
0.17	0.24	0.20	0.41	0.37	0.41	0.18	0.41	0.39	0.41
0.21	0.36	0.18	0.40	0.20	0.44	0.21	0.39	0.54	0.42
0.28	0.50	0.24	0.38	0.17	0.60	0.18	0.30		0.30
0.28	0.36	0.26	0.38	0.22	0.49	0.26	0.41		0.35
0.15		0.36	0.50	0.26	0.41	0.25	0.35		0.30
0.28		0.15	0.40			0.42	0.26		0.23
0.26		0.27	0.32			0.40	0.34		
0.33									
0.24	0.28	0.21	0.38	0.22	0.36	0.22	0.35	0.38	0.34

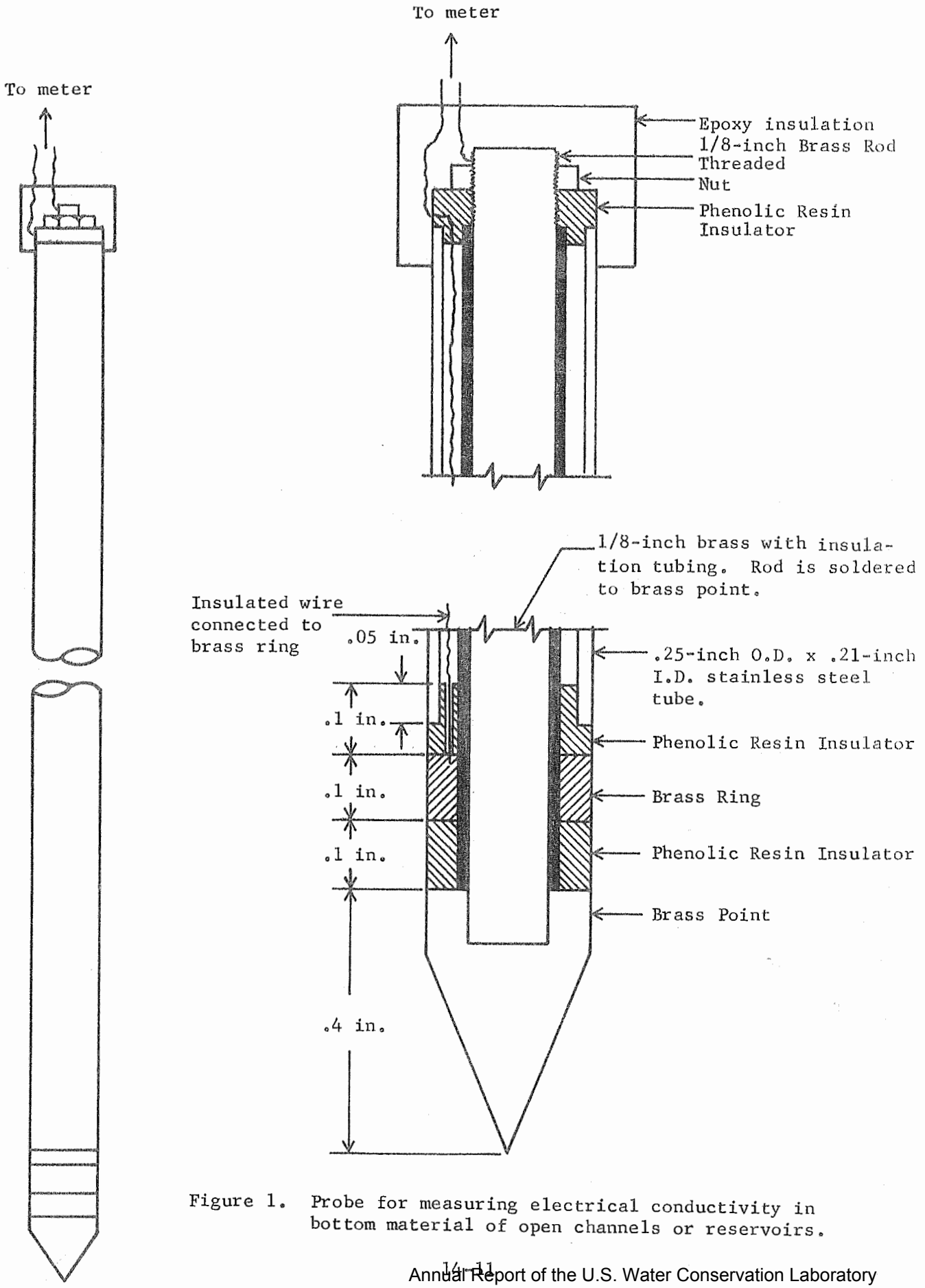

Figure 1. Probe for measuring electrical conductivity in bottom material of open channels or reservoirs.

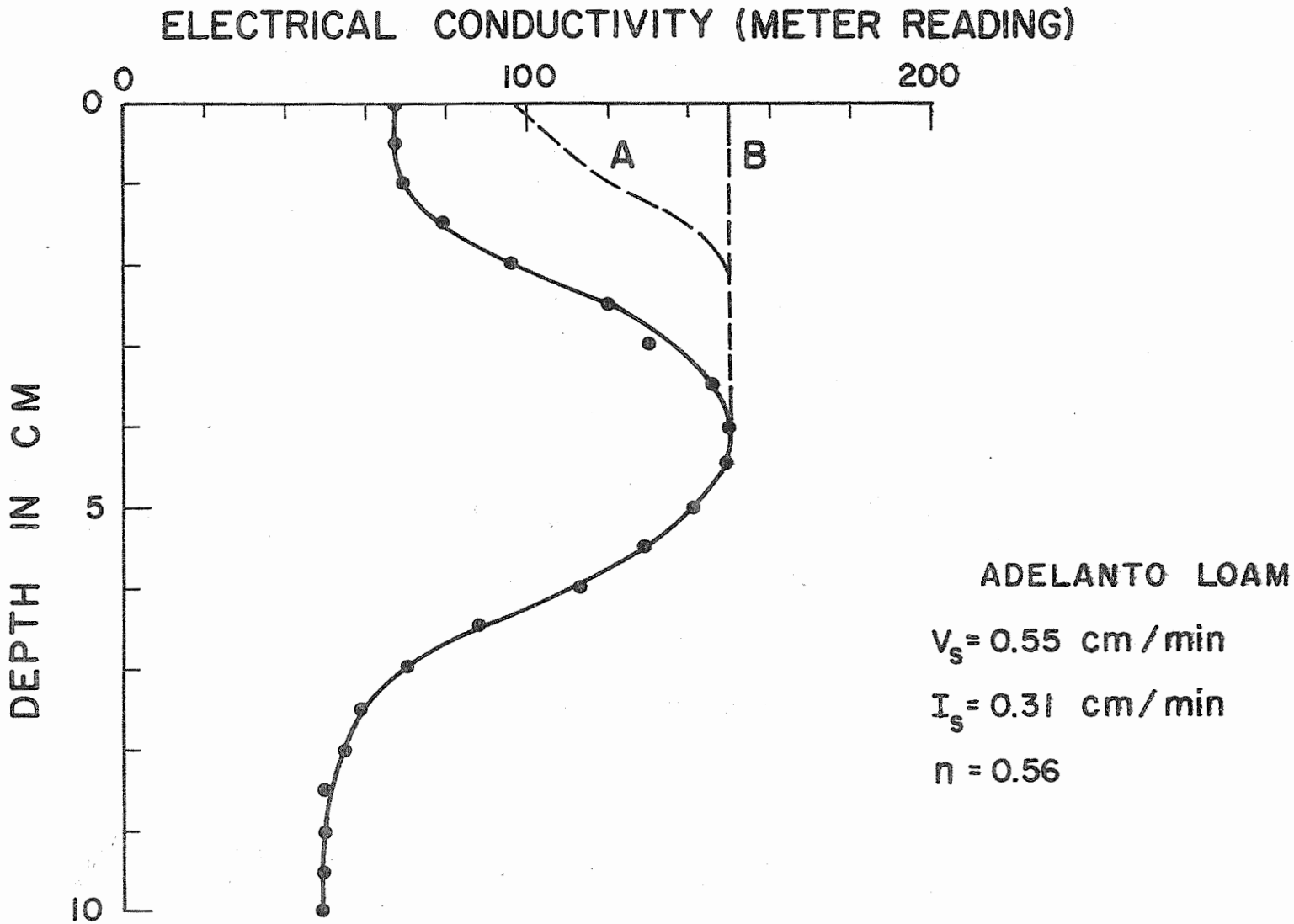

Figure 2. Electrical-conductivity profile after application of $CaCl_2$.

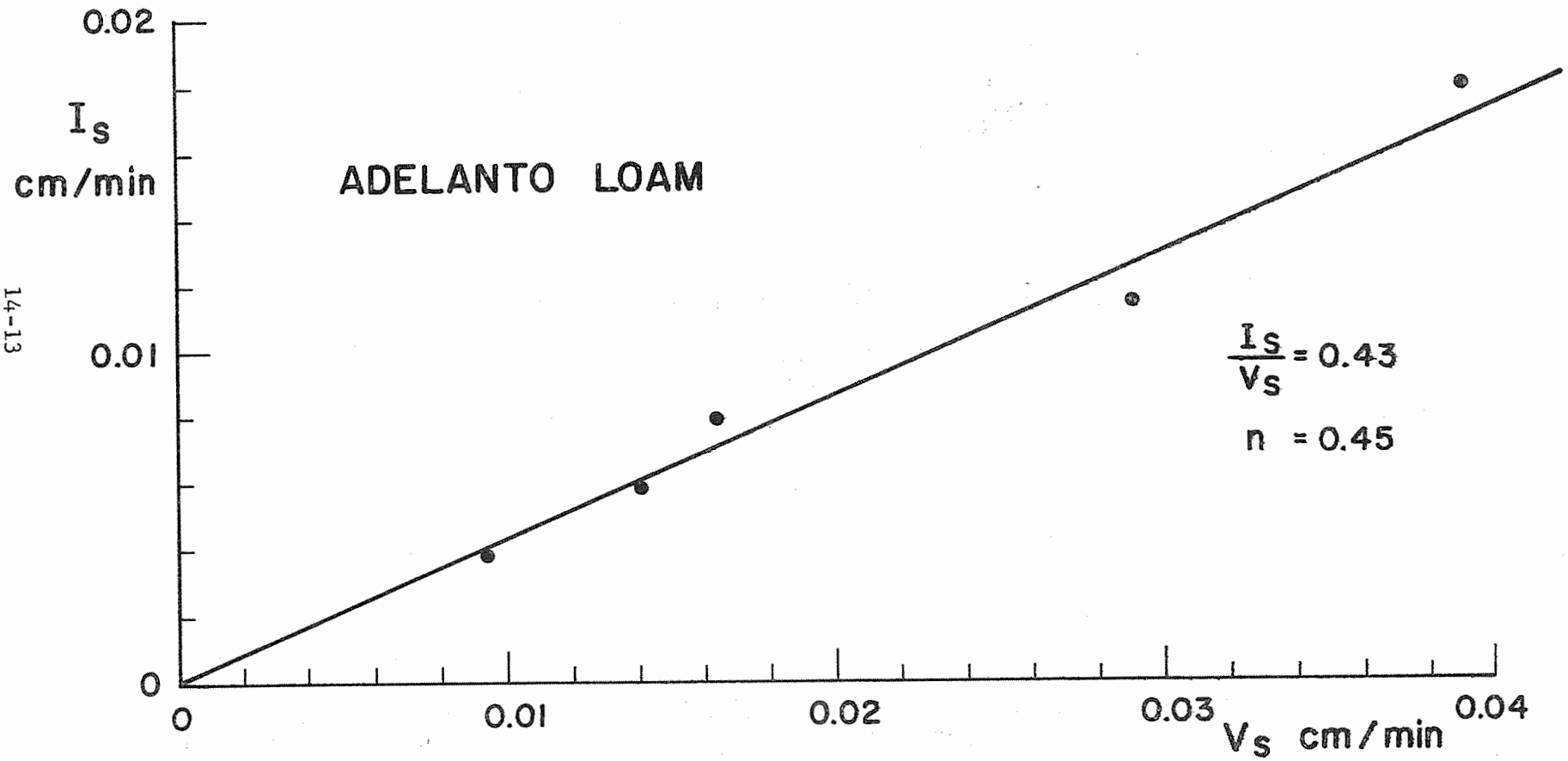

Figure 3. Graph of seepage rate versus velocity of peak of salt wave.

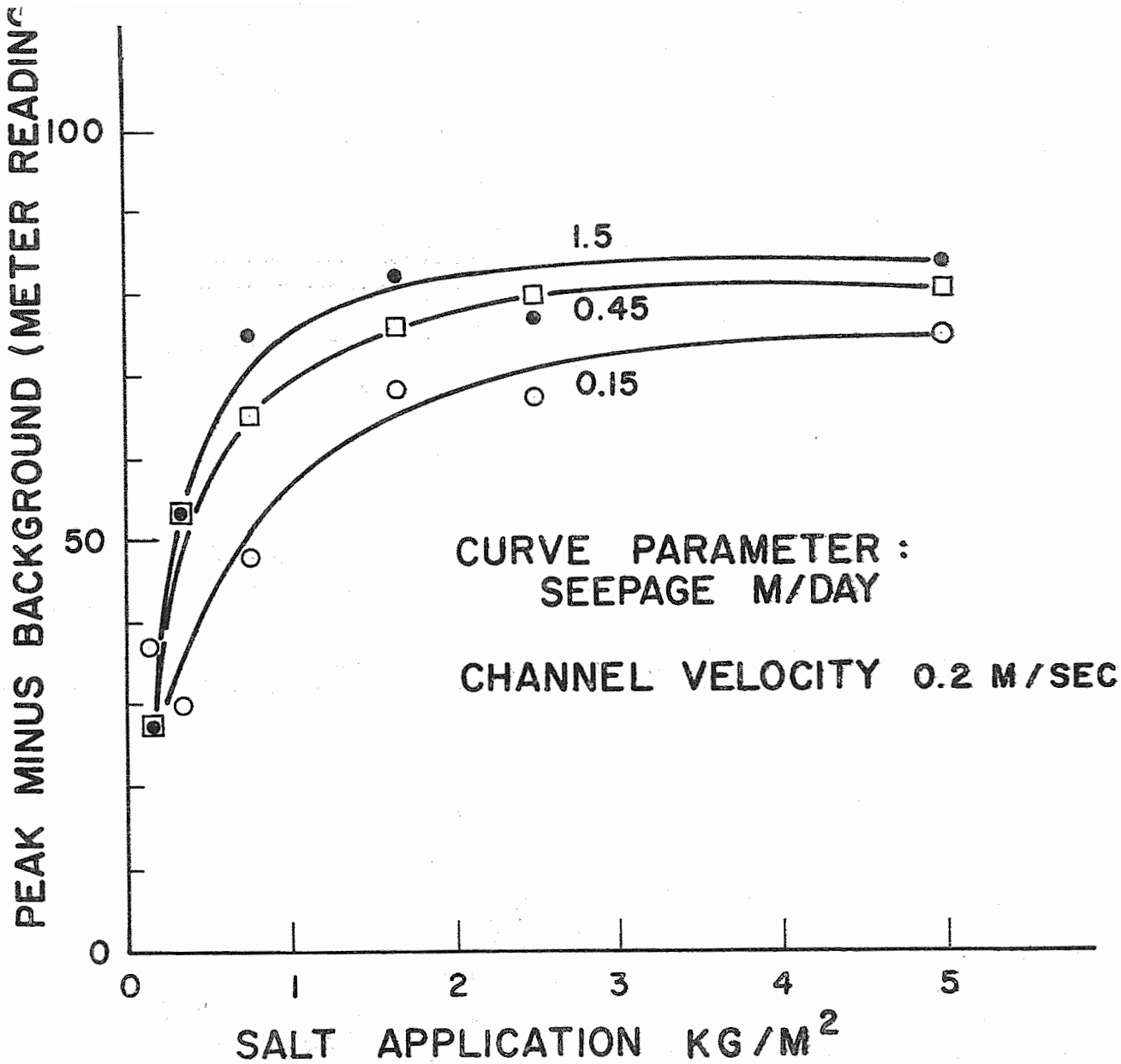

Figure 4. Graph of peak minus background conductivity reading versus rate of salt application for different seepage rates (on the curves) and a constant channel velocity.

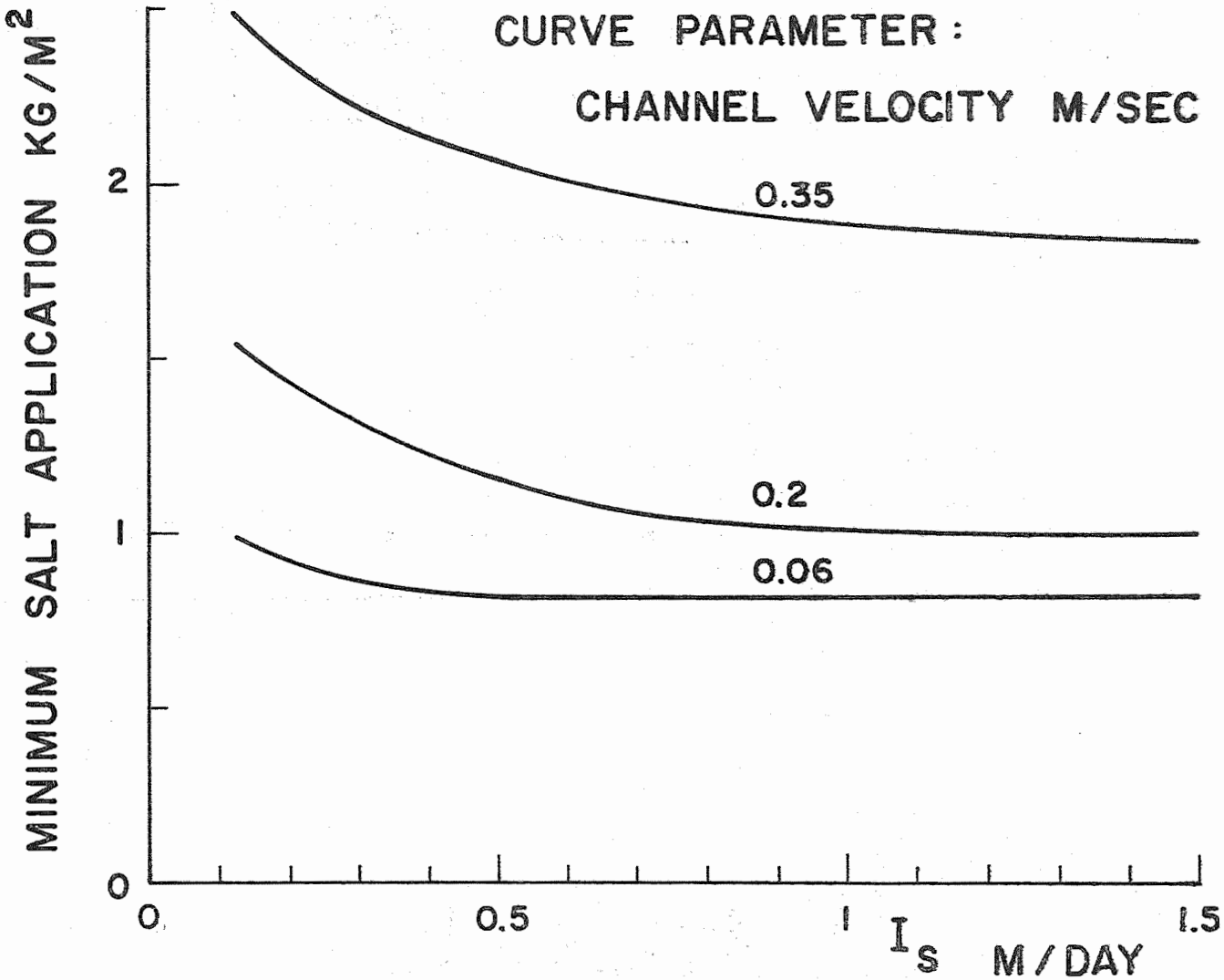

Figure 5. Minimum rate of salt application versus I_s for different channel velocities.

TITLE: FIELD APPLICATION OF FALLING-HEAD TECHNIQUES FOR SEEPAGE METER AND DOUBLE-TUBE METHOD FOR HYDRAULIC CONDUCTIVITY MEASUREMENTS

LINE PROJECT: SWC VII gG1 CODE NO.: Ariz.-WCL-14

PART II. DOUBLE-TUBE STUDIES

INTRODUCTION:

Field experience with the double-tube method over the last few years indicated that the diameter of the auger tube should be larger than the theoretical minimum because of suspected soil disturbance in the annular space between the inner and the outer tube. In view of this, studies were performed to evaluate the effect of different tube diameters on the measured values of hydraulic conductivity and to determine tube-size combinations required to eliminate most of the effects of soil disturbance.

PROCEDURE:

Values of K were obtained with an inner tube of 5 inches diameter in combination with outer tubes of 8, 10 and 12 inches diameter. Measurements were obtained in Adelanto loam and in river sand at a depth of approximately 80 cm. In addition to the value of K as determined with the double-tube method, the vertical hydraulic conductivity K_v below the inner tube was also measured, using the gradient-intake technique developed for anisotropy evaluation. The Adelanto loam was in Bermuda grass lawn and it had a well-developed structure with numerous root and worm holes. The river bed sand was only sparsely vegetated and some horizontal layering of sand of different textures could be detected. For each diameter of the outer tube, 6 replications were used for the loam and 4 for the sand. The auger holes were approximately 1 meter apart and the different sizes of the outer tube were alternated in space and in time.

In addition to studying the effect of increasing the diameter of the outer tube for a given inner tube, the effect of decreasing the diameter of the inner tube for a given outer tube was also studied. This study was included because, where double-tube equipment with the previously suggested diameters of 5 inches and 8 inches is already

available, reducing the size of the inner tube will be simpler than increasing the size of the outer tube. In this study, values of K were obtained with an inner tube of 4 inches diameter in combination with an 8-inch outer tube. The resulting values were then compared with those obtained with an inner tube of 5 inches in combination with an outer tube of 10 inches diameter, which in the light of the results from the studies described in the previous paragraph could be taken as a standard. The studies with the smaller diameter inner tube were again carried out at 80-cm depth in Adelanto loam and in river sand, using 6 replications for each soil and each combination of tube diameters.

RESULTS AND DISCUSSION:

The results of the study with the 5-inch inner tube and the 8-, 10-, and 12-inch outer tubes, respectively, are presented in Table 1. Since K_v can be expected to be unaffected by soil disturbance in the zone between the inner and outer tube, the ratios of K/K_v are indicative of the effect of the outer-tube diameter on the measured value of K. The ratios show that the 10- and 12-inch outer-tube diameters in Adelanto loam yielded K-values that were approximately four times those obtained with the 8-inch diameter. For the sand, the K-values were three times as high. For both soils, however, there was no significant difference between the values of K/K_v for the 10- and 12-inch outer tubes. Therefore, it is concluded that for a thin-walled inner tube of 5 inches diameter, a thin-walled outer tube of 10 inches diameter was sufficient to eliminate most of the effects of soil disturbance. The larger tube diameters do not only yield higher, but also more uniform values of K than the 8-inch outer tube.

The results of the studies with the smaller sized inner tube are shown in Table 2. It appears that the 4"-8" combination of tube sizes gives approximately the same results as the 5"-10" combination. The average values of K for the 4"-8" combination are only slightly lower than the ones obtained with the 5"-10" combination and, for the Adelanto loam, the relative scatter is only slightly higher. The high relative scatter of the data for both tube combinations for the

sand must be attributed to nonuniformity of the sand itself, since both combinations yielded a wide but similar range in values of K.

SUMMARY AND CONCLUSIONS:

Experiences with the double-tube method indicated that the diameter of the outer tube should be larger than the theoretical minimum because of suspected soil disturbance in the annular space between the inner and the outer tube. Field studies were conducted in Adelanto loam and in river sand using outer tubes of various diameters in combination with a constant diameter for the inner tube. The results indicated that, for an inner-tube diameter of 5 inches, an outer-tube diameter of 10 inches was sufficient to eliminate most of the effects of soil disturbance on the measured value of the hydraulic conductivity. Values of 4 inches and 8 inches for the diameters of the inner and the outer tube, respectively, also appeared to be satisfactory. This is of significance where double-tube equipment with the 5-inch and 8-inch diameters is already available, because it is easier to reduce the size of the inner tube than to increase the diameter of the outer tube. The choice between the 5"-10" and 4"-8" combination depends on the type equipment that may already be at hand, on considerations of the size of the auger hole and the workability of the method in the field, and on the size of the soil region from which K is determined. The latter is twice as large for the 5-inch inner tube as for the 4-inch inner tube. As regards workability, the larger diameter auger hole permits easier and better cleaning and preparing of the hole bottom. Regardless of which of the two combinations is used, however, the tubes should always be thin-walled, have a beveled edge, and should be carefully installed at minimum depth of penetration into the auger hole bottom.

Table 1. Comparison between K obtained with the double-tube technique and K_v calculated from intake rate and vertical gradient, for three diameters of the outer tube and two soils.

	Outer-tube diameter (inches)		
	8	10	12
Adelanto loam			
K (cm/min)	0.091 ± 0.068	0.40 ± 0.09	0.43 ± 0.08
K_v (cm/min)	0.33 ± 0.21	0.41 ± 0.12	0.47 ± 0.12
K/K_v	0.25 ± 0.16	1.0 ± 0.23	0.96 ± 0.16
River sand			
K (cm/min)	0.11 ± 0.03	0.36 ± 0.07	0.28 ± 0.08
K_v (cm/min)	0.22 ± 0.04	0.25 ± 0.07	0.19 ± 0.07
K/K_v	0.50 ± 0.06	1.55 ± 0.47	1.62 ± 0.38

Table 2. Comparison between K obtained with two combinations of tube diameters for two soils.

Tube diameters inches	K of Adelanto loam cm/min	K of river sand cm/min
4 and 8	0.36 ± 0.13	0.10 ± 0.05
5 and 10	0.38 ± 0.10	0.13 ± 0.06

TITLE: FIELD APPLICATION OF FALLING-HEAD TECHNIQUES FOR SEEPAGE METER AND DOUBLE-TUBE METHOD FOR HYDRAULIC CONDUCTIVITY MEASUREMENTS

LINE PROJECT: SWC VII gG1 CODE NO.: Ariz.-WCL-14

PART III. PROCESSING OF HYDRAULIC CONDUCTIVITY DATA.

INTRODUCTION:

Values of soil hydraulic conductivity, K, obtained with the double-tube method or other field techniques for K-evaluation generally apply to a small soil region. Thus, measurements at various points in a field invariably yield different values for K. If the K-data are to be applied in the analysis of a certain flow system (tile drainage, channel seepage, ground water recharge, etc.), processing of the data to obtain simple, uniform or layered profiles may be desirable. If there is no trend or bias in distribution of the K-values, the problem then consists of determining, for a seemingly random distribution, the "hydraulic" mean value for K. In the case of vertical flow through horizontal layers, which might be called series flow, the hydraulic mean is the arithmetic mean of the K-values of the individual layers. For horizontal flow through horizontal layers, which may be called parallel flow, the hydraulic mean is the harmonic mean of the K-values of the individual layers. Thus, for a multi-dimensional flow system in a medium with randomly distributed different values of K, the hydraulic mean can be expected to lie between the arithmetic and the harmonic mean. Another calculable mean that lies between the arithmetic and the harmonic mean is the geometric mean. Studies were carried out to obtain information of how the different means compare with the hydraulic mean value, as determined with a resistance network analog.

PROCEDURE:

Random distributions of K-values were obtained by drawing numbers from a box. The numbers were placed in a two-dimensional, square, network of 10 x 10 meshes in order of their drawing. Two types of random distributions of K-values were used. For the first type, paper slips with K-values of 1, 2, 3, 4, 5, 6, 7, 8, 9, and 10 in the amount of 60 slips for each value were deposited in a box. Drawing

these values yielded a random distribution of K-values from 1 to 10 with about equal representation of each value. The drawing of numbers was done three times (starting each time with the complete set of numbers) to yield three different random distributions. An example of the distribution of K-values is shown in Figure 1. The representation of the different K-values in all three systems is summarized in Table 1. This type distribution would be representative of the case where the K-data obtained in the field cover a certain range of values with no apparent preference for any particular value within the range.

For the second type, only two different K-values were used, a low value of 1 and a high value of 10. The relative proportion of these K-values in each system was varied. The proportions of the low and high values are shown in Table 2. Except for the first system, three replications were used for each system. An example of the K-distribution is shown in Figure 2, which applies to one of the replicates of system E. The second type of K-distribution is representative of the case where the K-data obtained in the field fall in two distinctive groups, one group of high K-values, and one group of low K-values. This may be encountered in alluvial deposits where fine and coarse soils occur in irregular fashion.

For each system, the arithmetic, harmonic, and geometric mean values, as defined below, were calculated.

arithmetic mean $$K_a = \frac{K_1 + K_2 + \text{----} K_n}{n}$$

harmonic mean $$K_h = \frac{n}{\frac{1}{K_1} + \frac{1}{K_2} + \text{----} \frac{1}{K_n}}$$

geometric mean $$K_g = \sqrt[n]{K_1 K_2 \text{-----} K_n}$$

The hydraulic mean, K_{hyd}, was determined by simulating the K-values in an electrical resistance network analog and determining the average resistance (or conductivity) from a measurement of the total voltage drop across the system and the total electrical current going through the system. For this purpose, two flow systems were created for each set of K-values. The first system was one of predominantly horizontal flow and it was obtained by using the left and right sides of the square network as equipotentials and the top and bottom as solid boundaries. The second system was one of predominantly vertical flow and it was obtained by using the top and bottom of the network as equipotentials and the left and right sides as solid boundaries.

RESULTS AND DISCUSSION:

The results of the analog determination of the hydraulic mean and the calculation of the arithmetic, harmonic, and geometric means for the systems in Table 1 with K-values from 1 to 10 are presented in Table 3. Because the K-values at the boundaries of each system are not identical, changing equipotentials to solid boundaries and vice versa slightly alters the distribution of the K-values involved. The differences between the values for horizontal and vertical flow are quite small, however. As could be expected, K_{hyd} is between K_a and K_h, but closer to K_a than to K_h. This reflects the ability of the flow to shunt itself around areas of reduced K, causing the series flow along the streamlines to take advantage of the higher K-values. Although K_g also lies between K_a and K_h, K_g appears to be lower than K_{hyd}. It seems that K_{hyd} is best estimated by the average of K_a and K_g, which for the data in Table 3 is 4.57. If, instead of the relatively uniform distribution of the K-values as in systems I, II, and III, a more Gaussian distribution would have been used, the values for the various means would be closer together because of the greater representation of K-values in the middle range.

The results of the analog analysis and computations for the system of Table 2 with K-values of 1 and 10 are shown in Figure 3. The values on the abscissa are the percentages of the number of K-values of 1 in

the system. The use of three replications and the application of horizontal and vertical flow in the analog analysis yielded six values of K_{hyd} for each ratio of K-values. The range of these six values is indicated by the vertical lines in Figure 3. The average of the six values is indicated by the dots. Because of the insignificant effect of flow direction on K_a, K_h, and K_g, the latter were calculated for all the K-values in the network without regard of which sides were the equipotential lines or the solid boundaries. The curves in Figure 3 show that again K_{hyd} lies between K_a and K_h. However, in this case, the agreement between K_{hyd} and K_g is very good. It is of interest to note that K_{hyd} is relatively close to K_a if the percentage of the K-values of 1 is low, and relatively close to K_h if this percentage is high. An explanation of this may be that when a permeable medium has occasional spots of low K, the flow will go around these spots and the resulting parallel flow will cause K_{hyd} to be relatively close to K_a. On the other hand, the occurrence of occasional spots of high K in a medium of otherwise low hydraulic conductivity will attract the flow to and through the permeable spots, yielding a flow pattern that more resembles series flow, and consequently a K_{hyd} that lies relatively close to K_h. The shape of the curve for K_{hyd} in Figure 3 is of interest because it is not what would be intuitively expected. Without factual data, it probably would be deduced that the curve should be S-shaped with K_{hyd} relatively close to 10 for the low percentages of K-values of 1 and relatively close to 1 for the high percentages of K-values of 1. This is because if the percentage of K-values of 1 is relatively low, the medium with K = 10 is continuous and K_{hyd} might be expected to be relatively close to 10, and vice versa. As shown by Figure 3, however, a small percentage of low hydraulic conductivity values already causes significant reductions in K_{hyd}.

SUMMARY AND CONCLUSIONS:

Most field techniques for measuring soil hydraulic conductivity (K) yield essentially point measurements, and tests at different

locations within a field or soil type invariably give different K-values. To apply these K-values in the analysis of a flow system, processing of the data to obtain simple, uniform or layered profiles may be desirable. This creates the problem of determining the "hydraulic" mean (K_{hyd}), which for a random distribution of K-values can be expected to lie between the arithmetic mean (K_a) and the harmonic mean (K_h). The geometric mean (K_g) also lies between the latter two. Studies were made to compare K_{hyd} as evaluated with a resistance network analog, with K_a, K_h, and K_g. This was done for a square network system of 10 x 10 meshes using two types of random distributions of K-values drawn from a box. The first type consisted of systems with K-values from 1 to 10 with a relatively uniform representation of each value in each system. The second type consisted of systems with K-values of 1 and 10, using different proportions for each system. Replicate systems and different flow directions were used for both types. For the first type, K_{hyd} appeared to lie just about midway between K_a and K_g. For the second type, K_{hyd} was very close to K_g. In all cases, $K_a > K_{hyd} > K_h$. Thus, where the average K-value of a soil or soil layer needs to be determined from point measurements seemingly yielding a random distribution with no preference for any one value, the geometric mean appears to yield a more realistic average K-value for flow system analysis than the arithmetic or harmonic mean.

PERSONNEL: Herman Bouwer and Robert C. Rice.

Table 1. Number of K-values from 1 to 10 in the three random-distribution networks.

K-value	System I	System II	System III
1	25	27	25
2	28	26	20
3	27	24	23
4	17	15	18
5	18	19	25
6	17	22	25
7	26	22	22
8	20	21	22
9	22	23	18
10	20	21	22

Table 2. Numbers of K-values of 1 and 10 in random-distribution networks.

System	Number of K-values K = 1	K = 10	Replications
A	10	210	2
B	20	200	3
C	35	185	3
D	60	160	3
E	80	140	3
F	100	120	3
G	120	100	3
H	160	60	3
I	200	20	3

Table 3. Values of hydraulic, arithmetic, harmonic, and geometric means for vertical and horizontal flow in systems I, II, and III.

	system I		system II		system III		average
	vertical	horizontal	vertical	horizontal	vertical	horizontal	value
K_{hyd}	4.60	4.70	4.59	4.47	4.62	4.55	4.59
K_a	5.14	5.10	5.02	5.06	5.19	5.22	5.12
K_h	2.97	2.84	2.88	2.85	2.93	3.09	2.93
K_g	4.03	3.96	3.96	3.98	4.10	4.17	4.03

°	4	°	2	°	8	°	3	°	2	°	7	°	6	°	9	°	7	°	3	°
6		10		2		7		3		3		1		3		8		4		10
°	7	°	1	°	5	°	9	°	3	°	1	°	6	°	5	°	3	°	7	°
2		6		9		6		10		7		3		9		5		10		6
°	10	°	2	°	4	°	8	°	8	°	3	°	6	°	3	°	5	°	6	°
6		4		5		2		6		3		8		5		10		6		8
°	5	°	4	°	2	°	7	°	3	°	1	°	3	°	2	°	1	°	1	°
2		7		6		9		1		6		2		1		7		8		7
°	10	°	4	°	9	°	5	°	1	°	10	°	9	°	6	°	1	°	10	°
1		4		10		1		1		7		9		3		10		6		2
°	5	°	7	°	5	°	1	°	5	°	8	°	7	°	4	°	3	°	10	°
7		1		3		2		7		9		5		4		2		2		3
°	1	°	4	°	7	°	5	°	5	°	6	°	8	°	5	°	2	°	5	°
8		6		8		1		10		5		2		7		2		8		7
°	9	°	1	°	4	°	7	°	8	°	1	°	10	°	7	°	5	°	10	°
6		8		1		10		5		4		4		6		10		6		9
°	5	°	9	°	1	°	7	°	10	°	6	°	10	°	7	°	4	°	9	°
1		5		8		6		3		9		2		9		10		3		8
°	10	°	4	°	6	°	9	°	5	°	1	°	9	°	1	°	8	°	3	°
4		1		5		6		8		3		4		2		5		10		2
°	4	°	8	°	8	°	5	°	3	°	8	°	3	°	8	°	6	°	9	°

Figure 1. Distribution of K-values for system III.

•	1	•	10	•	10	•	1	•	10	•	10	•	1	•	10	•	1	•	10
10		1		10		10		10		10		10		1		10		10	
•	1	•	10	•	10	•	10	•	10	•	10	•	10	•	1	•	10	•	1
10		10		10		1		10		10		10		1		10		10	
•	10	•	1	•	10	•	10	•	1	•	10	•	1	•	10	•	10	•	10
10		1		10		10		1		10		10		10		1		10	
•	1	•	1	•	10	•	10	•	1	•	10	•	1	•	10	•	10	•	1
10		10		10		10		10		10		10		10		10		1	
•	10	•	10	•	1	•	10	•	10	•	10	•	10	•	1	•	10	•	10
10		10		10		1		10		10		10		10		10		1	
•	1	•	10	•	10	•	10	•	10	•	1	•	10	•	1	•	10	•	1
1		1		1		10		1		1		1		10		10		10	
•	10	•	10	•	10	•	1	•	10	•	1	•	10	•	10	•	1	•	1
10		10		10		1		10		1		10		1		1		10	
•	10	•	1	•	10	•	10	•	10	•	10	•	1	•	10	•	1	•	10
10		1		1		10		10		1		1		10		1		10	
•	10	•	10	•	10	•	10	•	1	•	1	•	10	•	10	•	1	•	1
1		1		10		10		1		10		10		1		1		1	
•	10	•	10	•	10	•	10	•	1	•	10	•	1	•	1	•	10	•	1
10		10		1		10		1		10		10		10		1		1	
•	10	•	1	•	1	•	10	•	10	•	10	•	10	•	1	•	10	•	1

Figure 2. Distribution of K-values for one of the systems E.

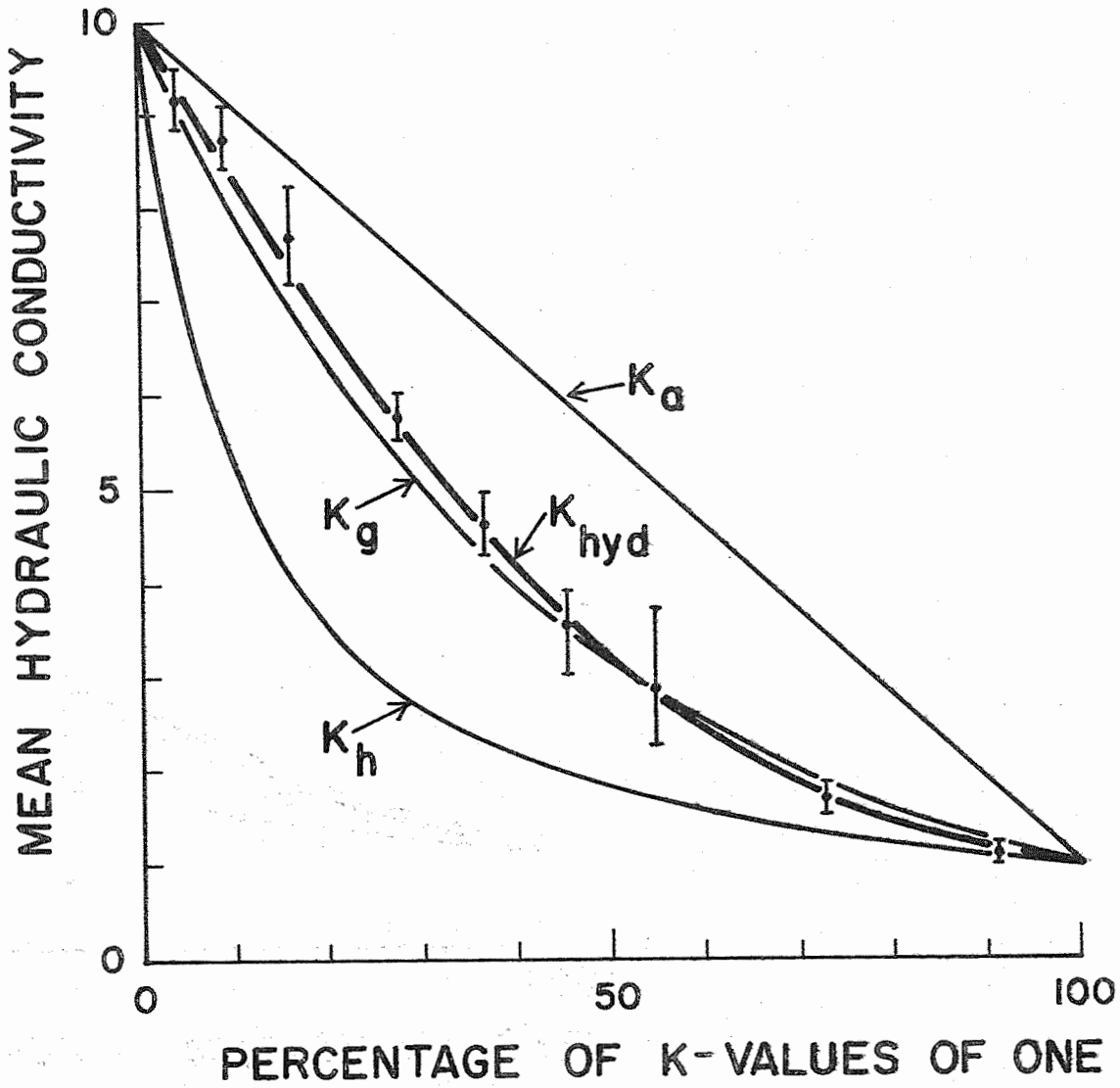

Figure 3. Results of analog analyses and calculations for systems in Table 2.

TITLE: EVAPORATION FROM THE SOIL SURFACE AND SOIL MOISTURE MOVEMENT

LINE PROJECT: SWC VII - gG5 CODE NO: Ariz-WCL-19

INTRODUCTION:

The annual report for 1965 sets forth reasons for the current investigation under the project outline. It consists of measurement of the surface temperature of bare, wet soil with an infrared radiation thermometer and the application of this measurement to the calculation of the evaporation from such a surface. The 1965 annual report also presents the theoretical background and the instrumentation which is being used. It details the method of calibration and the procedure whereby the emittance of the test surface and the unknown is determined, and, also, the method whereby incident radiation from the sky is measured.

In 1966, the entire procedure was put to the test by a series of outdoor measurements using the weighable lysimeters as the standard of comparison for evaporation. Also in 1966, an improved procedure was adopted for the measurement of the emittance of the natural surface, a procedure first published by Buettner of Washington State University.

The entire investigation with respect to evaporation from bare soil was concluded during 1966, and is currently being documented in three reports. For details of the investigation and its results these reports should be consulted. (See publication list under Conaway).

PROCEDURE:

In addition to the procedures listed in the 1965 annual report, a so-called emittance box was constructed according to the suggestions of Buettner, with minor modifications. This box consists of a gold-plated vertical enclosure with a grooved and blackened ceiling that can be covered with a gold-plated, sliding ceiling. The temperature of the black ceiling can be measured by means of thermocouples and the infrared thermometer views the bottom of the box, which is the unknown surface, through a small peep-hole in the ceiling. By placing the box over the natural soil surface and making two successive measurements with a radiation thermometer, one with the gold-plated ceiling in place, and one without it, the latter complemented by a measurement of

the black ceiling, the temperature emittance of the unknown surface is easily determined any time during the day or night, and in a relatively short period of time of several minutes. Since the measurements can be made over a natural undisturbed surface, the method is obviously superior to the one that was used in 1965, in which samples were brought into the laboratory for measurements.

As stated in the 1965 annual report, a cart was constructed on which the radiometer was mounted in such a way that it could be wheeled over a track in the field to various locations of interest. The cart was also made so as to enable the operator to push the reference surface in the beam of the infrared thermometer for the purpose of measuring the sky radiation. Using the weighable lysimeters as standards, a series of three experiments, each over a 24-hour period, was carried out in April and May of 1966. These consisted of measuring the actual evaporation rate and the soil surface temperature on all three lysimeters, together with observations on windspeed, air temperature, and air humidity at 1 m above the bare soil surface. Measurements were made every 15 or 30 minutes.

Using time-sharing computing procedures, the radiometer indications were converted into equivalent blackbody temperatures and, with the aid of the previously measured emittances of both the reference and the unknown surface, the actual blackbody radiation of the soil was found, and the surface temperature calculated. Knowing that the surface was wet and saturated, the vapor pressure at the soil surface was then known.

Using the vapor pressure at the surface and having measured the vapor pressure at 1 m above the surface, the evaporation was then calculated using the following equation:

$$E = (\rho r/p)\ (e_o - e_z)\ C_z\ u_z \qquad g\ sec^{-1}\ cm^{-2}$$

$$C_z = k^2/[\ln z/z_o]^2 \qquad \text{dimensionless}$$

in these two equations E is the evaporation rate, ρ is the density of

the air in grams per cubic centimeter, r is the water/air molecular rate ratio, p is the ambient pressure in millibars, e_o is the surface vapor pressure in millibars, e_z is the vapor pressure at elevation z, C_z is the drag coefficient, u_z is the windspeed at elevation z in centimeters per second, k is the von Karman constant, z the elevation in centimeters, and z_o the surface roughness parameter. The Expression for E is, of course, a Dalton equation based on the simple logarithmic wind law, and it has been used by us before in the use of the combination method. Using this formula with the known surface vapor pressure, the evaporation was calculated for hourly periods for each of the three days of the tests. The calculated values were then compared to those given by the weighable lysimeters.

RESULTS AND DISCUSSION:

The results of comparison between calculated and directly measured evaporation rates over bare soil were excellent. This is exemplified by the data shown for the 29th of April 1966 in Figure 1. On a daily basis the directly measured evaporation was 6.91 mm, whereas the evaporation calculated from surface temperatures was 6.88 mm. Since the entire calibration procedure of the radiothermometer, its use and the measurement of the emittance of the two surfaces involved must be considered as primary measurements, the results reported here are a test of the evaporation model. Since the log-law model is a very familiar one and used extensively, sometimes with apprehensions, our result is a most significant one. It demonstrates that the disturbing effect of instability or stability of the air over an evaporating surface does not interfere with the accuracy of the log-law, when the measurements are made close to the surface as we did. It should be mentioned that the value for the surface roughness parameter was determined several years ago by Fritschen on the same field. Since this value and the direct measurement with the lysimeters are the only critical values involved in the calculation, the entire result stands out as a simple and irrefutable test of the log-law.

An interesting side result of our studies had to do with the intensity and distribution in time of the sky irradiance. From

consulting the literature and others, doing similar work, we had obtained the impression that the radiance from the sky in the bandpass of the radiometer would, on clear days, not only be relatively small and perhaps negligible, but also rather invariant with time since it would, presumably, represent only radiation from ozone in the upper heights of the atmosphere. However, when we monitored sky radiance with the reference surface every 30 minutes on a number of days in 1966, it was soon found that there was a strong diurnal variation on many days, and that also that values could become quite high during the daytime, as high as 3 1/2 to 4 milliwatts per square centimeter. The latter value would correspond to equivalent blackbody temperatures of the order of 50 degrees centigrade, and obviously cannot be ignored in a calculation of the surface temperature, even if the surface emissivity is close to 1.

When we started to investigate the cause of these observations we could only find the ozone concentration close to the surface as a correlated parameter. These ozone data were made available to us by the Maricopa County Health Department as part of their routine air pollution monitoring. A comparison with the world wide data on ozone concentration revealed that, at the Phoenix site, ozone concentrations would often be in excess of a normal .04 parts per million on a volume basis during the daytime as a result of the emission from cars and the effect of sunlight. During the night ozone concentrations drop, and so does both the variability and the intensity of the sky radiance.

From these findings we have concluded that it is necessary to monitor the sky radiance continuously when surface temperatures are being monitored. With the use of the reference surface that we have introduced (see 1965 annual report) this is a simple matter. Also, at least for the purpose of computing evaporation, one can show that the neglect of the sky radiance in surface temperature computation may cause large errors in the computed evaporation rate, up to 10 percent of the hourly values.

In areas where air pollution is not as pronounced, and ozone concentrations are determined only by the exchange between the

troposphere and the stratosphere these considerations need not necessarily apply.

With the studies and results reported here the investigation of bare soil evaporation is concluded. We hope that it is possible to extend these methods to the measurement of the temperature of crop canopies. Whereas such measurements have already been made by others, they have not been applied to the problem of evaporation from a plant cover.

SUMMARY AND CONCLUSIONS:

During 1966 directly measured rates of evaporation from bare, wet soil, using weighable lysimeters, were compared with rates estimated from a simple micrometeorological model. This model embodied a transfer equation using a Dalton-type expression and the logarithmic wind law. It necessitated, beside the measurement of windspeed and vapor pressure at 1 m above the surface, a measurement of the true surface temperature.

The surface temperature measurement was successfully accomplished by using an infrared radiation thermometer (Barnes I-T-2) with some accessories developed especially for the purpose during 1965. The measurement of the surface temperature consists of a recording of the radiation from the surface, the radiation from the sky and a knowledge of the emittance of the soil surface. A number of measurements carried out during the late spring of 1966 showed that routine determination of surface temperatures within 0.2 degrees centigrade is feasible.

The comparison between calculated and measured evaporation rates from bare soil was extremely close, and it allows us to conclude that the simple log-law model of vapor transfer above a bare surface is accurate even though during part of the measuring period the air was unstable and, again, during others was quite stable. Nevertheless, the consideration of any corrections for air stability was apparently unnecessary. This conclusion is of considerable practical significance, because the log-law expression is widely used in other applications of micrometeorological data for the purpose of estimating

evaporation.

PERSONNEL:

J. Conaway, C. H. M. van Bavel

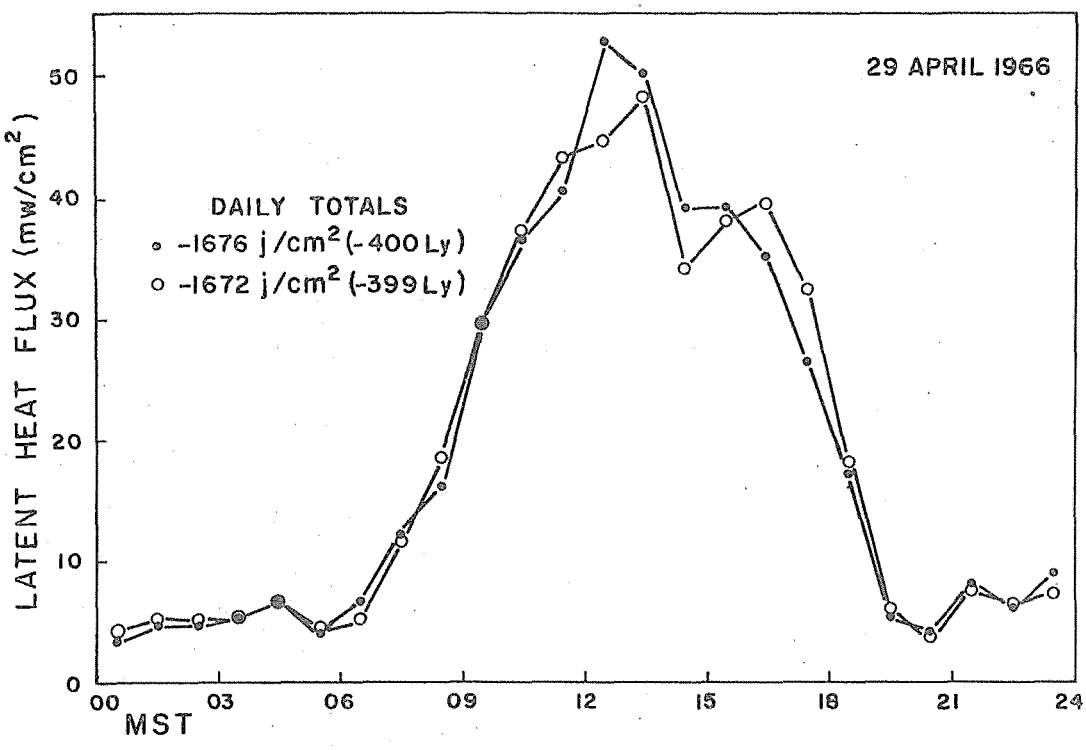

Figure 1. Measured (solid dots) and calculated (open dots) values of hourly evaporation rates from wet, bare soil using radiometrically obtained surface temperatures to obtain the surface vapor pressure e_o.

TITLE: CONSUMPTIVE USE OF WATER BY CROPS IN ARIZONA

LINE PROJECT: SWC IX-gG3 CODE NO.: Ariz.-WCL-23

SUBPROJECT TITLE: RELATIONSHIP OF METEOROLOGICAL MEASUREMENTS WITH CONSUMPTIVE USE FOR OPTIMUM COTTON PRODUCTION.

INTRODUCTION:

For need of study, see previous Annual Reports. Several new varieties have been introduced into Arizona cotton production. It was felt that these new varieties should be grown using recommended irrigation techniques developed several years ago.

OBJECTIVES:

1. To correlate certain meteorological measurements with water management on cotton.
2. Determine the comparative production of present-day cotton varieties with older varieties, under a previously determined irrigation schedule.
3. Determine the comparative consumptive use for various varieties of cotton.

PROCEDURE:

The experiment is located on Field C-1 at the University of Arizona Cotton Research Center, Phoenix, Arizona. The field had been in alfalfa for the previous two years. 120 pounds of nitrogen as urea was applied on February 23, the field plowed, furrowed out, and a pre-planting irrigation applied on March 18. On April 1, Deltapine Smoothleaf was planted on the East half of the field. The West half was planted in four-row plots to five varieties; Deltapine Smoothleaf, Stoneville 213, Acala 44-10, Hopicala, and Pima S-4, in a randomized block design replicated 4 times.

Irrigations were given when visual plant symptoms and soil moisture determinations indicated the plant needed water. In so doing, an attempt was made to duplicate the 65% concept recommended by this office. Varieties on the West side were irrigated on the same day, regardless of differences in soil moisture tensions.

"Piche" atmographs and net radiometers were installed in the East half of the field about June 15.

Yield measurements were made on 260 feet of the two inside rows of the four-row plots. Two pickings were made, the first with hand pickers and the second by machine. Samples were saved at each picking and processed to determine lint percentage.

Soil moisture measurements were made at three locations on the East side and on all varieties in three replications on the West side.

DISCUSSION:

Cotton was planted on April 1 and an excellent stand was obtained. Mean temperatures were higher than normal in April and the cotton made excellent early growth. Irrigations were given on May 18, June 17, July 6 and 27, August 17, and September 22. All irrigations, except that of July 6th, were given when soil moisture depletion from the top three feet was at, or near, 65%. Soil moisture depletion was somewhat greater before the July 6th irrigation, although no extreme plant stress conditions were noted. Some uneveness in distribution of water was noted, due to high and low spots within the field. During each irrigation, several rows on each set were connected together in an attempt to attain more even distribution.

Two dusters, along with heavy rains, occurred on August 17 and 18. Wind gusts reached 50 miles per hour during each of the storms. All varieties were damaged and cotton from open bolls was strung out to some degree. Cotton plants were flattened out to some extent and excessive secondary growth occurred when plants failed to return to their normal upright position. Maturity of late-season boll set was prolonged as no killing frosts occurred before the final harvest.

TABLE 1. Yield of Cotton from Two 260-Foot Rows.

VARIETY	HARVEST	SEED COTTON (lbs)	LINT PERCENT	LINT (lbs)	TOTAL LINT (lbs)	BALE/ACRE EQUIVALENT
ACALA 44-10	1st	58.0	36.9	21.4		
	2nd	69.8	38.1	26.6	48.0	2.44
HOPICALA	1st	97.0	36.6	35.5		
	2nd	46.8	38.7	18.1	53.6	2.72
DELTAPINE	1st	127.3	36.9	47.0		
	2nd	43.3	36.9	16.3	63.3	3.22
STONEVILLE	1st	143.3	37.2	53.3		
	2nd	47.5	37.5	17.8	71.1	3.61
PIMA	1st	71.0	32.9	23.4		
	2nd	50.3	34.9	17.6	41.0	2.08

TABLE 2. Soil Moisture Depletion by Depths in Inches and Percent

0 - 1	12.0 (30%)	12.0 (32%)	11.8 (31%)	12.1 (32%)	10.4 (31%)
1 - 2	8.8 (22%)	8.6 (23%)	8.4 (22%)	9.0 (24%)	8.1 (24%)
2 - 3	7.2 (18%)	6.3 (17%)	6.9 (18%)	6.4 (17%)	5.7 (17%)
3 - 4	5.6 (14%)	5.2 (14%)	5.0 (13%)	4.9 (13%)	4.4 (13%)
4 - 5	3.6 (9%)	3.0 (8%)	3.1 (8%)	3.4 (9%)	2.7 (8%)
5 - 6	2.8 (7%)	2.2 (6%)	3.1 (8%)	1.9 (5%)	2.3 (7%)
TOTAL	40.0	37.3	38.3	37.7	33.6

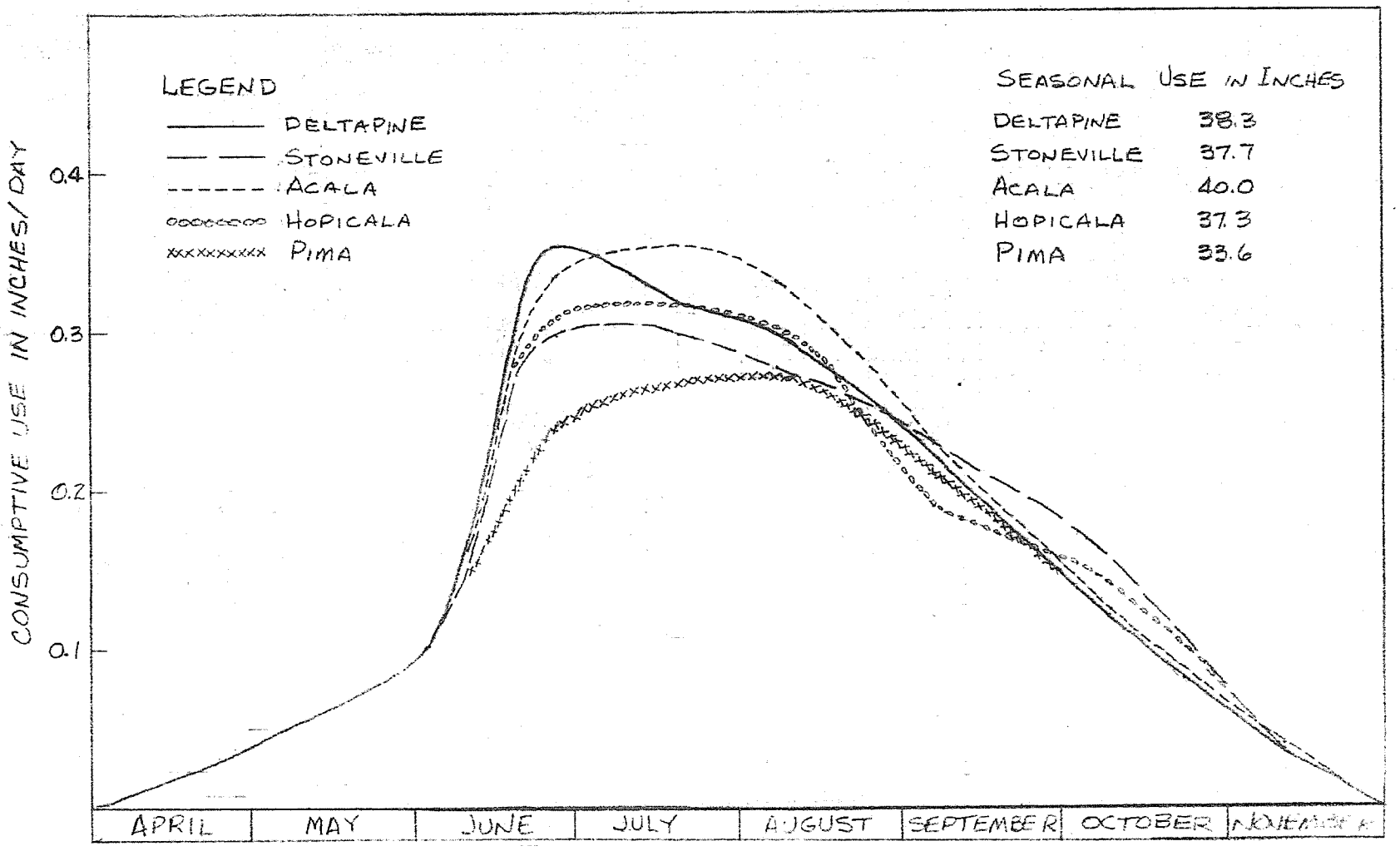

FIGURE 1. MEAN CONSUMPTIVE USE FOR 5 VARIETIES OF COTTON AT PHOENIX, ARIZONA. 1966

SUMMARY AND CONCLUSIONS:

Seasonal consumptive use as measured in 1966 under recommended irrigation management techniques was nearly equal to the mean developed from nine years of previous research. However, the seasonal use may have been affected by either of offsetting conditions -- lack of new growth on plants laid flat by severe winds, or secondary vegetative growth arising after the storms. The peak use occurred about two to three weeks earlier than expected. The early planting date and conditions favoring excellent early growth may account in part for this fact.

Percent soil moisture depletion was quite similar for all varieties at each depth. The fact that total consumptive use was somewhat less on Pima S-4 would indicate further research is justified on this variety.

Yields obtained in 1966 seemed desirable for cotton grown under presently recommended irrigation techniques. As much as 75% of the total yield was picked at the first harvest on all varieties except Acala. Over half of its yield was picked at the last harvest.

PERSONNEL: Leonard J. Erie and Orrin F. French.

TITLE: MEASURING HORIZONTAL AND VERTICAL CONDUCTIVITY OF THE SOIL WITH THE DOUBLE-TUBE METHOD

LINE PROJECT: SWC VII 4-gG1 CODE NO.: Ariz.-WCL-25

INTRODUCTION:

The development of the fast-response piezometers (see Annual Report 1965) has been extended to that of a multiple tensiometer system. Such a system can be used in ground water recharge, drainage, and infiltration investigations, or any other studies where pressure-head data at a number of points is desired. An interesting application would also be the determination of the unsaturated hydraulic conductivity characteristic in the field. For this purpose, pressure-head measurements at various depths are combined with water content measurements to obtain the desired information. The tensiometer system employs one transducer and a switching arrangement to accommodate a number of tensiometers.

PROCEDURE:

Tensiometer system. The tensiometer system consisted of ten tensiometer ceramics connected to a pressure transducer through a 12-port scanning valve (Figure 1). The signal from the transducer was recorded on a millivolt recorder. The valve is equipped with a solenoid switching motor that is energized with a timer. The switching time interval should be long enough for the system to essentially reach equilibrium at each tensiometer position yet fast enough to complete the entire scan without losing any significant events. The switching time interval, therefore, will depend upon the response time of the system and the type of soil in which the tensiometers are placed. The scanning valve is a shear type valve with precision machined parts which result in no detectable volume change when switching from one port to another. The tensiometer ceramics were 3 cm long, 1.3 cm in diameter, and had a bubbling pressure of 1300 mb. They were connected to brass-tubing fittings with epoxy (Figure 2). Nylon tubing, 3/16 inches O.D., was used to connect the tensiometer ceramic with the scanning valve. To facilitate installation and retrieval

of the tensiometers, the brass-tubing fitting with the ceramic was connected to ¼-inch galvanized steel pipe. For this purpose, a nut was soldered into the pipe at the bottom. The length of the steel pipe was such that the top of the pipe would be 15 cm below ground surface.

The transducer may undergo a zero shift or calibration change when exposed to temperature changes. For this reason, records of the zero reference and calibration were also maintained. The zero reference was obtained by connecting one port from the valve to a free water surface at the transducer level. The calibration was obtained by connecting another port to a reference level 100 cm below the transducer. For every complete scan of the tensiometer system, a calibration check and zero reference were obtained in this manner.

Laboratory experiment. When the nylon tubing leads from the ceramic to the transducer were exposed to the open air, considerable pressure fluctuations were observed which were likely caused by rapid changes in temperature. To study this phenomenon and to find ways to avoid the temperature effects, the tensiometer system was set up in a 55-gallon drum filled with Laveen loam. A gravel drainage layer was provided in the bottom of the drum. The pressure head in this layer could be controlled so that, at equilibrium conditions, the true pressure head for each tensiometer was known. After the soil was saturated from the bottom, tensiometers were installed at different depths. With the tensiometers in place, the drum was placed outside in the open air to determine the magnitude of the pressure fluctuations. Then the barrel was completely enclosed in a plywood box to prevent any rapid temperature changes resulting from air movement but allowing diurnal temperature variations inside the box. In another test, the barrel was in the open but only the nylon leads were insulated using 1 1/8-inch O.D. x ½-inch I.D. foam rubber insulation tubing. This was done because in most field experiments it is not feasible to completely enclose the tensiometer system.

The transducer and scanning valve were placed in a styrofoam insulated box adjacent to the barrel in all cases.

Field experiment. The field experiment was designed to test the field behavior of the system while measuring the pressure profile during infiltration and drainage. The tensiometer system was installed in Adelanto loam with a Bermuda grass cover 30 ft east of Building 5. A neutron access tube was used to obtain water content profiles in the center of the test plot. Location and depth of the tensiometers in the test plot is shown in Figure 3. Three tensiometers at the 55-cm depth were placed at varying distances from the neutron access tube. The plot area was 135 cm square and was divided into 36 sections with a series of sheet metal cells each 22½ cm sq and 12 cm high. The cells were driven into the ground 5 cm.

The leads from the tensiometers were insulated with the foam rubber tubing. After the profile was wet up, the plot area was covered to prevent evaporation. In this way, any change in water content would be due to drainage alone.

RESULTS AND DISCUSSION:

Laboratory experiment. A typical record of pressure head versus time with the barrel outside in the open and no shielding of the leads is shown in Figure 4A. Pressure fluctuations of ± 20 cm of water were caused by short-term temperature fluctuations around the nylon tubing. These temperature changes are probably caused by air currents and they are likely to be "instantaneous" in nature. The resulting volume changes, therefore, occur faster than can be dissipated by the ceramic which causes the diaphragm of the transducer to deflect. Thus, the pressure measured is that inside the tubing and not that of the soil-water.

When a box was placed over the barrel, there was no noticeable pressure fluctuation (Figure 4B). The diurnal temperature change of 18C did not cause any pressure fluctuations but resulted in a zero shift in the transducer. Because the zero reference is measured, the zero shift can be adjusted accordingly.

Shielding the tensiometer leads with insulation yielded pressure records similar to those when the entire barrel was covered by the box (Figure 4C). The diurnal temperature variation inside the insulated tubing was approximately 25C. The pressure records obtained with the system enclosed in a box and with the leads insulated agreed closely with the true pressure heads as calculated from the height of the ceramic above the water table level in the gravel drainage layer of the barrel.

The response time of the tensiometers in the Laveen loam was fast enough to permit a ½-minute scanning time at each port.

Field experiments. Most of the tensiometers had a response time constant (63 percent response) of less than 1 minute. This response time is somewhat longer than that in the Laveen loam, indicating that the system is soil limiting rather than instrument limiting. The response time constant of the tensiometer in water was less than 1 second. The response time constant of less than 1 minute would permit a switching interval of approximately 2 minutes. Since the pressure changes in the soil occurred at a relatively slow rate, however, a 5-minute interval was selected. With the 12 ports on the valve, this meant that a tensiometer reading was taken every hour.

Pressure profiles during infiltration are shown in Figure 5. During the first hour of infiltration when pressure changes were rapid near the surface, readings were alternated between the 10- and 25-cm depth. After the first hour, the rate of pressure change was sufficiently slow so that hourly readings would suffice. The "final" infiltration rate in the plot was approximately 0.2 cm/hr.

If drainage were allowed to occur with no evaporation or additional infiltration, the unsaturated hydraulic conductivity-water content relationship and the soil-water characteristic could be obtained. However, a complete drainage cycle was not completed because of rain which flooded the plot. The soil-water characteristic obtained from the pressure head and water content measurements during drainage is shown in Figure 6 for different depths. Plotting these

curves on one graph (Figure 7) shows that there are three different layers in the profile. The upper curve is the 25-cm depth. The next four curves, 44 to 100 cm in depth, are similar, indicating a uniform layer. The bottom curve is the 130-cm depth. Additional drainage cycles will be measured in the future.

SUMMARY AND CONCLUSIONS:

The multiple tensiometer system consisting of a small volume displacement transducer connected to a number of tensiometers through a scanning valve performed satisfactorily under field conditions. When the nylon tubing from the porous ceramic was exposed to the atmosphere, considerable pressure fluctuations due to short-term temperature changes occurred. Shielding the nylon leads with insulated foam rubber tubing eliminated these pressure fluctuations. Response time of the tensiometers in Adelanto loam was sufficiently fast to obtain a reading within 2 minutes. The switching interval for the scanning valve was taken as 5 minutes. The wetting front during infiltration could be adequately characterized. Using the tensiometer data in connection with water contents measured with the neutron scattering method, the soil-water characteristic can be obtained. If evaporation is prevented from the surface, the unsaturated-hydraulic-conductivity characteristic can be obtained by using the method of instantaneous profiles. The multiple tensiometer system enables the rapid-response measurement of a number of tensiometers while using only one transducer. The system should be of value wherever pressure-head data at a number of points in a dynamic soil-water system are desired.

PERSONNEL: Herman Bouwer and Robert C. Rice.

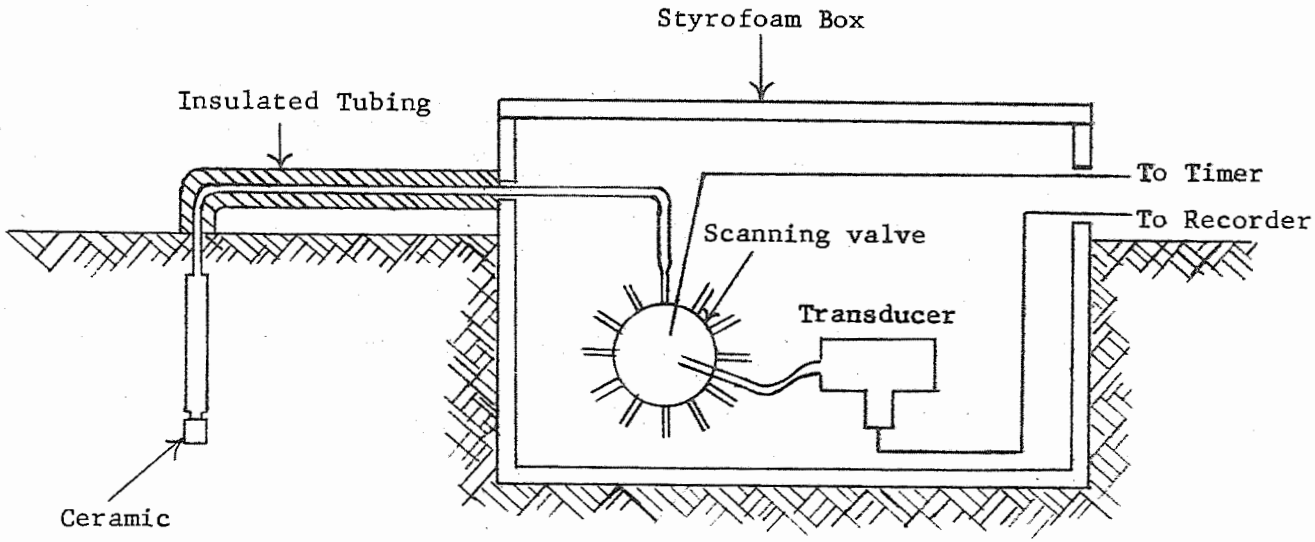

Figure 1. Sketch of tensiometer system in field.

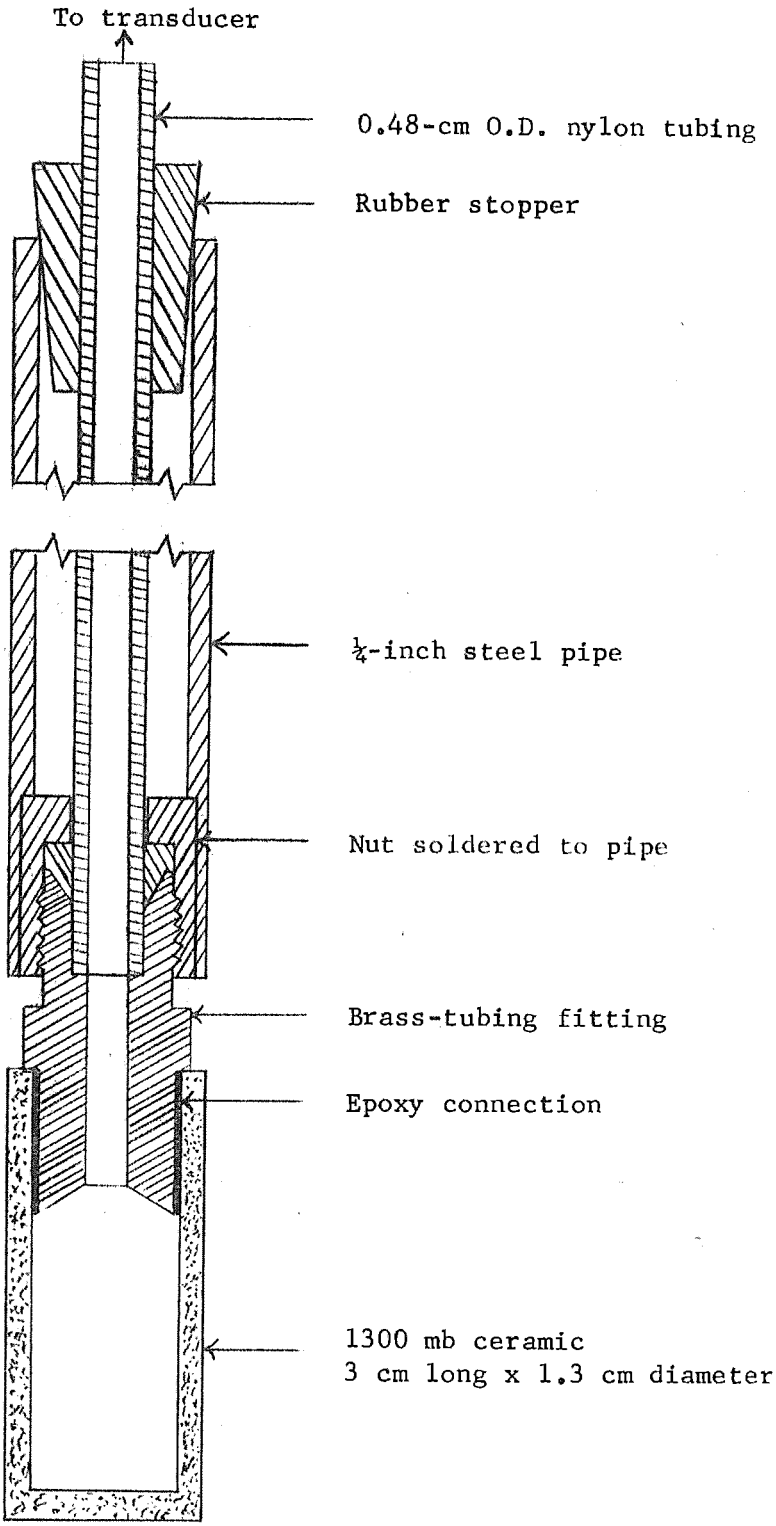

Figure 2. Schematic of tensiometer.

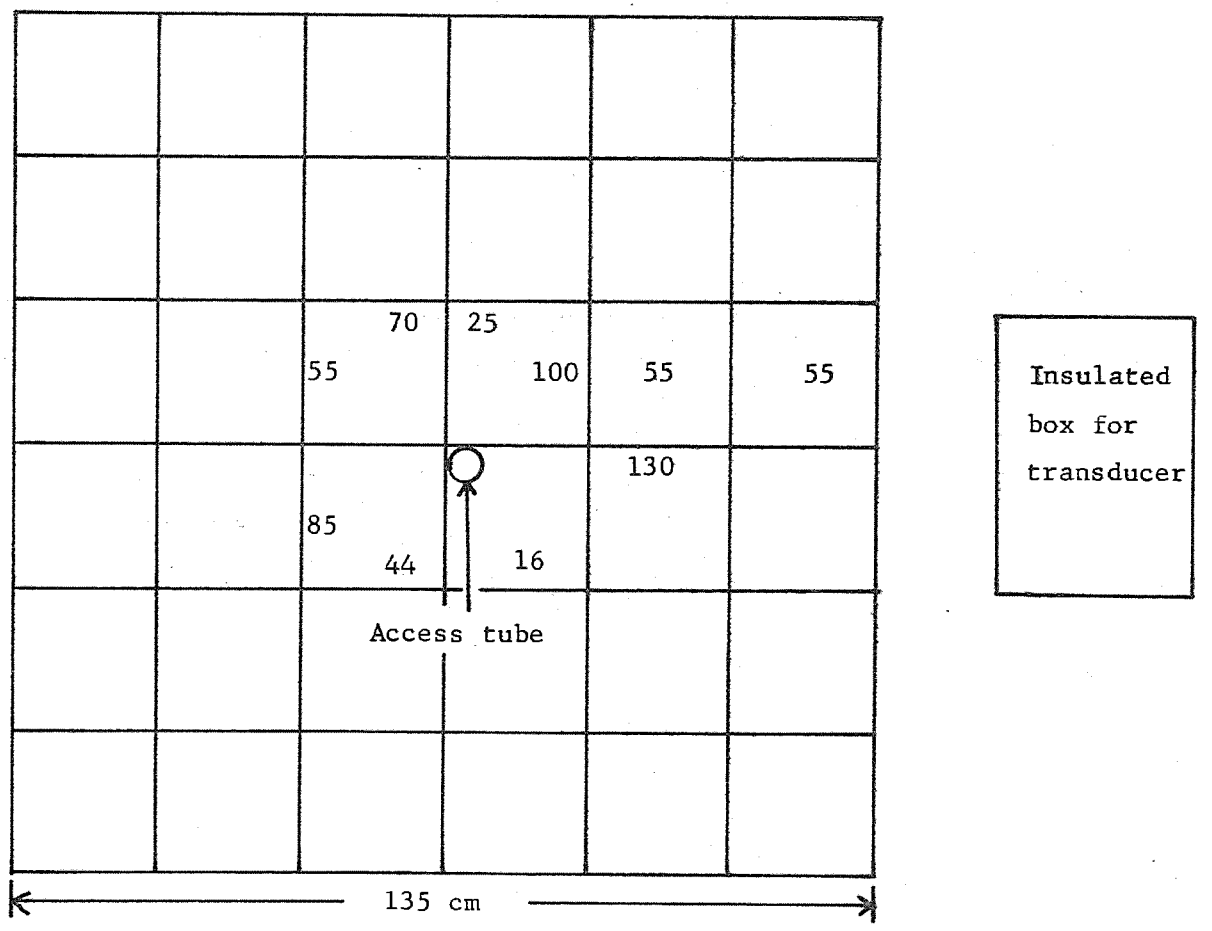

Figure 3. Location and depth in cm of tensiometer in field plot.

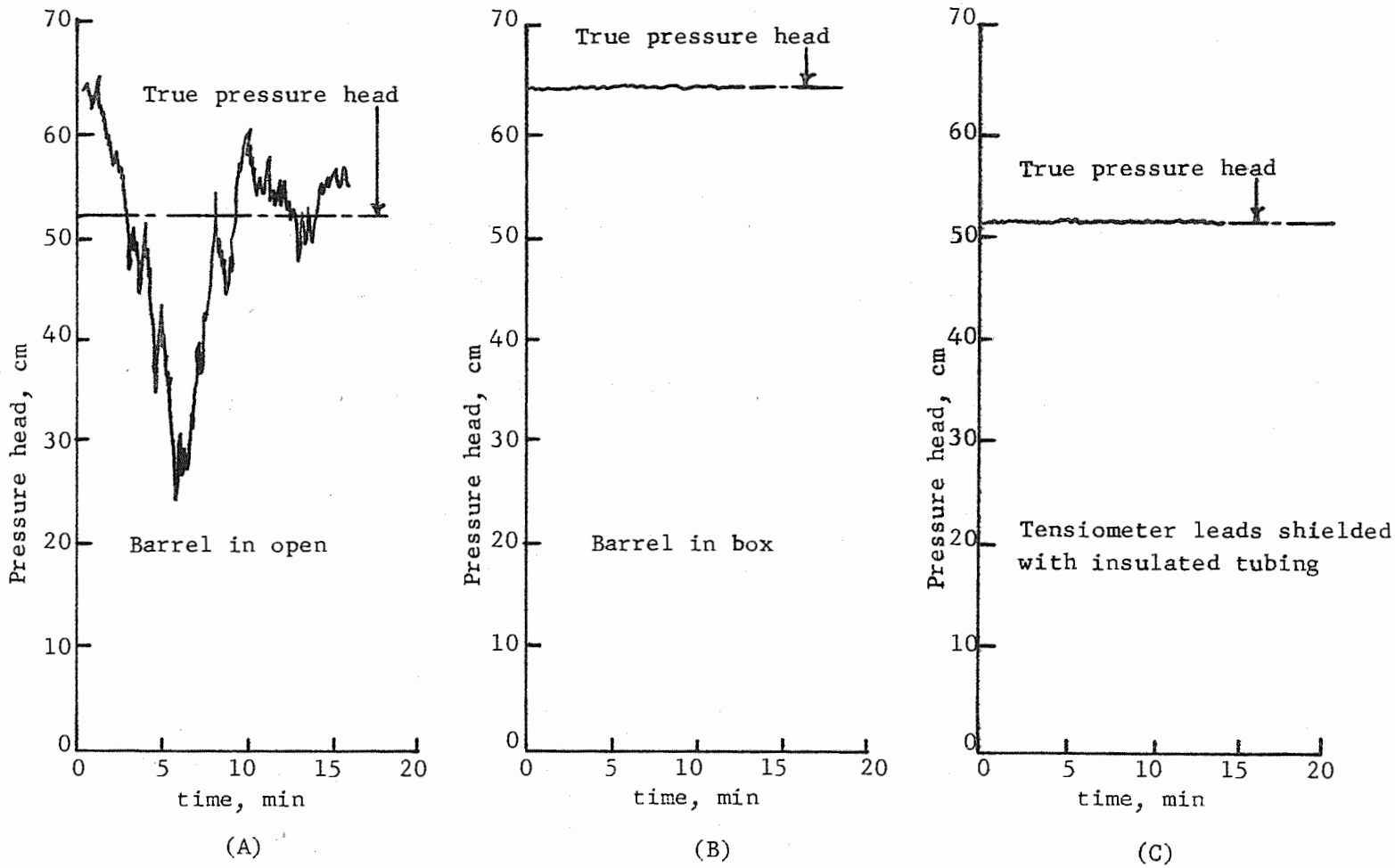

Figure 4. Pressure record of tensiometer in three different temperature environments. True pressure head refers to height of ceramic above water table in drainage layer.

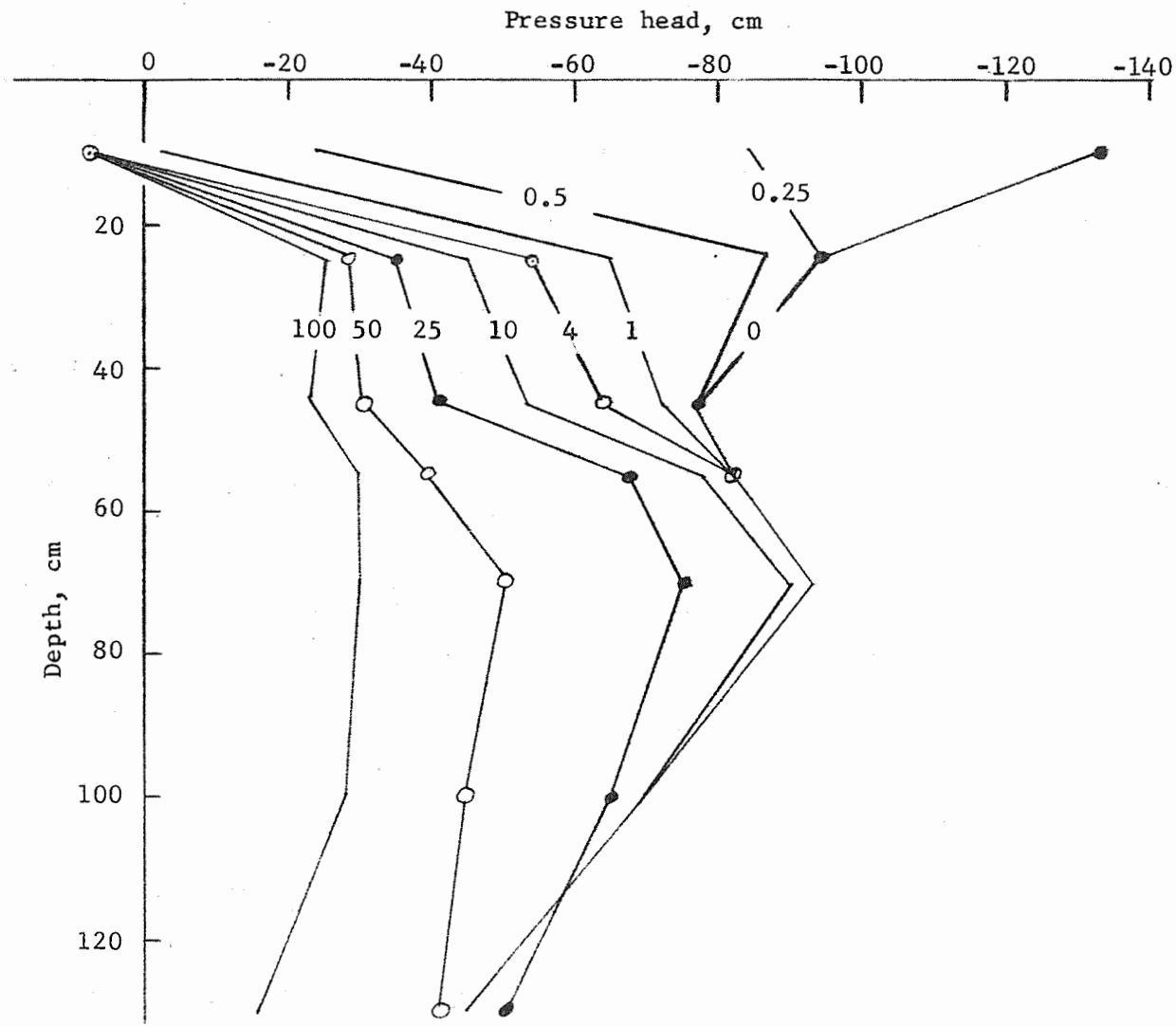

Figure 5. Pressure-head profile during infiltration at different times in hours.

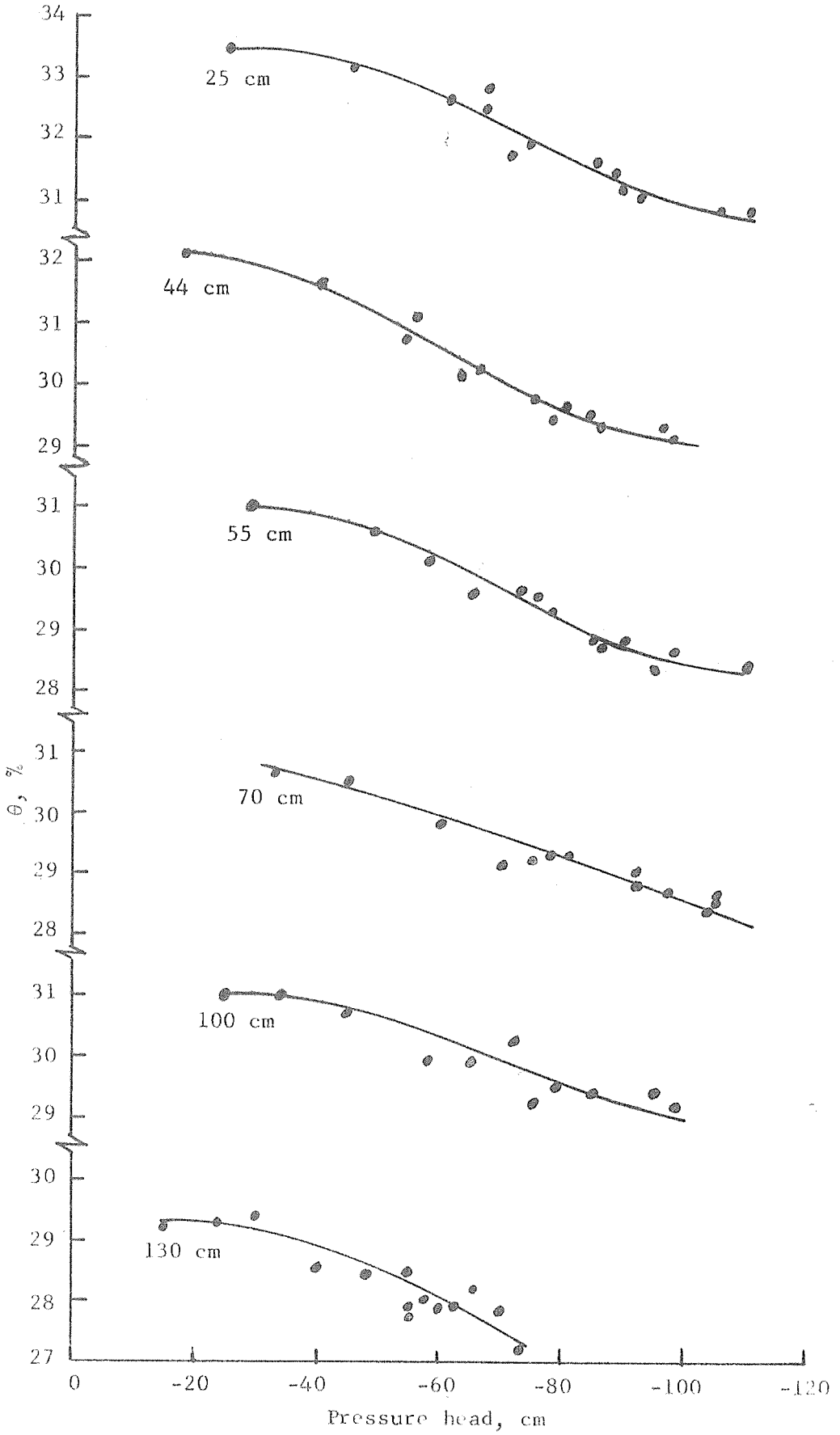

Figure 6. Soil-water characteristic for different soil depth during drainage.

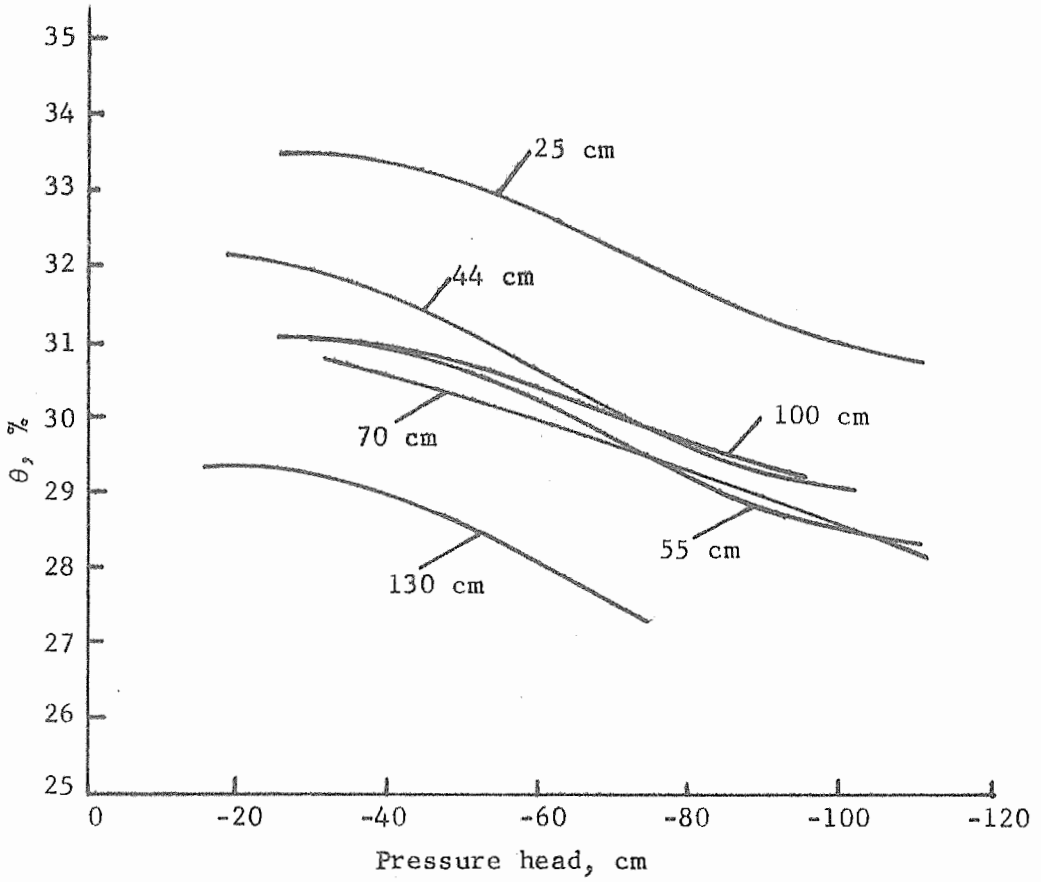

Figure 7. Composite soil-water characteristic curves for different depths (on the curves).

TITLE: WATER ABSORPTION, TRANSPIRATION, AND INTERNAL WATER BALANCE OF COTTON PLANTS AS AFFECTED BY CHANGES IN EVAPORATIVE DEMANDS

LINE PROJECT: SWC IX-gG1 CODE NO.: Ariz.-WCL-29

This report consists of three parts, followed by a General Summary and Conclusions Section.

PART I. INSTALLATION AND EVALUATION OF HIGH INTENSITY MERCURY VAPOR LAMPS IN THE CONTROLLED ENVIRONMENT ROOM

As pointed out in the annual report for 1965, the illumination level from the fluorescent light system, although satisfactory for many purposes, was insufficient to induce complete stomatal opening. To remedy this condition, and thereby more closely simulate the outdoor environment, a battery of high intensity mercury vapor lamps was installed as a replacement for the fluorescent lamps. The type used was 400-w, standard white, semi-reflective, No. H33-1-DN/C, a color-corrected lamp. The frequency multiplier previously used as part of the lighting system no longer was necessary, since the present system of mercury vapor lamps utilizes ordinary 60 cycle, 274 V. current.

The room has a floor area of 2.70 $\times$ 6.14 m and a ceiling height of 3.60 m. The bottom of the pear-shaped lamps is 3.10 m above the floor. A total of 184 of the lamps is arranged in eight symmetrical rows; up to 120 can be used at one time, either uniformly dispersed over the entire area or arranged in a double-density pattern over the center of the room. The diffuse spacing is 34 $\times$ 41 cm, the dense one 34 $\times$ 20 cm.

To promote uniform light distribution, the floor was coated with a glass-beaded white paint, and the walls and door were covered with aluminized mylar. An additional gain in illumination occurred when it proved feasible to dispense with the mylar panel formerly separating the lamps from the room proper. This could be done, because the lamp output no longer depended on ambient temperature, as with fluorescent lights.

Measurements of illuminance were made at 15 uniformly spaced sites in the room at three elevations for each site, first with the

diffuse and then with the dense lighting pattern. These measurements showed a very uniform distribution of illumination, but with somewhat lower levels at the corners of the room than in the center, primarily evident in the dense arrangement.

In general, conversion of the white plaster walls to a mirror-like surface by application of aluminized mylar not only significantly increased the illuminance throughout the room, but also somewhat improved the lighting uniformity. For example, with 120 lamps on in a diffuse arrangement, illumination at 1.5 m, the normal working distance, increased 9%, from 83.9 $\pm$ 5.6 kilolux, (with a coefficient of variation, C.V., of 6.7%) the value for white walls, to 91.4 $\pm$ 2.8 kilolux (C.V. 3.1%) for aluminized walls, the means being computed from 15 values. At the 2.5-m distance, illuminance rose from 67.0 $\pm$ 4.0 (C.V. 6%) to 82.5 $\pm$ 2.6 kilolux (C.V. 3.2%) for the diffuse arrangement; a 23 percent gain. The same percentage gains in illuminance occurred for the dense as for the diffuse spacing, but the absolute levels were about 8 percent higher at both distances from the lamps. No significant differences in illuminance were measured 0.5 m from the lamps, regardless of type of wall covering or lighting arrangement. At such a short distance from the lamps the mean readings of the 15 sites all were 100 kilolux.

Omission of the data from six sites near the ends of the room emphasizes the center, where experiments are carried out. Three specific examples of the very high levels of illuminance that were measured over the more restricted area are the following, each being the mean of the nine central sites, the information being obtained with the dense arrangement of 120 lamps that were reflecting on aluminized walls: at 2.5 m from the lamps, 95 $\pm$ 2 kilolux; 1.5 m, 117 $\pm$ 9 kilolux; 0.5 m, 140 $\pm$ 19 kilolux. These data illustrate the present capability of inducing full stomatal opening, since the light levels greatly exceed 65 kilolux, estimated to be the saturation value for full stomatal opening.

In regard to irradiance levels, simultaneous measurements with a Weston luxmeter, used to obtain the data cited above, and a Kipp

pyranometer established a conversion factor that is valid for light from the mercury vapor lamps described here: ly min^{-1} = kilolux $\times$ 0.01. Accordingly, for a specific value cited above, 117 kilolux, the irradiance was 1.2 ly min^{-1}, a level quite comparable to midsummer radiation intensities at solar noon out-of-doors in central Arizona. Therefore, the controlled environment room can simulate natural conditions quite closely in both illuminance and irradiance levels.

Spectral measurements over increments of 0.01 μ from 0.38 to 0.75 μ revealed five major peaks of output, which fact undoubtedly is related to the known line spectra of mercury. The area under the curve resulting from a plot of energy per unit band width against wave number was integrated over three spectral ranges. The energy distribution, in percent of the total, was as follows: 0.380-0.500 μ, 22.7; 0.500-0.600 μ, 47.0; 0.600-0.780, 30.3. Two of the peaks, those at 0.430 and 0.670 μ, are very close to those cited by Kuiper as required for maximal stomatal opening, 0.432 and 0.675 μ. The major difference in spectral composition between the mercury vapor light and sunlight is the low emission of the former in the region from 0.450 to 0.520 μ. Fortunately, however, this region is not important for either stomatal action or photosynthesis.

In summary, it appears that the present lighting system can simulate outdoor radiant conditions rather closely, in both illuminance and irradiance levels, and that the objective of the conversion from fluorescent to mercury vapor lamps was fully achieved. This objective was the capability to induce complete stomatal opening.

PART II. TRANSPIRATION AND LEAF DIFFUSION RESISTANCE

INTRODUCTION:

The ability to calculate transpiration from appropriate plant and environmental measurements would enhance our understanding of the complex process of plant water loss, and might lead ultimately to the resolution of evapotranspiration into its components of evaporation and transpiration. With the objective of attaining a closer agreement between calculated and measured transpiration, the research already carried out with three plant species was repeated more comprehensively, and was extended to a fourth species, bean.

As before, the aim was to obtain reliable data to satisfy the transpiration equation

$$E = \frac{\Delta d_v}{R_A + R_L}$$

where E is the evaporation (or transpiration) rate, Δd_v the gradient in water vapor density from leaf to air, R_A the boundary layer resistance, obtained by use of a synthetic plant, and R_L the leaf diffusion resistance. The transpiration calculated from the transpiration equation then was compared with the value obtained by weight loss. The extent of agreement in the two sets of data was a measure of the validity of the transpiration equation, providing that the transpiration rate was great enough to obtain accurate readings of weight changes.

PROCEDURE:

Briefly, a closely controlled environment was maintained, defined as follows: air temperature 30.0 $\pm$ 0.2C; vapor pressure 15.0 $\pm$ 0.2 mb; carbon dioxide content of the air 375 $\pm$ 10 ppm; wind speed constant at a low velocity; the plant in aerated, complete nutrient solution. A synthetic plant with leaves of green blotter paper shaped and oriented like those of the living plant was weighed on a balance located 30 cm from the living plant, for data permitting calculation

of R_A values by use of the same equation as above, but lacking the R_L term.

The assumption underlying the procedure is that evaporation from the blotter leaves is directly proportional to the evaporative gradient from blotter to air, and inversely proportional to the boundary layer resistance, which in turn depends primarily on wind speed, and secondarily on leaf dimensions. In contrast, although the leaf of the living plant could be assumed to have the same boundary layer resistance as the blotter leaf, it would have an additional internal resistance due to partial or complete stomatal closure.

Tiny copper-constantan thermocouples (0.1 mm diameter) embedded in the leaf midribs measured leaf temperature; this permitted calculation of the water vapor density within the leaf, on the assumption of saturation vapor pressure therein. The additional measurement of the vapor density of the air then permitted calculation of the gradient in vapor density from leaf to air, the numerator of the transpiration equation. In the same manner, thermocouples embedded in the blotter leaves established Δd_v for the blotter leaves.

A leaf resistance meter was used to measure R_L on both surfaces of every leaf. In early experiments the individual values were averaged harmonically to obtain a single R_L characteristic of the whole plant. In later experiments (E-4, E-5, E-6) each leaf was treated individually, so that transpiration for the whole plant was the sum of that for all the leaves.

After the greenhouse-grown plant had been equilibrated overnight in the desired environment, a very low level of light was established. The first series of measurements was made when the continuously recorded leaf temperatures showed steady plant behavior. Later the illumination was increased gradually to the desired high level. When plant equilibrium prevailed, the second set of measurements was made.

The experiments were repeated for sunflower and cotton; bean was the new species studied, all three species in the second series being exposed to mercury vapor light instead of fluorescent light. The new

lamps permitted radiation levels of around 60 kilolux (0.6 ly min^{-1}), values previously unattainable.

RESULTS AND DISCUSSION:

General - Experiments E-1, E-2, and E-3 were carried out under fluorescent light, the others under mercury vapor light. Associated with the change from one type of lamp to another was the removal of the mylar panel that separated the upper light plenum from the rest of the room. This apparently resulted in a slightly greater overall wind velocity in the room, due to the added air movement from the two refrigeration units used to cool the fluorescent lamps. Evidence for this effect is the decrease in R_A when E-1 is compared with E-5 (cotton) and E-2 with E-4 (sunflower), at both levels of illumination (Tables 1-A and 1-B).

Air temperature was maintained at 30.0 C in all experiments, with a deviation of $\pm$ 0.2 C at the low level of illumination, and $\pm$ 0.5 C at the high level.

As shown in Table 1, evaporation from the blotter leaves was sufficient to lower their temperature 8 or 9 C below air temperature in the low level of light, and from 5 to 6 C in the high level of light. Since ambient vapor density was held steady, the higher temperature of the evaporative surface directly determined the gradient for loss, and thereby led to the large increase in evaporation rate coincident with the higher radiant energy load.

Leaf size played a minor role in affecting R_A, since there was no pronounced difference in R_A values among species with rather large differences in length and width of leaves e.g., lemon vs. sunflower (E-2 vs. E-3). Nevertheless, the slight trend apparent in the series cotton, sunflower, lemon (E-1, E-2, E-3 at both light intensities) does coincide with a downward trend in leaf size, and may be just barely significant. The fact that a fourfold difference in area per leaf (lemon vs. cotton) exerted only a slight change in R_A means that wind velocity undoubtedly was the predominant factor in determining the boundary resistance. The uniformity of the R_A data attests to the

relative constancy of wind speed in the controlled environment room.

The close agreement in R_A values for a given species at both levels of illumination permitted subsequent calculations of transpiration to be made on the basis of the average R_A of the two levels of light, except for E-5.

I. Experiments at Low Illuminance Levels

During the first part of each experiment the plants were either in darkness or in light so low as to bring about R_L values similar to those in darkness, i.e., high values (Table 2). Even so, in all experiments the evaporative cooling due to the low transpiration rate was sufficient to bring about a leaf temperature somewhat below ambient, especially in sunflower. Slight differences among experiments in both leaf temperature and ambient vapor density led to some differences in the gradient in water vapor density from leaf to air, despite the uniform environment (30 C air temperature and a set point of 15 mb vapor pressure). These differences were small, however, since the gradients from the six experiments were encompassed in the range 16 ± 3 $\mu g\ cm^{-3}$. Therefore, significant differences in transpiration could be attributed primarily to differences in resistance to movement of water vapor, i.e., the denominator of the transpiration equation. Furthermore, the similarity of the R_A values among species necessarily points to the R_L data as the main source of transpiration differences. In general, the lower epidermis tended to show a lower R_L than the upper epidermis. Generally speaking, then, those species demonstrating lower overall R_L values had the highest transpiration rate; sunflower (E-4) is the notable example.

The poor agreement between calculated and measured transpiration in lemon may be due as much to the weighing error involved in measuring extremely low rates of water loss, as to the calculated value; this also may apply to cotton (E-1), but not necessarily. In general, the agreement between calculated and measured values was not as good at low as at high illuminance levels. Yet in the case of cotton (E-5), the error of only 9 percent represents an excellent

verification of the principles involved. On the whole, however, agreement between calculated and measured data can be described as only reasonably good.

II. Experiments at High Illuminance Levels

Levels of both illuminance and irradiance were considerably higher than in the first set of experiments (Table 3). In experiments E-4, E-5, and E-6 the radiant environment simulated outdoor conditions, although not at maximum levels. The additional radiant energy absorbed by the leaves caused leaf temperatures to equal or exceed air temperature in cotton, lemon, and bean, but not in sunflower. The ability of sunflower to develop a lower R_L than the other species led to a higher transpiration rate per unit area, as before. Therefore, the greater amount of evaporative cooling cancelled heat gain more effectively in sunflower than in the other species. Table 3 shows that the best agreement between calculated and measured transpiration rates occurred in cotton (E-5), as before, where the error was only 12 percent at the high illuminance level. For the experiments as a whole, the calculated value was an overestimate in all instances but one, bean (E-6). The usual discrepancy was about 20 percent. The large error for cotton (E-1) and sunflower (E-2-II) probably cannot be attributed to weighing error, since transpiration rates for all experiments at high light intensity were reasonably high. The expected improvement in accuracy due to instrumentation of each leaf was realized only for cotton (E-5, at both light intensities). For the other species the discrepancy was about 20 percent, representing no improvement over the previous results obtained by averaging leaf temperature over the upper and lower halves of the plant. This information nevertheless points to the most likely source of error, the R_L values. These R_L values are based on a sound calibration technique, one in which a resistance to diffusion of water vapor was achieved by imposing different path lengths between the source of water vapor and the sensor of the leaf resistance meter. The original calibration was confirmed last year. However, it is possible that an

alternate calibration method would be preferable to the one used. The alternate method would develop a resistance, analogous to the resistance of closed stomates, by the presence of different numbers of tiny perforations in a barrier imposed in a fixed position between source and sensor.

The conclusion is that the extent of agreement achieved between calculated and measured transpiration is sufficient to have verified the transpiration equation; therefore, the experimental data support a rational view of the whole transpiration process. No further refinement of the technique is contemplated in the laboratory. On the other hand, it might be worthwhile to adapt this method to the field, making use of plants on lysimeters. This approach, if successful, would lead to separate measurements of transpiration and soil evaporation, a problem that up to now has proved intractable.

Table 1. Grand summary of evaporation from blotter leaf replicates

Expt. No. 1/	Simulated Crop	Blotter Temp. 2/	d_v Blotter 3/	d_v Air	Δd_v	E 4/	R_A 5/
	A. - Darkness or low light intensity						
E-1	Cotton	21.9	19.81	11.62	8.19	4.88	1.7
E-2	Sunflower	21.2	19.02	12.40	6.62	4.71	1.4
E-3	Lemon	21.8	19.70	13.66	6.04	4.36	1.4
E-4	Sunflower	20.9	18.68	11.11	7.57	6.73	1.1
E-5	Cotton	21.0	18.83	10.70	8.13	5.82	1.4
E-6	Bean	20.9	18.65	11.24	7.41	7.10	1.0
	B. - High light intensity						
E-1	Cotton	24.8	23.49	11.62	11.87	6.60	1.8
E-2	Sunflower	24.1	22.58	12.38	10.20	6.41	1.6
E-3	Lemon	24.0	22.43	13.65	8.78	6.08	1.4
E-4	Sunflower	24.7	23.35	10.92	12.43	12.10	1.0
E-5	Cotton	24.3	23.07	10.50	12.57	12.45	1.0
E-6	Bean	25.1	23.98	11.24	12.70	13.58	0.94

1/ E-1, E-2, E-3 with mylar panel between the upper and lower plenum, and with fluorescent lights. E-4, E-5, E-6 without panel, and with mercury vapor lights. Standard conditions: air temperature, 30.0 C, vapor pressure, 15.0 mb.

2/ Degrees C. as measured by embedded thermocouples.

3/ Density of water vapor, in $\mu g\ cm^{-3}$, based on blotter temperature.

4/ Evaporation, in $\mu g\ cm^{-2}\ sec^{-1}$, on a total surface basis, i.e., the area being the sum of upper and lower surfaces.

5/ Boundary layer resistance, in $sec\ cm^{-1}$, obtained by dividing Δd_v by E.

Table 2. Summary of six experiments on calculation of transpiration

Expt. No. & Crop	Flux density 1/ 0.4-0.8μ	Flux density 1/ 0.3-2.3μ	Leaf 2/ Temp.	d_v 3/ Leaf	d_v 4/ Air	5/ Δd_v	6/ R_A	R_L 7/ Lo. epid.	R_L 7/ Up. epid.	Calc. 8/ Transp.	Meas. 9/ Transp.	Calc./Meas.
					Low light intensity							
E-1 Cotton	0.93	0.01	29.0	29.94	11.62	18.32	1.7	11.5	25.6	2.05	1.05	1.96
E-2 Sunfl.	0.00	0.00	28.0	28.29	12.40	15.89	1.4	9.0	19.1	2.28	1.49	1.53
E-3 Lemon	0.00	0.00	29.2	30.29	13.66	16.63	1.4	13.4	52.5	1.42	0.50	2.82
E-4 Sunfl.	7.0	0.07	(24.9) 10/	(24.56)	11.11	(13.45)	1.1	(3.4)	(2.8)	5.95	7.50	0.80
E-5 Cotton	2.8	0.03	(29.3)	(29.62)	10.70	(18.92)	1.4	(15.6)	(17.0)	2.02	1.86	1.09
E-6 Bean	2.2	0.02	(28.6)	(29.30)	11.24	(18.06)	1.0	(17.0)	(113)	1.14	2.51	0.45

1/ 0.4-0.8μ, in kilolux; 0.3-2.3μ, in ly min^{-1}

2/ ^{o}C

3/ Vapor density in the leaf, in μg cm^{-3}

4/ Vapor density of the ambient air, in μg cm^{-3}

5/ Gradient in vapor density from leaf to air

6/ Boundary layer resistance, in sec cm^{-1}

7/ Leaf diffusion resistance of the lower and upper epidermes, in sec cm^{-1}

8/ Calculated transpiration, in μg cm^{-2} sec^{-1}, single surface basis

9/ Transpiration measured by weight loss, in μg cm^{-2} sec^{-1}, single surface basis

10/ Values in parentheses are for comparative purposes only; the calculations were not made from the mean data given in the parentheses, but rather from data from individual leaves.

Table 3. Continuation of summary for six transpiration experiments

Expt. No. & Crop	Flux density 1/ 0.4-0.8μ	Flux density 1/ 0.3-2.3μ	Leaf 2/ Temp.	High light intensity: d_v 3/ Leaf	d_v 4/ Air	5/ Δd_v	6/ R_A	R_L 7/ Lo. epid.	R_L 7/ up. epid.	Calc. 8/ Transp.	Meas. 9/ Transp.	Calc./Meas.
E-1	34.6	0.31	31.5	34.52	11.62	22.90	1.8	7.2	11.0	4.37	2.23	1.96
E-2-I Sunfl.	28.1	0.25	26.9	26.56	12.38	14.18	1.6	1.4	1.9	9.05	7.43	1.22
E-2-II Sunfl.	28.1	0.25	28.6	29.23	12.38	16.85	1.6	2.2	4.3	7.43	5.43	1.37
E-3 Lemon	26.1	0.23	30.0	31.70	13.65	18.05	1.4	2.5	34.8	5.20	4.30	1.21
E-4 Sunfl.	65.6	0.66	(29.2) 10/	(30.32)	10.92	(19.40)	1.0	(1.6)	(0.26)	19.10	16.01	1.19
E-5 Cotton	61.2	0.61	(33.7)	(39.29)	10.50	(28.79)	1.0	(9.6)	(3.3)	9.07	8.07	1.12
E-6 Bean	53.3	0.53	(31.6)	(34.67)	11.24	(23.43)	0.9	(4.5)	(8.4)	6.92	8.92	0.78

1/ See the accompanying page (data for low light intensity) for explanation of foot notes.

PART III. CHANGES IN LEAF DIFFUSION RESISTANCE, LEAF TEMPERATURE, AND LEAF WATER CONTENT OF FIELD SORGHUM IN RESPONSE TO DECLINING SOIL WATER CONTENT.

INTRODUCTION:

It has become increasingly apparent that understanding a complex field environment requires multiple measurements of a large number of variables over an extended time. For the past two summers the lysimeter field has been planted to sorghum in an experimental approach to agricultural meteorology (Refer to WCL-33). In essence the experiments consisted of complete characterization of the crop response to a gradual decline in soil water content and to an abrupt restoring of soil water by a heavy irrigation. Changes in evapotranspiration, and the water vapor diffusion resistance of the whole canopy, and in associated meteorological parameters are dealt with elsewhere (WCL-33). This report is limited to the measurements and the responses of individual leaves. Data were obtained for stomatal aperture (leaf diffusion resistance, R_L), leaf temperature, and leaf water content, as well as for rate of growth in height and leaf area.

PROCEDURE:

More complete measurements were made in the repetition (June, 1966) than in the 1965 experiment, but over only one drying cycle instead of three. Only a brief description of the procedure will be given now; details are deferred until a complete presentation of the results in a later report.

The lysimeter field was planted to RS-610 sorghum broadcast over a total of seven borders, instead of being drilled in rows, as before. During crop development several measurements of leaf area, height, and general appearance (by photographs) were made. The experiment was terminated before mature grain was formed.

Leaf temperature was measured by four separate thermocouples, sewn into the leaf midrib, wired in parallel, each thermocouple being in the leaf of a separate plant. The four plants were located within a square meter of field area at a given site. This arrangement

was repeated at two elevations in the canopy, an upper, well-exposed one, and another two nodes down the stem. Five sites were instrumented in this manner, two in the field and one in each of the three lysimeters. The signals from the thermocouples were conducted to the data handling system, referenced against a cold junction, and put on punched tape at frequent intervals.

Leaf water content was assessed by beta ray gauge measurements on a representative leaf in a field plot and in lysimeter No. 1. Actually, beta ray gauges measure leaf thickness, with the assumption that changes in thickness are due almost exclusively to a net change in leaf water content. Leaf water content at dawn is used as a reference value, one indicating adequate hydration. Stronger sources of beta radiation were used in 1966 than in the previous year, and Tc^{99} instead of Pm^{147}, to gain the advantage of the longer half life of the former.

Leaf diffusion resistance readings were taken with the resistance meter on a routine basis three times per day at suitable intervals during the drying cycle. Readings were taken on the five plots used for temperature monitoring. Leaf temperature depression (leaf temperature minus air temperature of the bulk air) progressively rose with time as the drying cycle advanced. This indication, as well as the detection of a partial midday stomatal closure, as shown by a significant rise in leaf diffusion resistance, signalled the proper time for an intensive measurement period. This took place over a 24-hour period, when data on leaf response were taken every 15 or 30 minutes, depending on the parameter. All pertinent meteorological data, as well as evapotranspiration from the lysimeters, were recorded automatically, along with the specific types of leaf measurements reported here. Following a heavy irrigation, the same intensive measurements were repeated, to measure the crop's response to alleviation of a severe drought. This second set of measurements occurred on the next day after irrigation, in order to exclude possible effects of rapid regrowth of the plants after irrigation.

RESULTS:

Although the experimental data have been programmed and processed by the computer, they have not been thoroughly analyzed yet. No preliminary results are included in this report.

GENERAL SUMMARY AND CONCLUSIONS:

Close simulation of outdoor radiant conditions was achieved in the Controlled Environment Room by use of mercury vapor instead of fluorescent lamps. The flux density from 120 lamps (117 kilolux, 1.2 ly min^{-1} at 1.5 m) can induce full stomatal opening and impose a realistic heat load on leaves. The improvement is due to (1) high output lamps, (2) dense arrangement, (3) elimination of the mylar panel separating the lamps from the room proper, and (4) application of aluminized mylar to the walls. Despite the lower emission of mercury vapor light than sunlight from 0.450 to 0.520 μ, this spectral range is unimportant in stomatal opening or photosynthesis.

Plant and environmental measurements supplied data for calculating transpiration of cotton, sunflower, lemon, and bean under controlled conditions. In six experiments each species was tested in complete or virtual darkness and at high illuminance, up to 60 kilolux. In the last three experiments the temperature of every leaf was measured. Knowledge of leaf temperature, leaf diffusion resistance, ambient vapor density, and boundary layer resistance permitted calculation of transpiration for individual leaves, a more accurate method than that used earlier. Agreement between calculated transpiration and that measured gravimetrically ranged from poor, for lemon (where weighing error may be involved) to good, for cotton, with a 10 percent error. On the whole, calculated transpiration was within 20 percent of the reference value. The overall agreement is believed sufficient to have verified the transpiration equation. The consequent enhanced understanding of transpiration ultimately may lead to separation of transpiration from evaporation in the field.

As part of a comprehensive experiment on the agricultural meteorology of sorghum, leaf response to a declining soil water content was measured routinely over several weeks and intensively for 24 hours. After a heavy irrigation, intensive measurements were

repeated. Representative areas in the field (two sites) and in three lysimeters were monitored for leaf temperature at two heights on the plant, leaf water content changes (by beta ray gauging), and leaf diffusion resistance. Observations on crop development were made, including height, leaf area, and general condition (by photographs). These measurements were accompanied by precise determination of evapotranspiration and numerous meteorological measurements. The results are not yet ready for presentation.

PERSONNEL:

W. L. Ehrler and C. H. M van Bavel

TITLE: QUANTITATIVE MEASUREMENT OF WATER FLOW WITH CHEMICAL TRACERS

LINE PROJECT: SWC X-gG1 CODE NO.: Ariz.-WCL-30

INTRODUCTION:

See Annual Report for 1965.

Further studies designed to evaluate possible dye tracer losses to channel boundaries were postponed until the spring irrigation season of 1967. Active research on the project will resume at that time.

PROCEDURE:

No new data or analyses were collected or conducted during this calendar year.

RESULTS AND DISCUSSION:

Results and techniques developed were published in Proceedings of ASCE, September, 1966, pages 1 to 15 under the title "Flow Measurements with Fluorescent Tracers" by Replogle, Myers, and Brust, which summarizes the results reported in Annual Reports 1965 and previous.

SUMMARY AND CONCLUSIONS:

Laboratory studies were conducted to obtain information relative to the accuracy and precision with which fluorescent tracers can be used to determine stream discharge.

Fluorescent tracer concentrations of less than 10 ppb can be quantitatively detected in most natural stream waters with errors less than $\pm$ 1 percent. This permits stream gaging with a potential accuracy of this same order provided the tracer is not adsorbed on the stream boundaries and adequate mixing of tracer with stream flow is obtained.

Flow measurement with fluorescent dyes, using integrated sample dilution technique, requires no special handling of materials, presents no health hazard through the water supply being measured, and is convenient to apply to natural streams, since it eliminates the requirement for detailed channel data.

Loss of Rhodamine WT to the stream boundaries does not appear to be a significant problem.

Accurate flow measurements with fluorescent dye dilution methods require the use of precision procedures including preparation of comparison standards by weighing techniques, the use of continuous flow

sample cuvettes, the application of accurate temperature correction coefficients, and proper sampling techniques.

Reliable criteria for guaranteeing adequate lateral mixing require further study. The sampling technique indicates whether mixing was adequate, but this is "after-the-fact" and deserves improvement. Preliminary data indicate that the effects of tracer losses to the stream boundaries may be negligible.

PERSONNEL: J. A. Replogle

TITLE: DIRECT MEASUREMENT OF EVAPOTRANSPIRATION AND THE ENERGY BALANCE OF IRRIGATED CROPS

LINE PROJECT: SWC IX-gG1 CODE NO.: Ariz-WCL-33

INTRODUCTION:

In 1965 an experiment was conducted in the lysimeter field with a crop of sorghum planted in rows. The objective was to determine the relationship between leaf resistance and canopy resistance, and, also, to describe the total energy balance of the sorghum crop as it was subjected to different conditions of soil water availability during one or more prolonged irrigation cycles. The 1965 experiment was preliminary because several defects in the design and instrumentation resulted in inconclusive data. Nevertheless, it was found conclusively that soil water has to be depleted to a very large extent until measureable effects appear in the role that the canopy plays in the evaporation and, furthermore, that there seems to be a fairly straightforward relationship between leaf resistance and canopy resistance. It was also noted that the depletion of soil water as found from neutron measurements did not agree well with the actually measured values of evaporation from the lysimeters.

Therefore, it was decided to repeat the entire experiment in order to attain its principal objectives, as outlined above, more precisely. We also resolved to make a closer study of the entire question of soil water depletion under an evaporating crop as it pertains to the interpretation of such data in terms of water loss to the atmosphere (consumptive use). Thus, the 1966 experiment, although resembling the 1965 work to some extent, consisted essentially of two parallel efforts. The first, to characterize the energy balance of the sorghum crop, and to study the relation between leaf resistance and canopy resistance, and the second, to describe the hydraulic properties of the soil on which the crop was grown and to obtain precise data on soil water content. Thus, we proposed to study the relationship between soil water depletion and evaporation, on the one hand, and on the other, to test ideas, that have already been advanced in literature, on the correction of soil water depletion data for

the effect of downward flow of water.

The second phase of the study has been concluded during the 1966 year, and will be reported here. The data on the first phase, although completely available and ready for interpretation, have not been studied as yet and will, therefore, not be discussed.

PROCEDURE:

In order to facilitate the study of soil water depletion, which is basically a special case of distribution of soil water after irrigation, a test plot was built within the lysimeter field. The general nature of this plot is apparent from Figure 1.

By filling the upstream border with water and allowing the water to cover the test plot within a period of about three to four minutes by means of the gates in the plywood borders, a rapid and uniform application of water was possible. Following each irrigation the distribution of water within the 170 cm profile was followed by frequent measurements of soil water content with an improved neutron technique and by reading tensiometers installed at four sites within the plot and spaced at 10 or 20 cm intervals.

Prior to planting the sorghum, a distribution experiment was carried out in which the soil was bare and covered with a plastic sheet. This experiment should have provided all of the necessary data on the hydraulic properties of the soil but, unfortunately, a 7 mm rainstorm four days after irrigation made a good part of the data invalid or impossible to obtain. Therefore, two additional bare soil studies were carried out, but without the plastic sheet in place, the third irrigation being coincident with the planting of the sorghum on 27 April. The first planting was not entirely successful and it was therefore repeated on 6 May. The resulting crop, planted by broadcasting, developed into a complete cover, which had exhausted the greater part of the available soil water reserves by the 1st of June and exhibited symptoms of drought. The irrigation applied on the 1st of June provided the first opportunity to study soil moisture depletion under a crop throughout a thirty day period, at the end of which most of the soil water had again been used by the crop, so that

a last irrigation was applied on 2 July. The dates and quantities of irrigation, together with other pertinent information are summarized in Table 1.

Date	Application	Surface Condition
22 March	1st (140 mm)	Bare soil (covered 23 Mar-4 Apr.)
26 March	Rained ~7 mm	Bare soil
7 April	2nd (115 mm)	Bare soil
27 April	3rd (120 mm)	Bare soil (first planting)
6 May	4th (118 mm)	Bare soil (second planting)
1 June	5th (196 mm)	Sorghum crop (HT.~40 cm)
20 June	Rained ~0.4 mm	Sorghum crop (L.A.I.~5, heads emerging)
30 June	Rained ~ 0.8 mm	Sorghum crop
2 July	6th (328 mm)	Sorghum crop (L.A.I.~4, HT.~72 cm)

The improvements in the soil water measurement with the neutron technique consisted in using a 150 mc americium-beryllium neutron source, together with a line operated timer and scaler. Using half-minute counts we obtained a high degree of precision, equivalent to about .001 water content by volume. The details of the procedure have been documented in an article about to be published in the JOURNAL OF HYDROLOGY.

The hydraulic head in the profile was measured with Lark tensiometers using mercury manometers, grouped in banks around each access tube.

Using the data obtained during the three bare soil irrigations (No. 1, 2 and 3), both the soil water characteristic and the conductivity characteristic of the soil profile could be determined using an instantaneous flux method, as proposed for column studies by Watson, and making the computations by a time sharing computer method. This procedure gave the hydraulic properties for the soil on each of four sites, and in 10 cm layers. Subsequently, the data for the two crop irrigations (No. 5 and 6) could be used for a separation of the

hydraulic component and the root water absorption component making up the total depletion. A similar method has been used before by Ogata at the Salinity Laboratory and by Rose and Stern in Australia.

An alternate procedure for analyzing the data consisted in using the conventional method of computing the total water content of the profile and its change (depletion) with time. The depletion rates thus obtained were then compared with the directly measured values of evapotranspiration based on the lysimeter data. Careful management of the lysimeters and of the test plot, and comparative measurements of the energy balance and of canopy temperatures insured that conditions in and over the two sites were substantially equal.

RESULTS AND DISCUSSION:

The data obtained during the first three irrigations can be considered as the calibration of the test sites, whereas the actual data of interest were provided by the fifth and sixth irrigation (see Table 1.) Even though the calibration observations were marred by the rainstorm occurring during the first irrigation, and by the fact that a somewhat arbitrary correction for surface evaporation had to be applied during irrigations 2 and 3, the data resulted in a consistent picture of both the water and the conductivity characteristics of the soil in situ. It is important to note that very few studies of this kind have been conducted, most others being based on observations made on soil cores in the laboratory. An example of a typical result is given in Figure 2, which shows the conductivity characteristic at one site at 60 cm depth. It was found that the conductivity characteristic differed between sites at the same depth, and even more so between depths. Generally speaking, the profile exhibited a greater conductivity with depth until the 100-110 cm layer, where an abrupt change to a smaller conductivity was typically found.

The second significant result was that neither the water content characteristic nor the conductivity characteristic exhibited any sudden transitions, but that a smooth relation between water pressure and conductivity versus water content was found. A definite air entry value, for example, cannot be assigned to this material, which

is typically permeated with large root and worm holes, as a number of photographs of undisturbed material indicated.

A calculation of the distribution of root activity with depth becomes possible, when the hydraulic characteristics of the soil are known, by considering the following expression:

$$\partial\theta/\partial t - \partial v/\partial z = r_z$$

In words this formula says that the change of water content with time at any given point minus the vertical divergence of the flux equals the root extraction rate. Application of this method to the data of irrigation cycle No. 5 gave the result indicated in Figure 3. The root extraction rate, in this case, also includes the direct evaporation from the soil surface. The distributions given in Figure 3 are quite reasonable. The integration of r_z with depth should result in the total evaporation rate or the consumptive use rate. These integrals are also indicated in Figure 3, and they compare reasonably well with the measured evaporation rates, except that the latter are higher by 20 to 30 percent. This is attributed to the fact that all measurements leading to the Figure 3 were taken early in the morning, before the impact of the maximum evaporation rate on the depth distribution of hydraulic head and water content.

Of more practical interest is a comparison of the depletion rate with the evaporation rate. If the depletion refers to a 170 cm layer, the difference between the two quantities is the flux at the 170 cm depth. The flux at 170 cm, as obtained in this way, is shown in Figure 4, against the time from the start of irrigation. Figure 4 indicates that water continues to be highly mobile in the soil profile for a long time after the application of water. First of all, during the irrigation cycles 2 and 3 on bare soil one can see that water continues to leave the profile at substantial rates, in excess of 2 mm per day for as long as 100-200 hours after the irrigation. When a crop is present, as in irrigation cycles 5 and 6, an almost identical situation prevails until about 100 hours after the irrigation. The

flux becomes zero at 200 hours after irrigation, and reverses itself to become significantly negative. This finding is not generally recognized in literature. Generally, it is conceded that in the early part of an irrigation cycle there is considerable downward movement, but little thought is given to the possibility of significant upward movement from wet soil into the root zone above. Our data make it clear that this movement exists, and that it is significant: in fact by the end of the irrigation cycle it was contributing some 3 or 4 mm, or 30 percent of the total consumptive use rate of the crop.

The data shown, and others obtained during this study, make it plain that one cannot expect to draw any conclusions concerning short-time evaporation or consumptive use rates of a crop from soil moisture depletion data alone. In the beginning of the irrigation cycle the latter will give serious overestimates, and in the latter part of the cycle they give significant underestimates of the consumptive use.

It is worthwhile to inquire whether any reliable corrections can be made. One of these has been suggested in 1960 by Willcox in which he proposed to subtract the depletion rate of a bare and covered plot from the cropped plot at the same water content. This approach, we found, does an inadequate job of correcting for downward flux in the beginning of the period, and it cannot account at all for the upward flux that we described above.

A more fundamental approach would be to predict the flux at 170 cm from measurements of the hydraulic gradient and from the known water conductivity as it follows from water content measurements. Results from this procedure were equally disappointing. In the beginning of the period a fairly adequate correction could be obtained, but in the end of the period the estimated flux was considerably higher - in absolute terms - than the actually occurring one. Again, this is attributed to the fact that all measurements of the gradient and of the water content at 170 cm were made during the early morning, and so could not be representative of the situation during the principal time of water extraction. Correction of depletion amounts, using an estimate of the hydraulic flux is, at best, laborious and it is subject

to all the uncertainties that are brought into the picture by the lack of homogeneity of the soil and its hydraulic properties. Also, the conductivities for the lower water contents required extrapolation of the K-θ.

From our experience we are led to believe that a direct measurement of consumptive use, either by weighing methods or by micrometeorological methods is more precise and more representative of the true value than values obtained from measurements of soil water depletion, whether an attempt towards correction of the latter is made or not. Certainly, the depletion method should never be considered as a standard for other methods, but rather the reverse is true.

The details of this investigation are described in a series of publications entitled "Hydraulic Properties of a Clay Loam Soil and the Field Measurement of Water Obtained by Roots", in addition to the publication referred to above.

SUMMARY AND CONCLUSIONS:

An experiment was conducted on the lysimeter field in which the distribution of irrigation water in the profile was studied by means of frequent measurements of the water profile content and of the hydraulic head profile in three irrigation cycles of a bare soil. From this data the water retaining and water conducting properties of the soil were determined, so as to yield a complete hydraulic description of the material, as it varies with depth, and as it exists in the field. Data so obtained do not necessarily show a close resemblance to laboratory data obtained on soil samples.

Once the hydraulic properties of the soil had been ascertained the experiment was continued by studying the distribution of irrigation water at the same site and in the presence of an actively growing and transpiring sorghum crop. The measured changes in soil water content were divided in the two components, one attributable to root extraction and the other to flow of water under the influence of hydraulic gradients. The gradient involved was measured directly and the conductivity was obtained from the conductivity characteristics

obtained earlier. The distribution of root activity and its integral with depth gave reasonable values, but the latter did not agree perfectly with the rate of evaporation measured with lysimeters.

A direct comparison of the depletion for the entire profile and measured evaporation rates exhibited great discrepancies. In the first few days after irrigation, the depletion rate was several times larger than evaporation rate. Later, as much as four to six days after irrigation, depletion still exceeded evaporation significantly, then became equal to it and subsequently, the depletion became less than the evaporation. This implies a movement upward from wet soil, that is not permeated with roots, into the root zone proper. It is often assumed that this movement exists on paper, but in actuality does not amount to much. Our data showed such an idea to be false, and imply upward movement of water at 170 cm depth at rates of 3 to 4 mm per day. This is a significant part of the total consumptive use and is of special agronomic significance since it occurs in the latter part of the irrigation cycle.

Depletion rates, as usually obtained, can be corrected for downward flux and thus come closer to true evaporation rates. A correction for upward flux is also possible if the hydraulic properties of the soil are known and if the hydraulic gradients are measured. None of these corrections appeared to be very precise, and we are led to the conclusion that any depletion method is only an approximation of the true evaporation rate which, preferably, should be measured in some other way.

PERSONNEL:

C. H. M. van Bavel, K. J. Brust, W. L. Ehrler, G. B. Stirk

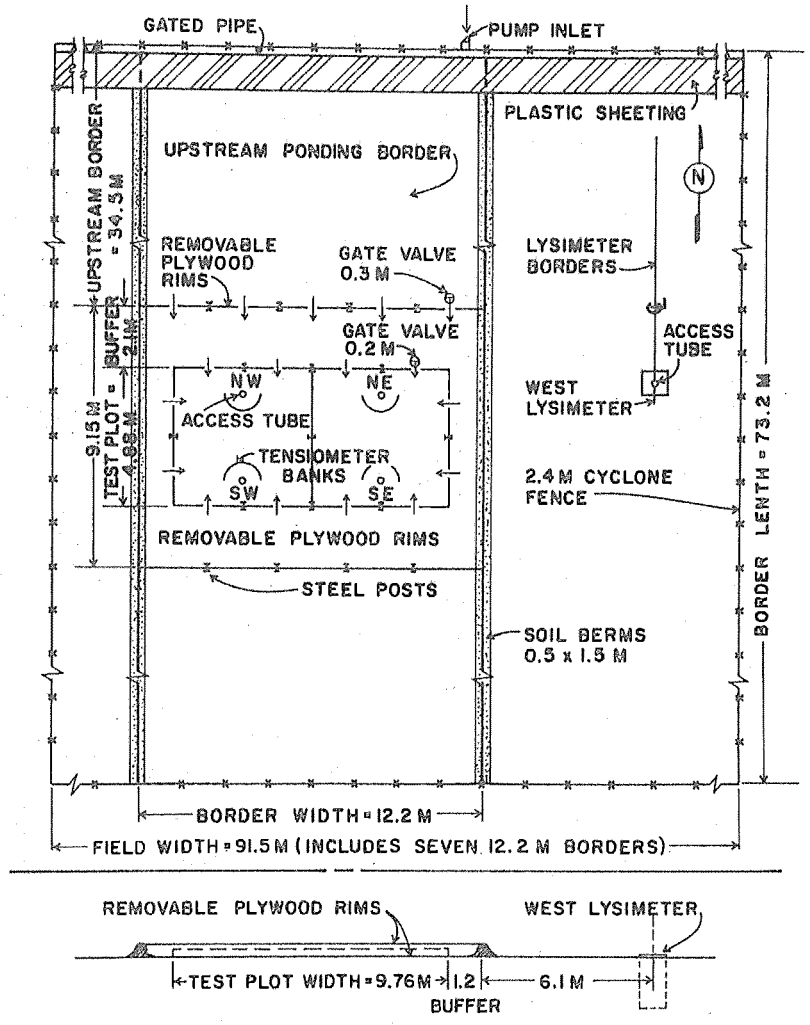

Figure 1. Layout of experimental plot for 1966 studies.

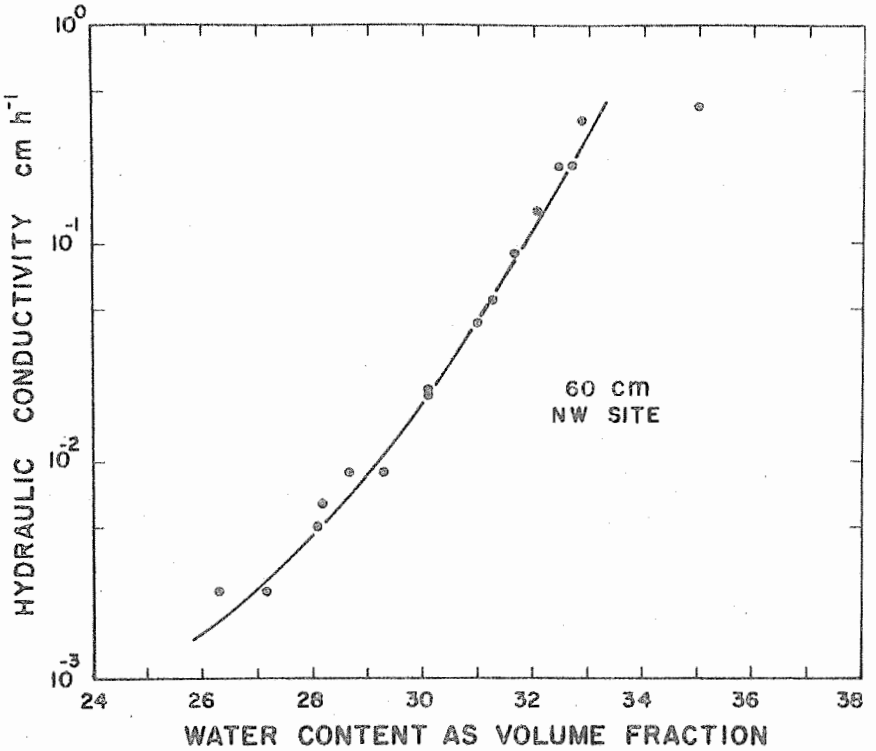

Figure 2. Hydraulic conductivity against water content at 60 cm depth at the NW site.

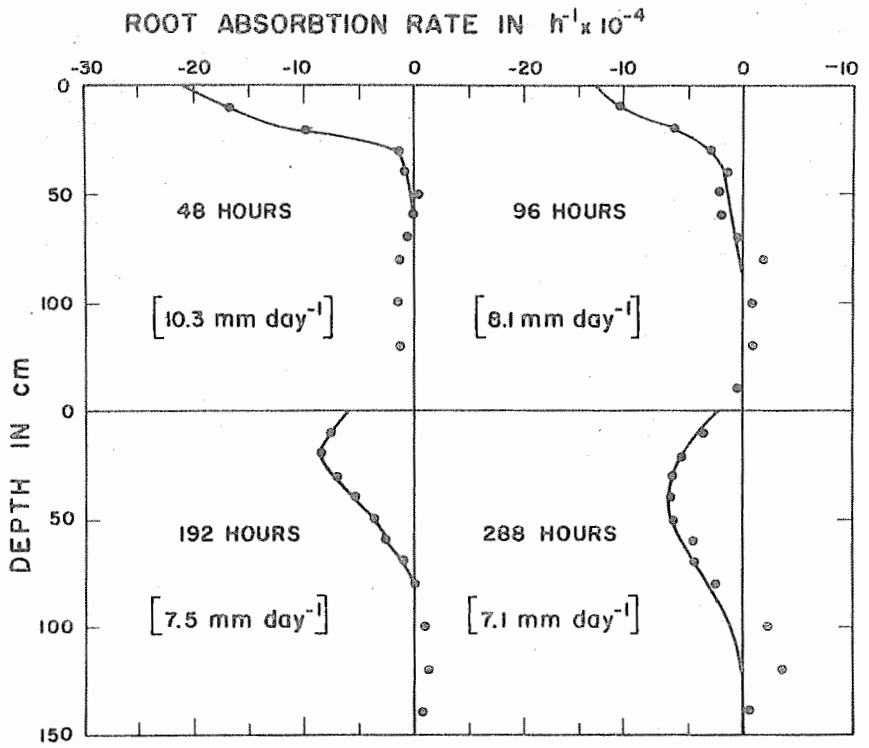

Figure 3. Root extraction rate with depth after irrigation.

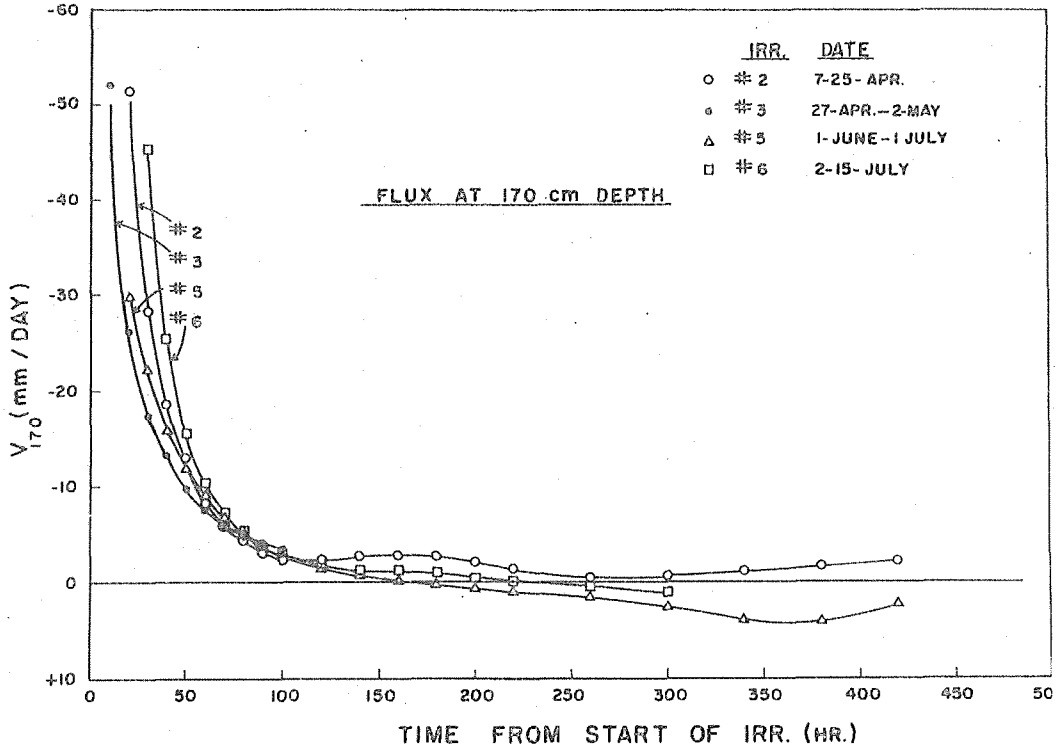

Figure 4. Hydraulic flux at 170 cm depth in mm day^{-1} against time in hours after irrigation No. 5.

TITLE: WATER MANAGEMENT FOR THE EFFICIENT IRRIGATION OF SUGAR BEETS

LINE PROJECT: SWC IX gG3 CODE NO.: Ariz.-WCL-36

INTRODUCTION:

See Annual Report for 1965. The objective of the experiment is to determine the irrigation requirements of sugar beets for maximum economic yield per unit of water.

PROCEDURE:

The experiment is located at the University of Arizona Experiment Farm, Mesa, Arizona.

Four borders, each 270 x 33 feet, were split into 48 plots (each 16.5 x 33 feet) containing eight rows of beets, planted September 22, two rows on a 40-inch bed. Eight irrigation treatments were replicated six times in a randomized block design. Eighty units of phosphate and 100 units of nitrogen were applied previous to planting of 301H monogerm beet seed. An additional 70 units of nitrogen were applied after thinning. The seed was germinated by irrigating up with at least one acre-foot applied. A pre-determined quantity of water was pumped and measured with a Sparling meter into the respective plots at each subsequent irrigation. Hand thinning, normal cultivation and weed control were conducted.

Treatments and Variables

A. Under investigation: (soil moisture)

Treatment 1 - irrigate when less than 40 percent of the available water in the top three feet of soil was depleted.

(1) 1A - irrigate continuously until harvest.

(2) 1A - 3A irrigate until April 5, then like 3A.

Treatment 2 - irrigate when 60 percent of the available water in the top three feet was depleted.

(4) 2A - irrigate continuously until harvest.

(6) 2A - 3A irrigate until April 5, then like 3A.

Treatment 3 - irrigate when 80 percent of the available water in the top three feet was depleted.

(7) 3A - irrigate continuously until harvest.

(8) 3A - 1A irrigate until April 5, then like 1A.

(9) 3A - 2A irrigate until April 5, then like 2A.

Treatment 4 - irrigate only when a visual moisture stress appeared.

(10) 4A - irrigate continuously until harvest.

The basic treatments, 1A, 2A, and 3A, were designed to cover the regime of very dry to wet. The April change in schedule was designed to determine if such a procedure was desirable from the standpoint of production and water conservation.

Data to be Obtained

1. Quantity of water applied by measurement with a Sparling meter.
2. Soil-moisture depletion by gravimetric sampling.
3. Growth rate measurements and plant physiology.
4. Yield and sucrose measurements on four harvest dates.

Methods of Interpreting Results

1. Analysis of variance.

Source	df
Main plots	47
Treatments	7
Replications	5
Error	35

FIELD PLAN

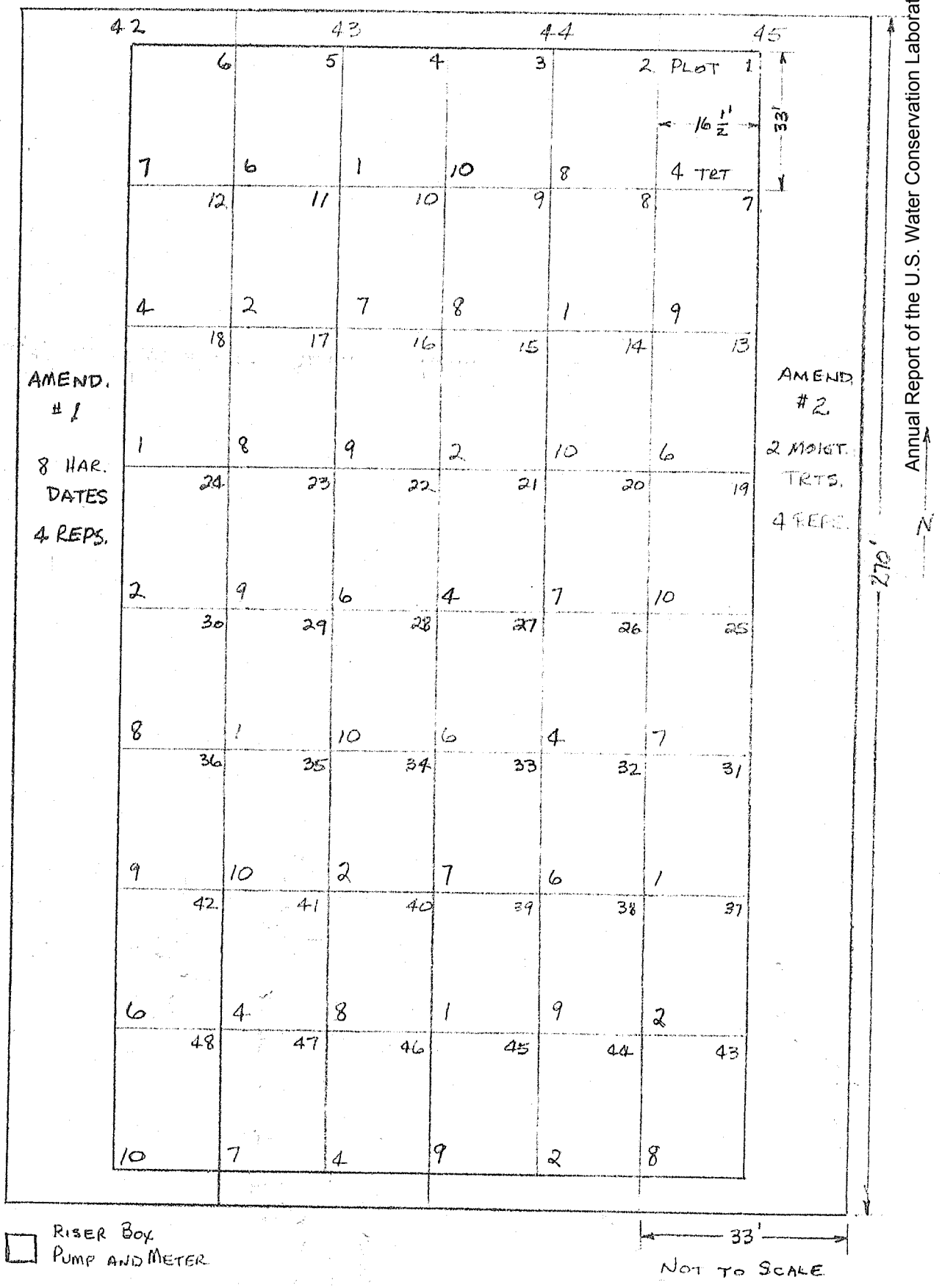
42
43
44
45
6 5 4 3 2 PLOT 1
16 1/2'
33'
7 6 1 10 8 4 TRT
12 11 10 9 8 7
4 2 7 8 1 9
18 17 16 15 14 13
AMEND. #1
8 HAR. DATES
4 REPS.
AMEND. #2
2 MOIST. TRTS.
4 REPS.
1 8 9 2 10 6
24 23 22 21 20 19
2 9 6 4 7 10
30 29 28 27 26 25
8 1 10 6 4 7
36 35 34 33 32 31
9 10 2 7 6 1
42 41 40 39 38 37
6 4 8 1 9 2
48 47 46 45 44 43
10 7 4 9 2 8
270'
N
33'
RISER BOX
PUMP AND METER
NOT TO SCALE

DATES

TRT.	9/24	11/6	3/10	3/16	3/30	4/4	4/7	4/18	4/27	5/4	5/15	5/12	5/20	5/28	6/12	6/14	6/23	6/27	TOTAL
1	X	X	X		X		X	X		X		X		X	X	X	X		12
2	X	X	X		X		X		X			X			X		X		9
4	X	X		X		X		X			X		X		X	X		X	10
6	X	X		X		X			X			X			X		X		8
7	X	X				X			X			X			X		X		7
8	X	X				X		X		X		X		X	X	X	X		10
9	X	X				X		X			X		X		X	X		X	9
10	X	X					X				X				X			X	6

SCHEDULE OF IRRIGATIONS

AMENDMENT 1

TITLE: DETERMINATION OF THE RATIO OF ROOT TO TOP GROWTH FOR FALL-PLANTED SUGAR BEETS

LINE PROJECT: SWC IX gG3 CODE NO.: Ariz.-WCL-36

INTRODUCTION:

See Annual Report for 1965.

PROCEDURE:

The experiment is located at the University of Arizona Experiment Farm, Mesa, Arizona.

Treatments and Variables

A. Under investigation: (Harvest dates)

1. Eight harvest dates, starting on February 23, and thereafter at three-week intervals. The February 23 harvest date was indicated as No. 1, and the last harvest as No. 8.

Beets were planted and thinned to about one foot between plants. Plots were irrigated on the same schedule as 2A, a medium treatment scheduled to be irrigated when 60 percent of the available water was depleted from the top three feet of soil. At each of the eight harvest dates, six lineal feet in each of four rows of beets were harvested. Top growth and roots were weighed separately. Representative beet samples from each of the four replications were processed, and sugar content analysis made. The beet area involved was split into 32 plots, each plot 8 rows wide and 8 feet long. Harvest dates were replicated four times in a randomized block design.

Data to be Obtained

1. Weights of top growth and roots.
2. Sucrose content, starting in April.

Methods of Interpreting Results

1. Analysis of variance.

Source	df
Main plots	31
Harvest dates	7
Replications	3
Error	21

AMENDMENT 2

TITLE: EFFECT OF LATE SEASON SOIL MOISTURE STRESS ON SUCROSE CONTENT OF SUGAR BEETS

LINE PROJECT: SWC IX gG3 CODE NO.: Ariz.-WCL-36

INTRODUCTION:

See Annual Report for 1965.

PROCEDURE:

The experiment is located at the University of Arizona Experiment Farm, Mesa, Arizona.

Treatments and Variables

A. Under investigation: (moisture stress)

1. Two moisture treatments, one medium and the other very dry, were established, starting in April.
2. Harvest was conducted whenever the dry treatments showed visual moisture stress.

Beets were planted and thinned to about one foot between plants. Plots were irrigated initially on the same schedule as 2A, a medium treatment scheduled for irrigation when 60 percent of the available water was depleted from the top three feet of soil. At the irrigation date previous to each harvest, the medium treatment was irrigated but the dry treatment was not, thus establishing the two treatments. The buffer area (8 rows wide by 270' long) was divided into eight plots, each 33' long. Yields and sucrose measurements were made whenever dry plots reached a visual soil moisture stress appearance, from six rows, each four feet long. After each harvest date, both medium and dry treatments were allowed to dry out further, at which time an additional harvest was made. A week to ten days of additional drying-out occurred. Dry and medium plots were replicated four times.

Data to be Obtained

1. Weight of beets at each harvest date.
2. Sucrose content of beets at each harvest date.

Method of Interpreting Results

1. Analysis of variance

Source	df
Main plots	7
Moisture levels	1
Replications	3
Main plot error	3

RESULTS AND DISCUSSION:

Sugar beets were planted September 22, 1965, and irrigated up on September 24. Plants were thinned to about nine inches between plants on October 18. Plants were side dressed with 70 units of nitrogen and all plots were given an irrigation on November 6.

Aphids were controlled with "Meta-Systox" on November 5 and again on March 15. The incidence of "yellows" was considerably less than in 1964-65, probably due to good aphid control and a larger, more vigorous plant. In April and May, the beets were sprayed with "Kelthane" for control of red spider mites.

Main-plot study beets were harvested May 2 and 26, June 22, and July 7. Beets were harvested on four rows, each six feet long. Root and top measurements on Amendment 1 commenced on February 23, and continued at three-week intervals until 8 harvests had been completed. On Amendment 2, beets were harvested on May 6 and 16, June 9 and 15, and July 11 and 19. All beets were counted, weighed, and representative samples kept for sucrose measurements.

The water for the first two irrigations applied was not measured, other than by soil moisture sampling. All other irrigation water was measured with a Sparling meter. Soil moisture samples were taken on the planting date, at intervals of no more than 10 days, before and after each irrigation, and on the final harvest date. Samples were taken on three plots for each irrigation treatment and two samples consolidated from each plot. Soil samples were taken at 1-foot increments through six feet. The average percent soil moisture depletion in the top three

feet before each irrigation was 49, 66, 85, and 92 for the wet, medium, dry, and stress treatments, respectively. Due to heavy winter rains in December and January, there were no soil moisture differences established until early in March. Apparently, early season growing conditions were desirable, as plants were large and healthy.

TABLE 1.

MEAN PLOT YIELD IN POUNDS OF BEETS AT HARVEST DATES (6 REPS.)

May 2		May 26		June 22		July 7	
TRT	$\bar{x}$	TRT	$\bar{x}$	TRT	$\bar{x}$	TRT	$\bar{x}$
6	48.6	1	64.0	1	72.3	4	72.2
2	47.5	6	60.3	4	70.1	8	71.3
9	46.3	10	59.2	8	68.8	1	69.4
4	45.8	7	58.1	6	67.0	9	69.4
1	45.2	8	57.8	2	66.2	10	68.1
7	45.2	2	57.4	9	65.8	7	67.8
8	44.1	9	57.1	7	64.8	6	67.2
10	43.5	4	55.2	10	63.8	2	66.0
No Sig.		No Sig.		No Sig.		No Sig.	

To convert plot yields to pounds per acre, multiply ($\bar{x}$) (1089).

TABLE 2.

MEAN SUGAR PERCENTAGE AT HARVEST DATES (6 REPS.)

May 2		May 26		June 22		July 7	
TRT	$\bar{x}$	TRT	$\bar{x}$	TRT	$\bar{x}$	TRT	$\bar{x}$
10	13.7 a	10	14.3 a	6	15.1 a	6	13.8
4	13.3 ab	2	13.8 ab	7	14.9 a	4	13.7
1	13.1 ab	7	13.7 ab	2	14.8 a	2	13.7
8	12.8 abc	4	13.5 abc	10	14.7 a	8	13.7
9	12.8 bc	6	13.5 abc	4	14.2 a	10	13.2
2	12.7 bc	9	13.4 abc	1	14.1 a	1	13.2
6	12.6 bc	8	12.9 bc	8	13.9 ab	7	13.1
7	12.2 c	1	12.6 c	9	12.8 b	9	12.8
Sig. 1%		Sig. 1%		Sig. 5%		No Sig.	
LSD 0.83		LSD 1.11		LSD 1.26			

TABLE 3

MEAN YIELD OF SUGAR IN POUNDS PER PLOT AT HARVEST DATES (6 REPS.)

TRT	$\bar{x}$	TRT	$\bar{x}$	TRT	$\bar{x}$	TRT	$\bar{x}$
6	6.11	10	8.46	1	10.19	4	9.89
4	6.10	6	8.12	6	10.10	8	9.72
2	6.04	1	8.02	4	9.96	6	9.29
10	5.95	7	7.98	2	9.78	1	9.12
1	5.93	2	7.93	7	9.66	2	9.02
9	5.91	9	7.62	8	9.48	10	8.99
8	5.66	8	7.46	10	9.33	7	8.91
7	5.47	4	7.42	9	8.44	9	8.87
No Sig.		No Sig.		No Sig.		No Sig.	

To convert plot yields to pounds per acre, multiply ($\bar{x}$) (1089)

TABLE 4

DAYS FROM IRRIGATION UNTIL HARVEST

HARVEST DATE	TREATMENT			
	Wet	Medium	Dry	Stress
May 2	14	14	4	24
May 26	3	6	14	21
June 22	8	8	20	20
July 7	14	10	14	10

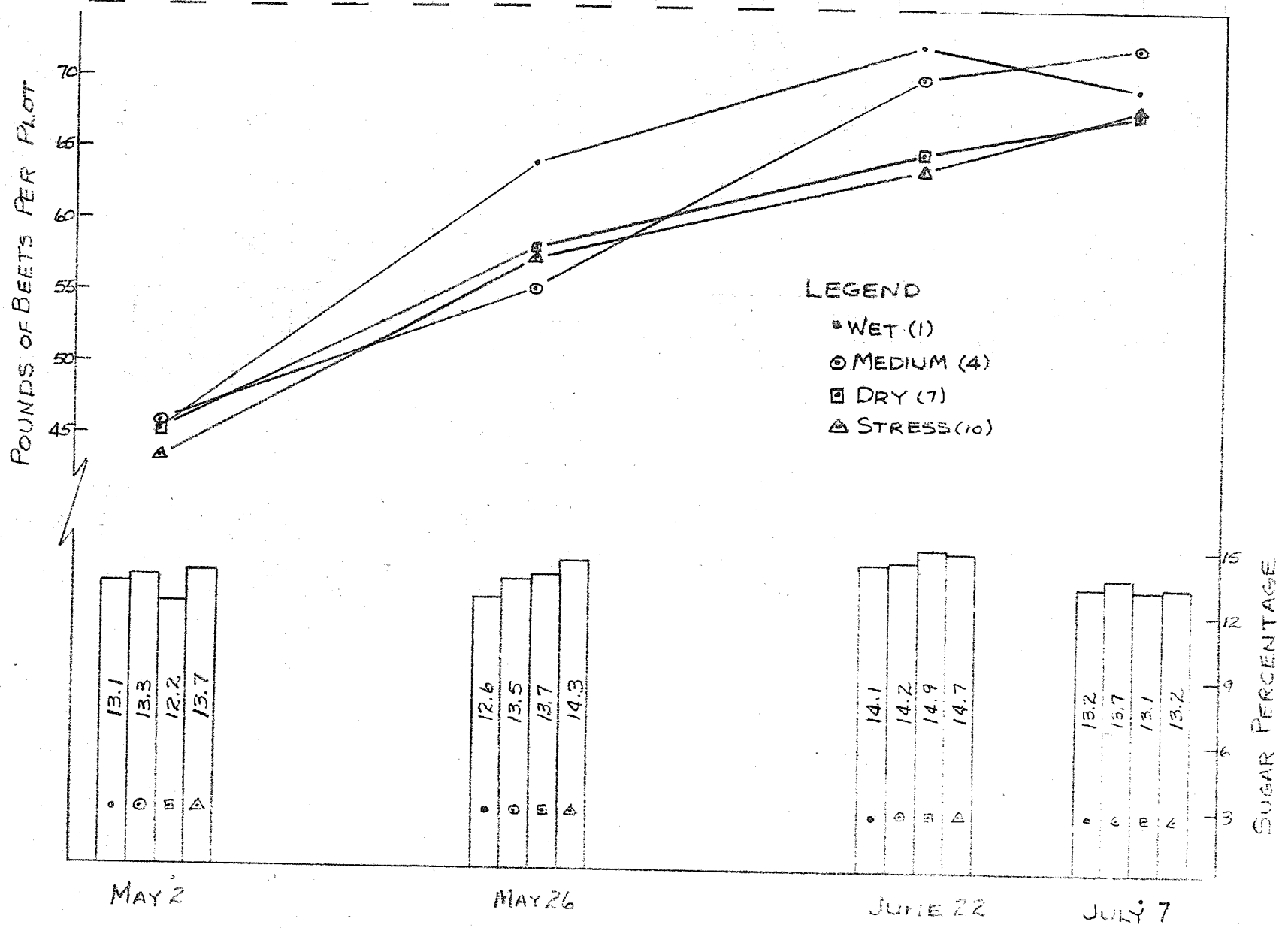

FIG. 1 MEAN PLOT YIELDS AND SUGAR PERCENTAGES FOR SUGAR BEETS BY HARVEST DATES

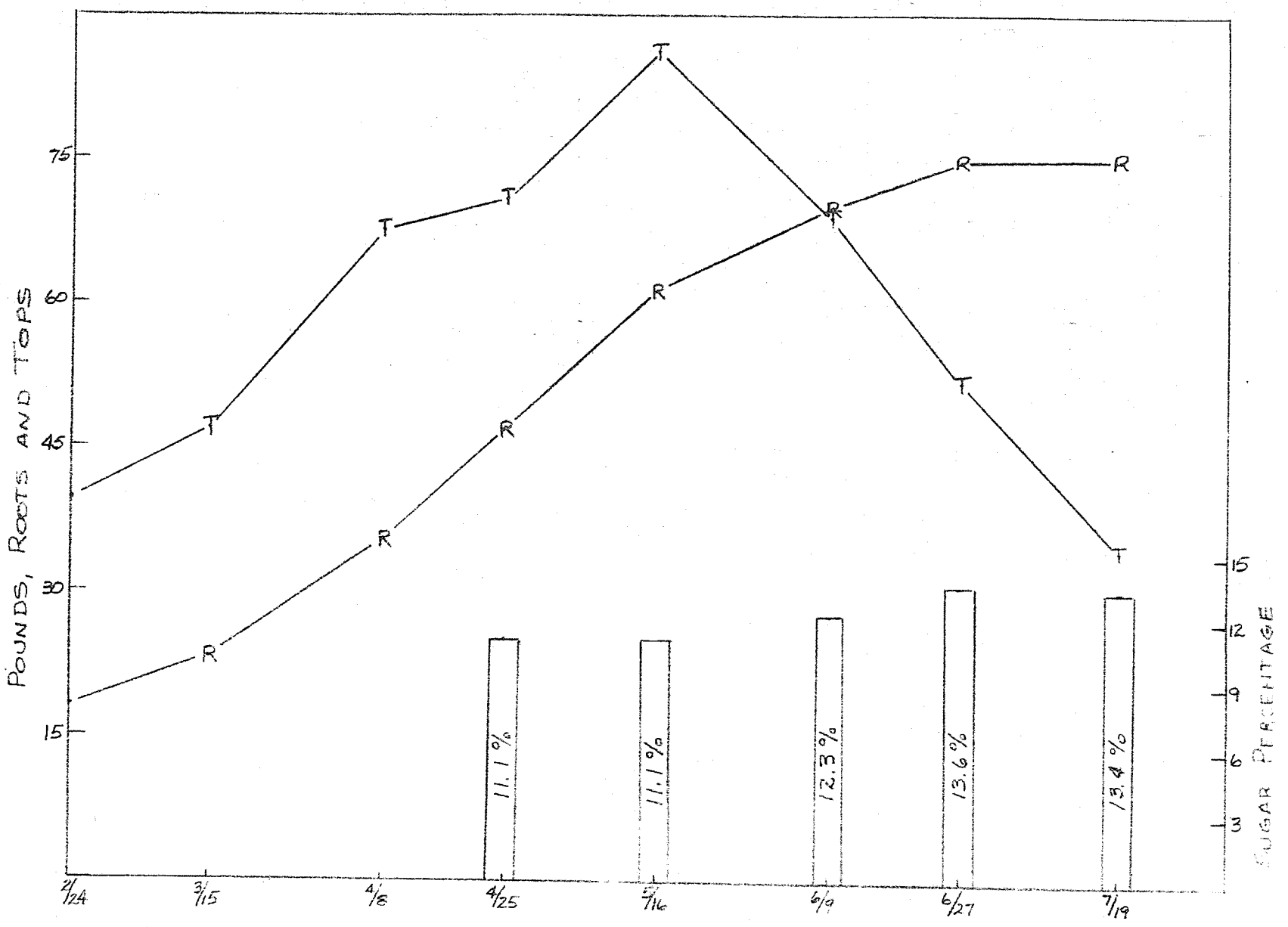

FIG. 2 A COMPARISON OF ROOT AND TOP WEIGHTS OF SUGAR BEETS FOR EIGHT HARVEST DATES WITH SUGAR PERCENTAGES FOR THE LAST FIVE DATES. EACH POINT ON THE CURVE IS A MEAN OF 4 REPS.

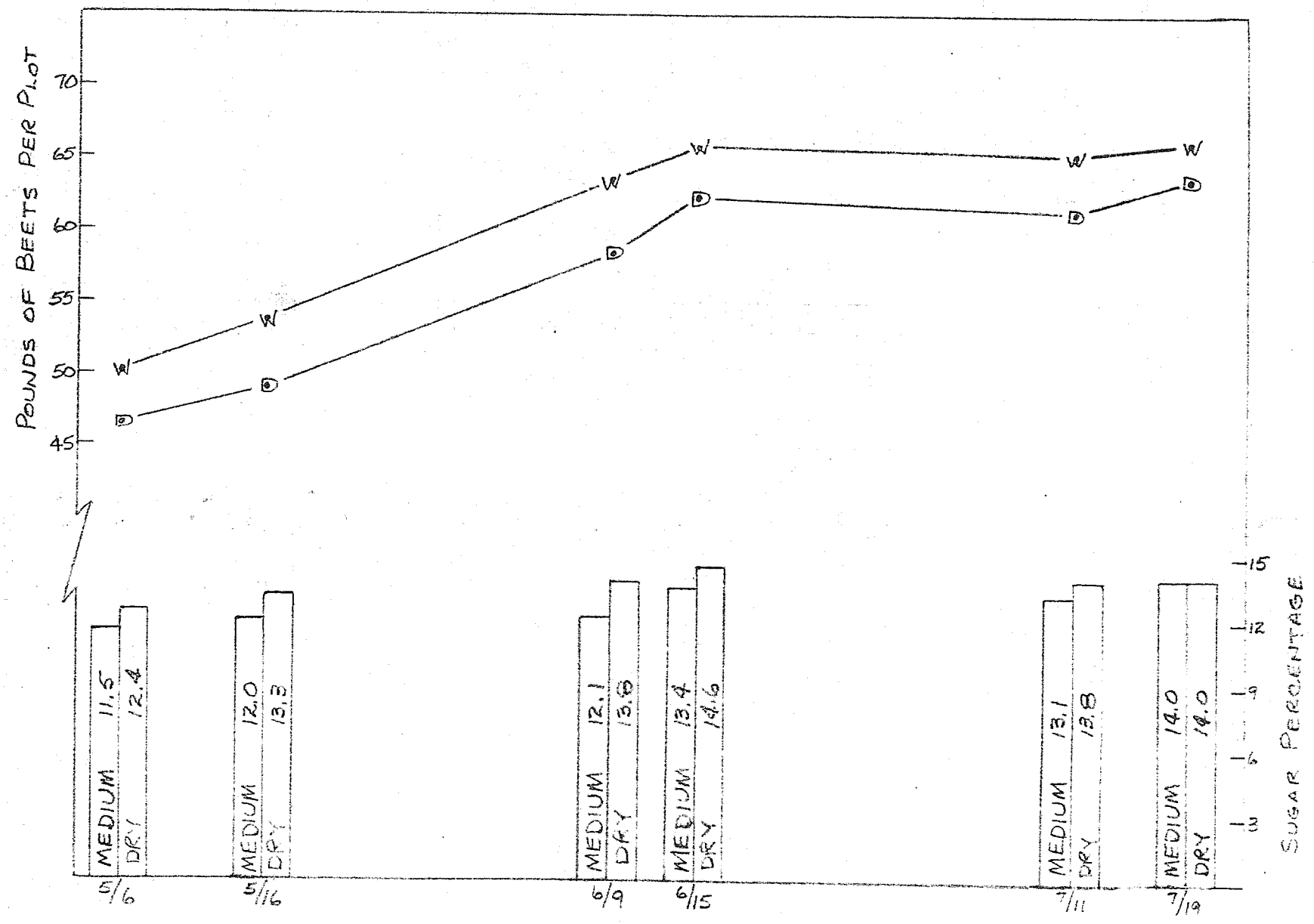

FIG. 3 EFFECT OF LATE-SEASON SOIL MOISTURE STRESS ON YIELDS AND SUGAR PERCENTAGE OF BEETS. EACH POINT ON CURVE IS A MEAN OF 4 REPS.

SUMMARY AND CONCLUSIONS:

Main Study

There was a difference in yields of beets between irrigation treatments ranging from 9 to 16 percent, but no harvest date showed differences that were statistically significant (Table 1). Yields increased as the season progressed, but to a lesser amount per unit time by the final harvest. Beet yield reached a maximum of 39.3 tons per acre, with a mean yield of 37.5 tons for all irrigation treatments.

Table 2 represents the sugar percentages for all harvest dates. There were statistically significant differences between treatments for the first three harvest dates. The differences can be associated with the soil moisture status at time of harvest. The longer the time between irrigation and harvest, the greater the sugar percentage. (Tables 2 and 4). Sugar percentage increased with each succeeding harvest through the third harvest. Percentage decreased on the last harvest date, at which time top growth was badly disintegrated.

To evaluate the potential of an irrigation treatment, sugar percentage must be applied to the beet yield weights. For the four harvest dates, there were no significant differences between treatments in pounds of sugar, however as much as 10 percent variance was noted. The maximum yield of sugar was 5.5 tons per acre, with a mean of 5.3 tons for all treatments.

It appears that the beet plant has the ability to produce sugar equally well under either dry or moist soil moisture conditions. Letting the soil dry out to near wilting point did not seem to have detrimental effects on the plant's ability to produce sugar.

Seasonal consumptive use for the different irrigation treatments was very similar to those in 1965. Consumptive use reached a small peak in November, decreased through the winter months, then increased abruptly in March to another peak by the end of May. Seasonal consumptive use was 44, 45, 40 and 35 inches for the wet, medium, dry, and stress treatments, respectively. Soil moisture depletion by soil depth calculations show that about 70 percent of the moisture used was from the top two feet.

Moisture was used from the 5th and 6th foot depth, but no more than could be stored by the germination irrigation on silt loam soils.

AMENDMENT NO. 1

Root tops increased in weight until a peak was reached in the middle of May, then declined very rapidly as the leaves began to mature. (Fig. 2). The yield of tops reached a peak of 47 tons per acre. Roots continued to increase in weight with each harvest until the last harvest. Final beet root yield was 40.8 tons per acre. A definite border effect was noted early in the season in the area utilized for this study, and may have increased the top growth. The sugar percentage increased until June 27, then declined slightly for the last harvest.

AMENDMENT NO. 2

The medium treatment had higher beet weights for each harvest, but lower sugar percentages, except on the last harvest. When sugar percentages were applied to the root weights, there was no difference in total yield of sugar on the May 6, May 16, and July 11 harvests. A 300 to 400 pound per acre increase of sugar in favor of the dry treatment occurred in the June 9 and June 15 harvests. The same difference in favor of the medium treatment occurred on July 19.

PERSONNEL: Leonard J. Erie and Orrin F. French.

TITLE: CLAY DISPERSANTS FOR THE REDUCTION OF SEEPAGE LOSSES FROM RESERVOIRS

LINE PROJECT: SWC VII gG1 CODE NO.: Ariz.-WCL-37

INTRODUCTION:

Observations and post-treatment soil and water analyses were made during 1966 on two stock tanks treated with sodium carbonate to reduce seepage. Dick Mason pond did not go dry and no soil samples were taken. Additions of sodium carbonate and sodium chloride were made to House Mountain No. 1 pond water in November 1966 to precipitate the calcium in the pond water and replenish sodium on the soil.

PROCEDURE:

Dick Mason Pond. During 1966 seepage measurements and soil solution extracts were taken periodically during the year on this pond.

House Mountain No. 1 Pond. Soil samples, soil solution extracts, and seepage measurements were taken periodically during 1966. Two hundred pounds of sodium carbonate and 300 pounds of sodium chloride were broadcast from a boat to the pond water (estimated volume 270,000 gallons) in November 1966. These amounts were calculated from a chemical analysis of the soil solution extracts. The purpose of this treatment was to precipitate the Ca^{++} and Mg^{++} in the pond water and add Na^{+} to the soil. Enough carbonate was added to reduce the Ca^{++} in the pond water by 100-fold and keep the pH below 9.5. Additional Na^{+}, in the form of sodium chloride was added to bring the ESP to 7 in the upper 2-3 inches of soil. Also a new stilling well and extraction cups were placed in the pond, close by the old units.

RESULTS AND DISCUSSION:

Dick Mason Pond. Seepage on this pond during the year averaged 4 mm/day. This low seepage rate equals the rate measured in August 1963, one year after treatment with TSPP. Chemical analyses of the pond water and soil solution extracts are given in Table 1. Assuming that the soil solution is in equilibrium with the soil, there is still quite a bit of sodium remaining in the top of the soil profile. We were unable to obtain extracts from the 22-cm deep ceramic cup

during 1966. Either the ceramic has become clogged or damaged or the soil water was under negative pressure.

It appears that the sodium carbonate treatment will be effective in reducing seepage longer than the TSPP treatment. This latter treatment failed 12 to 21 months after the salt was applied, whereas the sodium carbonate has been effective 13 months with little or no loss of sodium from the treated depth.

House Mountain No. 1. The seepage rate on this pond measured over a three-week period in mid May 1966 was 0.8 cm/day (evaporation was 0.7 cm/day for a total loss of 1.5 cm/day). Average water depth during this time was 120 cm. Chemical analysis of the pond water and soil solution extracts are given in Table 2. The data for November 1966 were taken a week prior to applying the sodium carbonate and sodium chloride to the pond water. The samples taken in December 1966 are four weeks after the salt addition.

Total water loss measured during the last two weeks of December 1966 and the first two weeks of January 1967 was 16 cm, or an average of 0.6 cm/day. Evaporation was not measured, but seepage losses would be on the order of 0.4 to 0.5 cm/day, a very low rate.

SUMMARY:

The use of sodium carbonate as a dispersing agent to reduce seepage in two stock ponds was evaluated. Dick Mason pond is still maintaining a low seepage rate, 0.4 cm/day, 13 months after treatment. The soil solution is still high in sodium, 10 to 12 meq/l in the top 16 cm of the soil profile. This indicates that very little leaching is taking place. To date, the sodium carbonate treatment has lasted as long as the TSPP treatment, and indications are that it may persist longer.

The seepage rate in House Mountain No. 1 pond increased from 0.4 cm/day in September 1965 to 0.8 cm/day in May 1966. Along with this increase was a decrease in sodium in the soil. In November 1966, 200 pounds of sodium carbonate and 300 pounds of sodium chloride were broadcast in the pond water to precipitate the calcium and magnesium

in the pond water and increase the sodium in the soil. Soil solution extracts taken in December 1966 showed a marked increase in sodium concentration down to the 22-cm depth. Seepage measured during the last two weeks of December 1966 and the first two weeks of January 1967 was 0.4 to 0.5 cm/day, the same low rate as measured in 1965.

The periodic addition of salt to the pond water appears to be a simple, inexpensive method of maintaining a low seepage loss. Continued seepage measurements and chemical and physical analyses of soil and water should indicate the longevity of the retreatment.

PERSONNEL: Robert J. Reginato and Lloyd E. Myers.

Table 1. Chemical analysis of pond water and soil solution extracts from Dick Mason pond.

Sample Site	Date	Na^+ meq/l	$Ca^{++} + Mg^{++}$ meq/l	Total Salts meq/l	pH
Runoff Water	9/65	0.13	0.77	0.92	7.0
Pond	5/63	1.55		1.75	
	5/64	0.70	0.79	<2	
	6/65	0.20	0.88	1.10	7.2
	9/65	.13	.58	.58	7.0
	10/65	.67	.56	1.10	7.0
	11/65	1.20	.54	1.60	6.9
	4/66	.55	.83	1.40	
	5/66	.70	.83	1.56	
	8/66	.70	1.17	1.20	
	11/66	.28	.74	.82	7.9
Soil Depth (cm)					
1-4	10/65	11.84	0.97	10.0	8.2
	11/65	16.19	.77	12.5	8.2
	4/66	7.93	2.07	9.0	
	8/66	10.87	2.17	11.2	
	11/66	10.05	1.45	12.2	8.7
7-10	10/65	7.82	2.90	8.5	7.5
	11/65	11.30	3.24	10.0	8.2
	11/66	12.23	2.42	11.0	8.8
13-16	10/65	4.62	2.32		
	11/65	10.94	5.12		
	8/66	9.56	6.91		
	11/66	11.14	6.35	13.5	8.2
19-22	10/65	3.26	2.51	4.4	
	11/65	6.30	4.82		

Table 2. Chemical analysis of pond water and soil solution extracts from House Mountain No. 1 pond.

Sample Site	Date	Na^+ meq/l	$Ca^{++} + Mg^{++}$ meq/l	Total Salts meq/l	pH
Runoff Water	9/65	1.83	0.97	3.10	7.2
Pond	11/63	0.55		2.0	
	5/64	1.63	2.12	3.1	
	6/65	0.18	1.46	1.7	7.1
	9/65	.87	1.16	2.0	7.4
	10/65	1.22	1.16	2.2	7.0
	11/65	1.42	1.73	2.6	6.9
	4/66	.27	1.89	2.2	
	5/66	.30	2.16	2.4	
	8/66	1.10	1.56	2.1	
	11/66	.15	1.25	1.4	8.5
	12/66	3.12	1.10	4.3	6.5
Soil Depth (cm)					
1-4	10/65	1.52	4.35	4.4	8.0
	11/65	1.44	4.84	4.7	7.5
	5/66	1.08	3.05	3.9	
	8/66	1.30	5.92	5.4	
	11/66	.73	4.65	4.4	7.6
	12/66	2.43	1.70	3.8	6.8
7-10	10/65	1.63	4.35	4.9	8.0
	11/65	.95	4.35	4.7	7.4
	5/66	.69	3.05	3.6	
	8/66	1.30	6.91	4.2	
	11/66	.82	4.65	4.0	7.4
	12/66	3.64	1.46	4.6	7.0
13-16	10/65	1.90	5.80	6.0	7.9
	11/65	1.52	5.43		
	5/66	1.23	4.04	4.9	

Table 2 (Continued).

Sample Site	Date	Na^{+} meq/l	$Ca^{++} + Mg^{++}$ meq/l	Total Salts meq/l	pH
13-16	8/66	1.73	5.92	4.7	
	11/66	.82	4.17	4.0	7.8
	12/66	2.04	1.46	3.5	7.1
19-22	10/65	1.25	3.87	3.5	8.0
	11/65	1.52	6.02		
	5/66	.59	4.93	5.7	
	8/66	2.71	4.44	2.5	
	11/66	1.49	3.03	5.3	8.2
	12/66	3.61	2.67	5.7	7.1

TITLE: WATERBORNE SEALANTS TO REDUCE SEEPAGE LOSSES FROM UNLINED CHANNELS AND RESERVOIRS

LINE PROJECT: SWC VII gG1 CODE NO.: Ariz.-WCL-38

INTRODUCTION:

During 1966, ten waterborne sealants were investigated in the laboratory. From these ten sealants, two petroleum emulsions were deemed acceptable for further tests. Additional laboratory studies were conducted to determine which of the two materials would be most effective in reducing seepage over a wide range of soil textures. Three reservoirs were treated in October 1966 with the emulsion found to be most effective in the laboratory tests.

PROCEDURE:

Laboratory. Procedures have been previously described except for changes in the seepage cylinder equipment. Pretreatment seepage rates are controlled by inserting various lengths of fine capillary tubing in the discharge lines.

Four soils, Cajon very coarse sand, Leetsville fine sand, Control sandy loam, and Laveen loam, were packed into cylinders. Two petroleum emulsions, 10A and 14MR, in concentrations of one, three, and five ppt were added to water ponded over the soils (one ppt is equivalent to 0.1 gallons emulsion per square yard). The supply water was stopped when the emulsions were added to the ponded water. Twenty-four hours after treatment, the cylinders were refilled with water and emulsion at the original concentrations. Twenty-four hours after the refill, clear water was added to the cylinders and a constant head maintained. All cylinders were run in duplicate.

Field. Emulsion 10A was added to three reservoirs with a positive displacement gear pump in October 1966. The purpose of the field trials was to determine the effectiveness of the treatment under field conditions and to determine the longevity of the treatment.

The first pond treated was in Laveen loam in Glendale, Arizona. It had a pretreatment seepage rate of 1 ft/day. Seven hundred fifty gallons of emulsion were added to the water as the pond filled, resulting in an application rate of 0.5 gal/yd^2. Two 8-inch diameter

infiltration cylinders were placed in the pond bottom 3 months after treatment. Infiltration measurements were made with clear water for a 24-hour period (with an initial head of about 1 ft). Emulsion 10A was then added to the water in the cylinders at the rate of 0.5 gal/yd^2 and the water level was brought up to the 1-ft depth. Water levels in the two cylinders were measured 1, 5, and 8 days after treatment, and clear water was added to bring the depth back to 1 ft after each measurement.

A falling-head permeameter was placed on the asphalt membrane 3 months after treatment to determine how good a seal was formed. A 3-ft head of water was placed on the 10-inch diameter cylinder. Hydraulic conductivity of the membrane was calculated.

Located in Salome, Arizona, the second pond was constructed in Cajon very coarse sand. Its pretreatment seepage rate was 2.3 ft/day. One thousand two hundred fifty gallons of emulsion were added to the filling water resulting in an application rate of 0.8 gal/yd^2. One 8-inch diameter infiltration cylinder was placed in the bank of the pond about 1 ft from the pond bottom 3 weeks prior to treatment. Infiltration measurements were made with clear water for a 100-minute period (with a head of about 1 ft). Emulsion 10A was then added to the water in the cylinder at the rate of 0.8 gal/yd^2 and the water level was brought up to the 1-ft depth. The water level was measured during the 100 minutes immediately after treatment.

A falling-head permeameter, described above, was placed on this asphalt membrane 2 months after treatment.

Reno, Nevada was the third test site. The pond, in Leetsville fine sand, was much smaller than the previous two, and only 30 gal of emulsion were used, resulting in a 0.25 gal/yd^2 application rate. Pretreatment seepage was 0.3 ft/day. This pond was located and treated by a cooperating field station. Initially, we were told that the pond had a seepage rate of about 2 ft/day, so we recommended a treatment rate of 0.5 gal/yd^2. However, the initial seepage rate

was actually much lower (0.3 ft/day) as well as the amount of emulsion added by the cooperator (0.25 gal/yd^2).

Immediate posttreatment seepage measurements were made on all three ponds.

RESULTS AND DISCUSSION:

Laboratory. Emulsion 10A reduced seepage in laboratory cylinders better than 14 MR over the entire range of soil textures investigated (see Table 1). The latter emulsion did not work well on the Cajon soil (13 and 39 percent reduction) but emulsion 10A did (92 percent reduction). Both emulsions showed poor seepage reduction at a low initial seepage rate (0.5 ft/day), a fact demonstrated in previous year's work. The effect of emulsion concentration appears to be important on the medium textured Laveen loam. Here 0.5 gal/yd^2 gives nearly 100 percent reduction, whereas 0.2 gal/yd^2 gives only 47 percent reduction. On the basis of laboratory investigations, it was decided that emulsion 10A would be used for the field trials.

Field. The results of the three field trials are shown in Table 1.

Although the pretreatment seepage rate and the amount of emulsion added to Laveen loam were the same in the field as in the laboratory, the seepage reduction was not (99+ percent in the laboratory versus 47 percent in the field). Posttreatment inspection of the pond revealed that the soil started to crack, exposing the soil under the asphalt (petroleum). The cause(s) of the cracking is/are currently under investigation in the laboratory.

Infiltration, measured with the cylinders, was reduced 60 percent 1 day after treatment and 93 percent 5 days later. There was no evidence of soil cracking in the cylinders. This reduction is nearly as great as was found in the laboratory. Hydraulic conductivity of the membrane, from permeameter data, averaged 2×10^{-4} ft/day, essentially an impermeable barrier.

Seepage reduction in the Salome pond was identical (93 percent) to that found in the laboratory studies. A heavy application of emulsion

(0.8 gal/yd^2) was made in the pond as the head of water (160 cm) would be greater than that used in the cylinders (50 cm). It was thought that more asphalt on the soil would better resist the water pressure, forcing the asphalt into the soil pores.

An infiltration reduction of 96 percent was obtained with the cylinders placed in pond bank. This compares favorably with the laboratory study and field trial (93% for each). Results from the permeameter gave a hydraulic conductivity for the membrane, of 1×10^{-4} ft/day, again, meaning a relatively impermeable seal.

The pond was pumped dry by the farmer several days after treatment, as he wished to refill with clear water and stock the pond with fish. Upon refilling the pond, the lining was torn along a small section on one side of the pond. The seepage rate increased to give a seepage reduction of 73 percent. The torn area was sprayed with a cationic asphalt emulsion (RSK) after the pond went dry. After refilling the pond again with clear water, the seepage reduction was 78 percent (based on the pretreatment rate).

Because there was a thick layer of silt and sand covering the membrane, we probably did not locate all the damaged areas. If the pond lining had not been damaged upon refilling, or if we had repaired all the broken areas, I feel that high seepage reduction (93 percent) would still be maintained. The lining did not have high erosion resistance to fast-flowing water.

In Reno, Nevada it is understandable why the waterborne sealant did not work (on the treated pond, seepage was reduced 53 percent 4 weeks after treatment, while the seepage rate in 2 control ponds declined by 66 and 47 percent). The initial seepage rate was too low (0.3 ft/day). From all previous work, we have shown that an initial rate of about 1 ft/day is necessary before the waterborne sealants we have investigated are effective. It is possible that the pond may be retreated next spring when the water table declines and the seepage rate increases.

SUMMARY AND CONCLUSIONS:

Laboratory experiments and three field trials were conducted to determine the suitability of an asphalt emulsion as a waterborne seepage-reducing agent. In the laboratory, four soils, ranging from a very coarse sand to a loam were packed in cylinders, and the emulsion added to the water ponded over the soil. For application rates of emulsion greater than 0.3 gal/yd^2 and initial seepage rates in excess of 1 ft/day, seepage was reduced by at least 92 percent.

A field trial in Cajon very coarse sand resulted in 93 percent reduction in the seepage rate, just as was predicted in the laboratory experiments. However, there was no seepage reduction in the pond in Leetsville fine sand. This lack of reduction is because the initial seepage rate was too low (0.3 ft/day) for the waterborne sealant to be effective. Although the seepage rate was reduced 99 percent in laboratory tests on Laveen loam, the rate in the pond was reduced only 45 percent. Posttreatment investigation of the pond revealed that the soil and asphalt had started to crack. Causes of this cracking are currently under investigation.

It is evident from our tests that the waterborne sealant we investigated is most effective in non-shrinking soils where the seepage rate exceeds 1 ft/day. Soil shrinkage causes the membrane to rupture. The membrane will also be mechanically damaged by fast-flowing water. To circumvent this problem, the treated pond should be kept full of water.

PERSONNEL: Robert J. Reginato and Lloyd E. Myers

Table 1. Percent reduction in seepage rate 72 hours after treatment.

		LABORATORY CYLINDERS															FIELD PONDS		
Material		14MR					10A										10A		
Emulsion Added (gal/yd^{-2})		0.3					0.2		0.3					0.5			0.25	0.5	0.8
Initial Seepage Rate (ft/day [1])		0.5	1.0	1.5	2.5	5.0	1.5	2.0	0.5	1.0	1.5	2.5	5.0	1.0	1.5		0.3	1.0	2.3
Soil	Texture																		
Cajon	Very Coarse Sand			13	39					92				93					93
Leetsville	Fine Sand									95							0		
Control	Sandy Loam	57		95		99		92	20		94		94						
Laveen	Loam						47							99+				45	

TITLE: CRACK SEALANTS FOR CONCRETE LINED CANALS

LINE PROJECT: SWC VII gG1 CODE NO.: Ariz.-WCL-39

INTRODUCTION:

Since the publication of ARS 41-121, "Repair of Cracks in Concrete Channel Linings," June 1966, work on this research outline has consisted mainly of inspecting test sections of canals where experimental crack sealers were sprayed.

RESULTS AND DISCUSSION:

Sprayable crack sealer S_2, commercially manufactured, was sprayed on a 500-ft section of the Tempe Canal in November 1964. This canal has water in it continuously eleven months of the year. Inspection of this site in November 1965 showed that the sealer had cracked above the water line but not below. Bonding of the material to the gunite was excellent on cracks that had been cleaned with a high pressure water jet or wire brushed, followed by a tack coat.

Two years after treatment, November 1966, the material was again inspected. Bonding was still good on the cracks cleaned as mentioned previously. However, the sealer had started to crack below the water line regardless of the cleaning treatment. At the water line, the sealer was blistering and peeling on all treatments except where a tack coat was used.

The general appearance of the sealer was not good. It seemed to have deteriorated considerably during the period one to two years after installation.

Other sprayable crack sealers, such as resinous polymers are being investigated, but no data are available at this time.

SUMMARY:

After two years of exposure in an operational canal, a commercially manufactured, sprayable crack sealer has cracked above and below the water line. The material is, however, still bonded to the gunite where the cracks had been cleaned with a high pressure water jet or wire brushed and a tack coat applied. All other cleaning treatments resulted in poor bonding of the sealer to the gunite.

Other sprayable crack sealers, such as resinous polymers, are currently under investigation, but no data are available at this time.

PERSONNEL: Robert J. Reginato and Lloyd E. Myers.

TITLE: DISPERSION AND FLOCCULATION OF SOIL AND CLAY MINERALS AS RELATED TO THE Na AND Ca STATUS OF THE AMBIENT SOLUTION

LINE PROJECT: SWC VII-gG4 CODE NO.: Ariz-WCL-40

INTRODUCTION:

The primary objectives of this project have been discussed in the Annual Report of 1964.

PART I. FLOCCULATION-DEFLOCCULATION BEHAVIOR OF SOILS AND CLAY MINERALS.

The purpose of this part of the study was to study the deflocculation-flocculation behavior of different materials as related to the electrolyte composition including both the kind of cations and the concentration.

PROCEDURE:

Separate 20g soil and clay mineral samples were washed and leached first with 200 ml of SAR solutions of 1, 5, 10, 15, 20, and 40 at a concentration of 30 meq/liter, followed by washing with a similar volume of SAR solutions, but at a concentration of 1 meq/liter. For the Wyoming bentonite, 2g samples were washed by centrifugation; the solution concentration used was 30 meq/liter followed by 10 meq/liter. The leached or centrifuged material was dispersed in 200 ml of the respective SAR solution at 1 meq/liter concentration. Two ml of the suspension were treated with 23 ml of constant SAR solution, but with a series of varying electrolyte concentrations in a graduated test tube. The mixture was shaken and allowed to settle for 18 hours.

The threshold concentration at which deflocculation-flocculation separation occurred for a given SAR treatment was noted visually. Concentration gradients used were 1 meq/liter. The condition of flocculation or deflocculation was easily observed within 1 meq/liter concentration ranges. In one case the suspension was analyzed for suspended materials by pipetting out part of the solution for comparison with the simple visual turbimetric technique. The suspension weight was corrected for the salt present.

The clay minerals used were illite (Goose Lake), bentonite (Wyoming), bentonite (Chambers), kaolinite (Macon), and kaolinite (Mesa Alta), which were obtained from Wards Natural Science Establishment. The

soil materials used were the Big Lake clay loam, Mason clay, and House Mountain silty clay from Arizona; Pachappa loam from California; and Hagerstown silt loam from West Virginia. The physical and chemical analyses of the soils are presented in Table 1.

The effect of Mg and Ca cations on the flocculation-deflocculation phenomena was also compared in the Mason soil. In this case, for a given SAR and electrolyte concentration, the amounts of Ca and Mg cations were varied.

The combination of SAR and electrolyte concentration at which the deflocculation and flocculation could be separated was plotted using the electrolyte concentration as the abscissa and the SAR as the ordinate. A line of best fit was drawn through the data points for a given material. Starting from the lowest concentration-SAR combination, the region to the right of the curve is the flocculated zone and that to the left is the deflocculated zone.

RESULTS AND DISCUSSIONS:

The pipette analyses of the suspension for the various SAR treatments at different electrolyte concentrations for the Mason soil are presented in Figure 1. The analyses showed two distinct zones of behavior; namely, the deflocculated and the flocculated zones. In the deflocculated zones the particles were not completely dispersed and, for a specified SAR, had varying degrees of dispersion, which was a function of the electrolyte concentration. The visual turbimetric separation of the flocculated and deflocculated state as shown by the asterisk in Figure 1 was considered accurate enough for our work. The turbimetric method required only a few minutes to run whereas the pipette analysis required three days to complete.

Wiklander and Hallgren (8) working with homoionic soil materials and a different technique noted that dispersion did not take place at a definite concentration, but increased successively with decreasing concentration in the percolating solution. The need for controlled deflocculation instead of complete dispersion has been alluded to for seepage control by the use of chemical dispersants. The exact degree of dispersion, however, has not been specified and research along these

lines may provide the required answers.

The illitic, montmorillonitic, and kaolinitic clay minerals behaved similarly in regards to the flocculated-deflocculated state under the various solute compositions as illustrated in Figure 2. Lines of best fit were drawn through the data points and the curve is similar to that reported by Collis-George and Smiles (3) for their single soil sample. For a specified SAR, the clay mineral materials required a lower concentration of electrolyte than the soil materials to go from the dispersed to the flocculated state (Figure 3).

Unlike the clay minerals, the various soil materials behaved very differently from each other in regard to the flocculation-deflocculation status as shown in Figure 3. The Big Lake and House Mountain soils were similar to the clay minerals, whereas the Pachappa and Hagerstown soils were not. For comparative purposes, the data of Collis-George and Smiles (3) are also plotted in the figure.

In the 1965 Annual Report it was noted that increasing the rate of application of NaCl and Na_2SO_4 in the Big Lake and Mason soils caused an eventual decrease in the amount of dispersed materials, whereas the Na_2CO_3 treatment increased deflocculation. On the other hand, data using the same treatment rates for the Pachappa soil showed no decrease in the amount of dispersed material with increasing rates for all the different Na salt treatments. The physical and chemical analyses of the equilibrium solution for the highest treatment rate of 32 meq per 100 g soil material are listed and compared with the predicted suspension status on Table 2 using the chemical analysis and the relationship developed in Figure 3. The comparison supports the explanation made in the earlier studies that an increase in electrolyte concentration was causing flocculation when the rate of salt treatment was increased. According to present theory on the behavior of dispersed charged colloidal particles, the flocculation caused by an increase in electrolyte concentration follows from the suppression of the diffuse double layer which results in the closer approach of the colloidal micelle, and subsequent attraction of the particles through van der Waal's forces.

A suitable explanation for the differences observed in the flocculation of the various soil materials is not available at present. The reason apparently lies in the physico-chemical nature of the colloidal micelle and investigations are being conducted to evaluate such properties.

From the practical field problem of selecting the rate of application of chemical dispersants, the data presented in Figure 3 indicate that the Hagerstown soil will require less Na-salt than the Mason soil to obtain soil dispersion for seepage control.

The effects of Ca + Mg on the flocculation-deflocculation process are compared for the Mason soil in Figure 4. In the comparison, systems of $NaCl-CaCl_2$, $NaCl-MgCl_2$, and mixed systems of $NaCl-CaCl_2-MgCl_2$ with different ratios of Ca and Mg were utilized. The results show that for a specified SAR, the $NaCl-CaCl_2$ system flocculated at a lower electrolyte concentration than the $NaCl-MgCl_2$ system. This is in agreement with the work of Jenny and Reitemeier (4) who showed that the flocculation value, amount of electrolyte needed to cause flocculation of homonionic Mg-clay mineral, was higher than that for the Ca-clay mineral. Furthermore, the replacement of 25 percent or 50 percent of the Ca by Mg cations resulted in systems which behaved more like the Mg dominant than the Ca dominant condition. In the usual procedure for calculating SAR, the Ca and Mg concentrations are combined. For flocculation-deflocculation behavior, although it is convenient to represent the relation between the monovalent and divalent cations by the sodium adsorption ratio, one must be more specific by designating the amount of Ca and Mg cations present.

PART II. MEASUREMENT OF Ca ACTIVITY: DISSOCIATION AND SOLUBILITY OF $CaSO_4.2H_2O$

INTRODUCTION:

In the present laboratory study on soil dispersion and field investigations on chemical control of seepage losses (Ariz-WCL-37) an attempt is made to replace the Ca of the soil exchange complex with Na to cause dispersion and swelling of the soil material. For a better understanding of the process of deflocculation and cation exchange, we must have reliable measurements of the Na and Ca status of the

ambient solution. The sodium salts encountered in soil studies are essentially completely dissociated. The Ca salts, such as $CaSO_4$ and $CaCO_3$, however, are not completely dissociated. Unfortunately, the existing chemical analytical procedures are capable of measuring the total amount of Ca in solution, but not the amount of dissociated and undissociated species.

A membrane Ca electrode has become available recently which is claimed to measure the Ca^{++} activity. In a preliminary study, the electrode was used to determine the dissociation and solubility of $CaSO_4.2H_2O$. Possibilities exist for using it with more complicated $CaCO_3$ and soil-water systems.

PROCEDURE:

Saturated solutions of $CaSO_4$ were prepared by dissolving $CaSO_4.2H_2O$ in deionized distilled water and also in NaCl and Na_2SO_4 solutions of various concentrations up to 0.1 M. Total Ca in solution, $[Ca^{2+}]_T$, was determined by the versenate method using hydroxy-naphthol blue as the complexing indicator. Ca activity (Ca^{2+}) was measured with the Orion Ca membrane electrode which was calibrated with standard $CaCl_2$ solutions, since $CaCl_2$ is completely dissociated. Calibration curves of $CaCl_2$ were run in water and in various concentrations of NaCl to simulate the ionic conditions anticipated for the $CaSO_4$-NaCl and $CaSO_4$-Na_2SO_4 systems. The EMF response of the Ca-electrode to Ca^{2+} was of the Nernstian type between 10^{-4} and 10^{-1} moles per liter of Ca^{2+}. EMF measurements were made on a Corning Model 12 expanded scale MV meter ($\pm$ 0.5 mv) at 25 $\pm$ 1 C. Triplicate measurements were made for each of the ionic strengths used.

With proper calibration, the Ca electrode measures the activity of the Ca^{2+} in solution and is not responsive to the undissociated or complexed Ca in solution. For a completely dissociated calcium salt, we have

$$(Ca^{2+}) = \gamma_{Ca^{2+}} [Ca^{2+}] , \qquad [1]$$

where ( ) refers to the activity, [ ] denotes the concentration, and γ the activity coefficient. For a partially dissociated Ca salt, however, the relation must be modified as follows:

$$(Ca^{2+}) = \alpha \gamma_{Ca^{2+}} [Ca^{2+}]_T \qquad [2]$$

where α is the degree of dissociation of the dissolved salt and $[Ca^{2+}]_T$ is the total calcium in solution as determined by the versenate or equivalent method. (Ca^{2+}) is the activity of the salt in solution as measured by the Ca electrode. The product $\alpha \gamma_{Ca^{2+}}$ can be calculated from experimentally determined values of (Ca^{2+}) and $[Ca^{2+}]_T$. α and $\gamma_{Ca^{2+}}$ are not independent of one another, being related to the ionic strength via the concentration of ions in solution.

In the calculation procedure α and $\gamma_{Ca^{2+}}$ were estimated by an iterative process from measured values of (Ca^{2+}) and $[Ca^{2+}]_T$. An arbitrary value between 0 and 1 was selected for $\gamma_{Ca^{2+}}$, and α was estimated using equation (2). From the calculated α, the concentration (Ca^{2+}) was determined using the relation $[Ca^{2+}] = \alpha [Ca^{2+}]_T$; consequently, the ionic strength, $\mu = \Sigma z_i^2 c_i/2$, and then the activity coefficient, $\gamma_{Ca^{2+}}$, from the relation $\log \gamma_{Ca^{2+}} = - A z^2 \sqrt{\mu}/(1 + B a_i \sqrt{\mu})$ were calculated. From the new value of $\gamma_{Ca^{2+}}$ another value of α was estimated and the process was repeated until the values of $\gamma_{Ca^{2+}}$ and α remained constant.

The apparent dissociation constant K_D' was determined by the relation

$$K_D' = \frac{([Ca^{2+}]_T \times \alpha \times \gamma_{Ca^{2+}}) ([SO_4^{2-}]_T \times \alpha \times \gamma_{SO_4^{2-}})}{(1 - \alpha) [Ca^{2+}]_T \gamma_{\overline{CaSO_4}}} \qquad [3]$$

The activity coefficient of the undissociated $\overline{CaSO_4}$ was taken as unity. In the sulfate concentration, corrections for the undissociated SO_4^{2-} as $NaSO_4^-$ were made using $K_{NaSO_4^-} = 0.19$. The formation of HSO_4^- was also considered, but under the experimental conditions the amount

of HSO_4^- present was calculated to be negligible compared to the SO_4^{2-} concentration, and thus was not included in the final computation.

The apparent solubility product was calculated from

$$K_S' = ([Ca^{2+}]_T \times \alpha \times \gamma_{Ca^{2+}})([SO_4^{2-}]_T \times \alpha \times \gamma_{SO_4^{2-}}) \qquad [4]$$

Molar concentration, instead of molal concentration was used throughout, and the differences between the two systems are insignificant at the low concentrations reported here.

RESULTS AND DISCUSSION:

The apparent dissociation and solubility product constants of $CaSO_4$ at the different ionic strengths are listed in Table 3 together with their respective degree of dissociation. Ca activities and concentrations in unsaturated $CaSO_4$ solutions including combinations of NaCl and Na_2SO_4 were also determined, but the experimental errors for these diluted samples became large due to the limitations in the chemical and electrode analyses and thus were not used in the calculation of K_D'. The apparent linear and logarithmic solubility product varied with the ionic strength as (a) $K_S' = 2.50 \times 10^{-5} + 6.27 \times 10^{-6}\ \mu$ and (b) $\log K_S' = -4.60 + 0.163\ \mu$, respectively. K_S at ionic strength of zero is $(2.50 \pm 0.10) \times 10^{-5}$ compared to K_S of 2.45×10^{-5} reported recently by Moreno and Osborne (6).

The apparent linear and logarithmic dissociation constants followed the relation (a) $K_D' = 5.32 \times 10^{-3} + 4.78 \times 10^{-3}\ \mu$ and (b) $\log K_D' = -2.28 + 0.363\ \mu$, respectively. K_D at infinite dilution is $(5.32 \pm 0.37) \times 10^{-3}$ compared to values of 4.9×10^{-3} (1) and 5.3×10^{-3} (5) obtained by solubility and conductometric methods. The irregularity of K_D was greater than that of K_S because the values of the former were accentuated by the use of both factors α and $(1 - \alpha)$. The similar K_D values (also K_S) obtained for the $CaSO_4$-H_2O, $CaSO_4$-NaCl and $CaSO_4$-Na_2SO_4 systems gives added confidence in the Ca-activity measurement using the Ca-electrode and the assumptions made in the calculation.

PART III. SWELLING BEHAVIOR OF SOIL MATERIALS AND CLAY MINERALS AND ITS RELATION TO HYDRAULIC CONDUCTIVITY.

INTRODUCTION:

In addition to the dispersive nature of the soil and clay materials, the swelling properties must also be taken into account when water flow in these materials is considered. Much time and effort have been devoted to predicting the value of the hydraulic conductivity, a constant used in evaluating the flow rate of fluids in porous materials. An important aspect of the conductivity is its relation to the alteration of the pore dimension as a result of the swelling of the material; the swelling in turn depends upon the composition of the surrounding solution. Portions of this investigation were conducted with the staff of the U. S. Soils Laboratory during the incumbent's assignment there (Oct 1965 - March 1966).

THEORY:

In this investigation a distinction is made between the pore space which is effective and that which is ineffective with regard to the macroscopic flow of water. The ineffectiveness is assumed to be due to the interaction between water (solution) and the colloidal fraction of the soil, causing the latter to swell. This process implies that an increasing number of water molecules is brought under the constraint of the electrical field forces existing in the immediate soil environment. The theory of the electrical double-layer was applied to describe the quantitative aspects of this problem.

Using the basic postulates developed (2) and ignoring momentarily the ionic species and valences, it is predicted that

$$\frac{dy}{dx} = \sqrt{\beta}\sqrt{\Sigma C - \Sigma C_c} \qquad [1a]$$

where y is the ratio between the electrical and thermal energies determining the equilibrium distribution of cations and anions between adsorbed and solution phase, x is the distance parameter with respect to the charged surface, β is a constant at constant temperature (1.06×10^{15} mmole cm^{-1} at 25 C) and ΣC is the total molar concentration

of cations and anions in the adsorbed phase. The absence of a subscript indicates their location anywhere in the adsorbed phase, while the subscript c indicates their location in the boundary layer of the adsorbed phase. This layer occurs either midway between opposing soil surfaces in the case of saturated flow, or at the interface between adsorbed water and the soil atmosphere in the case of unsaturated flow. In either case, $dy/dx = 0$, and $y = y_c$ at the boundary layer. Furthermore, according to the Boltzmann distribution equation, $C^+ = C_o e^y$, and $C^- = C_o e^{-y}$ for cations and anions anywhere in the adsorbed phase, whereas $C_c^+ = C_o e^{y_c}$ and $C_c^- = C_o e^{-y_c}$ for those ions in the boundary layer. In both cases C_o refers to the ionic concentrations in the equilibrium solution. Thus equation [1a] can be rewritten in the following general form:

$$\sqrt{\beta \Sigma C_o}\, dx = dy/\sqrt{ae^y - be^{y_c}} \qquad [1b]$$

where a and b indicate functional relationships determined by the number of ion species and their valences.

In the case of a mixed ion system containing monovalent and divalent cations and anions, by introducing N_o (= meq/L) instead of C_o for the total salt concentration in the equilibrium solution, and f for the equivalent fraction of divalent cations or anions (i.e., the system is symmetric), one may write:

$$\sqrt{\beta N_o}\, dx = \frac{du}{u[\{fu^2/2 + (1 - f)\, u + (1 - f)/u + f/2u^2\} - \{fu_c^2/2 + (1 - f)\, u_c + (1 - f)/u_c + f/2u_c^2\}]} \qquad [2a]$$

where $u = e^y$ and $u_c = e^{y_c}$ pertain to cations, and $1/u = e^{-y}$ and $1/u_c = e^{-y_c}$ to anions, while $dy = d\ln u = du/u$. Rearranging yields:

$$\sqrt{\beta N_o}\ dx = \frac{du}{u[\{f(u + 1/u)^2/2 - f + (1 - f)\ (u + 1/u)\} -}$$

$$- \{f(u_c + 1/u_c)^2/2 + f - (1 - f)\ (u_c + 1/u_c\}] \qquad [2b]$$

As a polynomial of the 4th degree in u, the righthand term of [2b] is an incomplete elliptic integral of the 1st kind. It can be solved if the denominator can be factorized to yield 4 real roots. In the present case, this is accomplished by introducing $v = (u + 1/u)/2 = \cosh y$, so that $dv = d(u + 1/u)/2 = [(1 - 1/u^2)/2]\ du$, or $du = 2dv/(1 - 1/u^2)$. Substituting into [2b], and integrating between y, or v, equalling infinity at a hypothetical plane behind the real soil surface, and y, or v, equalling zero at the outer boundary of the adsorbed phase, i.e. at distance D from the hypothetical plane mentioned, it follows that:

$$\sqrt{2f\beta N_o} \int_o^D dx = \int_\infty^{V_c} \frac{dv}{\sqrt{(v + 1)(v + 1)(v - v_c)(v + v_c + \frac{1 - f}{f})\ 2f}} \qquad [3]$$

in which all 4 roots are real. Conventionally, one may now write:

$$\sqrt{2f\beta N_o}\ D = \mu\ F(k,\varphi) \qquad [4]$$

where D, which henceforth will be considered the swelling thickness, is the sum of the real distance from the soil surface out into the adsorbed phase, x, and from the soil surface back to the hypothetical plane mentioned, d. The latter, therefore, is but a correction factor, to be calculated according to Schofield and Talibudeen (7). By properly combining the roots, one arrives at the following general formulation for μ, k, and φ in equation [4]:

	$0 < f < 1$	$f = 0$ (monovalent)	$f = 1$ (divalent)
$\mu =$	$\dfrac{2}{\sqrt{(v_c + 1)(v_c + 1 + \frac{1 - f}{f})}}$	$\dfrac{2}{\sqrt{(v_c + 1)\ 2}}$	$\dfrac{2}{v_c + 1}$
$k =$	$\sqrt{\dfrac{(2v_c + \frac{1 - f}{f})\ 2}{(v_c + 1)(v_c + 1 + \frac{1 - f}{f})}}$	$\sqrt{\dfrac{2}{v_c + 1}}$	$\dfrac{2 \sqrt{v_c}}{v_c + 1}$
$\varphi =$	$\sqrt{\dfrac{v_c + 1 + \frac{1 - f}{f}}{2v_c + \frac{1 - f}{f}}}$	1	$\sqrt{\dfrac{v_c + 1}{2\ v_c}}$

It is possible, therefore, to calculate the swelling thickness of the adsorbed phase for any combination of two symmetrical salts, such as NaCl and $CaSO_4$, provided one measures the total-electrolyte concentration and the proportion of monovalent to divalent ions, and assumes a value for v_c. Knowing also the specific surface of the soil, the swelling volume can be calculated. Assuming that the pore fraction occupied by the swelling prohibits free flow of water, subtraction of the swelling volume from the total pore volume, or of the pore fraction due to swelling from the total pore fraction, yields the pore volume or fraction that still permits unhindered flow.

The Kozenie-Carman equation, derived from Poiseuille's law, describes for viscous flow in unconsolidated porous media like soils the hydraulic conductivity in Darcy's equation as follows:

$$k = \frac{\rho\ g\ \varepsilon^3}{k'\eta\ S_o^2} \qquad [5]$$

where ρ is the liquid density, g is the gravitational constant, η is the liquid viscosity, S_o is the surface of the solid phase per unit volume of the porous bed that is in contact with solution, k' is an empirically determined constant depending mainly on particle size and shape, and ε is the porosity (pore fraction) of the medium filled with liquid. The porosity term lends itself to correction on account of swelling.

Comparing the results of a soil percolated with solutions of different compositions (subscripts i and j), it follows that the hydraulic conductivities are proportional to the flow rates as long as the hydraulic gradients do not differ. Thus, knowing from the flow rates the relation between the hydraulic conductivities, the Kozenie-Carman theory predicts that they compare as the third power of the corresponding porosities. Introducing the correction for swelling it would thus follow that:

$$\frac{k_i}{k_j} = \left(\frac{\varepsilon - \varepsilon_i^*}{\varepsilon - \varepsilon_j^*}\right)^3 \qquad [6a]$$

where ε indicates the total porosity, and ε^* the equivalent porosity due to swelling. This relationship would be valid as long as η_i and η_j, as well as ρ_i and ρ_j (equation [5]) do not differ significantly, and provided S_o is invariable under the conditions established by the different solutions. If S_o is not constant, however, but changes by a factor which is similar to the one characterizing the change in the porosity, it follows that

$$\frac{k_i}{k_j} = \frac{\varepsilon - \varepsilon_i^*}{\varepsilon - \varepsilon_j^*} \qquad [6b]$$

Between these two boundary cases, S_o may change but by a factor dissimilar to the one characterizing the change in porosity. In that case, the power function of the porosity lies between 1 and 3. An especially convenient case would be where

$$\frac{k_i}{k_j} = \left(\frac{\varepsilon - \varepsilon_i^*}{\varepsilon - \varepsilon_j^*}\right)^2 \qquad [6c]$$

Henceforth, the corrected porosity $\varepsilon - \varepsilon^*$ will be termed the effective porosity.

PROCEDURE:

A specially constructed lucite cell was used for the permeability measurements. The soil chamber itself was 5.08 cm high and 5.08 cm I. D.

The cell was assembled by fitting two sidearm inserts with plugs and a bottom insert without the plug onto the main cell body. Fiberglass filter papers were rubber-cemented to the faces of the inserts. The opening between the cell body and the insert was sealed with Apiezon wax to prevent solution and soil material from creeping down to the O-ring seal.

The cell was partially filled with the most concentrated of a set of mixed $NaCl-CaCl_2$ solutions. Mason clay loam (< 50μ), which was suspended also in the most concentrated $NaCl-CaCl_2$ solution, was poured into the cell and packing was continued by the wet-sedimentation process. During the settling process, solution was allowed to leak through the bottom insert. Additions of the suspension were made to get 5.08 cm of soil; the top insert was slowly fitted into the body to fit on top of the soil surface. A 6.62-cm head of solution was maintained on the soil column by means of a Mariotte-constant head arrangement. Percolation was continued with the most concentrated solution (100 meq/liter) and followed with a series of decreasing solution concentrations (60, 30, 10 meq/liter) causing an increase in swelling. This was to prevent possible leakage of solution between the soil mass and the cell wall. The solution was changed to the next dilute concentration each time the flow rate reached a steady value. In each set, the concentration ratio $R = Na^{+} / \sqrt{Ca^{++}}$, mmoles $liter^{-1/2}$, was kept constant. R of 0, 5, and 25 were used.

The flow rate was measured by weighing the solution percolating through the soil column for a prescribed time interval. By maintaining the hydraulic gradient constant, the hydraulic conductivities at the various solution concentrations for a given R could be interrelated. Predictions regarding the hydraulic conductivities relative to the one typical of the soil percolated with the most concentrated solution of each set were made according to equations [6a], [6b], or [6c], whichever fitted the best.

RESULTS AND DISCUSSION:

The hydraulic conductivities of the Mason soil for solutions of 60, 30, and 10 me/liter have been related to the solution of 100 me/

liter. Three sets of these solutions were used, viz., with values for R of 0, 5, and 25. Observed and predicted values for the relative hydraulic conductivities, henceforth called RHC, agreed well (Table 4). There may be some virtue in reporting in detail on some of the steps followed in the theoretical treatment. Knowing R, N (column 1), f (cf. equation [4]), and assuming v_c, values for D were computed using the IBM 1620 system (column 2). The value reported here for v_c, in conjunction with equation [6b], of all other combinations tried, eventually resulted in about the best achievable comparison with experimental data. Next, D was corrected for d as indicated (column 3). The actual swelling distance thus obtained was converted to the pore fraction occupied by swelling, ε^*, by multiplying D - d by a compound factor accounting for the weight of soil used to fill the chamber, the volume of the latter, and the specific surface of the soil (column 4). (In examining published data, information on soil density in the flow bed could sometimes be conveniently used.) The pore fraction due to swelling was subtracted from the total pore fraction in order to find the effective porosity (column 5). Effective porosities were related to the one pertaining to the soil treated with the most concentrated solution of the set (column 6), and the resulting values were considered to represent RHC.

This approach, admittedly, is empirical to the extent that one has to arrive by trial and error at values for v_c, and for the power function of the effective porosity, that give best agreement between theory and experiment. The choice of v_c determines the degree to which the decrease in concentration of the percolant is expressed by an increase in swelling. The ionic composition in each instance is the independent variable, and the swelling distance is the dependent one. As the swelling is restricted by physical confinement due to soil structure, the value of v_c chosen actually represents a complex of interacting conditions which are difficult to assess individually. Selecting a value for v_c implies considering the effect of concentration changes within each set

of solutions of constant R as being fully compensated for by changes in swelling rather than by changes in the distribution factor y_c. Obviously, this is an extreme assumption, which is only mitigated by the freedom of selecting the value for the power function of the relative porosity within the range 1 - 3. This course of action is deemed better, however, than the equally extreme alternative, namely considering the concentration changes of the solution to be fully compensated for by changes in y_c, ignoring any possible swelling. The latter, in fact, is the conventional approach.

The choice of the power function of the effective porosity depends on the extent to which the change in porosity due to the introduction of a different solution is accompanied by a change in surface area in contact with that solution. In particular, the choice indicates whether one considers the change in porosity due to swelling to be accompanied predominantly by a change in the density of pores, or by a change in the size of the pores. Where swelling affects pore density, one could visualize a rather wide range of sizes, the smaller ones of which are effectively blocked by swelling, thus reducing the surface mentioned. In the case where swelling is instrumental in reducing the overall size of the pores, one could think of a rather small range of pore sizes. Thus, all pores are about equally vulnerable to the effects of swelling, yet leave the surface area in contact with solution relatively unaffected. The former case seems to prevail in the case of the Mason soil.

The present use of a solution with R = 0 together with those typified by R = 5 and R = 25 affords the opportunity to consider a matter of ion distribution in the adsorbed phase. By definition, $v_c = \cosh y_c = (u_c + 1/u_c)/2$. Because, in the R = 0 case, the best fit was obtained with $v_c = 1.01$ (using the single power of effective porosity), it follows that $u_c = 1.15$. For the same soil saturated with monovalent cations, therefore, u_c would be $(1.15)^2$ or 1.32. In that case, v_c amounts to 1.04. The best fit in the cases of R = 5 and R = 25, which do not by any means correspond with Na-saturated soil, was obtained using $v_c = 1.25$ and 1.10, respectively,

well in excess of $v_c = 1.04$. The swelling appeared to be greater, therefore, than predicted on the basis of that characteristic of a Ca-saturated soil. The theory, to be consistent, thus would lead to the interpretation that Na and Ca are heterogeneously distributed, in that more Na ions are adsorbed on surfaces involved in swelling than a uniform distribution could account for.

SUMMARY:

The condition of flocculation or deflocculation of soil materials and clay minerals was determined when they were exposed to different electrolyte conditions. Zones of flocculation and deflocculation could be established by relating the deflocculation-flocculation behavior to the sodium adsorption ratio (SAR) and the electrolyte concentration. The kaolinitic, montmorillonitic, and illitic clay minerals behaved similarly to one another; the soil materials, however, behaved differently from each other and also from the clay minerals. For the same total electrolyte concentration, a higher SAR value was required to disperse the soil material in a $NaCl-CaCl_2$ system than in a $NaCl-MgCl_2$ system; or restated in terms of flocculation, the Ca ion is better than the Mg ion as a flocculating cation.

A calcium membrane electrode was used to measure the dissociation and solubility constants of $CaSO_4 \cdot 2H_2O$, which were $5.32 \pm 0.37 \times 10^{-3}$ and $2.50 \pm 0.10 \times 10^{-5}$ and compared favorably with those reported in the literature using other independent techniques. The good agreement obtained indicates that Ca activity measurement with the membrane electrode is reliable, particularly when the composition of the associated ions in solution is adequately defined.

The swelling of soil materials was computed as a function of electrolyte composition from the diffused double-layer theory. Using the Kozenie-Carman equation for flow in porous media, the porosity factor was corrected for swelling. Satisfactory agreement was obtained between the theoretical and experimental data.

PERSONNEL: F. S. Nakayama

REFERENCES:

(1) Bell, R. P. and George, J. H. B.
1953. The incomplete dissociation of some thallous and calcium salts at different temperatures. Faraday Soc. Trans. 49: 619-627.

(2) Bolt, G. H.
1955. Analysis of the validity of the Gouy-Chapman theory of the electric double layer. Jour. Colloid Sci. 10: 206-218.

(3) Collis-George, N., and Smiles, D. E.
1963. An examination of cation balance and moisture characteristic method of determining the stability of soil aggregates. Jour. Soil Sci. 14: 21-32.

(4) Jenny, H., and Reitemeier, R. F.
1935. Ionic exchange in relation to the stability of colloidal systems. Jour. Phys. Chem. 39: 593-604.

(5) Money, R. W., and Davies, C. W.
1932. The extent of dissociation of salts in water. Part IV. Bi-bivalent salts. Faraday Soc. Trans. 28: 610-614.

(6) Moreno, E. C., and Osborne, G.
1963. Solubility of gypsum and dicalcium phosphate dihydrate in the system $CaO-P_2O_5-SO_3-H_2O$ and in soils. Soil Sci. Soc. Amer. Proc. 27: 614-619.

(7) Schofield, R. K., and Talibudeen, O.
1948. Measurement of internal surface by negative adsorption. Faraday Soc. Disc. 3: 51-56.

(8) Wiklander, L., and Hallgren, G.
1944. Über die dispersion der bodenkolloide. Agr. Col. Sweden Annals. 12: 230-250.

Table 1. Physical and chemical analyses of soil materials.

	Big Lake	Mason	House Mountain	Pachappa	Hagerstown
Clay, %	37.8	48.0	44.7	17.7	18.5
Silt, %	38.4	36.8	47.4	42.1	66.7
Sand, %	23.8	15.2	8.0	40.2	14.8
pH (paste)	6.53	6.41	7.42	7.55	5.84
Ca (meq/100g)	12.6	20.2	40.3	9.16	5.23
Mg (meq/100g)	5.8	16.6	7.1	1.19	1.36
Na (meq/100g)	0.26	0.11	0.32	0.26	1.80
K (meq/100g)	0.45	0.41	2.61	0.43	8.19
Organic matter, %	0.31	2.32	1.32	1.45	2.18
$CaCO_3$ equiv., %	0.97	0.94	2.40	0.53	0.17

Table 2. Comparison of amount soil in suspension after salt treatment and predictable suspension status.

Soil and treatment 32 meq/100 g		SAR	Electrolyte conc., meq/L	Pipette analysis < 2μ, %	Predicted suspension status from Figure 3
Big Lake	NaCl	16.6	20	0	Flocculated
	Na_2CO_3	25.2	9	0.9	Deflocculated
	Na_2SO_4	9.8	17	0	Flocculated
Mason	NaCl	11.2	19	0.1	Flocculated
	Na_2CO_3	15.0	8	5.8	Deflocculated
	Na_2SO_4	12.3	16	0.3	Flocculated
Pachappa	NaCl	19.7	20	0.7	Deflocculated
	Na_2CO_3	26.9	13	1.9	Deflocculated
	Na_2SO_4	15.6	18	0.8	Deflocculated

Table 3. Dissociation and solubility product constants of $CaSO_4$ at various solution compositions.

	Electrolyte	$[Ca^{2+}]_T$ $\times 10^2$	(Ca^{2+}) $\times 10^3$	μ $\times 10^2$	α	K_D $\times 10^3$	K_S $\times 10^5$
1.	Satd. $CaSO_4$	1.47	5.4	4.21	0.76	6.37	2.67
2.	Satd. $CaSO_4$ + 0.001 M NaCl	1.47	5.2	4.17	0.69	5.60	2.55
3.	Satd. $CaSO_4$ + 0.01 M NaCl	1.59	5.3	5.44	0.70	5.12	2.44
4.	Satd. $CaSO_4$ + 0.025 M NaCl	1.69	5.5	7.43	0.73	5.83	2.66
5.	Satd. $CaSO_4$ + 0.050 M NaCl	1.86	5.6	10.58	0.75	5.38	2.50
6.	Satd. $CaSO_4$ + 0.075 M NaCl	2.00	5.7	13.80	0.78	5.83	2.56
7.	Satd. $CaSO_4$ + 0.1 M NaCl	2.13	5.9	16.80	0.80	5.90	2.51
8.	Satd. $CaSO_4$ + 0.001 M Na_2SO_4	1.45	5.0	4.24	0.68	5.17	2.40
9.	Satd. $CaSO_4$ + 0.01 M Na_2SO_4	1.23	3.5	5.59	0.61	5.08	2.44
10.	Satd. $CaSO_4$ + 0.025 M Na_2SO_4	1.08	2.6	7.74	0.56	6.16	2.92
11.	Satd. $CaSO_4$ + 0.050 M Na_2SO_4	1.01	2.0	17.28	0.57	6.56	2.85

Table 4. Measured and predicted values of the relative hydraulic conductivities of the Mason clay loam (102 m^2/g, 0.567 me/g).

N	D	D − d	ε*	ε − ε*	RHC		
me/l	Å	Å			Theor.	Exptl.	Ratio
R = 0	R = 0.715	d = 0.3Å	v_c = 1.01		p = 1		
100	22.9	22.6	0.176	0.539	(1)	(1)	
60	29.4	29.1	0.224	0.491	0.91	0.85	1.07
30	41.8	41.5	0.320	0.395	0.73	0.70	1.04
10	72.4	72.1	0.550	0.165	0.31	0.60	0.52
R = 5	R = 0.698	d = 0.3Å	v_c = 1.25		p = 1		
100	12.3	12.0	0.098	0.600	(1)	(1)	
60	16.4	16.1	0.131	0.567	0.95	0.95	1.00
30	24.4	24.1	0.196	0.502	0.84	0.82	1.02
10	47.2	46.9	0.382	0.316	0.53	0.62	0.86
R = 25	R = 0.701	d = 0.7Å	v_c = 1.10		p = 1		
100	21.1	20.4	0.164	0.537	(1)	(1)	
60	28.7	28.0	0.226	0.475	0.87	0.90	0.97
30	43.1	42.4	0.342	0.359	0.67	0.69	0.97
10	80.2	79.5	0.640	0.061	0.11	0.10	1.10

Legend: N = total electrolyte concentration in me/liter, D = swelling thickness from hypothetical plane of infinite potential, D − d = swelling thickness from real surface, both in Angströms, ε* = pore fraction occupied by swelling volume, ε − ε* = pore fraction effective for flow, RHC = relative hydraulic conductivity, p = power function of the effective porosity. $R = Na/\sqrt{Ca}$, concentrations in millimoles/liter.

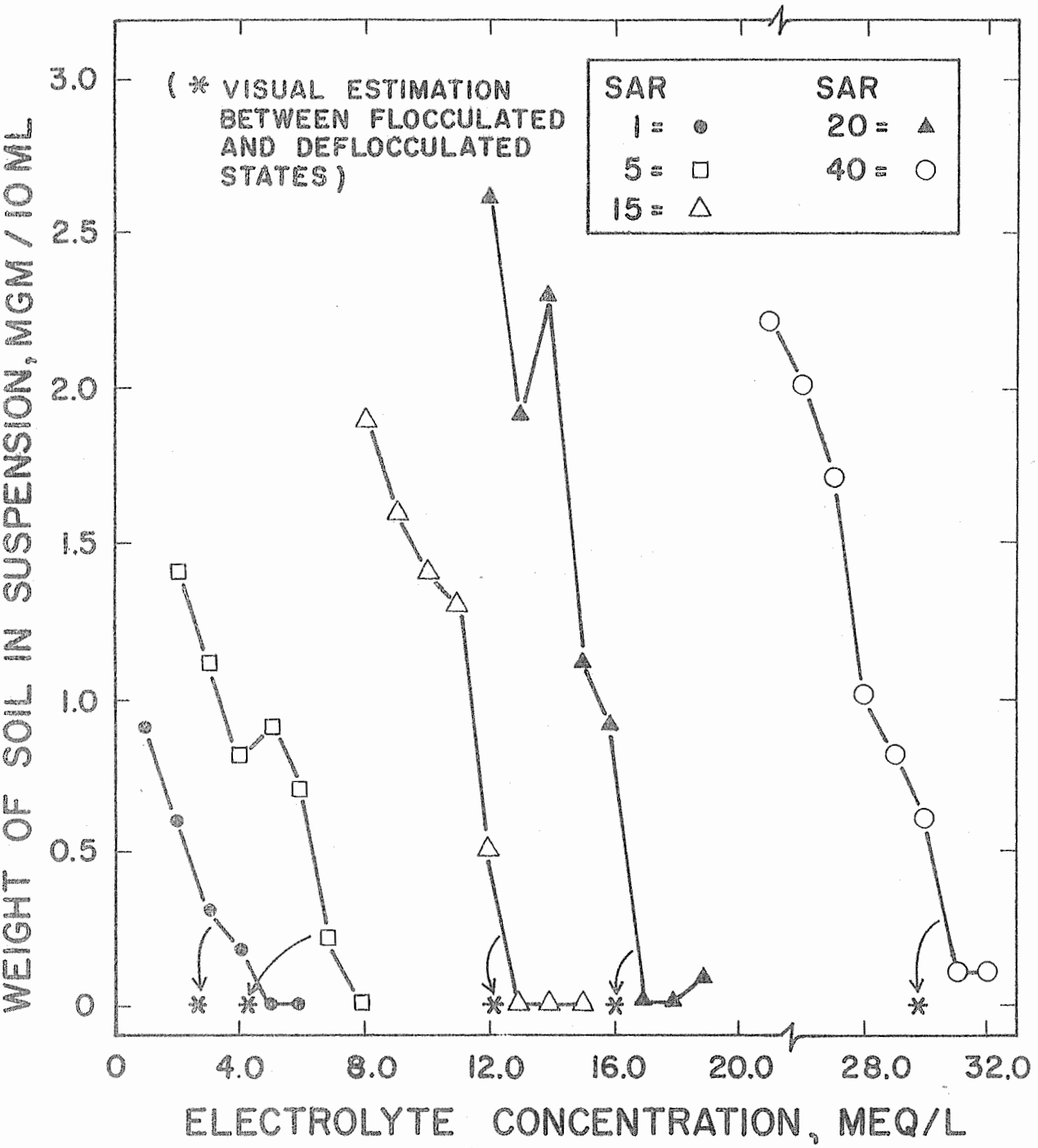

Figure 1. Comparison of pipette and visual methods for determining the dispersed state of soil suspensions.

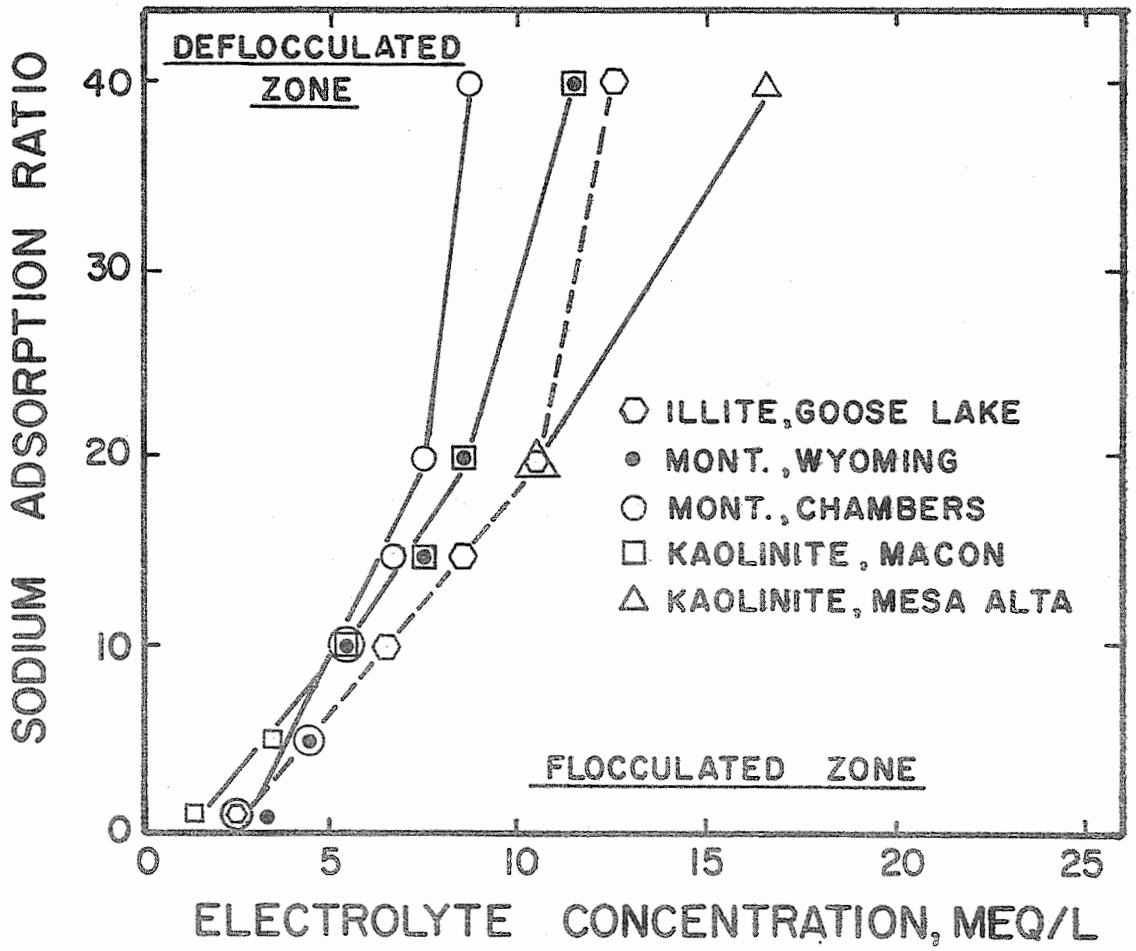

Figure 2. Deflocculated-flocculated states of clay minerals as related to SAR and electrolyte concentration.

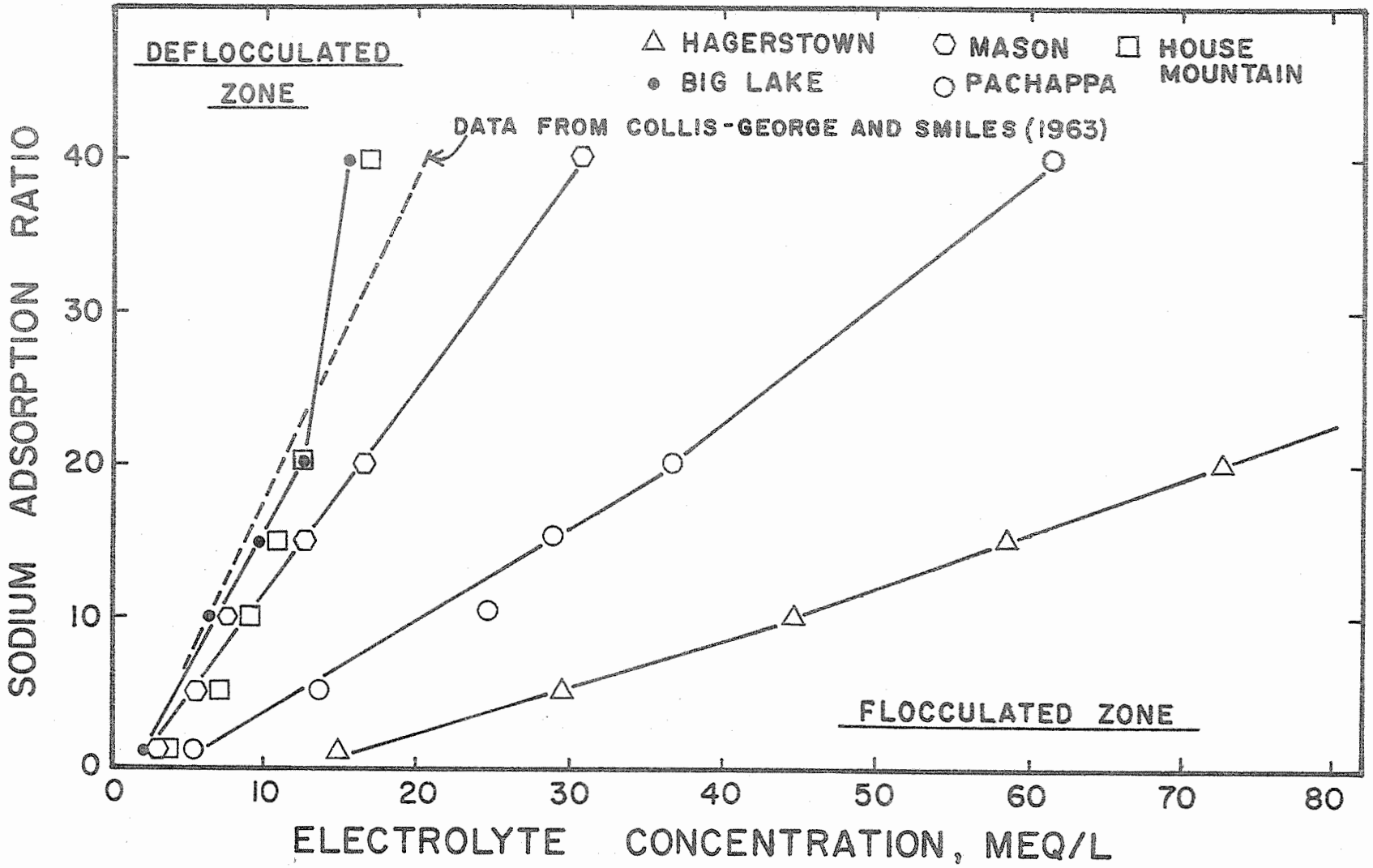

Figure 3. Deflocculated-flocculated states of soil materials as related to SAR and electrolyte concentration.

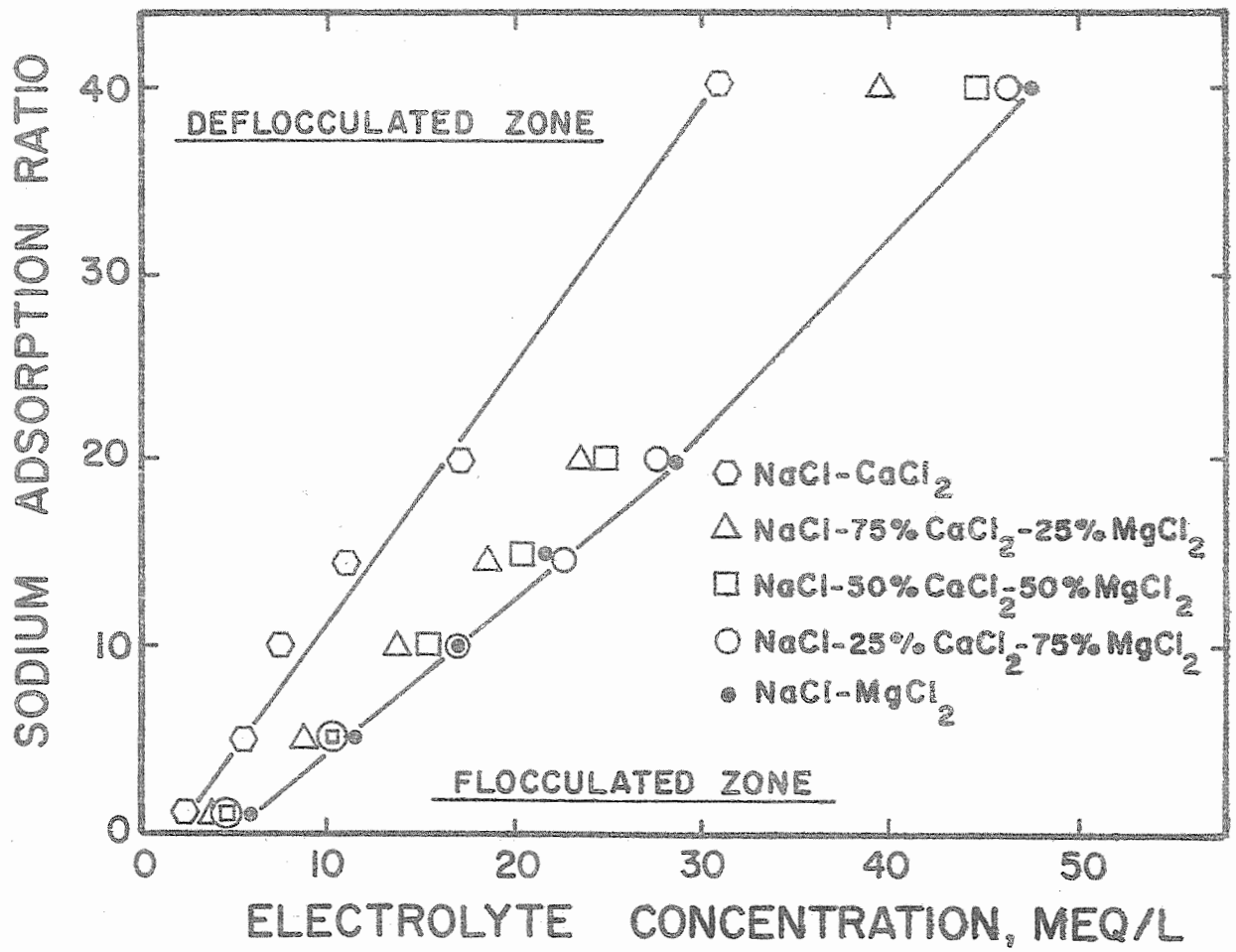

Figure 4. Deflocculated-flocculated states of Mason soil as related to the Ca-Mg-Na status and electrolyte concentration.

TITLE: MATERIALS AND METHODS FOR WATER HARVESTING AND WATER STORAGE IN THE STATE OF HAWAII

LINE PROJECT: SWC III-gG3 CODE NO.: Ariz.-WCL-42

INTRODUCTION:

Water harvesting in the State of Hawaii is highly feasible, but due to lack of information concerning design criteria and materials specifications suited to Hawaiian conditions, the maximum benefits of this source of water are not being fully realized. For preliminary investigation of the problems, two experimental water harvesting structures were installed in Hawaii in June 1966. One installation is an operational catchment and storage reservoir combination on the Island of Hawaii. The other installation is a four-plot test unit on the Island of Maui. These structures permit evaluation of installation procedures and provide weathering and runoff data from various treatments and materials under high-rainfall climatic conditions.

PROCEDURE:

Kukaiau catchment. This catchment, on the Island of Hawaii in a 100-inch rainfall zone, consists of a 10,225 ft^2 catchment and a 750,000-gal storage reservoir. The installation was a cooperative effort by Kukaiau Ranch, Wisdom International Rubber Company, Soil Conservation Service, and the U. S. Water Conservation Laboratory. Materials were furnished by Dow Chemical Company, Wisdom Rubber Company, and DuPont de Nemours Company.

The grass and brush in the reservoir and catchment areas was removed with a bulldozer and the soil surface hand raked to remove all loose rocks. After raking, the entire area was compacted smooth with 4-wheel drive vehicles. Rocks which were too big to remove were rounded with a sledge hammer and covered with a 1-inch layer of soil. The area was then sprayed with soil sterilant, a combination of Dowpon, Karmex, and 2-4D. The reservoir was lined with a 30-mil-thick experimental Nordel rubber sheeting supplied by DuPont Company. The sheeting, supplied in rolls 13 1/2 ft wide and lengths up to 170 ft long, was field seamed together with 4-inch wide lap joints.

The catchment was covered with 20-mil-thick modified, black polyethylene furnished by Dow Chemical Company. The material, supplied in rolls 54 inches wide, was solvent welded together with 3-inch lap joints. The lower edge of the catchment sheeting was bonded directly to the reservoir lining with butyl tape. A 6-inch capacity raingage was installed at the site and arrangements made for installation of a 20-inch capacity gage at a later date. The entire area was fenced with five rows of barbed wire and a 5 ft high woven wire.

Maui catchments. This installation on the Island of Maui is in an 80-inch rainfall zone and consists of four test plots 40 × 80 ft on a 5 percent slope. The installation was a cooperative effort by East Maui Irrigation District, Hawaiian Commercial and Sugar Company, Wisdom International Rubber Company, Soil Conservation Service, and the U. S. Water Conservation Laboratory. Materials for the installation were furnished by DuPont Company, Wisdom International Rubber Company, Hodgeman Rubber Company, and the U. S. Water Conservation Laboratory.

Plots 1, 2, and 3 were rough shaped to the desired slope and berms pushed into place with a bulldozer. Final shaping of the berms was done by hand. On plots 1 and 2 the soil surface was hand raked smooth and compacted with 4-wheel drive vehicles. Plot 3 was smoothed but not compacted. The three plots were then sprayed with a soil sterilant (DuPont DCMU).

Plot No. 1 was covered with a 20-mil-thick Hypalon 45 sheeting furnished by DuPont. The material, furnished in 54-inch width rolls, was field seamed with 3-inch lap joints. The laps originally were to be solvent welded, but the material had undergone partial self-vulcanizing and would not bond properly. It was necessary to seal the laps with a butyl cement adhesive.

Plot No. 2 was covered with a 20-mil cotton-reinforced butyl sheeting furnished by Hodgeman Rubber Company. The sheeting, supplied in rolls 54 inches wide, was bonded to the soil with SS-1

asphalt emulsion applied at a rate of 0.3-gal emulsion yd^{-2}. The asphalt was sprayed on in a strip 10 ft wide, then the butyl unrolled and pressed into place with a foam covered roller. The lap joints were then sealed with a butyl cement adhesive.

Plot No. 3 was treated with the two-phase asphalt application. Laboratory studies with soil from the site had indicated a satisfactory pavement could be obtained with RC-250 cutback asphalt as a soil stabilizer with an asphalt emulsion sealcoat. The spray equipment available did not have equipment for heating the asphalt, therefore, we could not spray the RC-250 which requires heating to 200°F. It was decided to use an MC-800 cutback asphalt which was available in heated tanks and would not require additional heating. Laboratory studies had shown the MC-800 would also stabilize the soil, but would not cure as fast as the RC-250. Prior to spraying, the plot was smoothed using the backs of rakes which formed an aggregated soil structure that would allow the asphalt to penetrate. The asphalt was sprayed on the plot at a rate of 1.40-gal of cutback yd^{-2} at a temperature of 180°F. Arrangements were made for application of a sealcoat after the basecoat had cured. On 3 October 1966 a sealcoat of SS-1 asphalt emulsion was applied at a rate of 0.7-gal emulsion yd^{-2}.

Plot No. 4 is an undisturbed surface which has a good cover of grass. The soil surface is very rough and irregular around clumps of grass within the area. Soil berms were pushed up around the plot from the outside.

The instrumentation at the site consists of one, 12-inch capacity - 8-day weighing raingage and water measuring flumes with recorders on plots 1, 2, and 3. The flumes are a precalibrated V-notch critical depth type with capacity range of 0.01 to 10 cfs. They are equipped with 24-hour water stage recorders which start automatically as water flows through the flume and stops when flow ceases. Initially, the flumes were installed only on plots 3 and 4. A third flume was installed on plot 2 in December 1966. The flume on plot 4 is fenced so cattle may graze the area.

RESULTS AND DISCUSSION:

The installations at both sites were inspected in December 1966. The reservoir at Kukaiau was approximately three-fourths full, but the rainfall

in the area had been quite low in October and November. The only visible damage to the installation was a blade of grass growing through the catchment sheeting in one corner. A later report at the end of December from the manager of Kukaiau Ranch stated the reservoir had filled and was overflowing by 30 December 1966.

The plots at the Maui site were considered in excellent condition when inspected in December. Plots 1 and 2 showed no signs of deterioration. Some grass was starting to grow through the asphalt on plot 3. Again, this was believed a result of poor soil sterilization. The asphalt sealcoat appeared good, but there was a sponginess in the basecoat.

The runoff data collected from the plots was not complete for the year. Problems were encountered with the clocks on the recorders failing to start when water started flowing through the flume. We are investigating various methods of insuring that the clocks will start each time.

SUMMARY AND CONCLUSIONS:

Water harvesting in Hawaii to supplement existing water supplies is highly feasible and badly needed. The present biggest deterent from large scale use is a lack of information concerning design criteria and materials specifications suited for Hawaiian conditions. For a preliminary evaluation, two experimental water harvesting structures were installed in Hawaii in June 1966. One is an operational catchment and storage reservoir combination on the Island of Hawaii. The other is a four plot test unit of plastic sheetings and asphalt treatments on the Island of Maui. Runoff from three of the Maui plots is being recorded with water stage recorders on calibrated flumes. Runoff from the various treatments will be compared to the rainfall as measured with a recording raingage. The installations were considered in good condition when inspected December 1966. Analysis of the data will be started in the near future.

PERSONNEL: L. E. Myers, G. W. Frasier

TITLE: INTEGRATING VELOCITY PROFILE METERS

LINE PROJECT: SWC X-gG1 CODE NO.: Ariz.-WCL-43

INTRODUCTION:

See Annual Report for 1965.

PROCEDURE:

Similar to 1965 except as noted.

Tests on meter No. 2 were conducted in a laboratory channel 2 ft wide and 32 ft long. The vane meter was inserted vertically into the established flow which was varied from about 6 inches deep to 1 ft deep. The torsional force necessary to prevent the vane blade of the meter from pivoting about the hinged side was read from a dial mounted on the frame that supported the blade. This total force reading was compared to the total force calculated from a pitot-tube traverse of the channel at the same point where the meter was inserted.

A Prandtl-type pitot tube was used on the tests conducted in the 2-ft wide channel because of mechanical difficulties of providing the necessary floor manometer taps to be used with the total head probe, as was done in the 1-ft wide laboratory channel.

RESULTS AND DISCUSSION:

Laboratory Study. Table 1 contains a comparison of the average velocity determined with vane meter No. 2 and the average velocities calculated from the pitot traverses. The results of the tests in the 2-ft wide channel were not as consistant as was expected. Values obtained ranged from about 1 percent above to as much as 4 percent below the velocities determined from the pitot tube traverses. This is attributed to the unsteady flow conditions that prevailed in the larger laboratory channel. The channel entrance section and flow baffling devices have been rebuilt in an effort to produce a more steady flow for a period long enough to obtain a stable pitot tube traverse and a vane-meter reading. At the time the tests listed in Table 1 were conducted, it was difficult to repeat either the pitot traverse or the vane meter reading because of wide fluctuations in flow.

Theoretical Study. Frequently, it is desirable to have a direct discharge-rate indicating device in a channel rather than a velocity

indicating mechanism. Such a vane-type device is commercially available for several specific channel geometries (1). Because the blade of this meter is allowed to deflect, which changes the impact area and the angle of contact, theoretical analysis is difficult.

The integrating vane meter, which in its present form is a velocity indicating device, is not allowed to deflect appreciably from a broadside-to-flow attitude. Thus, theoretical analysis of the fluid forces on the blade is simplified and should permit theoretical prediction of the necessary blade shape for any specified channel geometry so that discharge rate is indicated directly. This requires, for example, that a rectangular channel flowing 1 ft deep at a velocity of 2 ft per second would cause the same deflection as when it was flowing 2 ft deep at a velocity of 1 ft per second.

Calculation of the required blade shape for prismatic channels of any geometry is presented below. Assumptions are that the drag coefficient remains constant for any width of blade and that the momentum distribution coefficient is small.

Let

A_b = Area of vane blade

A_c = Area of channel section for which blade is to indicate discharge rate

C_d = Drag coefficient

F_d = Total force on blade

g = Acceleration due to gravity

Q = Discharge

v = Average velocity

w = Unit weight of fluid

β = Momentum distribution coefficient

then from previously derived equations, (see Annual Report, 1965),

$$F_d = C_d \frac{\beta w}{2g} v^2 A_b \qquad [1]$$

or since

$$Q = A_c v \qquad [2]$$

$$F_d = C_d \frac{\beta w Q^2}{2g} \frac{A_b}{A_c^{\,2}} \qquad [3]$$

Thus, for F_d to remain constant for a constant value of Q, it is necessary that

$$\frac{A_b}{A_c^{\,2}} = k, \text{ a constant} \qquad [4]$$

Whatever its final shape, the area of the blade can be described as a function of the blade width, b, and the distance from the channel bottom, y, or

$$A_b = \int_o^y b\,dy = k\,A_c^{\,2} \qquad [5]$$

taking the derivative of equation [5] with respect to y,

$$b = 2k\,A\,\frac{dA_c}{dy} \qquad [6]$$

but, $dA_c/dy = T_c$, the top width of the channel at the depth y in question, so that for any channel geometry

$$b = 2k\,A_c\,T_c \qquad [7]$$

Thus, the width of the blade is proportional to the area of the channel below the depth, y, in question times the top width for the same depth.

SUMMARY AND CONCLUSIONS:

Two models of a fluid-velocity indicating device have been constructed and tested in laboratory channels. The meter is of the force-deflection type and uses a rectangular blade placed into the flowing stream. The total force exerted on the 1-inch wide blade by the velocity profile registers as a torque about a hinged edge of the blade.

Tests made using the improved model were inconclusive because steady flow rates without wide fluctuation in the current patterns were not achieved. Remedial work has been completed on the channel entrance section and flow baffling devices in order to stabilize the flow

conditions. Additional testing has not been completed on the modified flow system.

Theoretical analysis indicates that, with proper blade shape, the meter can be extended to indicate direct discharge in any prismatic channel independent of depth of flow. Shapes for rectangular, triangular, trapezoidal, parabolic, and circular channels have been calculated, but none have been constructed for testing as yet.

REFERENCES:

(1) Robinson, A. R.
1963. Evaluation of the vane-type flow meter. Agric. Engin. 44:374-375.

PERSONNEL: J. A. Replogle

Table 1. Comparison of average velocities determined with a pitot tube and with integrating velocity-profile meter number 2.

Test no.	Flow depth y	Average velocity, $\bar{v}$ Pitot tube	Vane meter	$\Delta\bar{v}$
	(ft)	(ft/sec)	(ft/sec)	(%)
1	0.757	1.668	1.602	3.96
2	0.817	1.652	1.582	4.24
3	0.817	1.176	1.181	-0.43
3b	0.894	1.220	1.204	1.31
4	0.629	1.582	1.581	0.06
5	0.946	1.241	1.229	0.97
6	1.09	1.631	1.561	4.29

TITLE: EXPERIMENTAL AND ANALYTICAL STUDIES OF THE FLOW AND OXYGEN REGIMES IN SOIL INTERMITTENTLY INUNDATED WITH LOW QUALITY WATER

LINE PROJECT: SWC IV gG2 CODE NO.: Ariz.-WCL-44

INTRODUCTION:

The objective of this project is to develop a theoretical foundation for the scheduling of intermittent inundation of recharge basins with low quality water. The project will be conducted with special reference to the experimental recharge facility in the Salt River bed about 1 mile west of 91st Avenue (Project Flushing Meadows). It is expected, however, that the methodology will be sufficiently general to permit extension of the principles to facilities with other conditions of soil, water table, and recharge water. The initial objectives of the project are:

a. Design and construction of column traversing equipment and associated electronic instrumentation for non-destructive, simultaneous measurement of water content, pressure head and pore air pressure in laboratory columns of porous materials.

b. Use of this equipment for the measurement under dynamic conditions of the hydraulic characteristics of porous materials.

c. Laboratory measurement of the water content and pressure head changes occurring in soils columns under intermittent inundations.

d. Development of numerical solutions of the flow problems under c, using a digital computer, and the comparison of the computed profiles with those experimentally obtained.

The above techniques for measuring unsaturated hydraulic conductivity and water content characteristics of soil and for numerical solution of vertical drainage and infiltration systems will be used to develop theoretical schedules for intermittent inundation of low quality water for ground water recharge under various soil and water table conditions. Inundations and dry-ups should be rotated such that maximum recharge per unit area is obtained while allowing

sufficient dry-up time to permit a sufficient amount of air to enter the soil to satisfy the oxygen demand of the infiltrated water.

PROCEDURE:

1. Design and construction of column instrumentation. A large drill press assembly with a movable table was used for the vertical traversing of the columns. The column of the drill press was machined to give a shallow longitudinal slot to house several lengths of rack which permitted the traversing of the table over the entire column length. The table was cut to form a yoke for clearance around the soil column. The gamma source (100 mc Cs^{137}) and detector along with the lead shielding and collimators were mounted on the table, which was counterweighted. The gamma source and detector were collimated by two slits 0.2 cm high and 2.0 cm wide. The electronic equipment for the measuring of the gamma radiation was of standard make. The detector was a Baird Atomic Scintillation Probe Model 815 CL. It was powered by a Baird Atomic Power Supply Model 312A. The signal was fed into a Baird Atomic non-overloading Amplifier Model 215. After amplification, the signal entered a Baird Atomic Single Channel Pulse Height Analyzer Model 510. The pulse rate was counted by a Baird Atomic High Speed Scaler Model 134 with a Baird Atomic Precision Timer Model 630. In addition, a Nuclear Chicago Ratemeter Model 8733 connected to a Leeds & Northrup speedomax-W recorder was used.

To measure the water content of the soil in a cylindrical plastic column by the gamma attenuation method, it was necessary to specially machine the inside and outside of the 5" O.D. plastic cylinder on diametrical faces to give a uniform soil and column-wall thickness over the full collimation width. Soil columns up to 180 cm in length can be accommodated and access ports are available at 1-cm vertical intervals. A Statham bi-directional differential pressure transducer, type PM-131-TC was used as the pressure sensor. The signal was fed from it into a Leeds & Northrup Strain Gage module and recorded by a Leeds & Northrup "H" Azar recorder. By joining two multiple-port selector valves in parallel, it was possible to rapidly scan the pressure at 22 tensiometer points.

2. Temperature effects in the tensiometer-pressure transducer system. The existence of some instability in the pressure record was traced to a temperature effect on the nylon hydraulic pressure leads. A mathematical model explaining this effect, which included diffusion through the tube walls, was developed. Predictions were then made of pressure amplitudes and phase shifts as observed experimentally. The experiment was carried out in a controlled temperature room where an almost perfect sinusoidal temperature variation appeared to occur. The temperature was monitored by a rapid response thermistor connected to a potentiometric recorder. The experiment was carried out with both a tensiometer on one end of the nylon tubing and with that end being blocked off. The other end was connected to the transducer system. This was done to avoid calculating the temperature distribution across the nylon tubing walls. The experiment then consisted of measuring the pressure and temperature fluctuations with the hydraulic line terminated either by the blanked-off fitting or by a tensiometer kept at atmospheric pressure. The rate of diffusion of water vapor through the tubing walls was determined by periodically weighing a water-filled but sealed length of tubing.

3. Tensiometer behavior under conditions of changing pore air pressure. Intermittent watering schedules may cause zones of air in the profile to attain pressures in excess of atmospheric. Under these conditions, the response behavior of the tensiometer-pressure transducer system requires careful interpretation. A theoretical and experimental study of this response behavior was made. A small cell was made in which a tensiometer (connected to the transducer) and a rapid response air pressure measuring device was inserted. The cell was successively filled with sand of different water contents. For each condition, an air pressure was applied and the tensiometer response was recorded.

4. Entrapped air method of measuring the hydraulic conductivity-water content relationship. When a fully saturated column of porous material is partially drained and then rewet at the upper surface so

that air can not escape, a hydraulic situation is produced which yields a bell-shaped water content profile. Since, with correct timing of the rewetting phase, steady-state conditions are quickly achieved, it is possible to measure the steady-state flux, water contents and pressure heads using the equipment listed under 1. This information permits the determination of the relationship between the hydraulic conductivity, K, and water content, θ, in one simple experiment. The procedure reduces considerably the time required to measure the hydraulic characteristics of soil materials in columns. This method was used on two materials; #17 Ottawa sand and Banding sand.

5. Laboratory column experiments. Using the equipment described under 1 of this section, the following experiments have been completed at least for one run to provide the basic experimental information for the numerical comparisons.

a. Drainage of 180-cm column of #17 Ottawa sand to a constant water table at the bottom of the column for both fully saturated and resaturated conditions. The resaturated condition is meant to imply that the column had entrapped air in it after rewetting.

b. Infiltration into the 180-cm column following two stages of drainage. The first infiltration was timed to start approximately 24 hours after the commencement of the drainage cycle when the flux of water out the bottom of the column was extremely small. The second rewetting was initiated just 30 minutes after the start of drainage involving thereby wetting while drainage is still going on.

c. Redistribution of water in the column following partial wetting up from above.

d. Drainage of stratified columns using a 30-cm layer of the #17 sand on top of a 70-cm layer of the Banding sand, and vice versa.

6. Numerical approach. Computer programs have been prepared for the numerical solution of the problems listed as 5a, 5b, and 5d above. The programs have been written in Fortran IV for the Univac

1107 but plans have been made to revise the programs slightly and run them on the IBM 7094 at the University of Illinois. This change is being considered due to the big price differential for computer time.

7. Recording tensiometer for field measurement. The recharge program with which the laboratory investigations are closely related requires an accurate field recording of water pressure changes in the soil profile to considerable depths. For this purpose, a self-contained tensiometer-pressure transducer unit for field application was designed, constructed and tested. The transducer was the same model as in 1 and a diagram of the system is shown in Figure 1.

RESULTS AND DISCUSSION:

The numerical subdivision of this section follows that of the section on Procedure.

1. The laboratory instrumentation has been used for several different phases of this study. The water content, θ in cc/cc, versus pressure head, h in cm of water, relationships are shown in Figures 2 and 3 for the #17 Ottawa sand and the Banding sand, respectively. The dots on the curves are the experimentally determined points, the solid lines were sketched through these points and the dashed lines are extrapolations. As can be seen, the Banding sand is finer, having a higher air-entry value and a smaller value of $d\theta/dh$. The rewetting scanning curves for the Banding sand and the drying scanning curves for each sand have not as yet been determined.

2. The measured amplitudes of pressure changes brought about by temperature changes for two tensiometers were 6.9 and 2.8 mb. The computed values from theory were 7.6 and 2.8 mb, respectively, giving very good agreement. The phase shifts measured experimentally were 0.64 and 0.76 min and the predicted values were 0.61 and 0.71 min. The diffusion of water vapor through the walls of the tubing was measured to be 2.0×10^{-7} cm^3/min and the predicted values were 1.6×10^{-7} cm^3/min. The theory has been developed and the work

reported in the following manuscript: K. K. Watson and R. D. Jackson, "Temperature effects in a tensiometer-pressure transducer system." Proc. Soil Sci. Soc. of Am. In press.

3. The results of the experimental procedures indicated earlier were: for coarse ceramics and wet sand, the applied air pressure was always immediately recorded as a step change in the transducer output. However, for fine ceramics and drier conditions, only a portion of the applied air pressure was detectable on the output record. This was not a response effect but a "water limiting" condition. The independent air pressure measuring system records the entire air pressure change but only a part of this change appears in the output. Since capillary pressure changes are occurring simultaneously, it becomes impossible to separate the capillary pressure change from the nonrecorded air pressure component. The following manuscript, giving the results in detail, has been presented for publication: K. K. Watson, "The response behavior of a tensiometer-pressure transducer system under conditions of changing pore air pressure." Soil Sci. In review.

4. The results of the entrapped air method of determining the $K(\theta)$ relationship for the #17 Ottawa sand and the Banding sand are shown in Figures 4 and 5. The points are experimentally determined, the solid lines are drawn through the points, and the dashed lines are extensions of the solid lines. Since part of the column is wetting and part is drying, this gives information on the hysteresis behavior of the $K(\theta)$ relationship. In the two sands examined, no such hysteresis effects can be observed. A manuscript on this work is in preparation.

5. The first runs on the experiments outlined in the previous section have been made and the data are in the process of correlation with the numerical results. An extremely interesting and fundamental observation was made in the stratified column experiment in which the fine sand overlays the coarse. The pressure head in the bottom coarse layer became much more negative than the air-entry value with no change in water content. This was due to the fact that no air could

enter this layer until the fine layer drained. After air had entered the coarse sand, the pressure head actually increased while the water content was decreasing. The observed phenomenon relates to the system dependence of the water content-pressure head relationship. A manuscript has been prepared on this observation. K. K. Watson and F. D. Whisler, "System dependence of the water content--pressure head relationship." Note in Proc. Soil Sci. Soc. of Am. In review.

6. The computer program written for the numerical analysis of drainage to a constant water table has been checked against several published results (1, 2, 3, 4, 5). Figure 6 shows the $\theta(h)$ relationships and Figure 7 shows the $K(\theta)$ relationships which describe the materials which have been tested. Figure 8 shows a comparison between the experimental results in terms of the h(z) relationship as a function of time and the numerical predictions for the material, Botany sand, reported by Watson. Figure 9 shows the comparison between the experimental results obtained by Prill, Johnson, and Morris for a Fresno sand and the numerical results. As can be seen, the agreement is very good for Botany sand and not so good for the Fresno sand. The latter may be due to the fact that (1) tensiometers and manometers were used to follow the pressure head changes and (2) the characteristics used in the computer were the averages of two columns. A manuscript is being prepared to report on these and other comparisons and to discuss the physics of the processes involved. The numerical programs will also be used to predict the results observed in the columns of sand set up in the Laboratory. This will take considerable time both experimentally and numerically.

7. A pilot field study indicated that the tensiometer system described earlier was very satisfactory. With a transducer of $\pm$ 5 psi range and a ceramic of 600 mb bubbling pressure, the time constant of the system is 0.2 seconds. Field calibration of this equipment can be made by using the reference port of the transducer and a portable, well regulated air pressure system. A manuscript describing the equipment and its performance has been accepted for publication in the Journal of Hydrology. K. K. Watson, "A recording field tensiometer with rapid response characteristics."

SUMMARY AND CONCLUSIONS:

In order to develop a theoretical foundation for the scheduling of intermittent inundation of recharge basins with low quality water, both laboratory and mathematical studies have to be made. A vertical traversing system using a drill press has been adapted to the laboratory study of vertical flow of water in soil columns. The study has been instrumented so that the water content of the columns can be measured nondestructively by a gamma radiation system and the soil-water pressure can be measured simultaneously using a strain gage transducer-tensiometer system.

The existence of some instability in the pressure record was traced to a temperature effect on the nylon hydraulic pressure leads. A mathematical model explaining this effect, which included diffusion through the tube walls, was developed. Predictions were then made of pressure amplitudes and phase shifts as observed experimentally. These predictions compared closely with those determined experimentally.

Intermittent watering schedules may cause zones of air in the profile to attain pressures in excess of atmospheric. Under these conditions, the response behavior of the tensiometer-pressure transducer system requires careful interpretation. A theoretical and experimental study of this response behavior was made. The theory gives a satisfactory explanation of the phenomenon and the correction approach to be used.

When a fully saturated column of porous material is partially drained and then rewet at the upper surface so that air can not escape, a hydraulic situation is produced which yields a bell-shaped water content profile. Since, with correct timing of the rewetting phase, steady-state conditions are quickly achieved, it is possible to measure the steady-state flux, water contents, and pressure heads using the equipment mentioned earlier. This information permits the determination of the relationship between hydraulic conductivity and water content in one simple experiment. It also yields valuable information on the lack of hysteresis in the relationship.

In order to have experimental information to compare to the mathematical solutions of the flow equation, the following experiments were run:

a. Drainage of 180-cm column of #17 Ottawa sand to a constant water table at the bottom of the column for both fully saturated and resaturated conditions. The resaturated condition is meant to imply that the column had entrapped air.

b. Infiltration into the 180-cm column following two stages of drainage. The first infiltration was timed to start approximately 24 hours after the commencement of the drainage cycle when the flux of water out the bottom of the column was extremely small. The second rewetting was initiated just 30 minutes after the start of drainage involving thereby wetting while drainage is still going on.

c. Redistribution of water in the columns following partial wetting up from above.

d. Drainage of stratified columns using a 30-cm layer of the #17 sand on top of a 70-cm layer of Banding sand, and vice versa. When the Banding sand, a finer sand, was on top, the coarser sand did not drain at its "usual" air-entry value. Thus, the moisture characteristic is not always unique, but can be system dependent.

Computer programs have been written for numerically solving the flow equation and predicting the results of parts a, c, and d above. The programs are still being tested and the stage has been reached where extensive computer time is required to obtain the necessary numerical solutions. When this is completed, the numerical and experimental results can be compared and conclusions reached on the accuracy of the numerical predictive approach and the accuracy of the data needed for such an approach.

The recharge program requires an accurate field recording of water pressure changes in the soil profile to considerable depths. For this purpose, a self-contained tensiometer-pressure-transducer unit for field application was successfully designed, constructed, and tested.

REFERENCES:

(1) Day, P. R., and Luthin, J. N.
1956. A numerical solution of the differential equation of flow for a vertical drainage problem. SSSAP 20:443-447.

(2) Jensen, M. E.
1965. Nonsteady-state drainage of fluid from porous media and drainable porosity. Unpublished Ph. D. thesis. Colorado State University.

(3) Liakopoulos, A. C.
1965. Retention and distribution of moisture in soils after infiltration has ceased. Internatl. Assoc. Sci. Hydrol. B. 10:58-69.

(4) Prill, R. C., Johnson, A. I., Morris, D. A.
1965. Specific yield-laboratory experiments showing the effect of time on column drainage. USGS Water-Supply Paper 1662-B.

(5) Watson, K. K.
1966. An instantaneous profile method for determining the hydraulic conductivity of unsaturated porous materials. Water Resources Research 2:709-715.

PERSONNEL: K. K. Watson, Herman Bouwer, F. D. Whisler.

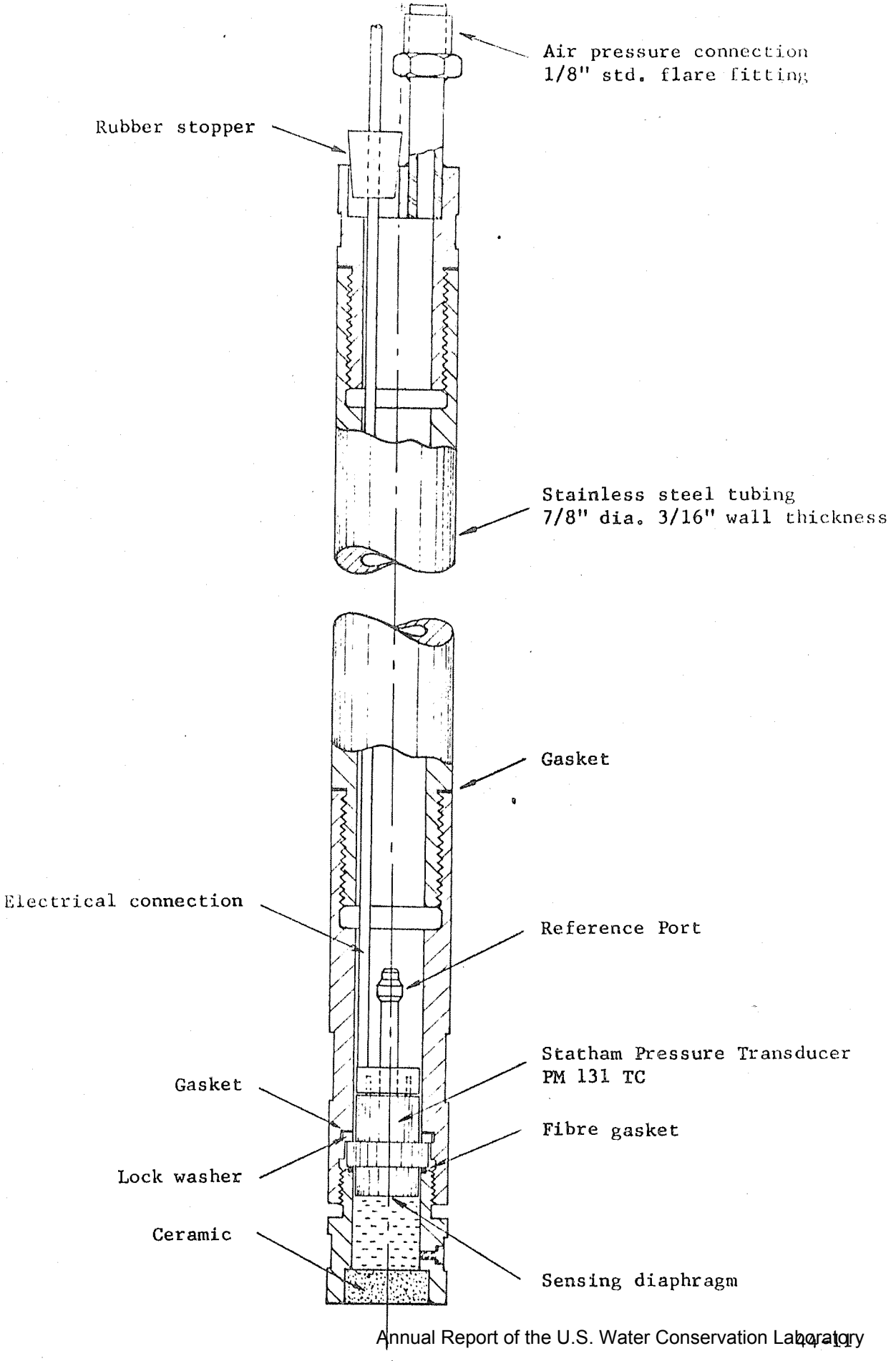
Air pressure connection
1/8" std. flare fitting
Rubber stopper
Stainless steel tubing
7/8" dia. 3/16" wall thickness
Gasket
Electrical connection
Reference Port
Statham Pressure Transducer
PM 131 TC
Gasket
Fibre gasket
Lock washer
Ceramic
Sensing diaphragm

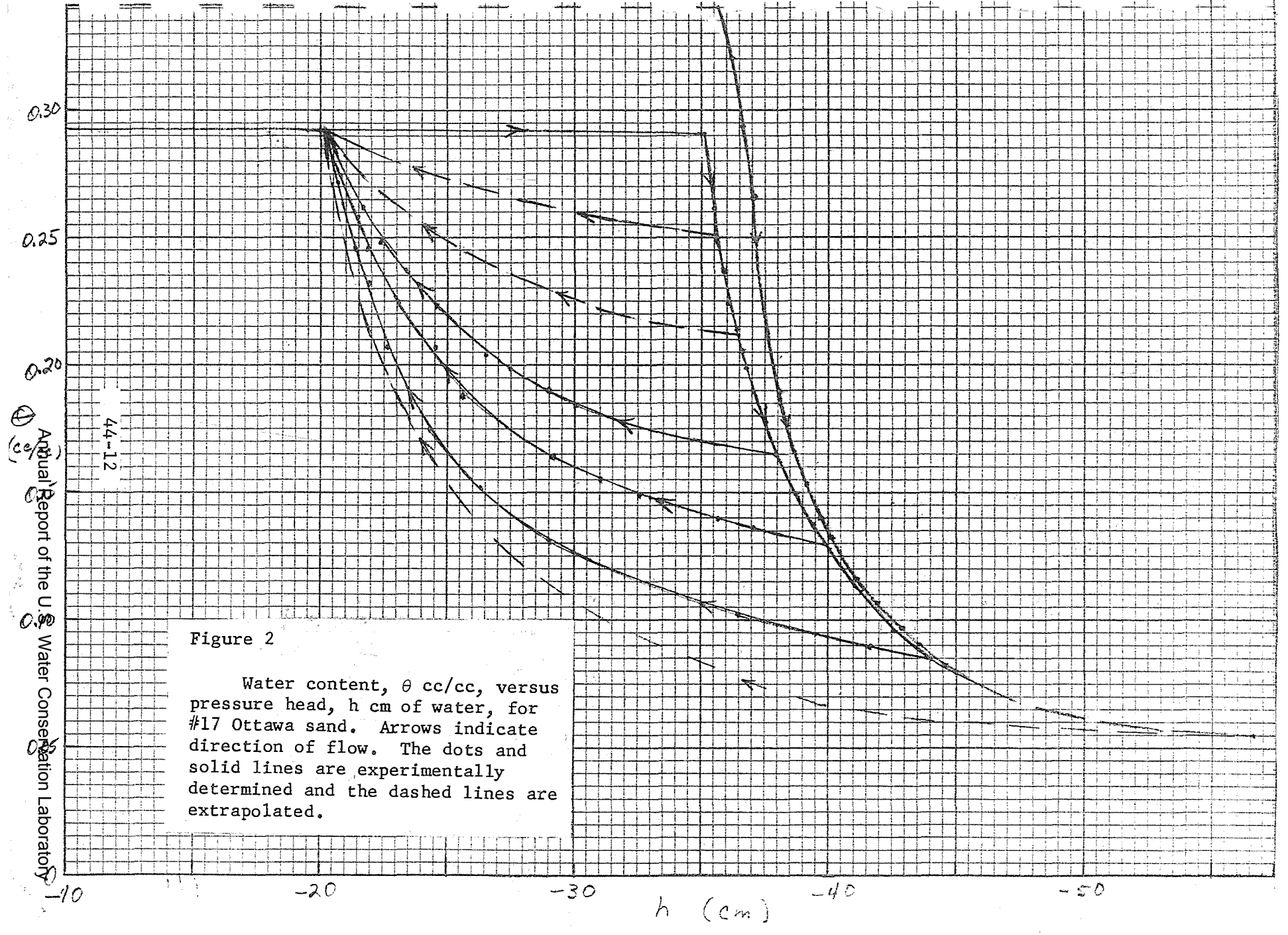

Figure 2

Water content, θ cc/cc, versus pressure head, h cm of water, for #17 Ottawa sand. Arrows indicate direction of flow. The dots and solid lines are experimentally determined and the dashed lines are extrapolated.

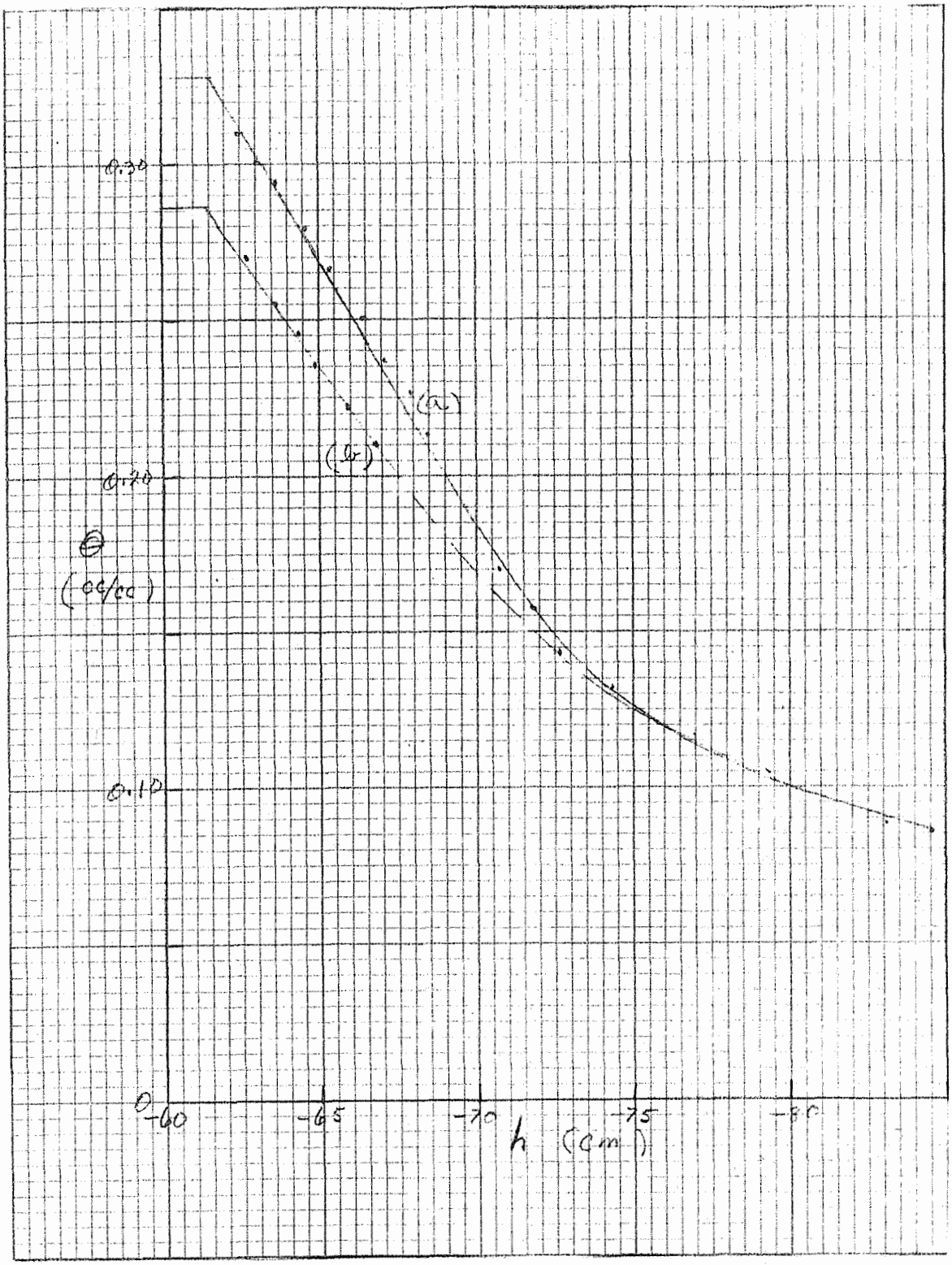

Figure 3

Water content, θ cc/cc, versus pressure head, h cm of water, for Banding sand during drainage. Curve (a) is drainage from saturation and curve (b) is drainage from "resaturation."

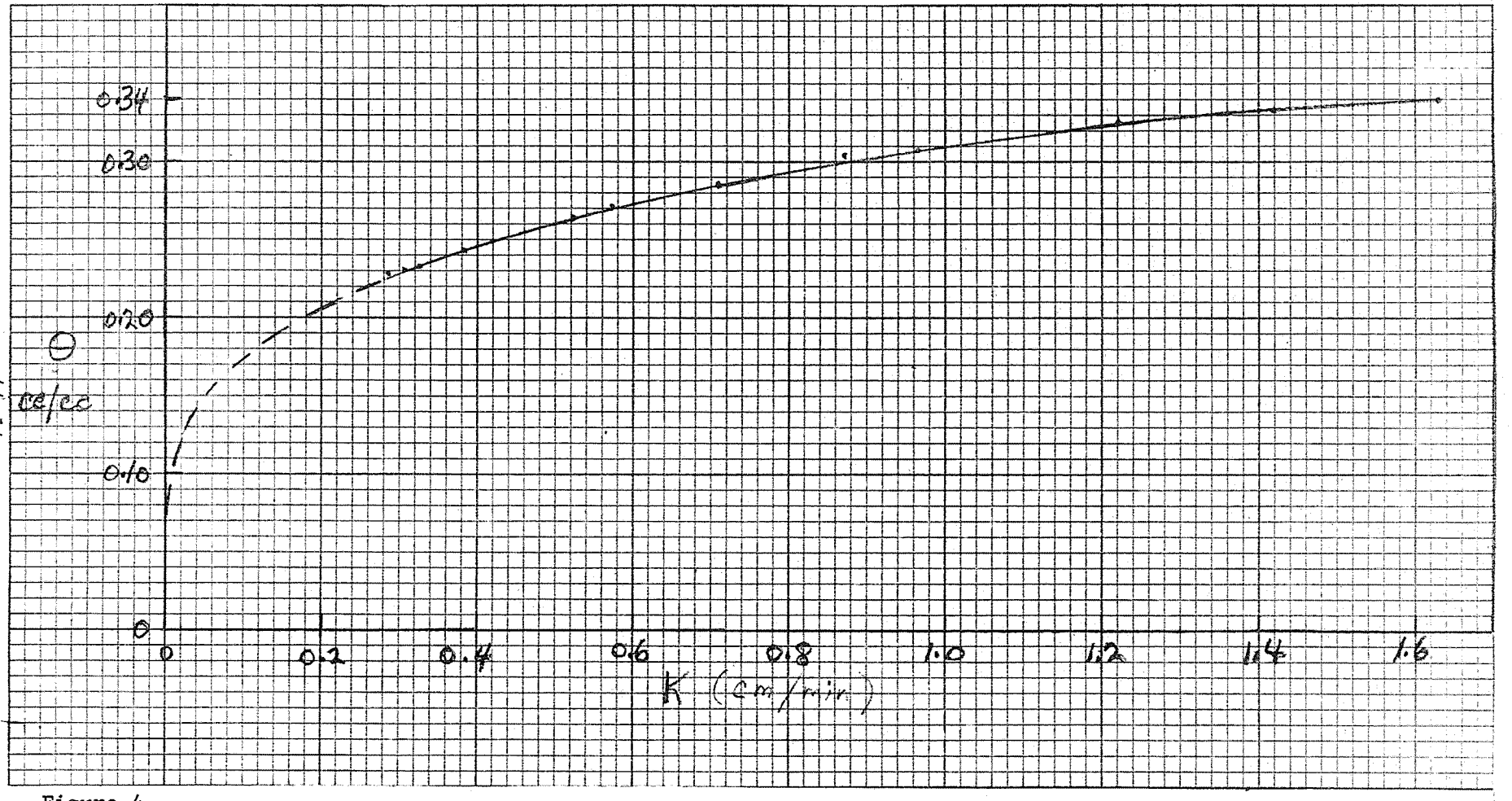

Figure 4

Water content, θ cc/cc, versus hydraulic conductivity, K cm/min, for #17 Ottawa sand. The dashed part of the curve is an extrapolation.

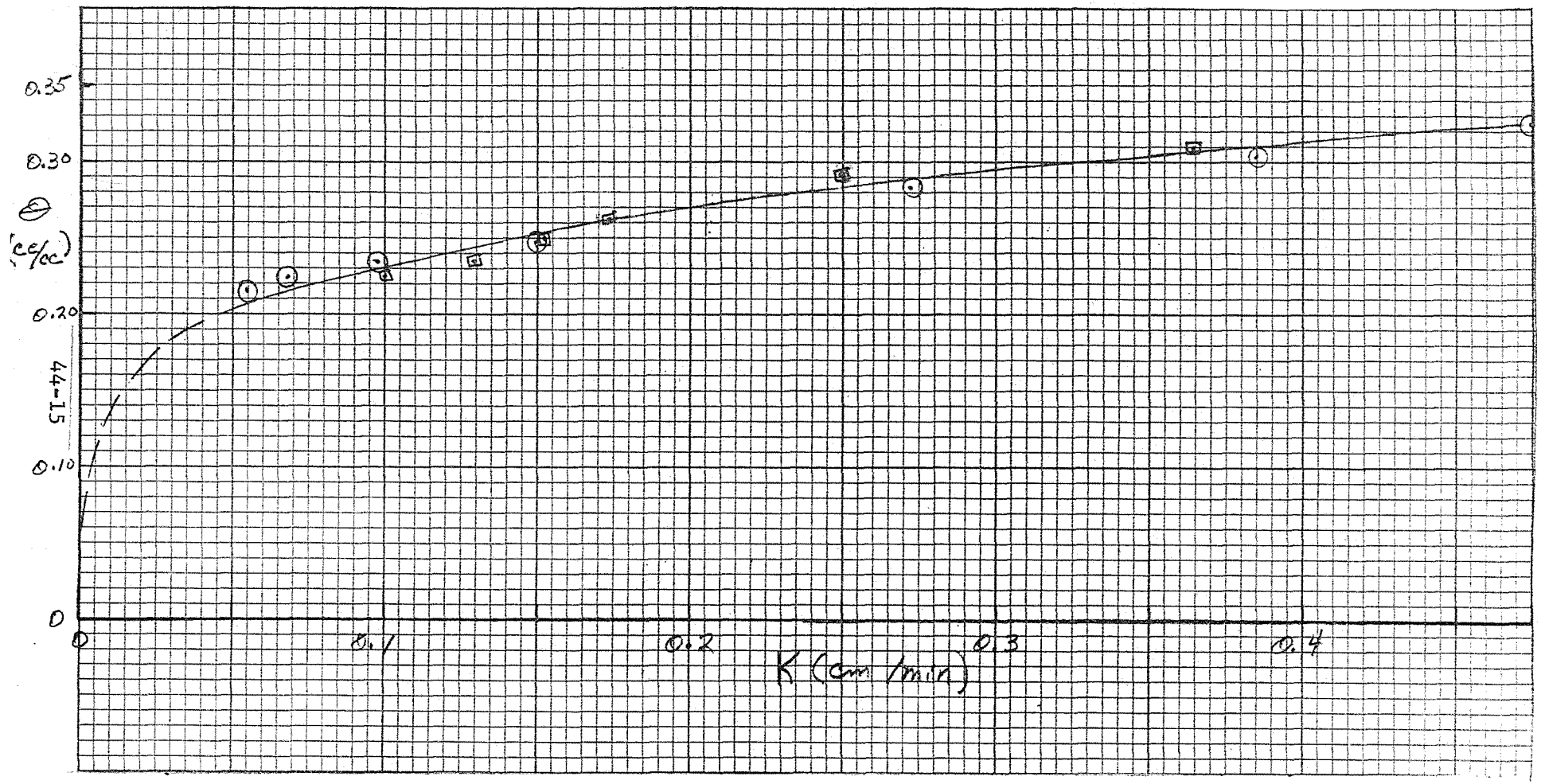

Figure 5

Water content, θ cc/cc, versus hydraulic conductivity, K cm/min, for Banding sand. Circles are for wetting and squares are for drying.

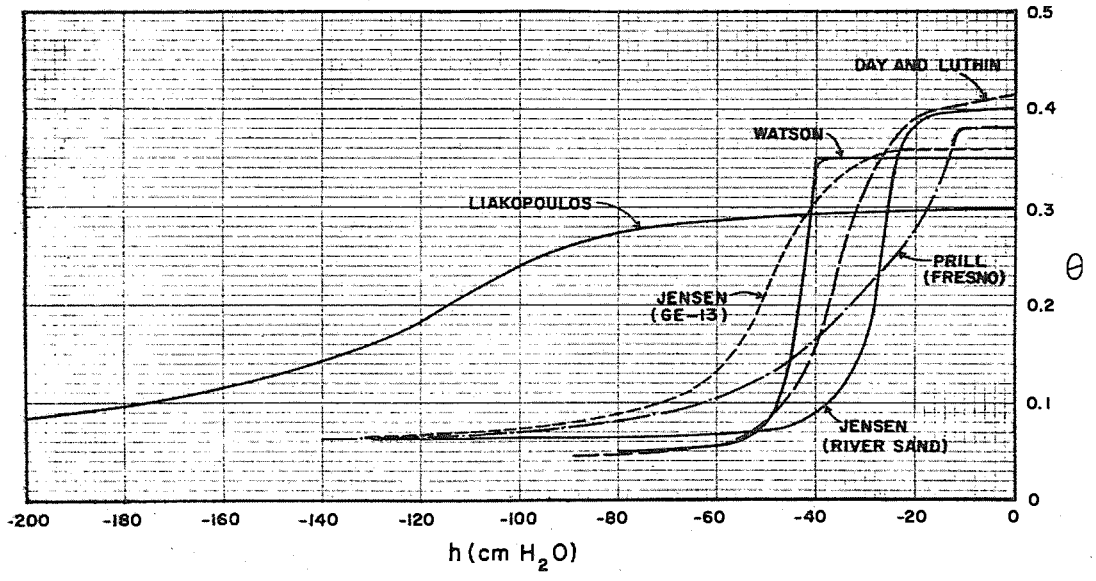

Figure 6

Water content, θ, versus pressure head, h, for published drainage relationships which have been tested.

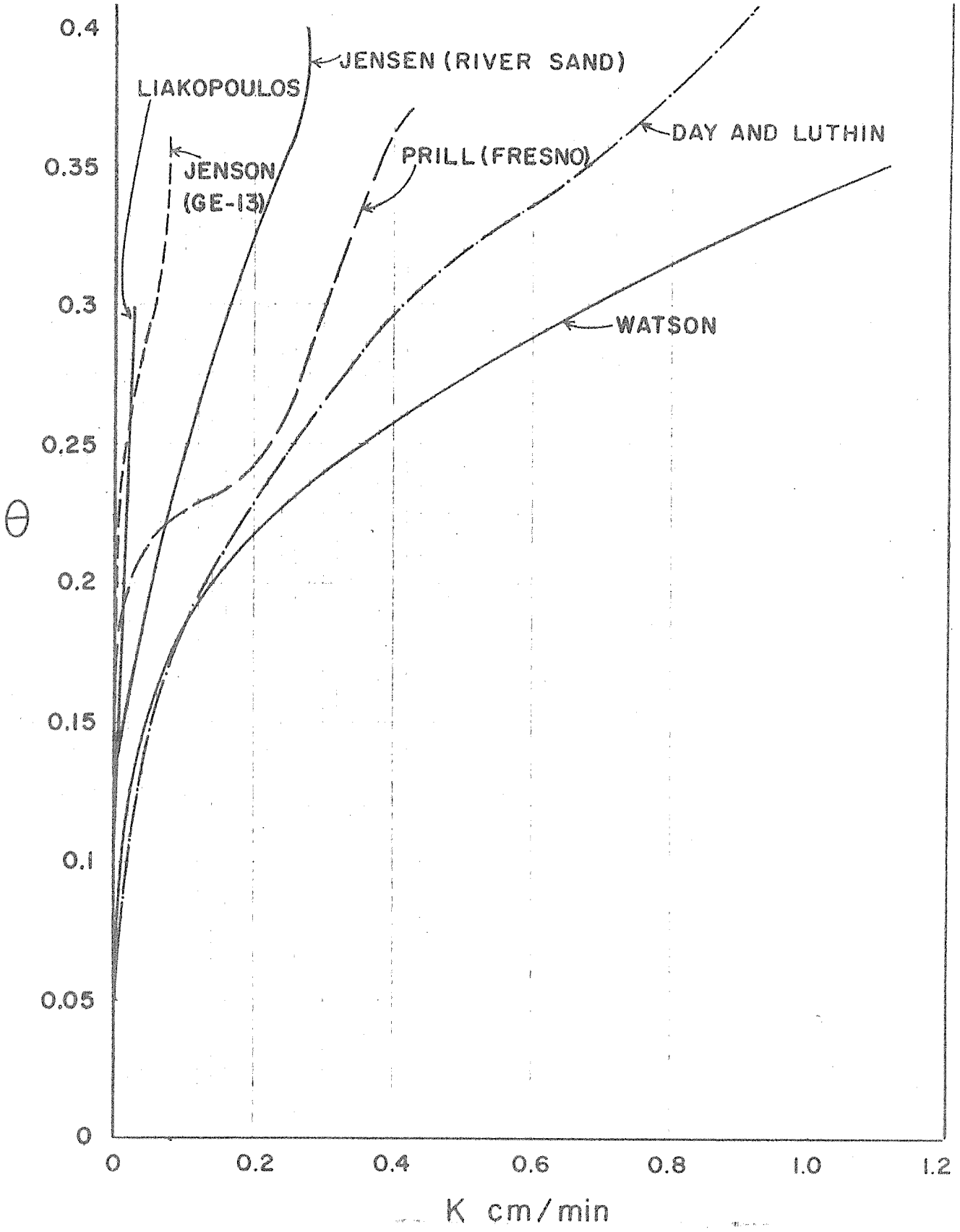

Figure 7

Water content, θ, versus hydraulic conductivity, K, for published drainage relationships which have been tested.

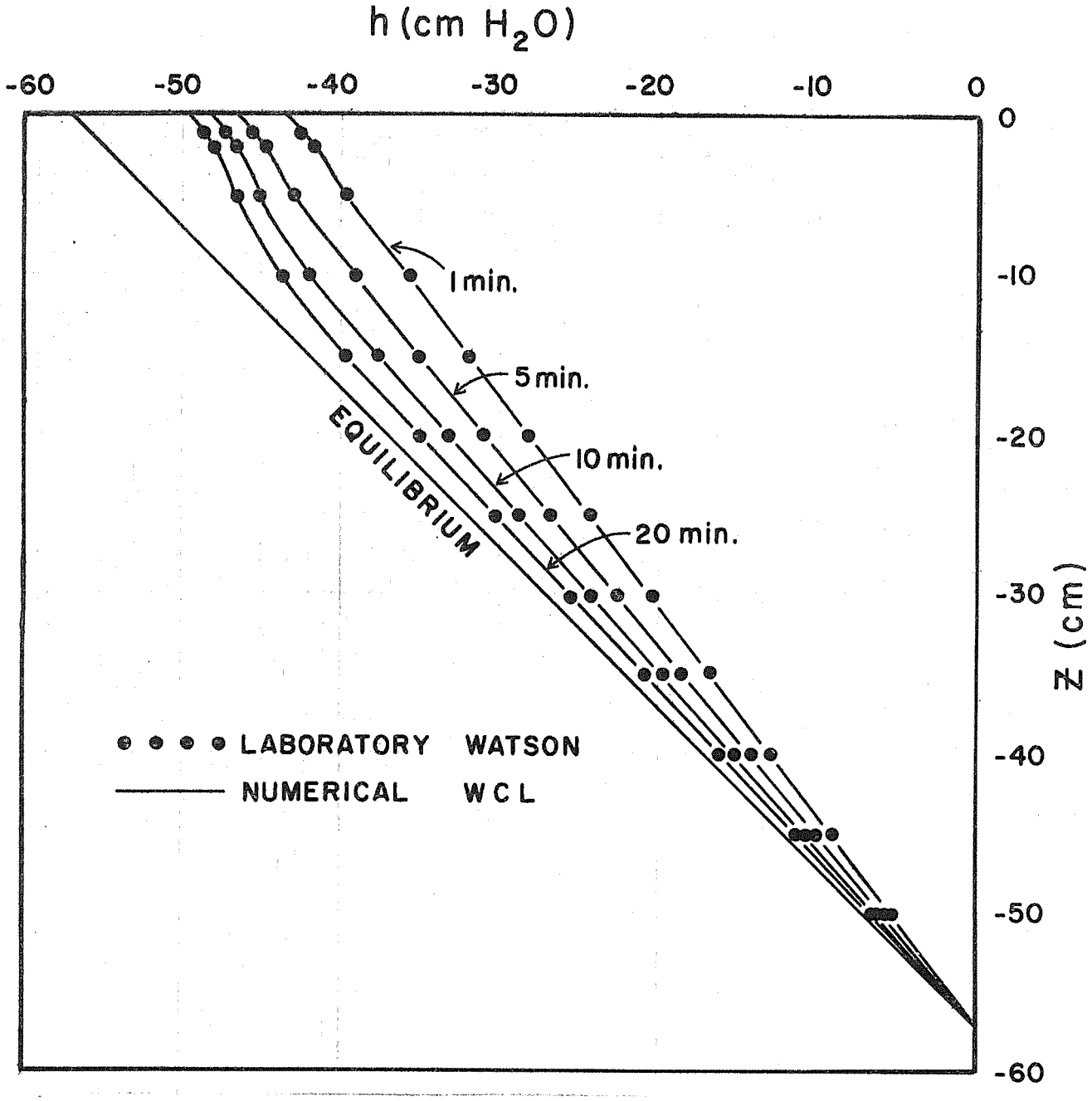

Figure 8

Pressure head, h, versus depth, z, for various times of drainage of Botany sand. The dots are experimentally determined and the solid lines are numerical predictions.

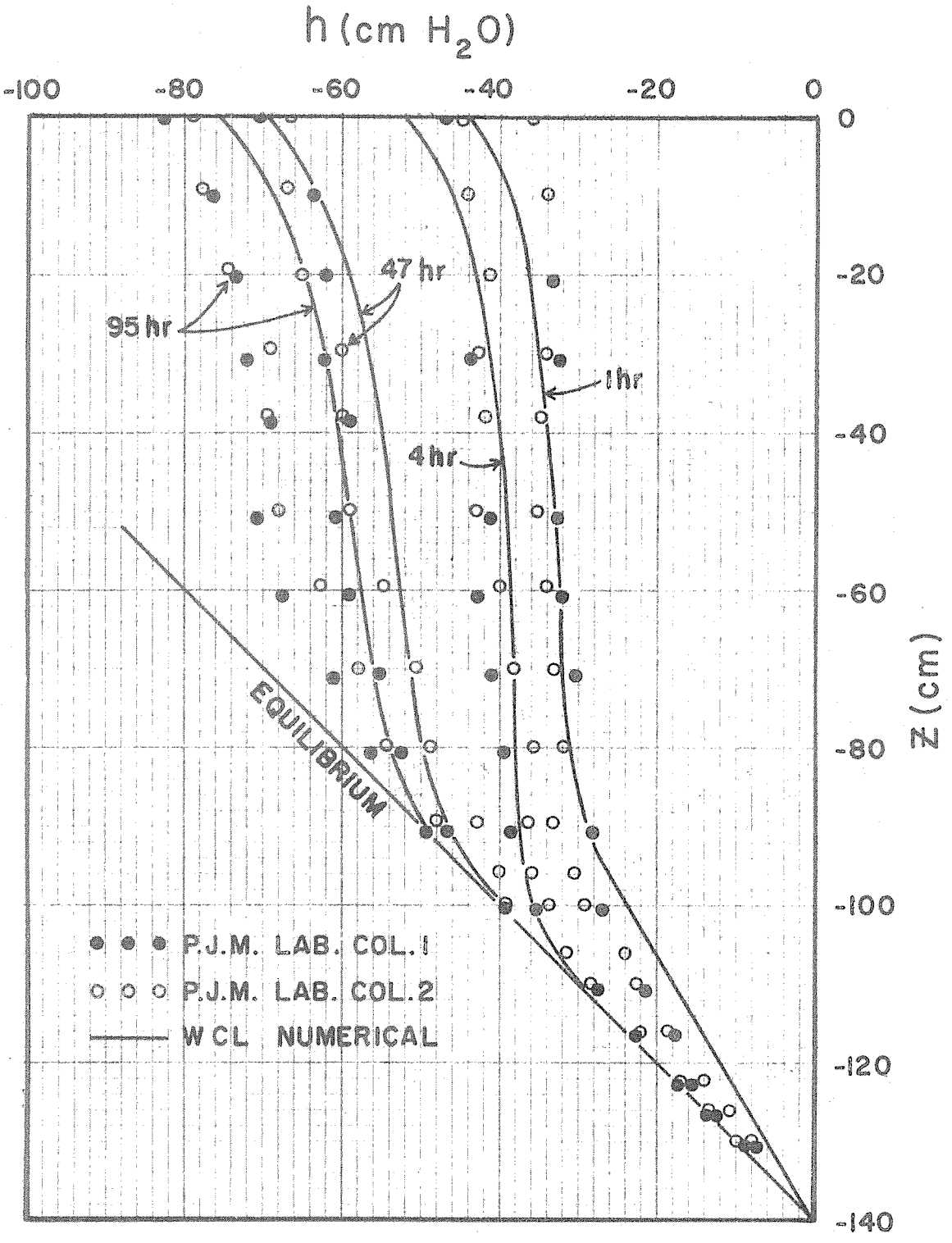

Figure 9

Pressure head, h, versus depth, z, for various times of drainage of Fresno medium sand. The solid dots are for column 1 and the open circles are for column 2, both experimentally determined. The solid lines are numerical predictions.

TITLE: IRRIGATION OUTLET STRUCTURE TO DISTRIBUTE WATER ONTO EROSIVE SOILS

LINE PROJECT: SWC X-gG1 CODE NO.: Ariz.-WCL-45

INTRODUCTION:

The objective of the experiment is to obtain design criteria for low-cost irrigation outlets that will distribute water onto sandy soils without excessive erosion.

As high-quality land, accessible to irrigation water, has become less plentiful, marginal lands are being developed for irrigation. Much of this land is sandy, requiring large quantities of water in short periods of time to efficiently accomplish the job of irrigation. Trends in the Southwest are to construct the irrigated areas so that they are nearly level, and then to apply water in large quantities in short periods of time.

Labor costs have encouraged the farm irrigation operators to apply large flow rates onto fields through some type of gated tile outlets from the concrete distribution ditches. These tile outlets range from 12 inches to 18 inches in diameter, and each may carry 900 to 4000 gallons per minute. The labor required to stop the flow in one irrigation border and start it in the next is small compared to other methods, such as using many siphon tubes which must be moved frequently when irrigating sandy soils.

In view of the low operational labor requirements, the tile outlet method is advantageous. However, these large flow concentrations have eroded deep holes in the field at the outlet, collapsing the tile by undermining the soil support, and in many cases threatening to destroy the supply ditch itself.

PROCEDURE:

Literature concerning erodibility of sands, as related to flow velocities on tractive forces, will be reviewed. The field problems will be examined and a one-fourth scale model will be constructed in the laboratory representing a typical field prototype installation. Various methods for distributing the flow onto the field will be studied, using this model. The more promising hydraulic designs will then be considered for full-scale field testing based on ease and expense of construction.

Concrete structures are anticipated for the field installations, hence plaster of paris models will be used in the laboratory.

TREATMENTS AND VARIABLES:

A. Under investigation:

1. Hydraulics of irrigation ditch outlets to include:

a. The maximum flow velocities over sand that will not cause erosion.

b. Velocity distribution patterns over the field surface near the outlet.

c. Methods to distribute the flow onto the field without causing erosive velocities.

2. Construction techniques that are compatible with farm labor capabilities and which use low-cost materials.

B. Not under investigation.

1. Irrigation application requirements of sandy soils.

2. Erosion on other than sandy soils.

3. Outlet pipe size requirements.

DATA TO BE OBTAINED:

A. Discharges used in typical installations.

B. Flow velocities, determined in the field, associated with the erosion patterns in typical installations.

C. Model data to indicate outlet structure dimensions, or characteristics, versus discharge rate.

METHODS OF INTERPRETING RESULTS:

The flow conditions observed in the field will hopefully be modeled in the laboratory. Models that distribute the flows without causing erosion damage will be considered satisfactory and will be further studied on the basis of economy and ease of construction. The design dimensions and flow rate relationships of the successful models will be used to establish design criteria for determining the most economical size for particular discharge rates.

RESULTS AND DISCUSSION:

Two outlets were constructed on sandy soil of the Ray Hensley Ranch, located at the east end of the Welton-Mohawk irrigation project. Sixteen-inch concrete outlets had been used on this sandy soil. A basin had formed at the outlets because of the erosive action of the water, which had left deposits of sand 200 ft from the outlet. One outlet structure was a box constructed by forming concrete in place around the existing pipe outlet, while the other was made by chiseling a rectangular opening in the top of the existing tile outlet, near the end, and blocking the former outlet with a pre-cast plug. The purpose was to cause the flow to exit vertically in order to dissipate some of the erosive energy. A thin-shell concrete apron about 2 inches thick was placed around the opening. It extended 3 ft into the field beyond the opening, was about 6 ft wide in the direction paralleling the ditch, and had a flange turned up on the ditch side in order to protect the fill. The edges of the apron and the flange were thickened somewhat to provide reinforcement and retard undercutting.

Nearly 3000 gallons of water per minute have discharged through these structures at various times since March 1965, with no erosion damage.

Four structures were built on the Jim Cannon Citrus Farm, located near Tacna, Arizona, having various-sized aprons and box elevations. Soils are Superstition sand, and ditches have 14-inch outlets. About 1000 gallons per minute are carried through these outlets and considerable Bermuda grass exists. Structures were built in July 1965, and if they failed, they were replaced. Since July 1965, one new structure was built and two were replaced. Replacements were required when the apron elevation was above the general elevation of the field. Bermuda grass destroyed one structure where concrete was too thin, with cracks existing between boxes and aprons. A two-foot apron seemed to be adequate for streams of this size in conjunction with 14-inch outlets, when aprons are below field elevation.

Two outlets were constructed on the Fred Enke Ranch near Maricopa, Arizona, in November 1965. Soils were silt loams and outlets were 14 inches in diameter. Different elevations, sized aprons and box types were used. One to two thousand gallons per minute were carried by these outlets. Whenever outlets failed, they were reconstructed. Two additional structures were built in 1966. Failures occurred when apron elevations were above field elevations. Two-foot aprons seemed to be marginal and might be feasible when aprons are well below field elevations. A step-down type of structure was built in 1966, to compensate for an outlet that was above field elevation, in order to get the apron below field elevation. The step-down type of outlet, with a two-foot apron, appears to be successful, to date.

One outlet was constructed at the Jack Currie Ranch in July 1965, on a sandy loam soil, using 14-inch outlets. The outlet apron was at field elevation, and a two-foot apron was used. This outlet still exists, but slight erosion has taken place on the flange corners. In March 1966, No. 2 outlet was constructed. An 18-inch apron was used, and a pre-fab box. The apron was below field elevation, but an erosion excavation existed in front of the apron. By the end of 1966, machinery had apparently hit this outlet, as it was destroyed.

In July 1965, four sites were selected on the Spencer and Spencer Ranches where very serious erosion problems exist on Superstition sands planted to new citrus. Concrete outlets were constructed at the existing elevations, which were generally above field elevation. Apron lengths varied from two to three feet at similar elevations. These concrete outlets carry about 1500 gallons per minute, and are 14 inches in diameter. Since July 1965, all of these have been replaced with different modifications, including rectangular pre-fab boxes instead of square ones, various sized aprons, various types flange corners, and step-down type structures, which lower the aprons to cope with the existing tile outlet elevations relative to the field elevations.

In general, it can be concluded from the Spencer structures that tile outlets above field elevation must be lowered in order to use the type box we have designed. Utilizing the step-down approach solved the problem. It is still questionable whether an apron of less than three feet can be used. No. 2 - Spencer is operating without erosion after flanges had been tucked back. It has a 42-inch apron. Flanges should be tucked back and be back into the ditch banks. No decision is possible, yet, on the square versus the rectangular box.

The use of pre-fab boxes was adopted and a form designed to construct same. Pre-fab boxes hold more promise than field-set forms. All boxes should be constructed with reinforcing on top to completely attach the aprons to the box, mainly because of the Bermuda grass problem.

LABORATORY STUDY:

A one-quarter scale model of the ditch outlet and field conditions was constructed in an 8 x 16 ft box. Commercially available "engine sand" was used as the erodible material. Even though it failed to model exactly the sandy soils found in the field, it closely approximated the erosion patterns that had been observed below 12- to 16-inch diameter outlets.

The most obvious requirement of the outlet is to place water onto the erodible surface at non-erosive velocities. Non-erosive velocities for the field conditions were determined with a target meter device that provided information on the average velocity in the sheet flow. Measurements were made at the outer boundary of noticeable erosion, because it was reasoned that at this location, the average velocity was at the threshold value. Results indicated a threshold velocity of 0.8 ft per sec.

An outlet structure for these field conditions should distribute water onto the sand at less than the threshold value. Knowing the desired total discharge and the flow depth of the sheet used, only a simple computation is required to determine the length of apron necessary to distribute the discharge if uniform spreading is achieved.

The major effort of both the field and laboratory work is directed toward methods of assuring uniform spreading and distribution, while avoiding concentrations of flow, or jets, that will cause failure of the structure and ditch fill. Several elaborate baffles and distributors operate satisfactorily from the standpoint of hydraulics, but cannot be economically constructed for field use. Work is continuing on evaluation of various configurations that will perform satisfactorily and yet be constructed inexpensively.

SUMMARY AND CONCLUSIONS:

Labor costs have encouraged irrigation operators to apply large flow rates, which are required on sandy soils, through some type of gated tile outlet, 12 to 18 inches in diameter. These large outlets, though economical with regard to labor, cause erosion that has collapsed the tile, and in many cases has threatened the irrigation ditch itself. Outlet structures to control and properly distribute the discharge are being investigated through a field study of existing devices, construction of some preliminary field models, and a laboratory investigation using a one-quarter scale model in a sand tank.

The most promising basic design for the structure consists of discharging the flow vertically through the top of a box attached to the large tile leading from the ditch, or by breaking an opening in the top of the tile near the existing outlet and capping the end. The vertical discharge helps dissipate the erosive energy and, with suitable baffling or outlet design, should permit uniform distribution of the flow onto the soil at less than threshold erosion velocity. The threshold velocity was measured in the field to be about 0.8 ft per second. Aprons around the outlet opening must be of such a size that they can deliver the desired flow rate at less than the threshold velocity. This size is a function of the sheet flow depth and the efficiency of distribution of the outlet shape.

Eighteen field structures of the same basic design have been installed. A few have failed. The failures are attributed to insufficient sheet depth; i.e., the structure aprons were set above the general field elevation,

causing the sheet flow on the apron to exit onto the sand at erosive velocities. Those which were reconstructed with lower apron levels have remained serviceable.

Problems encountered in the field have included erosion of the ditch fill at the end of the turned-up flange, Bermuda grass growing in small cracks in the concrete and causing further breakage, and damage from field machinery. Reshaping the upturned portion of the apron, or flange, by thickening the rim so that it extended several inches into the ditch fill has helped prevent undercutting at the interface of structure and sandy soil.

The laboratory study has not been completed.

PERSONNEL: L. J. Erie and J. A. Replogle

TITLE: FLOW MEASUREMENT IN OPEN CHANNELS WITH CRITICAL DEPTH FLUMES

LINE PROJECT: SWC X-gG1 CODE NO.: Ariz-WCL-48

INTRODUCTION:

Increasing attention is being directed toward measurement of water in open channels, especially as related to irrigation distribution systems and watershed runoff investigations. In the latter case, wide ranges of flow rate must be accomodated. In both instances, critical depth flumes provide a satisfactory means of gaging. The structures are rugged, require little maintenance, and can be fitted with devices for continuous recording of discharge rate. The basic theory of their operation has been long known, dating back to Bélanger's work reported in Paris in 1849-50 on broad crested weirs, and culminating with the publications of Ackers (1), Ackers and Harrison (2), Diskin (3), and Robinson (4).

Diskin presented a solution for predicting the rating curves for flumes with exponential throats (rectangular, triangular, and parabolic), and Ackers presented a general solution for trapezoidal-throated flumes and introduced a correction for friction losses in the flume throat.

Even though the basic theory of operation is known, the stage-discharge relation is still generally determined empirically (4), because the application of the theoretical knowledge is tedious and requires detailed computations best accomplished with electronic computers. Furthermore, certain physical dimensions and relationships need to be determined in order to insure that the flume produces a flow that satisfies the assumptions in the derivation of the theoretical calibration equation.

This study involves the design of flumes based on theoretical concepts which hopefully will permit the laboratory calibration of a few flumes to be confidently applied to a wide variety of shapes.

PROCEDURE:

Numerous publications concerning critical depth flumes were studied in detail with emphasis directed toward theoretical derivations and the associated assumptions. Based on the theoretical study, four

triangular-throated flume sizes were initially designed for immediate use on associated projects. These flumes were calibrated under laboratory conditions as soon as each was constructed and the laboratory calibration compared to the theoretical derivation. Additional studies were conducted on some of the flumes to evaluate the effects of installation and construction anomalies.

RESULTS AND DISCUSSION:

Theoretical Considerations. Critical depth is obtained in a horizontal flume or channel when

$$\alpha_c \frac{v_c^2}{2g} = \frac{D_c}{2} \qquad [1]$$

where

α = velocity distribution coefficient

v = average velocity in the cross section

g = gravitational constant

D = hydraulic depth = A/T

A = cross-sectional area of flow

T = top width of flow

c = a subscript relating to conditions at the critical section

Since $Q = Av$, equation [1] can be expressed as

$$Q = \sqrt{\frac{gA_c^3}{\alpha_c T_c}} \qquad [2]$$

For trapezoidal channels

$$A_c = y_c(b_c + z_c y_c) \qquad [3]$$

$$T_c = b_c + 2z_c y_c \qquad [4]$$

where

b = channel bottom width

$1:z$ = channel side slope, vertical:horizontal

y = flow depth in the channel

From equations [2], [3] and [4]

$$Q^2 = \frac{g\, y_c^3 (b_c + z_c y_c)^3}{\alpha_c (b_c + 2 z_c y_c)} \qquad [5]$$

Equation [5] expresses the discharge in a trapezoidal channel or flume, in terms of the depth at the critical section, but in practice it is usually necessary to measure upstream depths because the exact point of critical depth in a flume throat is difficult to locate. Thus, an essential step is to convert the equation into a form relating head to discharge.

The total head, H_c, or specific energy in the throat of a flume measured relative to its invert is given by

$$H_c = y_c + \frac{\alpha_c v_c^2}{2g} \qquad [6]$$

or, since v = Q/A and using equations [2], [3], and [4],

$$H_c = y_c + \frac{A_c}{2T_c} \qquad [7]$$

or

$$H_c = y_c + \frac{y_c(b_c + z_c y_c)}{2(b_c + 2z_c y_c)} \qquad [8]$$

This is a quadratic that can be rearranged into the form

$$y_c^2 + \left(\frac{3b_c}{5z_c} - \frac{4H_c}{5}\right) y_c - \frac{2b_c H_c}{5z_c} = 0 \qquad [9]$$

with two roots, the negative root not satisfying the physical conditions. Thus the positive root is selected, which is

$$y_c = \frac{1}{10z_c}\left[\sqrt{(3b_c + 4z_c H_c)^2 - 8z_c b_c H_c} + 4z_c H_c - 3b_c\right] \qquad [10]$$

Equation [5] can now be evaluated using the physical dimensions of the channel and the total specific energy, H. Since H at the critical section is given by equation [8], the specific energy at an upstream measuring point must be the same except for a minor energy loss between this point of measurement and the critical section in the flume throat. Thus, H can be calculated by using the channel dimensions and flow depth approaching the flume. At a measurement section upstream from

the flume throat,

$$H_1 = y_1 + \frac{\alpha_1 Q^2}{2g\, y_1^2\, (b_1 + z_1 y_1)^2} \qquad [11]$$

where y is the depth of flow and the subscript 1 refers to the upstream section where the measurement is made. If the flow lines at this section are curving, then y will require a slight correction if the flow depth is sensed by using a pressure tap near the channel bottom. Equations [11] and [5] define Q implicitly and require iterative techniques for the evaluation of the theoretical calibration curve. This can be most readily accomplished with a computer.

For flumes to have predictable calibrations, the flow lines at the measurement section and the point of critical depth should be parallel. This eliminates the necessity of making corrections for streamline curvature.

Because of the usual converging channel section needed between the upstream point of measurement and the flume throat, the velocity profile is usually not well developed at the critical section and α_c can be assumed equal to unity. On the other hand, the velocity profile at the measurement section may be expected to be well developed and α_1 could have values between 1 and 1.04 or greater.

If the friction losses, f_1, between the measurement section and the critical section are not small then

$$H_c = H_1 - f_1 \qquad [12]$$

and some method of evaluating f_1 must be devised. This has been done by Ackers and Harrison (2) using boundary layer theory and also using the more conventional friction factor method.

Equations [5] and [11] simplify somewhat for triangular-throated flumes, $b_c = 0$, and for rectangular throats, $z_c = 0$, to become, respectively, if $\alpha_c = 1.00$ and $g = 32.16$,

$$Q = H^{5/2} \sqrt{\frac{2g}{\alpha_c}}\ 16\ \left(\frac{1}{5}\right)^{5/2}\ z_c \qquad [13]$$

$$= 2.296\ z_c\ H_c^{5/2}$$

and

$$Q = H^{3/2} \sqrt{\frac{2g}{\alpha_c}}\ 2b_c\ \left(\frac{1}{3}\right)^{3/2} \qquad [14]$$

$$= 3.087\ b_c\ H_c^{5/2}$$

Design Considerations. To operate as a critical depth flume requiring only one point of depth measurement, the outlet depth of flow must be sufficiently reduced to prevent submergence. In a rectangular-throated flume, the theoretical ratio between channel depth and critical depth is

$$y_c = \frac{3}{2} H_c \qquad [15]$$

where H is given by equation [6]. Thus, the submergence for a rectangular-throated flume would occur when the downstream depth exceeded the critical depth in the flume, which is approximately 0.67 times the upstream head, H_1.

In a triangular-throated flume,

$$y_c = \frac{5}{4} H_c \qquad [16]$$

and submergence would not occur until the downstream depth exceeded y_c or 0.80 times the upstream head, H_1. Trapezoidal-throated flumes are expected to vary between these values.

Theoretically, it appears that a triangular-throated flume is not as easily submerged as a rectangular flume. This makes it attractive for flow measurements in irrigation ditches where head losses must be kept low and submergence is not easily avoided.

Specific Designs. Detailed designs have been made for a few specific cases where submergence is avoided by selective design of

the flume throat. The procedure involves determining the normal depth of flow in the channel, then selecting a flume configuration that will cause sufficient ponding to maintain the minimum submergence relationship between upstream and downstream water levels.

30° Throat. One flume, based on passing 3.5 cfs at a depth of 2 ft in a concrete ditch, bottom width 1 ft and side slopes 1:1, was designed for portable use in irrigation channels with energy gradients as low as 0.0002. A triangular throat was chosen with a 30-degree opening. This flume had an 18-inch long approach section with 9-inch bottom width and 1:1 side slopes. The upstream edges were fitted with rubber flaps which prevented leakage past the flume when it was placed in the channel. A converging section, 2 ft long, adapted the approach section to the 30°-V throat section. The latter was initially 2 ft long, but laboratory tests indicated that above 1-ft operating head, the flow lines failed to attain the necessary parallel flow condition in the throat. The drawdown from the free discharging throat section carried back far enough to meet the drawdown curve at the throat entrance. Thus, parallel, or nearly parallel flow, was not achieved in the flume throat at the higher flow rates, causing an increase in discharge over that determined theoretically for a given head.

Based on the above observations, the average surface slope from upstream head to free overfall depth at the throat outlet was calculated. For triangular free overfalls, the end depth is approximately $0.8\ y_c$, and in turn, $y_c = 0.8\ H_1$. Using the observed 1-ft approach depth as the limiting upper value for a 2-ft long throat, it is obvious that for a 2-ft flow depth, a 4-ft throat is necessary. (Interestingly, since rectangular throats have an overfall depth of $0.715\ y_c$, the same average water surface slope in the throat dictates a throat length of 6 ft for a 2-ft depth of flow.) A laboratory check of the increased throat length has not been completed.

60° Throat, Large Flumes. Designed to pass 10 cfs at a maximum head of 2.25 ft, this flume was built to measure runoff from experimental field plots. The triangular throat opening was 60° with an

approach section having the same side slopes but with an 8-inch bottom width. A converging section connected the latter with the former. All sections were approximately 28 inches long and 27 inches deep. The calibration results were essentially as analytically predicted with a gradual departure from the theoretical solution at high flows. The error at maximum flow rate, however, was approximately 2 percent. Four flumes of this size have been built. Three have been calibrated in the laboratory and placed into field service. The three calibrations were essentially identical, as expected.

These flumes were subjected to several tests to evaluate effects of improper construction and installation. The tests and results are as follows:

1. Torsional twist of flume: The flume was twisted so that one side of the flume was 0.6 inches higher than the other. Less than 1 percent effect was noted at a head of 1.23 ft.

2. Inward deflection of throat section: A 0.75-inch inward deflection of the throat section as measured at a point 13 inches above the floor, caused approximately 1 percent change in calibration at a head of 1.23 ft.

3. End elevated: The end of the flume was elevated 0.75 inches. While it changed the zero reference for the point gage, the net flume calibration changed less than 1 percent. Elevating the end section by 1.5 inches caused approximately 2 percent change. The head again was approximately 1.2 ft.

4. End lowered: When the end of the flume was lowered about 0.75 inches below the level position, at the same heads used above, the calibration changed approximately 1.5 percent.

5. Effect of sediment in approach section: Concrete blocks, 8 inches by 16 inches, and 1.5 inches thick were placed in the approach section of the flume where the pressure head is sensed. One layer of blocks failed to produce a noticeable change in head, but when an additional layer of blocks was added, the change in calibration was approximately 2 percent for a head of 1.2 ft. This is thought to be caused by the turbulence induced near the pressure tap rather than to significant changes in flow area and hence velocity-of-approach changes.

6. Effect of approach into the flume: The normal entrance conditions at the approach section of the flume resulted from bolting it onto the flat side of an 8-ft square head box with the floor of the flume flush with that of the head box. Wingwalls spread at 45°, simple straight extensions of the entrance section and one extension only (causing flow to enter from one side) were tested for a midrange head of 1.2 ft. Effects of all conditions were noticeable but less than 1 percent.

7. Effects of additional divergent sections: Frequently it may be desirable to attempt to recover some head by constructing divergence sections to add to the downstream end of the flume. Two flumes were placed end-to-end with one of the throat sections disgarded, making a five-section flume combination. A flow depth was chosen to assure adequate throat length. The downstream section was removed while the flow was permitted to continue uninterrupted, and was again replaced under the same flow conditions. The head detected in the stilling well remained unchanged. This indicated that, if the throat length is adequate, no differences should be noted between the free-fall condition and the divergent-section condition.

8. Effect of submergence: With the divergent sections in place, downstream obstructions were introduced to cause backwater and to prevent free, ventilated discharge. Again, heads were chosen to provide adequate throat length of at least 2H. The lowest head was 0.38 ft and the highest was 0.95 ft. The ratio of downstream depth to upstream depth, when submergence effects were noted by a change in the stilling well reading, was approximately 0.90, for all flow rates. The theoretical value is 0.80 H, indicating that some head is recovered without causing submergence.

60° Throat, Small Flumes. These are similar to the larger size, but at one-fourth scale. They were chosen to be used on small runoff plots and to provide a means of checking inconsistencies reported by Robinson (4) on flumes of the same size. He noted a substantial difference in calibration when divergence sections were added. This might be explained by the likelihood that, because of their small sizes,

the observations reported were for heads which exceeded the recommended depth for the short throat length.

SUMMARY AND CONCLUSIONS:

Increasing attention to measurement of water in irrigation channels and from small watersheds has stimulated new interest in critical depth flumes. While much of the basic theory has been long known, the stage-discharge relations are still generally determined empirically because the application of the theoretical knowledge is tedious and requires detailed computations. Computers can now provide the means to apply the theoretical knowledge routinely.

Several flume design features required further study. Among these are flume throat length and its relationship to flow depth, methods to insure parallel flow at appropriate locations in order to avoid having to estimate coefficients to account for curving flow lines, and effects of friction losses in the flume throat.

Theoretical equations for the stage-discharge relation in trapezoidal-throated flumes were derived which are also applicable to rectangular and triangular throats. The equations are implicit in both discharge rate and flow depth, and must be solved iteratively.

Four sizes of flumes with triangular throats have been constructed and two of these have been checked in the laboratory. The theoretical calibration and the laboratory rating curves agreed well except at high flow rates. The deviation was attributed to insufficient throat length, which was less than 2 times the head, the value recommended by previous investigators.

The flumes should be installed level when possible. Negative, or adverse, slope has about half the influence on the calibration as positive flume slope.

REFERENCES:

(1) Ackers, P.
1961. Comprehensive formulae for critical-depth flumes. Water and Water Engineering, July, pp. 296-306.

(2) Ackers, P., and Harrison A. J. M.
1963. Critical-depth flumes for measurements in open channels. Hydraulics Research Station, Dept. of Scientifc and Industrial Research, Wallingsford,

Berkshire, England. Hydraulics Res. Paper No. 5, April. 49 pp.

(3) Diskin, M. H.
1963. Rating curves for venturi flumes with exponential throats. Water Power, August. pp 333-337.

(4) Robinson, A. R.
1966. Water measurement in small irrigation channels using trapezoidal flumes. Amer. Soc. Agr. Engin., Trans. 9: 383-385, 388.

PERSONNEL: J. A. Replogle

TITLE: WATERPROOFING OF SOILS - AN EVALUATION OF TREATMENTS AND INFLUENCING FACTORS

LINE PROJECT: SWC VII-gG4 CODE NO.: Ariz.-WCL-49

INTRODUCTION:

Large portions of the earth's land area suffer from a water imbalance, whereby the potential water loss through evapotranspiration exceeds the natural rainfall. In desert and semidesert areas, most of the rather limited rainfall is rapidly soaked up by the dry upper soil layers, only to be quickly re-evaporated and lost into the atmosphere. Intensive utilization of these land areas has, in the past, been possible only through importation of water supplies. However, if the soils in these areas could be waterproofed so as to prevent this wasteful infiltration, the resulting increased runoff could provide a very substantial new water source.

One promising technique for doing this is to make the soil water repellent by applying monolayer coverages of low surface energy, organic additives (see Annual Report - WCL-7). These additives are not readily wetted by water, and since the cohesional forces of the water exceed the adhesional forces of the water for the treated soil surface, the water "balls up" and runs off.

Preliminary experiments using silicone additives have shown exceptional promise. Runoff yields from experimental plots have been high. The additives are easy to apply and are relatively inexpensive. However, information on expected performance of these waterproofing agents based on their chemical and physical properties and those of the soil to which they are applied, is largely lacking. Furthermore, laboratory methods for obtaining this information quickly and inexpensively also are lacking.

The immediate objective of this project has been to develop experimental techniques for quantitatively evaluating the water-repellency of treated soils. Water-repellency for soils means they will shed water, but the term implies that if sufficient

positive pressure is applied to water at the porous, solid-liquid interface, the water can be forced into the capillary system of the soil. This pressure may be mathematically described in terms of the influencing parameters:

$$P = \frac{2\gamma \cos \theta}{r} \qquad [1]$$

where γ is the surface tension of the water, θ is the advancing contact angle at the water-soil interface, and r is the effective capillary radius of the soil. Preliminary experimentation has been directed at effectively measuring this "breakthrough" pressure, P, for treated soils.

PROCEDURE:

Preliminary experimental results suggest that the following procedure will effectively measure the breakthrough pressure of water into water-repellent soils. Essentials of the apparatus are shown in Figure 1. The soil container is a lucite cylinder 2 inches wide by 2 1/2 inches long, cemented to a lucite base. A Pyrex glass immersion tube having a 30 mm fritted glass disk of 10-15μ pore size was snugly fitted through a hole at the center of the lucite base, and then paraffined on the sides. Plastic tubing connects the immersion tube to a glass standpipe, which in turn is firmly mounted against a meter stick. Seventy-five g of water-repellent soil is poured into the lucite cylinder (this is sufficient to cover the immersion tube to several cm) and is uniformly packed by dropping a 240 g weight onto the soil ten times from a height of 33 cm. Water is then dripped into the standpipe at a uniform rate. The water rises in the standpipe and the immersion tube until it reaches the water-repellent soil. After this point is reached, the rate of rise of water in the standpipe becomes linear until the breakthrough pressure of the soil is reached. This point is determined from a plot of water head versus time.

The soil selected for testing the utility of the apparatus was Pachappa loam. The particle size distribution of this soil has been published (1). The soil was made water repellent with a surface application of Union Carbide R-20 Silicone, mixed with the soil from a 10 percent acqueous solution at the rate of 0.1 g R-20 per 100 g soil. The treated soil was dried and sieved into the following mesh size distributions: <40, 40-60, 60-140, and >140 mesh.

The apparatus also has been tested on a natural water-repellent soil from a wildfire area in the chaparral forests of southern California (2). The water-repellency of these soils apparently derives from natural organics distilled onto the soil by the heat of the fire.

RESULTS AND DISCUSSION:

Typical curves of increasing water head versus time for the water-repellent Pachappa soil appear in Figure 2. After the immersion tube is filled with water, the plot of water head (h_w) versus time becomes linear, the rate of increase depending solely on the rate of water addition and the cross-sectional area of the standpipe. The plot remains linear until the breakthrough pressure of the soil is reached.

The compiled results for the preliminary testing of the apparatus for the measurement of breakthrough pressure appear in Table 1. The testing was done on a water-repellent, fractionated series of Pachappa soil and on a California soil. The standard error of observation (σ) is low enough to give a fair degree of confidence for the continued use of the method.

These results show that the breakthrough pressure is inversely related to the soil particle size. This, of course, is predicted by the equation for breakthrough pressure (equation 1),

which when written in terms of breakthrough head for water (h_w) is:

$$h_w = \frac{2\gamma \cos \theta}{g \rho_w r} \qquad [2]$$

As particle size decreases, so does the effective radius r. Cos θ also is affected by the particle size distribution, since the contact angle not only depends on the surface energy of the treated soil surface, but also depends on the roughness of the soil-water interface. The rougher the surface, the more negative cos θ becomes (for $90^\circ < \theta < 180^\circ$). Since θ and r are both related to particle size, they, undoubtedly, are also both influenced by bulk density, and, as such, are certainly influenced by sample preparation techniques, e.g., packing procedures. Therefore, to get repeatability in the determination of h_w, it will be necessary to maintain strict uniformity in sample preparation.

SUMMARY:

A technique has been developed to quantitatively evaluate water-repellency of soils treated with organic chemical additives. The technique is based on the characteristic of water repellent soils that even though they shed water, i.e., the contact angle at the water-soil interface is greater than 90°, they still maintain a porous nature and therefore, if sufficient pressure is applied, water can be forced into the soil capillary system. This pressure called the breakthrough pressure may be described by the relation

$$h_w = \frac{2\gamma \cos \theta}{g \rho_w r}$$

where the pressure is here described in terms of a breakthrough head of water, h_w, and where γ is the surface tension of the water, θ is the contact angle of the water at the soil-water interface, r is

the effective soil capillary radius, ρ_w is the density of water, and g is the gravity.

It has been found that the breakthrough head, h_w, may be determined from plots of increasing water head versus time. Adding water at a constant rate to a standpipe directly connected to the water-repellent soil results in a linear rate of increase of pressure head until the breakthrough pressure of the soil is exceeded, after which the rate of pressure head increase decreases.

Preliminary results using a Pachappa soil treated with a silicone additive show that h_w may be determined with sufficient repeatability such that the standard error of measurement is less than 10 percent of the true value. Such accuracy should suffice for evaluating soil-water-repellency treatments.

REFERENCES:

(1) Jackson, R. D.
1963. Temperature and soil-water diffusivity relations. Soil Sci. Sci. Am. Proc. 27:363-366.

(2) Krammes, J. S. and Debano, L. F.
1965. Soil wettability: a neglected factor in watershed management. Water Resources Res. 1:283-286.

PERSONNEL: D. H. Fink

Table 1. Breakthrough heads (h_w) of water at the water-soil interface of water-repellent soils.

Soil	Pachappa				California
Mesh Size	< 40	40-60	60-140	> 140	< 1 mm
h_w	1.2	8.0	13.8	31.4	4.5
n	1	2	24	4	4
σ	-	0.6	1.3	1.3	0.2

h_w = average water breakthrough head

n = number samples run

σ = standard error of an observation

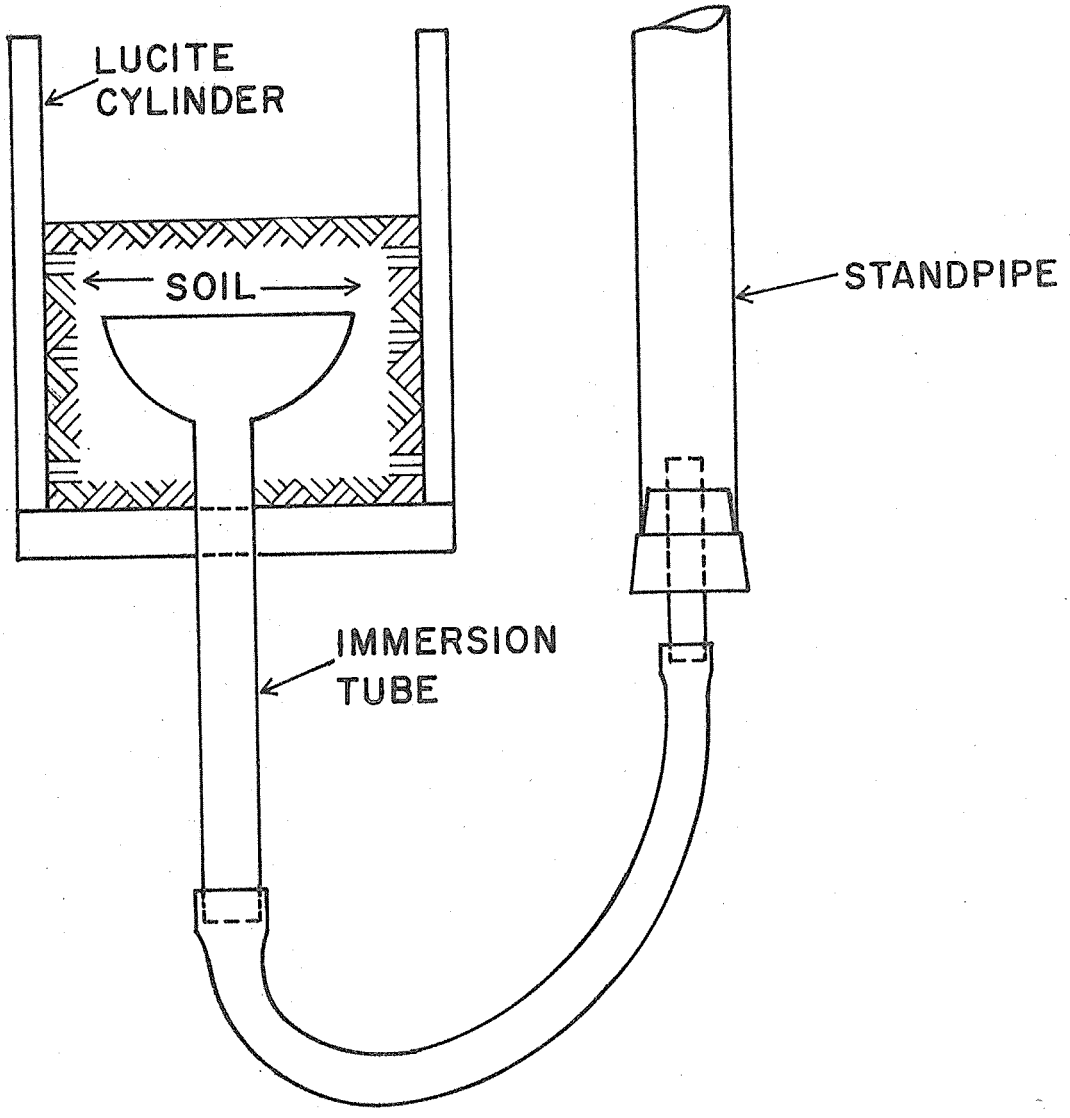

Figure 1. Apparatus for measuring breakthrough pressures of water-repellent soils.

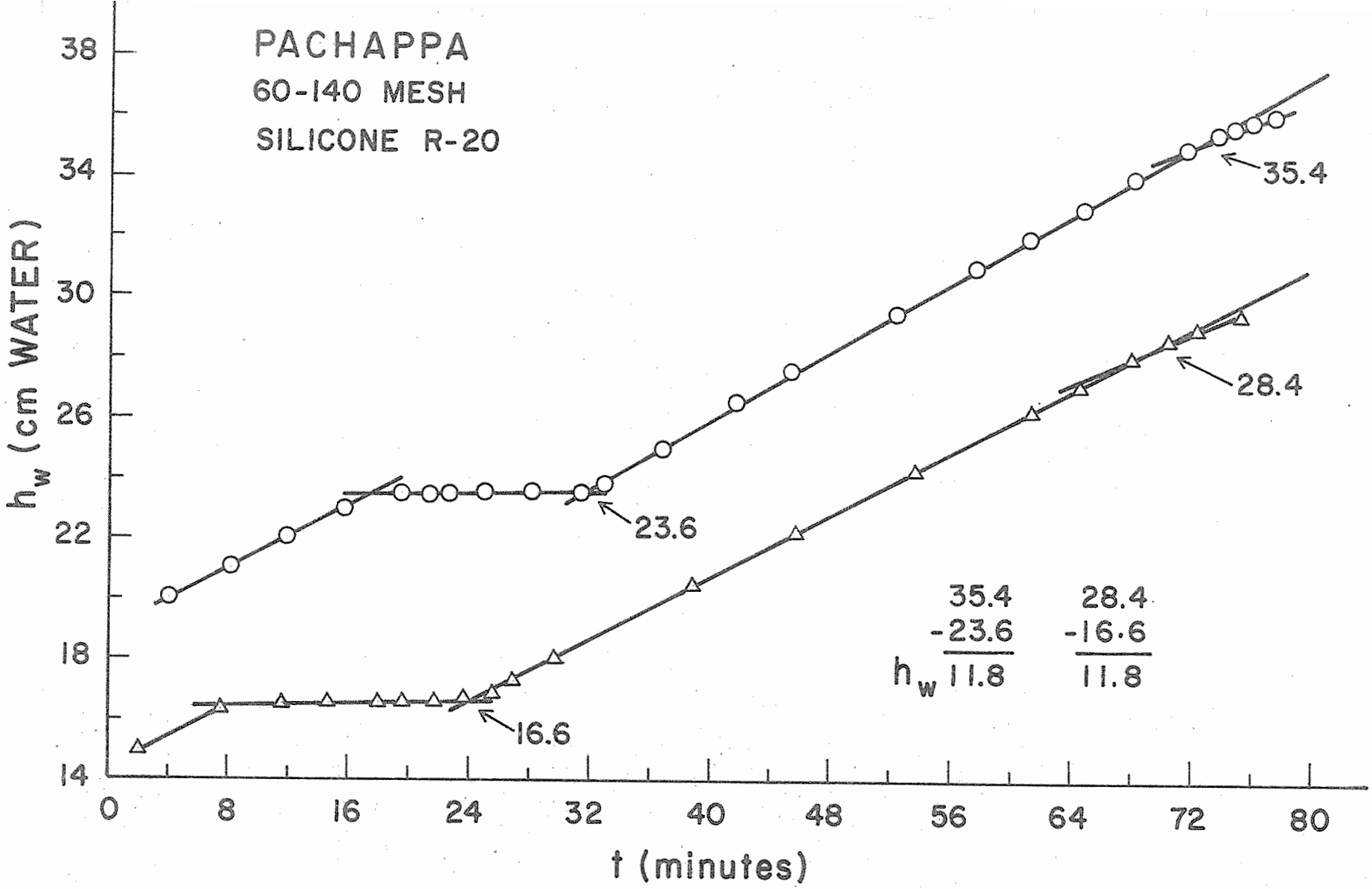

Figure 2. Typical plots of increasing water head versus time used in determination of breakthrough head (h_w) of water-repellent soils.

TITLE: USE OF FLOATING MATERIALS TO REDUCE EVAPORATION

LINE PROJECT: SWC-VII-gG2 Code No.: Ariz.-WCL-50

INTRODUCTION:

Previous studies on 2.7 m diameter tanks have shown it is economically possible to reduce evaporation with floating covers made from plastic or rubber sheeting. (See 1965 Annual Report WCL-9.) Because these materials are very light, it is possible the covers could be damaged or blown off, particularly when covering larger areas. Preliminary studies were conducted to evaluate the design and performance of large floating covers under field conditions.

Studies were conducted on evaluation of the long-term effect of floating white granular materials which reduce evaporation by reflecting solar radiation and reducing water temperature. The effect of wind moving the materials and the resulting effect on evaporation reduction was studied on a lined pond at the Granite Reef testing site.

A preliminary investigation was initiated on the use of lightweight floating concrete blocks for reducing evaporation.

PROCEDURE:

Procedures were the same as outlined in the 1965 Annual Report, WCL-9, with the following additions.

Two covers of 6.4 mm thick, white foamed polyethylene were constructed. A design was developed whereby the edges of the covers are held in contact with the water, thus reducing the possibility of wind damage. The covers are made in 6 m square sections and then tied together for larger areas. The covers were placed on a 12 x 30 m lined pond at the Granite Reef testing site. The movement of the cover by wind is being observed and the windspeed and direction are being recorded with a multipoint recorder at 30 min intervals.

The effect on evaporation of the relative size of cover to water surface area was studied on the 2.7 m diameter tanks. Three covers, 2.59 m diameter, 1.95 m diameter, and 1.32 x 1.32 m square, covering 92.1, 52.1, and 30.6 percent of the area, respectively, were constructed. The evaporation compared to an uncovered tank was recorded on waterstage recorders.

The long-term effectiveness of expanded perlite ore particles was evaluated on the 2.7 m diameter tanks. The effect of wind moving the perlite was studied on the lined pond at Granite Reef. The pond had previously been calibrated against two buried Young evaporation pans. The pond was then covered with the perlite and the reduction in evaporation as compared to the evaporation pans was determined. At the same time, the windspeed and direction was continuously recorded with a multipoint strip chart recorder.

Various types and proportions of aggregate materials for low-cost floating concrete blocks were investigated. Half of the most promising blocks were coated on the sides and bottom with an asphalt-clay emulsion after they had cured for two to three weeks. After the asphalt had dried, these blocks and the untreated ones were placed on a tank of water to evaluate their floating, water absorption, and other physical properties.

RESULTS AND DISCUSSION:

Foamed Polyethylene. The two foamed polyethylene covers installed at Granite Reef in December 1966 have been subjected to winds up to 25 mph with no apparent difficulties. During the period the covers have been on the pond, rainfall followed by freezing temperatures have been encountered with only minor problems. Rainfall collected on the cover, and four small holes were necessary on each cover to allow this water to drain. Because of the low evaporation rate, the effectiveness of the cover to reduce evaporation was not determined.

During the spring and summer of 1966, studies on the 2.7 m diameter tanks with covers of different sizes showed the reduction in evaporation is not equal to the area covered. With 92 percent of the area covered the reduction was 90 percent; with 52 percent of the area covered the reduction was 43 percent; and a square sheet covering 31 percent of the area reduced evaporation 25 percent. The daily untreated evaporation rate was 2-6 mm day^{-1}. Further studies will be conducted to determine the effect of shape and percent coverage.

Floating Powders. A study was conducted from 26 January 1966 to 21 June 1966 to evaluate the long term effectiveness of the perlite ore for reducing evaporation. Approximately 2500 grams of perlite was placed on a tank. This initially reduced evaporation by 30 - 35 percent. Five months later the reduction was 10 percent. At this time the remaining perlite was removed, dried and weighed. A total of 994 grams of discolored perlite and a small amount of debris was collected. During this period 60 percent of the perlite had been lost. The untreated evaporation rate was 2 mm day^{-1} initially and increased to 6 mm day^{-1} at the end of the study.

A study at the Granite Reef testing site was conducted from 19 October 1966 to 6 December 1966. Sufficient perlite was added to the water for complete coverage. The reduction for the period compared to the evaporation pans was 30 - 40 percent. This includes periods when 20 - 50 percent of the area was uncovered because of wind moving the perlite. The untreated evaporation rate was 3 - 5 mm day^{-1}. It was observed as the wind decreased the material would respread itself. Also the perlite used is believed to have been of inferior quality. It is estimated that 50 percent sank in the first two days.

Floating Concrete Blocks. The ability of concrete blocks to float has been the main concern to this point; therefore, only the floating characteristics, general texture and appearance have been tested to date. Evaporation suppression has not been evaluated due to low rates of evaporation during the winter months.

Some of the blocks have been floating for over two months and it appears that they will continue to do so.

The use of expanded 0.3 mm average diameter perlite ore as the main aggregate produces the best results. Tests to date do not indicate any benefit derived from the asphalt coatings.

SUMMARY AND CONCLUSIONS:

Studies were continued on floating covers constructed of 6.4 mm thick, white foamed polyethylene for reducing evaporation. Present 6 m square covers with weighted edges have been subjected to winds up to

25 mph with no damage. Small holes located at selected points on the covers are allowing rain water to drain through the cover. Continued studies will evaluate treatments to protect the sheeting from weathering, and also durability of the present design under field conditions.

Limited studies with floating covers on 2.7 m diameter tanks have shown the reduction in evaporation is less than the percentage of area covered. Further studies will be conducted to evaluate the effect of cover shape on evaporation reduction.

Studies on the long-term effect of perlite ore on the 2.7 m diameter tanks showed evaporation was initially reduced by 30 - 35 percent. After five months the evaporation reduction was 10 percent. Untreated evaporation was 2 - 6 mm day^{-1} for the period. During this time 60 percent of the perlite was blown off or sank. A test on a 12 x 30 m lined pond at Granite Reef for two months showed the perlite would reduce evaporation 30 - 40 percent. This included periods when 20 - 50 percent of the pond was uncovered because of wind moving the cover.

Concrete blocks have been developed which float on a water surface. Preliminary studies indicate the blocks will float for some time, and because of their light color and nontransparency, they should reduce the water temperature and evaporation. Further studies will be conducted to determine evaporation reduction efficiency, cost, most desirable ratio of constituents, and value of protective coatings. Large scale investigations will also be conducted to determine durability and efficiency under field conditions.

PERSONNEL: K. R. Cooley.

APPENDIX I

MANUSCRIPTS APPROVED AND/OR PUBLISHED IN 1966

	MS Number
Bouwer, Herman. Limitation of the Dupuit-Forchheimer assumption in recharge and seepage. Trans., Amer. Soc. Agric. Engin. 8(4):512-515.	139
Bouwer, Herman. Developing design requirements for parallel drains. Proc., Drainage for Efficient Crop Production Conference, Chicago, Ill. Dec. 6-7, 1965. Pp. 62-65.	156
Bouwer, Herman. Closure: Theoretical aspects of seepage from open channels. Jour. Hydraul. Div., Proc. Amer. Soc. Civ. Engin. 92(HY 3):90-95. May, 1966.	158
Bouwer, Herman. Digest: Theoretical aspects of seepage from open channels. Trans., Amer. Soc. Civ. Engin. (Submitted)	160
Bouwer, Herman. Rapid field measurement of air entry value and hydraulic conductivity of soil as significant parameters in flow system analysis. Water Resources Res. 2(4):729-738.	164
Bouwer, Herman. Analyzing subsurface flow systems with electric analogs. Water Resources Res. (Submitted)	178
Bouwer, Herman. Field measurement of saturated hydraulic conductivity in initially unsaturated soil. Proc., Symp. on Artificial Recharge and Management of Aquifers, Haifa, Israel, March 1967. (Submitted)	185
Bouwer, Herman, and Rice, R. C. Modified tube diameters for the double-tube apparatus. Note, Soil Sci. Soc. Amer. Proc. (Submitted)	188
Conaway, A. W., and Van Bavel, C. H. M. Radiometric surface temperature measurements and fluctuations in sky radiance emittance in the 600-1300 cm^{-1} waveband. Agron. Jour. (Submitted)	190
Ehrler, W. L., and Van Bavel, C. H. M. Sorghum foliar responses to changes in soil water content. Agron. Jour. (Submitted)	191

	MS Number
Erie, Leonard J., French, O. F., and Patterson, Lloyd. Water management to cope with the contrary cotton plant. Proc., Western Cotton Production Conference, Phoenix, Arizona, March 1-2, 1966. Pp. 15-16.	165
Erie, Leonard J. Irrigation. Chapter in Alfalfa for Forage Production in Arizona, Univ. of Arizona Agric. Experiment Sta. Bul. A-16, Revised July, 1966. Pp. 12-15.	170
Erie, Leonard J. Consumptive use data as a tool for increasing irrigation efficiency. Proc., 1966 Arizona Water Resources Committee Symposium, Phoenix, Arizona, Sept. 21, 1966. (Submitted)	186
Fritschen, Leo J. Evapotranspiration rates of field crops determined by the Bowen ratio method. Agron. Jour. 58:339-342. 1966.	145
Fritschen, Leo J. A sensitive cup-type anemometer. Jour. of Appl. Meteorol. (Submitted)	166
Fritschen, Leo J., and Nixon, Paul R. Microclimate before and after irrigation. Science (Special Issue). (Submitted)	167
Fritschen, Leo J. Report to State of California Department of Water Resources. California State Dept. of Water Resources Report. (Submitted)	180
Jackson, Ray D., and Van Bavel, C. H. M. Pocket-model solar still obtains water for survival. Arid Lands Research Newsletter (CODAZR) No. 19-20, Pp. 4-5. May-July, 1966.	149
Jackson, Ray D., and Van Bavel, C. H. M. Water for survival: An unusual application of plastic film. Proc., 6th Natl. Agric. Plastics Conference, Phoenix, Arizona, Nov. 16-18, 1965. Pp. 38-41. (Published, June, 1966)	153
Jackson, Ray D., and Van Bavel, C. H. M. A drink from the desert. Chap. 27, 1967 Yearbook of Agriculture. (Submitted)	174
Jackson, Ray D. Solar still: Water for survival. McGraw-Hill Encyclopedia of Science and Technology. 1967. (Submitted)	175

	MS Number
Jackson, Ray D., and Klute, Arnold. Estimation of dead-end pore volume in soils from transient- and steady-state diffusion coefficients. Soil Sci. Soc. of Amer. Proc. (Note). (Submitted)	179
Myers, Lloyd E. Water harvesting with plastic films. Proc., 6th Natl. Agric. Plastics Conference, Phoenix, Arizona, Nov. 16-18, 1965. Pp. 31-34. (Published, June, 1966)	154
Myers, Lloyd E. Recent advances in water harvesting. Jour. Soil and Water Conservation. (Submitted)	181
Myers, Lloyd E., Frasier, Gary W., and Griggs, John R. Sprayed asphalt pavements for water harvesting. Jour. Irrig. and Drain. Div., Proc. Amer. Soc. Civ. Engin. (Submitted)	182
Nakayama, Francis S. Deflocculation of soil materials by sodium salts. Soil Sci. 102(6):388-393. 1966.	155
Reginato, Robert J., and Myers, Lloyd E. Repair of cracks in concrete channel linings. USDA, ARS 41-121. June, 1966. (8 pp.)	159
Reginato, Robert J., and Myers, Lloyd E. Recent water management research. Proc., 34th Annual Meeting, California Mosquito Control Assoc., Monterey, California, 31 Jan.-2 Feb., 1966. Pp. 19-22.	161
Replogle, John A., and Chow, Ven Te. Tractive-force distribution in open channels. Jour. Hydraul. Div., Proc. Amer. Soc. Civ. Engin. 92(HY 2):169-191. March, 1966.	138
Replogle, John A., Myers, Lloyd E., and Brust, Kenneth J. Stream flow measurements with fluorescent tracers. Jour. Hydraul. Div., Proc. Amer. Soc. Civ. Engin. 92(HY 5):1-15. Sept. 1966.	152
Replogle, John A., Myers, Lloyd E., and Brust, Kenneth J. Evaluation of pipe elbows as flow meters. Jour. Irrig. and Drain. Div., Proc. Amer. Soc. Civ. Engin. 92(IR 3): 14-31. Sept. 1966.	157

MS
Number

Replogle, John A. Low-pressure differential measurements in liquid flows. Agric. Engin. (Submitted) 173

Rice, Robert C. Dynamic response of small piezometers. Trans., Amer. Soc. Agric. Engin. (Submitted) 171

Van Bavel, C. H. M. Potential evaporation: the combination concept and its experimental verification. Water Resources Res. 2(3):455-467. 1966. 151

Van Bavel, C. H. M. Physical factors determining water use by crops. Proc., First Pan American Soil Conservation Congress, Sao Paulo, Brazil, April 12-29, 1966. (Submitted) 162

Van Bavel, C. H. M. The three-phase domain in hydrology. Proc., UNESCO Symp. on Unsaturated Flow, Wageningen, The Netherlands, June, 1966. (Submitted) 168

Van Bavel, C. H. M. Changes in canopy resistance to water loss from alfalfa induced by soil water depletion. Agric. Meteorol. (Submitted) 172

Van Bavel, C. H. M. Use and abuse of information processing by machine. Proc., Symp. on Collection and Processing of Field Data, Canberra, A. C. T., Australia, Sept. 1, 1966. (Submitted) 176

Van Bavel, C. H. M. Summary of papers presented in Section I-b of UNESCO Symposium on Water in the Unsaturated Zone. Proc., UNESCO Symp. on Water in the Unsaturated Zone, Wageningen, The Netherlands, June 19-25, 1966. (Submitted) 183

Van Bavel, C. H. M., and Stirk, G. B. Soil water measurement with an Am^{241}-Be neutron source and an application to evaporimetry. Jour. of Hydrology. (Submitted) 189

Watson, K. K. An instantaneous profile method for determining the hydraulic conductivity of unsaturated porous materials. Water Resources Res. 2(4):709-715. 1966. 163

Watson, K. K. Experimental and numerical study of column drainage. Jour. Hydraul. Div., Proc. Amer. Soc. Civ. Engin. (Submitted) 169

	MS Number
Watson, K. K., and Jackson, Ray D. Temperature effects in a tensiometer-pressure transducer system. Soil Sci. Soc. Amer. Proc. (Submitted)	184
Watson, K. K. A recording field tensiometer with rapid response characteristics. Jour. Hydrol. (Submitted)	187
Watson, K. K. The response behavior of a tensiometer-pressure transducer system under conditions of changing pore air pressure. Soil Sci. (Submitted)	192

Reports -- The following reports of the U. S. Water Conservation Laboratory were released during the year. Such reports are not considered as formal publications, are not distributed to libraries, and should not be cited.:

Ehrler, W. L., Fritschen, L. J., and Van Bavel, C. H. M. Atmospheric and soil-plant-water relations studies. Research Report No. 388-2, prepared for U. S. Army Electronics Command, Atmospheric Sciences Laboratory, Research Division, Fort Huachuca, Arizona. October, 1966.

Frasier, Gary. A back-up power system for recorders. WCL Report No. 6. 24 October 1966.

Fritschen, Leo J. Plans for "a sensitive cup-type anemometer." April, 1966.

Van Bavel, C. H. M., Ehrler, W. L., Fritschen, L. J., and Jackson, R. D. Atmospheric and soil-plant-water relations studies. Research Report No. 388-1, prepared for Atmospheric Sciences Laboratory, Research Division, U. S. Army Electronics Command, Fort Huachuca, Arizona. July, 1966.

Van Bavel, C. H. M., and Fritschen, L. J. Evaporation and energy balance of alfalfa. Research Report No. 381, prepared for Meteorology Department, U. S. Army Electronics Research and Development Activity, Fort Huachuca, Arizona. January, 1966.